ADAPTATION OF TREES TO CLIMATE CHANGE: MECHANISMS BEHIND PHYSIOLOGICAL AND ECOLOGICAL RESILIENCE AND VULNERABILITY

EDITED BY: Andrea Ghirardo, James D. Blande, Nadine K. Ruehr, Raffaella Balestrini and Carsten Kulheim

PUBLISHED IN: Frontiers in Forests and Global Change and Frontiers in Ecology and Evolution

frontiers Research Topics

frontiers

ISSN 1664-8714
ISBN 978-2-88974-487-9
DOI 10.3389/978-2-88974-487-9

About Frontiers

Frontiers is more than just an open-access publisher of scholarly articles: it is a pioneering approach to the world of academia, radically improving the way scholarly research is managed. The grand vision of Frontiers is a world where all people have an equal opportunity to seek, share and generate knowledge. Frontiers provides immediate and permanent online open access to all its publications, but this alone is not enough to realize our grand goals.

Frontiers Journal Series

The Frontiers Journal Series is a multi-tier and interdisciplinary set of open-access, online journals, promising a paradigm shift from the current review, selection and dissemination processes in academic publishing. All Frontiers journals are driven by researchers for researchers; therefore, they constitute a service to the scholarly community. At the same time, the Frontiers Journal Series operates on a revolutionary invention, the tiered publishing system, initially addressing specific communities of scholars, and gradually climbing up to broader public understanding, thus serving the interests of the lay society, too.

Dedication to Quality

Each Frontiers article is a landmark of the highest quality, thanks to genuinely collaborative interactions between authors and review editors, who include some of the world's best academicians. Research must be certified by peers before entering a stream of knowledge that may eventually reach the public - and shape society; therefore, Frontiers only applies the most rigorous and unbiased reviews.
Frontiers revolutionizes research publishing by freely delivering the most outstanding research, evaluated with no bias from both the academic and social point of view. By applying the most advanced information technologies, Frontiers is catapulting scholarly publishing into a new generation.

What are Frontiers Research Topics?

Frontiers Research Topics are very popular trademarks of the Frontiers Journals Series: they are collections of at least ten articles, all centered on a particular subject. With their unique mix of varied contributions from Original Research to Review Articles, Frontiers Research Topics unify the most influential researchers, the latest key findings and historical advances in a hot research area! Find out more on how to host your own Frontiers Research Topic or contribute to one as an author by contacting the Frontiers Editorial Office: frontiersin.org/about/contact

ADAPTATION OF TREES TO CLIMATE CHANGE: MECHANISMS BEHIND PHYSIOLOGICAL AND ECOLOGICAL RESILIENCE AND VULNERABILITY

Topic Editors:
Andrea Ghirardo, Helmholtz Center München, Helmholtz Association of German Research Centres (HZ), Germany
James D. Blande, University of Eastern Finland, Finland
Nadine K. Ruehr, Karlsruhe Institute of Technology (KIT), Germany
Raffaella Balestrini, Institute for Sustainable Plant Protection, National Research Council (CNR), Italy
Carsten Kulheim, Michigan Technological University, United States

Citation: Ghirardo, A., Blande, J. D., Ruehr, N. K., Balestrini, R., Kulheim, C., eds. (2022). Adaptation of Trees to Climate Change: Mechanisms Behind Physiological and Ecological Resilience and Vulnerability. Lausanne: Frontiers Media SA.
doi: 10.3389/978-2-88974-487-9

Table of Contents

frontiers in Forests and Global Change

EDITORIAL
published: 21 January 2022
doi: 10.3389/ffgc.2021.831701

Editorial: Adaptation of Trees to Climate Change: Mechanisms Behind Physiological and Ecological Resilience and Vulnerability

Andrea Ghirardo[1]*, *James D. Blande*[2], *Nadine K. Ruehr*[3], *Raffaella Balestrini*[4] and *Carsten Külheim*[5]

[1] Research Unit Environmental Simulation, Institute of Biochemical Plant Pathology, Helmholtz Zentrum München, Oberschleißheim, Germany, [2] Department of Environmental and Biological Sciences, University of Eastern Finland, Kuopio, Finland, [3] Institute of Meteorology and Climate Research—Atmospheric Environmental Research, Karlsruhe Institute of Technology KIT, Garmisch-Partenkirchen, Germany, [4] Institute for Sustainable Plant Protection (IPSP)-National Research Council (CNR), Turin, Italy, [5] College of Forest Resources and Environmental Science, Michigan Technological University, Houghton, MI, United States

Keywords: acclimation, adaptation, abiotic/biotic stress, climate-resilient tree, gene variation, plasticity, recovery, root-associated microbiota

Editorial on the Research Topic

Adaptation of Trees to Climate Change: Mechanisms Behind Physiological and Ecological Resilience and Vulnerability

OPEN ACCESS

Edited and reviewed by:
Heather R. McCarthy, University of Oklahoma, United States

***Correspondence:**
Andrea Ghirardo
andrea.ghirardo@helmholtz-muenchen.de

Specialty section:
This article was submitted to Forest Ecophysiology, a section of the journal Frontiers in Forests and Global Change

Received: *08 December 2021*
Accepted: *30 December 2021*
Published: *21 January 2022*

Citation:
Ghirardo A, Blande JD, Ruehr NK, Balestrini R and Külheim C (2022) Editorial: Adaptation of Trees to Climate Change: Mechanisms Behind Physiological and Ecological Resilience and Vulnerability. Front. For. Glob. Change 4:831701. doi: 10.3389/ffgc.2021.831701

Climate change exposes plants to physiological conditions that are often outside their evolutionary limits (Shaw and Etterson, 2012). Multiple (a)biotic stressors such as heatwaves, drought, and insect/pathogen outbreaks are selective pressures on plant species and populations. However, the range of environmental conditions to which plants are adapted and their ability to acclimate to new conditions varies intra- and interspecifically. Plants can acclimate to stress by complex molecular and biochemical processes involving stress perception, signal transduction, gene expression, biochemical, physiological and morphological changes, and interactions with beneficial symbionts. Plant adaptation occurs through natural selection and ultimately relies on phenotypic plasticity, epigenetic modulations, and intraspecific genetic variation at individual and population levels.

This volume collected 11 articles, including primary research articles, opinions, and reviews that address fundamental questions and provide new insights into plant responses to climate change factors, focusing on biochemical and physiological adjustments underlying plant resilience and vulnerability.

Plant plasticity—the ability to change in response to stimuli or environments—can affect plant morphology and physiology by profound changes at molecular and metabolic levels. Alderotti et al. showed the anatomical, physiological, and biochemical responses triggered by a heatwave in *Cistus incanus* L., a shrub species adapted to hot and arid conditions typical of the Mediterranean basin. As an acclimation mechanism to heatwaves, the leaves had increased palisade parenchyma, resulting in a thicker lamina that enhanced resistance to dehydration and improved carbon assimilation. In addition, induction of secondary metabolites (tannins and terpenoids) indicated biochemical responses to counteract increasing oxidative stress. High plasticity is also characteristic of early successional species (Valladares et al., 2000). Carter et al. have studied *in situ* the effects of warming on photosynthesis and respiration of *Psychotria brachiata* and *Piper glabrescens,* which are early successional and mid-successional tropical shrubs. *P. brachiata* was able to acclimate the temperature optimum of photosynthesis (T_{opt}), whereas *P. glabrescens* lowered stomatal

conductance to decrease water loss resulting in lower photosynthesis. Shifts in T_{opt} and rate of photosynthesis during acclimation to hot and dry environments can be explained by protein expression plasticity in the date palm (*Phoenix dactylifera*), a plant species well-adapted to xeric and hot environments (Kruse et al., 2019; Ghirardo et al., 2021). This highlights the importance of plasticity in acclimating to higher temperatures.

Plant resistance and resilience to drought stress are essential for plant survival. Xylem hydraulic failure is a ubiquitous factor in drought-driven tree-mortality. Drought-resistant species have meristematic cells with an enhanced ability to relocate stored water in tissues to avoid plasmolysis (Mantova et al., 2021). Schröter and Oberhuber reported that phloem is less susceptible to environmental influences, although knowledge on phloem adaptation to extreme climate conditions at the high-elevation treeline is scarce. Besides extreme conditions, global warming shifts precipitation and temperatures, extending the growing season and increasing the evapotranspiration of forest and cropland areas in Baltic countries (Montibeller et al.). At high latitudes, the warmer autumn seasons affect cold acclimation—the process that prepares evergreen conifers for the winter season. Noordermeer et al. found that low temperature is the dominant signal for the downregulation of photosynthesis and upregulation of photoprotection in cold acclimation of Douglas-fir. Autumn warming disrupts the key components of the autumn cold acclimation process, which is usually initiated by the shorter photoperiod and then triggered by sub-zero temperatures. Oksanen further reviewed the actual understanding of the responses and acclimation mechanisms of silver birch (*Betula pendula*) to changing environmental conditions. This deciduous tree species has high plasticity and is widely distributed in boreal forests, thus it has an excellent acclimation ability. The high genetic variation and the availability of genome data make silver birch a good model system for elucidating the adaptation mechanisms of northern trees to climate change.

Acclimation to stress can persist between generations toward adaptive transgenerational plasticity by epigenetics (Crisp et al., 2016). It relies on plant memory; the ability to remember a stress condition and respond faster and stronger upon subsequent stress. It also depends on the ability of plants to repair stress-induced damages (Ruehr et al., 2019). Li et al. showed that antecedent water limitation primes the responses and recovery dynamics of *Eucalyptus camaldulensis* upon subsequent drought stress, and the effects extend during post-stress recovery. Deciphering the role of stress legacy and memory on plant physiology and growth will be critical to foresee changes in plant community composition and function. However, understanding the ability of trees to adapt to climate change also requires knowledge of functional traits under selection. Directional selection—the natural selection that favors extreme phenotypes of a population—leads to great changes in allele frequencies in a population and increases the adaptiveness of plants. Costa e Silva et al., studied the population-level variation in functional traits of *Eucalyptus pauciflora* seedlings in dry and mesic sites and compared it to controlled experimental drought. Upon acute water limitation, the trait of lamina length exhibited a directional selection pattern in line with a shift in the mean of the mesic population toward that of the dry population. Therefore, past adaptation and gene variation reduce the plant's susceptibility to stress.

Root symbiosis with ectomycorrhizal and arbuscular mycorrhizal fungi can further mitigate the tree sensitivity to stress. Affnity for specific fungal symbionts is part of a tree's phenotype and may serve as a form of adaptation. Usman et al., reviewed the role of mycorrhizal symbioses in attenuating climate-driven increases in abiotic stresses. In general, the mechanisms in trees are similar to those found in non-woody plants and knowledge on the protective mechanisms gained on non-woody plants may help the manipulation of the tree microbiome to support the health and resilience of forests.

Biotic attacks often appear alongside climatic stresses, amplifying forest vulnerability. Therefore, large-scale monitoring of forest ecosystems is crucial for assessing forest health and tree mortality (Hartmann et al., 2018). Moreover, developing detection methods for tree diseases will be paramount to assist forest management. Antimicrobial peptides (AMPs) are a group of proteins of innate immunity mostly known in herbaceous plants. AMPs are secreted in the apoplastic space of peripheral cell layers and act in plant defense against pathogenic fungi, bacteria, viruses, and herbivores. To counteract the increasing spread of pathogenic infection, Nosenko et al. suggested using AMPs as markers for early detection of forest diseases. Yet, its development requires advanced knowledge of the AMPs-based defense mechanisms in woody plants. To prepare our forests for fighting climate change, Schroeder et al. proposed the selection of oak genotypes from natural forest stands based on molecular markers of single nucleotide polymorphisms. This strategy would enable the screening for resistant genotypes to (a)biotic stress while maintaining a rich gene pool. Resistant members of tree populations may be then used in seed orchards to assist climate-resilient reforestation programs.

This Research Topic highlights the increasing number of studies addressing various aspects of woody plant adaptation, resilience, and vulnerability to climate change. There is a strong potential for adaptation under selective forces of climate change for plant species that have high variation in plasticity, genetics, trait expression and gene flow.

AUTHOR CONTRIBUTIONS

AG wrote the first editorial draft. All authors contributed to the article and approved the submitted version.

FUNDING

AG acknowledges the Fachagentur Nachwachsende Rohstoffe e. V. (FNR) in the programme Waldklimafond (28W-B-4-113-01/2), funded by Federal Ministry of Food and Agriculture and Federal Ministry for Environment, Nature Conservation, and Nuclear Safety, Germany. NR was supported by the German

Research Foundation through its Emmy Noether Program (RU 1657/2-1). RB acknowledges National Research Council (CNR) project FOE-2019 DBA.AD003.139. CK received financial support from a US Department of Agriculture, National Institute of Food and Agriculture, McIntire Stennis, Grant Accession Number 1017893.

REFERENCES

Crisp, P. A., Ganguly, D., Eichten, S. R., Borevitz, J. O., and Pogson, B. J. (2016). Reconsidering plant memory: intersections between stress recovery, RNA turnover, and epigenetics. *Sci. Adv.* 2:e1501340. doi: 10.1126/sciadv.1501340

Ghirardo, A., Nosenko, T., Kreuzwieser, J., Winkler, J. B., Kruse, J., Albert, A., et al. (2021). Protein expression plasticity contributes to heat and drought tolerance of date palm. *Oecologia* 197, 903–919. doi: 10.1007/s00442-021-04907-w

Hartmann, H., Schuldt, B., Sanders, T. G. M., Macinnis-Ng, C., Boehmer, H. J., Allen, C. D., et al. (2018). Monitoring global tree mortality patterns and trends. Report from the VW symposium 'Crossing scales and disciplines to identify global trends of tree mortality as indicators of forest health.' *New Phytol.* 217, 984–987. doi: 10.1111/nph.14988

Kruse, J., Adams, M., Winkler, B., Ghirardo, A., Alfarraj, S., Kreuzwieser, J., et al. (2019). Optimization of photosynthesis and stomatal conductance in the date palm *Phoenix dactylifera* during acclimation to heat and drought. *New Phytol.* 223, 1973–1988. doi: 10.1111/nph.15923

Mantova, M., Herbette, S., Cochard, H., and Torres-Ruiz, J. M. (2021). Hydraulic failure and tree mortality: from correlation to causation. *Trends Plant Sci. In press*. doi: 10.1016/j.tplants.2021.10.003

Ruehr, N. K., Grote, R., Mayr, S., and Arneth, A. (2019). Beyond the extreme: recovery of carbon and water relations in woody plants following heat and drought stress. *Tree Physiol.* 39, 1285–1299. doi: 10.1093/treephys/tpz032

Shaw, R. G., and Etterson, J. R. (2012). Rapid climate change and the rate of adaptation: insight from experimental quantitative genetics. *New Phytol.* 195, 752–765. doi: 10.1111/j.1469-8137.2012.04230.x

Valladares, F., Wright, S. J., Lasso, E., Kitajima, K., and Pearcy, R. W. (2000). Plastic phenotypic response to light of 16 congeneric shrubs from a panamanian rainforest. *Ecology* 81, 1925–1936. doi: 10.1890/0012-9658(2000)0811925:PPRTLO2.0.CO;2

Conflict of Interest: The authors declare that the research was conducted in the absence of any commercial or financial relationships that could be construed as a potential conflict of interest.

Publisher's Note: All claims expressed in this article are solely those of the authors and do not necessarily represent those of their affiliated organizations, or those of the publisher, the editors and the reviewers. Any product that may be evaluated in this article, or claim that may be made by its manufacturer, is not guaranteed or endorsed by the publisher.

frontiers in Forests and Global Change

ORIGINAL RESEARCH
published: 30 September 2020
doi: 10.3389/ffgc.2020.576320

Photosynthetic and Respiratory Acclimation of Understory Shrubs in Response to *in situ* Experimental Warming of a Wet Tropical Forest

Kelsey R. Carter[1,2], Tana E. Wood[3], Sasha C. Reed[4], Elsa C. Schwartz[1], Madeline B. Reinsel[5], Xi Yang[5] and Molly A. Cavaleri[1]*

[1] College of Forest Resources and Environmental Science, Michigan Technological University, Houghton, MI, United States, [2] Earth and Environmental Sciences Division, Los Alamos National Laboratory, Los Alamos, NM, United States, [3] U.S. Department of Agriculture, Forest Service, International Institute of Tropical Forestry, Río Piedras, PR, United States, [4] U.S. Geological Survey, Southwest Biological Science Center, Moab, UT, United States, [5] Department of Environmental Sciences, University of Virginia, Charlottesville, VA, United States

OPEN ACCESS

Edited by:
Nadine K. Ruehr, Karlsruhe Institute of Technology (KIT), Germany

Reviewed by:
Tomoaki Ichie, Kōchi University, Japan
Drew Peltier, Northern Arizona University, United States

***Correspondence:**
Kelsey R. Carter
kelseyrcarter@gmail.com

Specialty section:
This article was submitted to Forest Ecophysiology, a section of the journal Frontiers in Forests and Global Change

Received: *25 June 2020*
Accepted: *09 September 2020*
Published: *30 September 2020*

Citation:
Carter KR, Wood TE, Reed SC, Schwartz EC, Reinsel MB, Yang X and Cavaleri MA (2020) Photosynthetic and Respiratory Acclimation of Understory Shrubs in Response to in situ Experimental Warming of a Wet Tropical Forest. Front. For. Glob. Change 3:576320. doi: 10.3389/ffgc.2020.576320

Despite the importance of tropical forests to global carbon balance, our understanding of how tropical plant physiology will respond to climate warming is limited. In addition, the contribution of tropical forest understories to global carbon cycling is predicted to increase with rising temperatures, however, *in situ* warming studies of tropical forest plants to date focus only on upper canopies. We present results of an *in situ* field-scale +4°C understory infrared warming experiment in Puerto Rico (Tropical Responses to Altered Climate Experiment; TRACE). We investigated gas exchange responses of two common understory shrubs, *Psychotria brachiata* and *Piper glabrescens*, after exposure to 4 and 8 months warming. We assessed physiological acclimation in two ways: (1) by comparing plot-level physiological responses in heated versus control treatments before and after warming, and (2) by examining physiological responses of individual plants to variation in environmental drivers across all plots, seasons, and treatments. *P. brachiata* has the capacity to up-regulate (i.e., acclimate) photosynthesis through broadened thermal niche and up-regulation of photosynthetic temperature optimum (T_{opt}) with warmer temperatures. *P. glabrescens,* however, did not upregulate any photosynthetic parameter, but rather experienced declines in the rate of photosynthesis at the optimum temperature (A_{opt}), corresponding with lower stomatal conductance under warmer daily temperatures. Contrary to expectation, neither species showed strong evidence for respiratory acclimation. *P. brachiata* down-regulated basal respiration with warmer daily temperatures during the drier winter months only. *P. glabrescens* showed no evidence of respiratory acclimation. Unexpectedly, soil moisture, was the strongest environmental driver of daily physiological temperature responses, not vegetation temperature. T_{opt} increased, while photosynthesis and basal respiration declined as soils dried, suggesting that drier conditions negatively affected carbon uptake for both species. Overall, *P. brachiata,* an early successional shrub, showed higher acclimation potential to daily temperature variations, potentially mitigating negative effects of

chronic warming. The negative photosynthetic response to warming experienced by *P. glabrescens*, a mid-successional shrub, suggests that this species may not be able to as successfully tolerate future, warmer temperatures. These results highlight the importance of considering species when assessing climate change and relay the importance of soil moisture on plant function in large-scale warming experiments.

Keywords: experimental warming, photosynthesis, respiration, stomatal traits, thermal acclimation, TRACE, tropical forests

INTRODUCTION

Tropical forests cycle a disproportionate amount of Earth's carbon dioxide (CO_2) relative to their total land area and have the highest photosynthetic rates and aboveground carbon density of all terrestrial ecosystems (Beer et al., 2010; Pan et al., 2013; Schimel et al., 2015). These critical biomes are expected to approach temperatures outside their historical climate boundaries within the next decade (Diffenbaugh and Scherer, 2011; Mora et al., 2013). However, the magnitude and direction of the effects of climate warming on tropical forest carbon balance are not well constrained (Korner, 2004; Lloyd and Farquhar, 2008; Booth et al., 2012; Wood et al., 2012; Cavaleri et al., 2015). Plant carbon balance is determined by the uptake of CO_2 into the system through photosynthesis, and the release of CO_2 through respiration, however, these two processes respond differently to changes in temperature. Instantaneous photosynthetic rates increase with increasing temperatures until an optimum is reached, after which net photosynthesis rates decline (Berry and Bjorkman, 1980), whereas respiration rates rise with temperature in an exponential fashion and eventually decline at very high temperatures that cause membrane dysfunction (reviewed in Atkin et al., 2005; O'Sullivan et al., 2013; Heskel et al., 2016). Reduced photosynthesis and increased respiration with warming above photosynthetic optimum temperatures could result in CO_2 release exceeding uptake, possibly inducing a positive feedback that would exacerbate climate warming (Cox et al., 2000; Zhang et al., 2014; Drake et al., 2016; Hubau et al., 2020).

Forest upper canopies receive a higher proportion of direct solar radiation; such that, more carbon is cycled in sun leaves than shade leaves (Ellsworth and Reich, 1993). However, even though forest understory layers show lower CO_2 uptake rates per unit leaf area compared to upper canopy leaves, shaded leaves absorb the light that is scattered and refracted past the upper leaves, significantly contributing to forest productivity. In fact, due to their high leaf area index, the shaded canopy and understory leaves can contribute more than 50% of gross primary productivity of tropical forests (Chen et al., 2012; He et al., 2018). The role that shaded leaves play in tropical forest carbon cycling may further increase as temperatures rise if upper canopies surpass their thermal thresholds (He et al., 2018; Mau et al., 2018; Pau et al., 2018). Shaded leaves could continue to play an even larger role in forest carbon cycling if elevated CO_2 lowers transpiration (Kirschbaum and McMillan, 2018) and, therefore, evaporative cooling in the upper canopy leaves, as this could potentially further increase upper canopy leaf temperatures and reduce photosynthesis (Doughty and Goulden, 2008; Fauset et al., 2019). While some *in situ* tropical warming studies have focused on upper canopy leaves (Doughty, 2011; Slot et al., 2014), no study - to date - has investigated the physiological responses of tropical understory plants to experimental warming *in situ*, and rarely do warming experiments in any ecosystem investigate acclimation responses of *both* photosynthesis and respiration within the same study.

Both photosynthesis and respiration have the capacity to thermally acclimate (i.e., make adjustments to conserve carbon balance), which could mitigate the negative effects of increasing temperatures. Over time periods ranging from days to weeks, photosynthetic thermal acclimation can be measured as an *up-regulation* of either the optimum temperature of photosynthesis (T_{opt}), the rate of photosynthesis at that optimum temperature (A_{opt}) (Berry and Bjorkman, 1980; Way and Yamori, 2014), or through a broadened width of the photosynthetic temperature response curve (Ω) (Slot and Winter, 2017; **Table 1**). Respiratory acclimation to warming, on the other hand, manifests as a *down-regulation* of either the temperature sensitivity or the basal rate of respiration (Atkin and Tjoelker, 2003). Tropical forests experience more narrow variations in temperature than other latitudinal zones and plant function is determined by their growth environment and evolutionary history. Therefore, tropical species may not have the plasticity necessary to acclimate to climate warming to the same degree as organisms in systems that experience wider diurnal, seasonal, and inter-annual temperature ranges (Janzen, 1967; Cunningham and Read, 2003; Drake et al., 2015). Global meta-analyses (Way and Oren, 2010; Slot and Kitajima, 2015) and an *in situ* tropical canopy warming experiment (Slot et al., 2014) have shown that tropical plant respiration will likely acclimate to warmer temperatures, however, there is still large uncertainty and conflicting evidence surrounding photosynthetic acclimation (Cunningham and Read, 2003; Slot and Winter, 2017; Smith and Dukes, 2017; Crous et al., 2018). Recent studies on tropical seedlings suggest that some tropical species can photosynthetically up-regulate with increased temperatures (Slot and Winter, 2017; Smith and Dukes, 2017), however, an *in situ* warming study on tropical canopy leaves resulted in lower photosynthetic rates (Doughty, 2011). Respiration often acclimates even when photosynthesis does not, because a lack of photosynthetic acclimation can lead to less photosynthate available for respiration (Dewar et al., 1999; Atkin and Tjoelker, 2003; Aspinwall et al., 2016), resulting in lower respiration rates due to substrate limitation. There are limited examples of how tropical species will respond to experimental warming *in situ* (Doughty, 2011; Slot et al., 2014), and to date,

TABLE 1 | Abbreviations and descriptions.

Variable	Description	Units
A_{net}	Net photosynthesis	μmol $m^{-2}s^{-1}$
A_{opt}	Rate of photosynthesis at T_{opt}	μmol $m^{-2}s^{-1}$
A_{25}	Rate of photosynthesis at 25°C	μmol $m^{-2}s^{-1}$
g_{s_opt}	Rate of stomatal conductance at T_{opt}	mol $m^{-2}s^{-1}$
J_{max}	The maximum rate of photosynthetic electron transport	μmol $m^{-2}s^{-1}$
J_{opt}	The rate of J_{max} at T_{optJ}	μmol $m^{-2}s^{-1}$
Q_{10}	Factor that describes the rate respiration increases for every 10°C increase in temperature	unitless
R:A	Ratio of respiration at 25°C to photosynthesis at 25°C	unitless
R_d	Dark respiration	μmol $m^{-2}s^{-1}$
R_{25}	Rate of respiration at 25°C	μmol $m^{-2}s^{-1}$
T_{leaf}	Leaf temperature	(°C)
T_{opt}	The optimum temperature for net photosynthesis	(°C)
T_{optJ}	Optimum temperature of maximum photosynthetic electron transport	(°C)
T_{optV}	Optimum temperature of maximum rate of Rubisco carboxylation	(°C)
T_{veg}	Surface vegetation temperature of experimental plots	(°C)
T_{vegMAX}	Mean maximum daily surface vegetation temperature	(°C)
$T_{vegMEAN}$	Mean daily surface vegetation temperature	(°C)
T_{vegMIN}	Mean minimum daily surface vegetation temperature	(°C)
V_{cmax}	Maximum rate of Rubisco carboxylation	μmol $m^{-2}s^{-1}$
V_{opt}	The rate of V_{cmax} at T_{optV}	μmol $m^{-2}s^{-1}$
VPD	Vapor pressure deficit	kPa
VWC_{10}	Soil volumetric water content from 0 to 10 cm depth	m^3 m^{-3}
VWC_{20}	Soil volumetric water content from 20 to 30 cm depth	m^3 m^{-3}
Ω	The difference in T_{opt} and the temperature where the rate of photosynthesis is 37% of T_{opt}	(°C)

no studies have investigated how tropical plants respond to larger-scale, *in situ* whole-plant warming.

A major consequence of the scarcity of data in tropical forests, particularly for *in situ* studies, is uncertainty in our capacity to accurately model tropical ecosystem carbon exchange (Cavaleri et al., 2015; Lombardozzi et al., 2015; Mercado et al., 2018). In particular, data that inform models on how vegetation will respond to climate warming are severely lacking for tropical systems (Arneth et al., 2012; Booth et al., 2012; Cernusak et al., 2013; Huntingford et al., 2013; Wood et al., 2019). Although these models are based on the same empirical acclimation functions which were derived mostly from temperate species (Kattge and Knorr, 2007), the degree of this physiological acclimation varies (Lombardozzi et al., 2015; Smith et al., 2016; Mercado et al., 2018). Using a land-surface model, Mercado et al. (2018) recently predicted that photosynthetic capacity will be up-regulated as tropical regions acclimate to warmer temperatures, positively stimulating carbon storage in tropical regions, however, emerging empirical data do not support the idea of increased carbon uptake in African and Amazonian tropical forests (Hubau et al., 2020). To more accurately model future carbon cycling of these key ecosystems, we need to understand if these systems are able to adjust, or acclimate, to warmer temperatures (Huntingford et al., 2013).

To improve the understanding of how tropical understory plant carbon cycling will respond to climate warming, we investigated plant physiological responses of two understory shrubs to elevated temperature using a field-scale warming experiment in a wet tropical forest that heated the understory vegetation and soil using infrared heating panels (Kimball et al., 2018). While we controlled for as much variability as possible, *in situ* manipulative experiments are inherently variable both spatially and temporally. As a result, treatment differences may be obscured by high environmental variability, especially if sample size is relatively low, as is often the case with time-intensive gas exchange response curve measurements. To address this challenge, in addition to analyzing a binary treatment effect (control vs. warmed), we also assessed plant acclimation capacity by investigating photosynthetic and respiratory responses to daily environmental fluctuations using a more granular statistical approach. Physiological plasticity is directly related to thermal acclimation, as plasticity determines whether a plant has the potential to acclimate (Piersma and Drent, 2003; Atkin et al., 2006; Gunderson et al., 2010). Species that show an ability to adjust in response to environmental variation are likely to perform better under multiple aspects of climate change compared to species with limited physiological plasticity (Nicotra et al., 2010); therefore, assessing plastic responses to environmental variations provide an additional approach for examining plants' capacity for thermal acclimation.

Based on previous *in situ* studies showing a lack of up-regulation of net photosynthesis with warming (Doughty, 2011), evidence that tropical plants are operating near physiological thresholds (Doughty and Goulden, 2008; Mau et al., 2018), and the fact that tropical forests have evolved within a very narrow climatic envelope (Janzen, 1967), we expected these tropical

shrubs to have limited photosynthetic acclimation potential. We further hypothesized that respiration would acclimate to experimental warming, as respiratory acclimation has been shown in tropical plants developed *in situ* (Slot et al., 2014).

MATERIALS AND METHODS

Study Site and Meteorological Variables

This study was conducted at the Tropical Responses to Altered Climate Experiment (TRACE) site located at the USDA Forest Service Sabana Field Research Station, within the Luquillo Experimental Forest (18°18′N, 65°50′W) in northeastern Puerto Rico. This site is located at 100 m elevation in a tropical wet forest, with Ultisol soil classification (Scatena, 1989). Mean annual precipitation during 2014–2016 was 2271 mm, with each month averaging 112–324 mm rainfall. Mean annual temperature is 24°C (Harris et al., 2012). The wet season is May through November, and January through April is drier on average, however, this tropical forest experiences relatively low temperature and precipitation seasonality. In 2016, the site's basal area of trees >1 cm was 38.76 m^2 ha^{-1} and stand density was 3100 trees ha^{-1}. Canopy height averages ca. 20 m, and light level at mid canopy is approximately 600 μmol m^{-2} s^{-1}. The site is a secondary forest that, at the time of this study, had been regenerating from abandoned pasture land for approximately 70 years.

Tropical Responses to Altered Climate Experiment is comprised of three heated and three control 4 m-diameter plots located in the forest understory. The heated plots (initiated September 2016) were warmed +4°C using six infrared (IR) heating panels, each positioned in a hexagonal ring and raised approximately 2.6 m above the ground (**Figure 1**). Control plots had identical infrastructure, but with no electrical power cabling and non-heated black metal panels instead of IR panels. See Kimball et al. (2018) for more detail of experimental design and infrastructure. Plots experienced less than 20% canopy openness (Reed et al., 2020). In August 2017, canopy cover was similar between treatments, where leaf area index was 6.60 ± 0.27 (mean ± sd) in control and 6.34 ± 0.22 in heated plots.

Above-canopy daily rainfall and air temperatures used to display conditions throughout this study were collected from a 25 m tower weather station located approximately 2 km from the TRACE site (**Figure 2A**). Daily rainfall (mm) at the tower station was collected using a 10 cm plastic funnel draining into a 180 ml plastic bottle. Surface vegetation temperatures (T_{veg}) of each plot were monitored using infrared thermometers (SI-121, Apogee Instruments, Logan, UT), which measured vegetation (across multiple plants) and surface soil temperature at the center of each plot with an 18° half angle field of view. Below-canopy air temperature at the study site (CS215, Campbell Scientific, Logan, UT, United States; **Supplementary Table S1**) and T_{veg} were recorded using a multiplexer and datalogger (AM16/32, CR1000, Campbell Scientific; **Figure 2B**). Soil moisture and temperature were measured at the edge, center, and midway between center and edge of each plot at 0–10 cm depth, and additional probes were installed at 20–30 cm depth at the plot center (CS655, Campbell Scientific; **Figures 2C,D**). Air temperature (T_{air}) and relative humidity (RH) were measured inside each plot (∼1 m from the ground) using dataloggers (MX2301, Onset Computer Corp., Bourne, MA, United States) from June 20 to August 31, 2017, after the majority of plant gas exchange sampling was completed. Vapor pressure deficit (VPD) was calculated from T_{air} and RH using the Tetons equation from Monteith and Unsworth (2008).

FIGURE 1 | Photograph of one of the experimental warming plots. Photo credit: Aura M. Alonso-Rodríguez.

Sampling Design

We measured net photosynthesis, leaf respiration, and stomatal traits during four measurement campaigns: two before and two after the initiation of warming. Pre-warming measurements were taken in January (winter) and August 2016 (summer). Warming was initiated on September 28, 2016, and post-warming measurements were taken in January (winter), after 4 months of warming, and May–June 2017 (summer), after 8 months of warming (**Figure 2**).

Measurements were conducted on the first fully expanded leaf of the two most common species within the plots: *Psychotria brachiata* Sw., an early successional shrub that can be prevalent in the shaded understory but performs well in an open canopy environment (Devoe, 1989; Valladares et al., 2000; Pearcy et al., 2004), and *Piper glabrescens* (Miq.) C. DC., a mid-successional shrub species (Myster and Walker, 1997). Including seedlings under 30 cm height, there were 14–58 individual *P. brachiata*

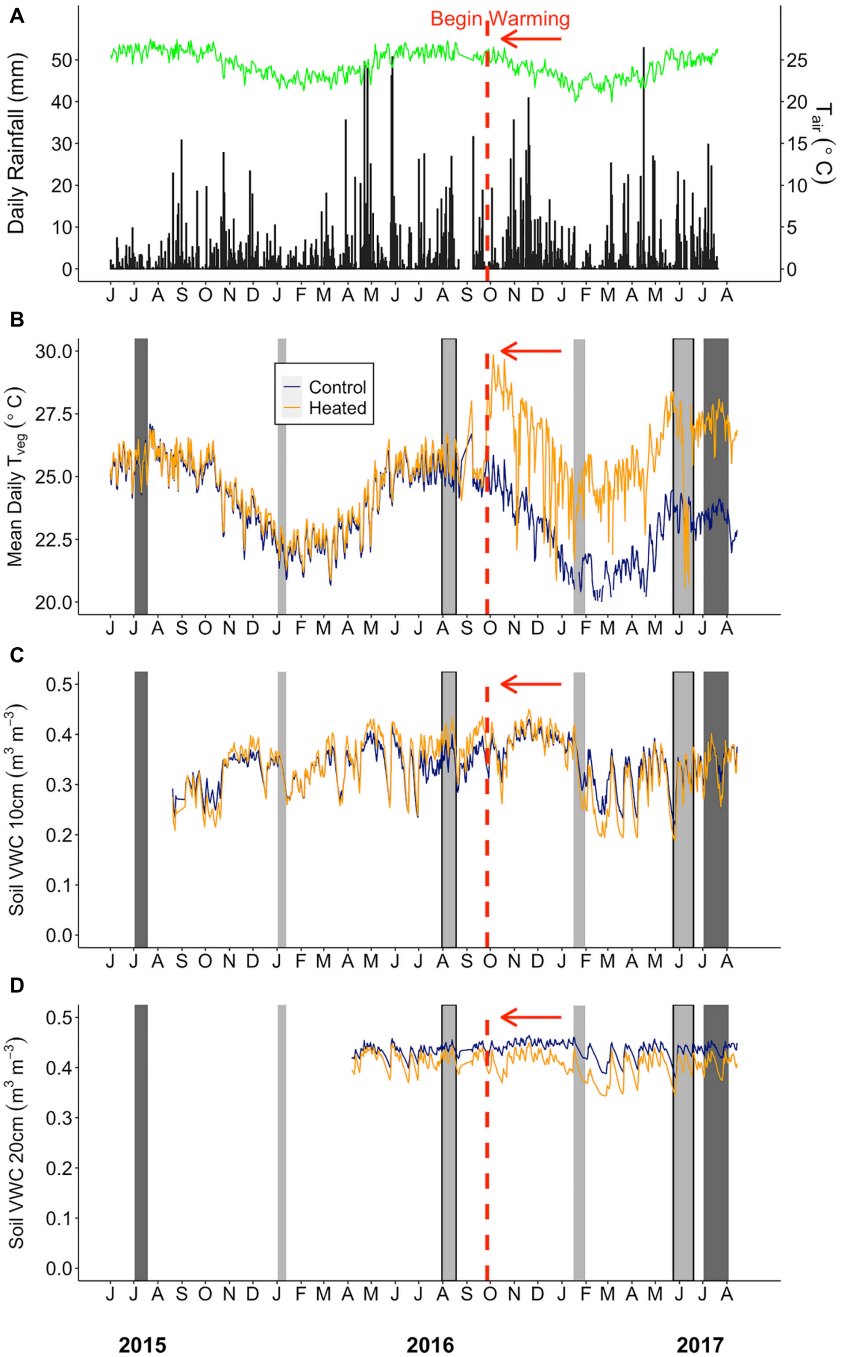

FIGURE 2 | Environmental summaries throughout the duration of the pre-warming and post-warming campaigns. **(A)** Daily rainfall (black bars) and average daily air temperature (T_{air}; green line). **(B)** Mean daily surface vegetation temperature of the heated (orange) and control (dark blue) plots. Mean daily soil moisture at **(C)** 0–10 cm and **(D)** 20–30 cm depth for the heated and control plots. The dates shown range from July 1st 2015–August 15th 2017. The vertical red dashed line depicts the beginning of the warming treatment in the heated plots. The light gray bars depict A_{net} and R_{dark} sampling campaigns. The sampling campaigns that are light gray bars outlined in black (August 2016 and June 2017) depict campaigns where stomatal size and density was measured. The dark gray bars depict the V_{cmax} and J_{max} sampling campaigns. Rainfall and air temperature were collected from an above canopy weather station. Air temperature (°C) (HMP50-L, Campbell Scientific) was logged using a datalogger (CR1000, Campbell Scientific).

and 2–84 individual *P. glabrescens* individuals per plot in 2017. *P. brachiata* comprised 30% and *P. glabrescens* comprised 5% of the number of woody plants greater than 30 cm height within the plots. The heights of individuals measured within each plot ranged from 25.5 to 209.0 cm for *P. brachiata* and 12.0 to 110.0 cm for *P. glabrescens*. Average stem diameter of

individuals measured 2 cm above the soil surface ranged from 3.6 to 37.6 mm for *P. brachiata* and 3.6 to 10.4 mm for *P. glabrescens*. Two to four leaves per species per plot were sampled during each campaign from separate individual plants whenever possible (**Supplementary Table S2**). In the cases where three leaves for a species were not available within a plot, extra leaves were measured from a separate plot. In some instances, there were not enough individual plants throughout the plots to get an adequate samples size; in this case, two leaves from the same individual plant were measured (**Supplementary Table S2**).

Net Photosynthesis and Stomatal Conductance Response to Temperature

We measured photosynthetic temperature response at 20, 25, 27, 30, 33, 35, 37, and 40°C on attached leaves using an LI6400XT infrared gas analyzer fitted with the 6 cm^2 leaf chamber (6400-02B, Li-COR Inc., Lincoln, NE, United States). Temperature was controlled by cycling hot or cold water through the Expanded Temperature Control Kit (6400-88, Li-COR Inc.) using gravity (Mau et al., 2018). Photosynthetic photon flux density was controlled at saturating irradiance (800 $\mu mol\ m^{-2}\ s^{-1}$) based on photosynthetic light response curves performed on these understory plants (data not shown), CO_2 concentration at 400 ppm, and flow rate between 150 and 500 $\mu mol\ m^{-2}\ s^{-1}$ to keep chamber VPD between 1 and 2 kPa. It was sometimes difficult to keep VPD below 2 kPa at temperatures above 35°C, however. Each leaf was allowed approximately 5 min to equilibrate to new chamber conditions. Measurement duration for a single temperature response curve ranged between 40 and 75 min, and measurements were conducted between 8 am and 4 pm. Each measurement campaign lasted 21–35 days. Environmental conditions were variable throughout the day and throughout campaigns.

Net photosynthetic temperature response parameters were extracted using the following equation from June et al. (2004):

$$A_{net} = A_{opt} \times e^{-\left(\frac{T_{leaf} - T_{opt}}{\Omega}\right)} \quad (1)$$

where A_{net} is net assimilation at the instantaneous leaf temperature (T_{leaf}), and Ω is the difference in T_{opt} and the temperature where photosynthesis is reduced to 37% of A_{opt}. The parameter Ω is a measure of the width of the temperature response curve, where a larger value of Ω indicates a wider curve, or broader photosynthetic thermal niche. In eight of the 124 curves, A_{net} peaked outside the range of measured temperatures, and in these instances, T_{opt} and A_{opt} were determined as the temperature at the maximum rate of photosynthesis, and Ω was not extracted. Therefore, Ω statistical analyses were based on 116 of the 124 temperature response curves. For each curve, we also extracted stomatal conductance at T_{opt} (g_{s_Opt}). The parameter g_{s_Opt} was extracted by fitting linear regressions to each g_s - temperature responses and extracting the rate of g_s at the photosynthetic optimum temperatures. Before g_{s_Opt} was extracted, $g_s > 3$ standard deviations away from the mean were determined to be outliers outside the range of instrumental error and were removed.

A-C_i Curves

To further investigate mechanisms underlying photosynthetic acclimation, we performed photosynthetic CO_2 response curves (A-C_i curves), at multiple temperatures to measure temperature responses of the maximum rates of Rubisco carboxylation (V_{cmax}) and the maximum rates of electron transport (J_{max}). Due to the time intensive nature of performing multiple A-C_i curves across a range of temperatures, only the most common species, *P. brachiata*, was used for V_{cmax} and J_{max} measurements. Pre-warming measurements were collected in July 2015 and post-warming measurements were taken July–August 2017, after approximately 9 months of warming (**Figure 2** and **Supplementary Table S2**). A-C_i curves were measured on the same leaf at 20, 25, 30, 35, 40°C using a LI6400XT (Li-COR Inc.) fitted with an Expanded Temperature Control Kit (6400-88, Li-COR Inc). V_{cmax} and J_{max} were extracted from each curve constructed from 400, 300, 200, 100, 50, 0, 450, 600, 850, 1000, and 1200 ppm CO_2 concentrations, at saturating irradiance (800 $\mu mol\ m^{-2}\ s^{-1}$) and a flow adjusted to control chamber VPD from 1 to 2 kPa (A-Ci curves at different temperatures shown in **Supplementary Figure S1**). V_{cmax} and J_{max} were extracted from the net assimilation rate (A_{net}) response to internal CO_2 concentration (C_i) using the "Ecophys" package (Duursma, 2015) in R version 3.5.0 (R Core Team, 2018), which implements the Farquhar, von Caemmerer, and Berry model (Farquhar et al., 1980; von Caemmerer and Farquhar, 1981). Biochemical parameters were extracted by fitting the J_{max} and V_{cmax} vs. temperature response curves to a peaked Arrhenius function (Medlyn et al., 2002):

$$(T_k) = (k_{opt}) \frac{H_d \exp\left(\frac{H_a(T_k - T_{opt})}{(T_k R T_{opt})}\right)}{H_d - H_a 1 - \exp\left(\frac{H_d(T_k - T_{opt})}{(T_k R T_{opt})}\right)} \quad (2)$$

where T_k is the measured leaf temperature in Kelvin, (k_{opt}) is the value of J_{max} or V_{cmax} at the optimum temperature ($\mu mol\ m^{-2}\ s^{-1}$), H_a is the activation energy, or exponential increase, in an Arrhenius function ($kJ\ mol^{-1}$), H_d is the decrease in J_{max} or V_{cmax} after T_{opt} and was held constant at 200 $kJ\ mol^{-1}$(Medlyn et al., 2002), and R is the universal gas constant (8.314 $JK^{-1}mol^{-1}$). Equation 2 was fit as one curve for all measurements made within a single plot; therefore, all measurements collected in one plot were calculated as one sample.

Leaf Dark Respiration

Foliar dark respiration (R_d) was measured on the same leaves that we used to measure net photosynthesis whenever possible. R_d measurements were conducted using a LI6400XT fitted with the 6400-05 conifer chamber head wrapped in aluminum foil and a water jacket (Expanded Temperature Control Kit 6400-088 Li-COR Inc., Lincoln, NE, United States). We used this chamber because it fit larger leaf areas, providing more accurate detection of the low R_d rates. For each measurement, a single leaf

was rolled or folded loosely to fit in the chamber and to allow adequate air mixing. Whether or not entire leaves fit inside of the chamber, respiration rates were corrected by the actual leaf area inside the chamber. For respiration – temperature response curves, we measured CO_2 efflux rates at 25, 30, 35, 37, and 40°C for each leaf. Measurements began at least 1 h after sunset, from approximately 7:00 pm to no later than 2:00 am. Chamber reference CO_2 was controlled at 400 ppm. Each curve took approximately 25–35 min to complete.

Leaf respiration generally declines at temperatures higher than 50°C (O'Sullivan et al., 2017), but shows an exponential increase with temperature below this threshold. We measured the rate of respiration at temperatures up to 40°C; therefore, each respiratory response curve was fitted to the exponential, non-linear equation as in Cavaleri et al. (2008) and Slot et al. (2014):

$$R_d = \beta_0 \times exp\left(T_{leaf} \times \beta_1\right) \quad (3)$$

where R_d is the respiration rate (μmol m^{-2} s^{-1}) at T_{leaf} and b_0 and b_1 are model parameters. The change in respiration rate with every 10°C (Q_{10}) is calculated as:

$$Q_{10} = exp\left(10 \times \beta_1\right) \quad (4)$$

R_{25} was calculated using:

$$R_{25} = \frac{R_{Tleaf}}{Q_{10}^{(T_{leaf}-25)/10}} \quad (5)$$

where R_{Tleaf} is the respiration rate at T_{leaf}. R_{25} was calculated for each measurement temperature and then averaged to obtain one value for each leaf.

R:A Ratio

To assess leaf carbon balance, the ratio of leaf respiration to photosynthesis (*R:A*) was calculated by dividing R_{25} by the photosynthetic rate at 25°C (A_{25}). A_{25} was extracted from Eq. 1 by setting T_{leaf} equal to 25. For the eight curves that would not fit Eq. 1, the actual photosynthetic rate measured at 25°C was used for the values of A_{25}. When respiration and photosynthesis were measured on separate leaves, measurements were matched from the same individual plant.

Stomatal Traits

To provide further mechanistic insight to photosynthetic responses, we measured stomatal size and density during August 2016 (pre-warming) and late June 2017 (post-warming) for *P. brachiata* only. Stomatal traits were collected on fully expanded leaves that developed during the warming treatment. Stomatal impressions were collected by applying clear nail varnish to the abaxial side of the leaf. Clear cellophane tape was used to remove the dried varnish and mounted to glass microscope slides. Photos of the slides were taken under 20× magnifications using a compound light microscope (Eclipse 400, Nikon Instruments Inc., Melville, NY, United States) and camera (DFC295, Leica Microsystems Inc., Buffalo Grove, IL, United States) fitted with a 55X coupler. Stomatal density was calculated as the number of stomata within the 20× magnified area and divided by total visible area using ImageJ v.1.50. Stomatal size was calculated by multiplying the length and width, including guard cells, of each stoma visible within the magnified area.

Detecting Acclimation by Analyzing Gain Score Treatment Effects

We found differences between plant temperature response parameters in the heated and control plots prior to the initiation of the warming treatment (**Figures 3**, **4**). To account for this natural variation and to avoid spurious treatment effects, the changes in measured physiological parameters (A_{opt}, T_{opt}, Ω, g_{s_Opt}, Q_{10}, R_{25}, *R:A*) in response to warming were analyzed using a gain score analysis, rather than simply comparing treatment versus control plants after warming initiation. Gain scores were calculated as the difference between post-warming and pre-warming plot averages, and were analyzed using two-way ANOVAs by treatment, season, and their interaction. Stomatal size and density gain scores were calculated as the difference between post-warming and pre-warming plot averages, measured during summer only, using Student's *t*-tests to compare treatments. J_{max} and V_{cmax} data were also only collected once pre- and post- warming (**Figures 2B–D**); therefore, Student's *t*-tests were used to compare differences between the optimum temperature of V_{cmax} (T_{optV}), the optimum temperature of J_{max} (T_{optJ}), the rate of V_{cmax} at T_{optV} (V_{opt}), the rate of V_{cmax} at 25°C, the rate of J_{max} at T_{optJ} (V_{opt}), and the rate of J_{max} at 25°C. V_{cmax} and J_{max} parameters were successfully extracted for two control and three heated plots; therefore, control plot gain scores were analyzed using two of the three control plots.

Gain scores were also used to analyze how plot environmental variables [daily maximum (T_{vegMAX}), mean ($T_{vegMEAN}$), and minimum (T_{vegMIN}) surface vegetation and soil volumetric water content at 10 cm (VWC_{10})] differed between treatment and season, calculated using dates of measurement campaigns only. Student's *t*-tests were used to compare VPD between the heated and control plots using hourly means, then comparing mean VPD between heated and control plots during daytime hours.

Acclimation Effect Size

To assess acclimation potential of the physiological parameters in a synthetic meta-analytic way, we calculated effect size of each gain score for all gas exchange and stomatal traits. Effect size was calculated as in Gurevitch et al. (1992) and Hedges and Olkin (1985):

$$d = \frac{Y_e - Y_c}{s} \times J_m \quad (6)$$

where d is the effect size, Y_e is the mean of the experimental gain score, Y_c is the mean of the control gain score, and s is the standard deviation calculated as:

$$s = \sqrt{\frac{\left((N_e - 1) \times s_e^2\right) + \left((N_c - 1) \times s_c^2\right)}{N_e + N_c - 2}} \quad (7)$$

where N_e is the experimental gain score sample size, N_c is the control gain score sample size, s_e is the standard deviation of the

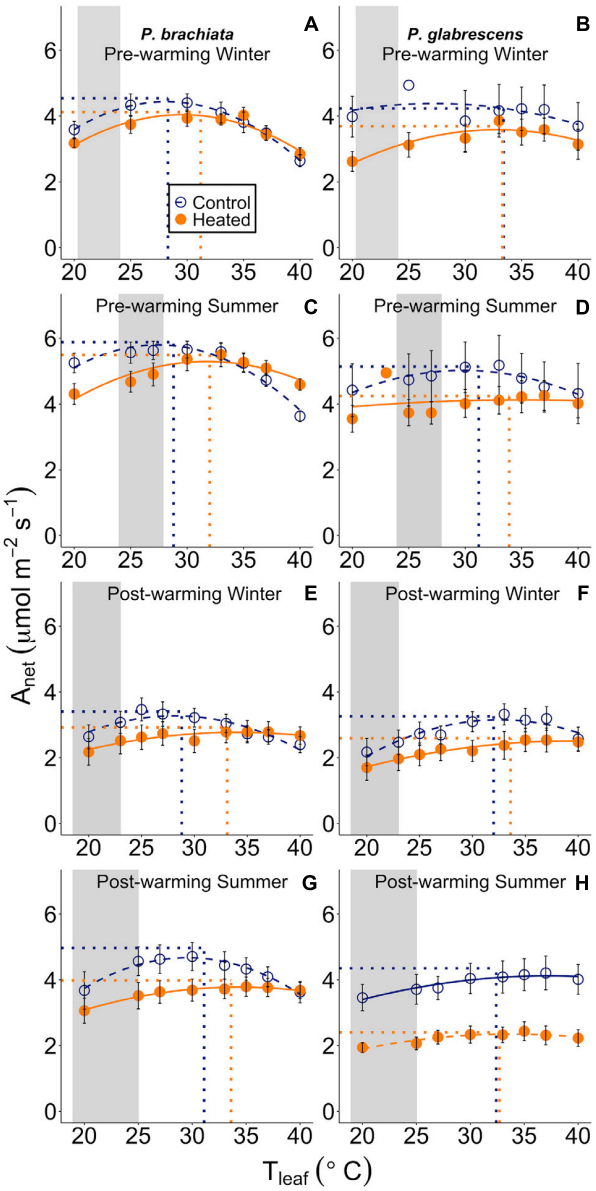

FIGURE 3 | Net photosynthetic (A_{net}) response to instantaneous leaf temperatures (T_{leaf}). The relationship between net photosynthesis and temperature was plotted separately for each measurement campaign and species: **(A)** *Psychotria brachiata* pre-warming winter season, **(B)** *Piper glabrescens* pre-warming winter season, **(C)** *P. brachiata* pre-warming summer season, **(D)** *P. glabrescens* pre-warming summer season, **(E)** *P. brachiata* 4 months post-warming winter season, **(F)** *P. glabrescens* 4 months post-warming winter season, **(G)** *P. brachiata* 8 months post-warming summer season, **(H)** *P. glabrescens* 8 months post-warming summer season. Control plot (dark blue open circles) and heated plot (orange closed circles) are means ± se at each leaf temperature. Lines are fit to each temperature response using the June et al. (2004) method (Eq. 1) for control (dark blue; dashed) and heated (orange; solid) plots separately. Dotted vertical lines represent the optimum temperature for photosynthesis. Dotted horizontal lines represent the rate of photosynthesis at the optimum temperature for plants in control (dark blue) and heated (orange) plots separately. Gray boxes represent the range of the average minimum and maximum daily vegetation temperature observed for the control plots. Average minimum and maximum temperatures are calculated for each measurement campaign separately.

experimental gain score, and s_c is the standard deviation of the control gain score.

J_m is a correction for small sample size biases and is calculated as:

$$J_m = 1 - \frac{3}{4m - 1} \tag{8}$$

Where m is calculated as:

$$m = N_e + N_c - 2 \tag{9}$$

Seasons were pooled for effect size analysis.

Detecting Acclimation by Analyzing Responses to Environmental Variables

The large variation in actual environmental conditions across space and time represented in "warmed" and "control" plots of a large-scale *in situ* manipulative experiment and the nature of these time-intensive physiological measurements resulted in rather low statistical power for the gain score analysis (i.e., using only binary categorical data). Additionally, we compared plots rather than individual plants across time when calculating gain scores because we did not always measure the same plants in each campaign, which decreased our sample size further for this analysis. To increase our statistical power for detecting acclimation, we took advantage of our rich datasets of actual environmental conditions experienced by these plants and investigated physiological plasticity in response to environmental variables (i.e., using continuous data). First, mixed effects models were used to investigate how photosynthetic temperature response parameters responded to daily values of temperature (T_{vegMAX}, $T_{vegMEAN}$), and soil volumetric water content at depths of 0–10 and 20–30 cm (VWC_{10}, and VWC_{20}, respectively) for each season. Respiratory temperature response parameters were analyzed in response to T_{vegMIN}, $T_{vegMEAN}$, VWC_{10}, and VWC_{20} because respiration was measured at night, when minimum temperatures occur. Models were run for each species separately with plot as the random variable, where individual plant was the sampling unit. In cases where multiple leaves were measured for a single plant, the mean of the dependent parameter of the two leaves were used as a single sample. Two Q_{10} values > 3 standard deviations from the mean were removed. Environmental variables on the day prior to gas exchange sampling were used because the heaters were turned off for safety during sampling days. Mixed effects models were analyzed using the "lmer" function in the "lme4" package (Bates et al., 2015). *P*-values were extracted for the mixed effect model using the "Anova" function from the "car" package in R (Fox and Weisberg, 2011), which calculates *p*-values based on Wald chi-square tests. In addition, we used a hierarchical partitioning approach to quantify the explanatory power of each environmental variable on parameter variance using the "heir-part" package in R (Walsh and Mac Nally, 2013). By using these additional approaches to assess acclimation potential of our study species, we were not only able to capture responses to the high spatial and temporal variability in environmental conditions that were obscured when only comparing binary treatment effects, but we also were able to tease apart the most important environmental drivers.

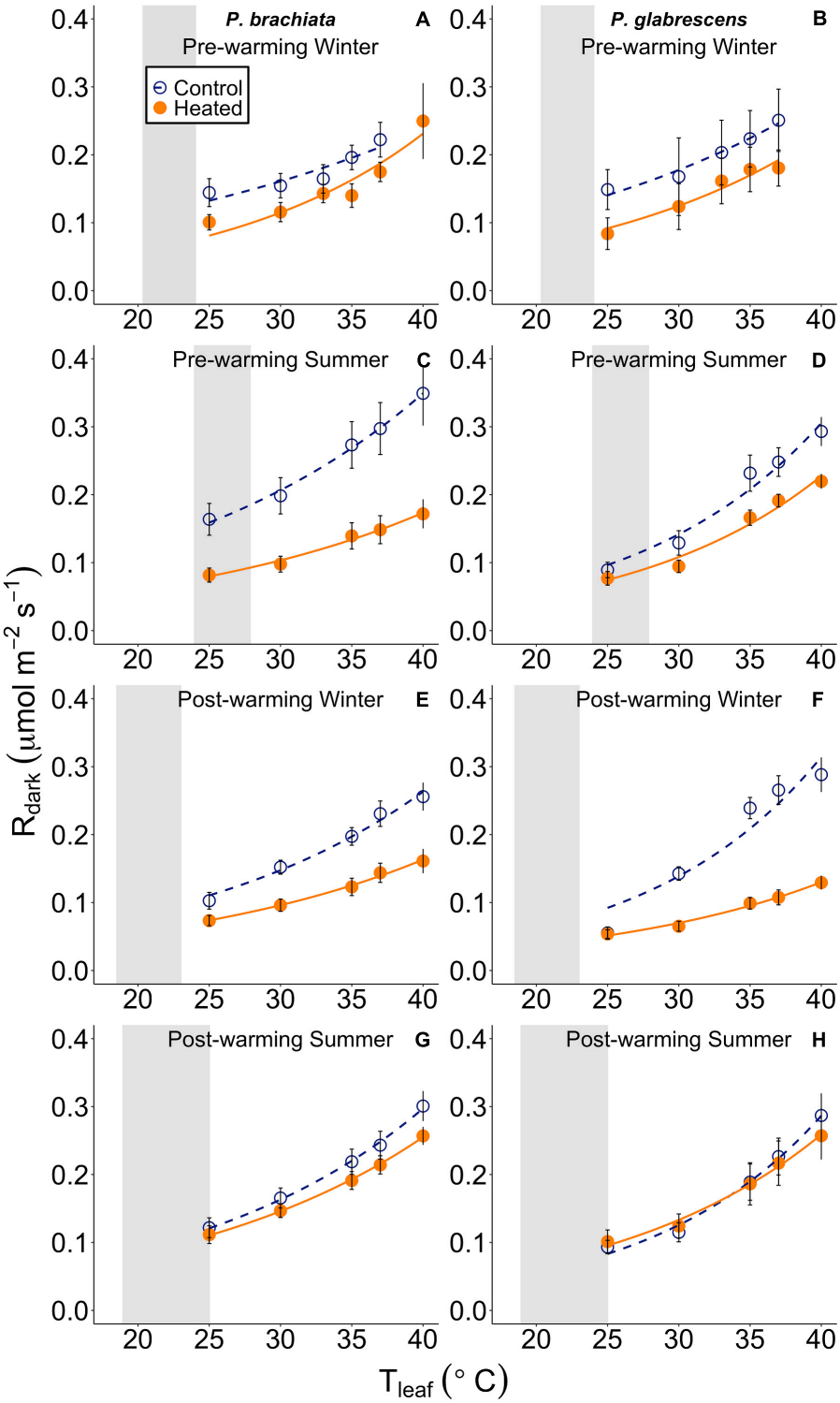

FIGURE 4 | Leaf respiratory (R_{dark}) response to instantaneous leaf temperatures (T_{leaf}). The respiratory response to temperature was plotted separately for each measurement campaign and species: **(A)** *Psychotria brachiata* pre-warming winter season, **(B)** *Piper glabrescens* pre-warming winter season, **(C)** *P. brachiata* pre-warming summer season, **(D)** *P. glabrescens* pre-warming summer season, **(E)** *P. brachiata* 4 months post-warming winter season, **(F)** *P. glabrescens* 4 months post-warming winter season, **(G)** *P. brachiata* 8 months post-warming summer season, **(H)** *P. glabrescens* 8 months post-warming summer season. Control plot (dark blue open circles) points and heated plot (orange; closed) points are means ± se at each leaf temperature. Exponential fit lines were fit to control (dark blue; dashed) and heated (orange; solid) plots separately. Gray boxes represent the range of the average minimum and maximum daily vegetation temperature for the control plots. Average minimum and maximum temperatures are calculated for each measurement campaign separately.

RESULTS

Environmental Variables

On average, the summer sampling campaigns were both hotter and rainier than the winter campaigns. Average daily precipitation was 3–6 times higher, and average daily below-canopy air temperature (T_{air}) was ∼3.5°C warmer in summer than winter (**Supplementary Table S1** and **Figure 2A**). Daily average minimum T_{air} showed slightly less variability between seasons (∼1–4°C), while maximum T_{air} showed a greater difference between summer and winter (∼3–7°C; **Supplementary Table S1**). Similarly, control plot mean daily vegetation temperature ($T_{vegMEAN}$) ranged from 23.5 to 25.3°C during summer and 20.7 to 21.9°C during winter campaigns (**Figure 2B**).

The infrared warming treatment resulted in hotter vegetation and drier soils compared to the control plots during both seasons. Daily mean, maximum, and minimum vegetation temperature gain scores (i.e., the difference between post- and pre- warming) showed a treatment effect (**Supplementary Table S3**), where heated leaf T_{vegMAX} was ∼4°C greater, heated leaf $T_{vegMEAN}$ was ∼ 3°C greater, and heated leaf T_{vegMIN} was ∼2°C greater compared to the control plots for both seasons (**Supplementary Figures S2A–C**). We did find a "seasonal" effect for $T_{vegMEAN}$, T_{vegMIN}, and VWC_{10} (**Supplementary Figures S2B–D**), however, this does not indicate environmental parameter differences between summer and winter. Gain scores measure the change from pre- to post-warming; therefore, a "seasonal" effect indicates that there is more inter-annual variation during one of the seasons compared to the other. Additionally, soil volumetric water content at 0–10 cm (VWC_{10}) gain score was ∼34% lower in the heated plots than the control (**Supplementary Table S3** and **Supplementary Figure S2D**), showing that the warming treatment did significantly alter the heated plants' growth environment through both higher vegetation temperatures and lower soil moisture (**Figures 2B,C**) and this treatment effect was consistent across seasons. Environmental gain scores were only calculated during our campaigns; therefore, differences outside of this timeframe could have had higher or lower gain score results.

Vapor pressure deficit (VPD) was not measured in the heated and control plots prior to warming, so we could not calculate gain scores for this variable. From data that coincided with our final measurement campaign only (late summer 2017), heated plots showed a mean daytime VPD of 0.36 ± 0.03 kPa, which was higher than the control plots (control VPD = 0.19 ± 0.03 kPa, $p = 0.002$, **Supplementary Figure S3**).

Treatment Effects on Net Photosynthesis and Foliar Respiration

While *Piper glabrescens* did not show treatment effects for any photosynthetic parameters, *Psychotria brachiata* did shift to a broader photosynthetic thermal niche under the warming treatment. Gain score analysis showed the optimum temperatures of photosynthesis (T_{opt}) and the rates of both photosynthesis and stomatal conductance at that optimum temperature (A_{opt} and g_{s_opt}) were not statistically different between warmed and control plots for either species (**Supplementary Table S4** and **Supplementary Figures S4A–D,G,H**). However, the photosynthetic thermal niche (**Ω**) gain score of *P. brachiata* was ∼6°C wider in the heated plots compared to the control plots (**Supplementary Table S4** and **Supplementary Figure S4E**), while *P. glabrescens* **Ω** did not differ between treatments (**Supplementary Figure S4F**).

For both species, photosynthetic optimum temperatures exceeded maximum daily vegetation temperatures in both heated and control plots during all measurement campaigns. T_{opt} values ranged from 30 to 32°C in control plots and 32 to 34°C in heated plots for both species (**Supplementary Table S5**). Control plot T_{opt} was ∼7°C higher than maximum vegetation temperature for *P. brachiata* and ∼6–9°C higher for *P. glabrescens,* with greater differences during the winter (**Supplementary Table S5** and **Figure 3**).

We found no evidence of a warming treatment effect on foliar respiration temperature response or the ratio between respiration and photosynthesis at 25°C (*R:A*) for either species. Neither *P. brachiata* nor *P. glabrescens* showed significant treatment, season, or interaction effects on the gain scores of Q_{10}, R_{25}, *or R:A* (**Supplementary Table S4** and **Supplementary Figures S5A–F**).

Treatment Effects on Component Processes of Net Photosynthesis and Stomata

We investigated underlying mechanisms of photosynthetic thermal acclimation by exploring the shifts in temperature responses of component processes of net photosynthesis, including the maximum rates of Rubisco carboxylation (V_{cmax}) and the maximum rates of electron transport (J_{max}) (**Supplementary Table S6**). Consistent with our analyses of net photosynthesis, we detected no warming treatment effects for the temperature responses of J_{max} or V_{cmax}. Neither the optimum temperature of V_{cmax} (T_{optV}; Student's *t*-test $p = 0.304$), rate of V_{cmax} at T_{optV} (V_{opt}; $p = 0.824$), the rate of V_{cmax} at 25°C ($p = 0.503$), the optimum temperature of J_{max} (T_{optJ}; $p = 0.546$), the rate of J_{max} at T_{optJ} (J_{opt}; $p = 0.747$), nor the rate of J_{max} at 25°C ($p = 0.468$) gain scores differed between treatments (**Supplementary Figure S6**).

Psychotria brachiata leaves had slightly smaller stomata in the heated (−23.80 ± 26.75 μm^2) compared to the control (67.28 ± 31.70 μm^2) plot gain scores after 8 months of warming ($p = 0.095$). There was no alteration in stomatal density ($p = 0.443$), where control density was −0.57 ± 42.24 m m^{-2} and heated density was 54.29 ± 49.50 m m^{-2}.

Acclimation Effect Size for All Variables

Effect size calculations were used to show acclimation responses of gas exchange and stomatal trait gain scores in a standardized meta-analytic framework. Photosynthetic acclimation indicates an up-regulation of photosynthesis with experimental warming; therefore, photosynthetic parameter (T_{opt}, A_{opt}, **Ω**, g_{s_Opt}, T_{optV}, T_{optJ}, V_{opt}, J_{opt}) effect size greater than zero indicates acclimation. With an effect size of 1.36 ± 0.41 (effect size ± variance), *P. brachiata* thermal niche (**Ω**) was the only photosynthetic

parameter that was not close to overlapping zero (**Figure 5**). Evidence of respiratory acclimation would result in Q_{10} and R_{25}, and *R:A* parameter effect sizes lower than zero (i.e., down-regulation). Agreeing with the gain score analyses, neither species showed high magnitude respiratory effect sizes (**Figure 5**). Adjustment of stomatal traits can result in either increasing or decreasing stomatal size and/or density (e.g., Shen et al., 2017), however, the only stomatal trait showing acclimation was *P. brachiata* stomatal size. With an effect size of -1.43 ± 0.84, *P. brachiata* adjusted to have slightly smaller stomata under experimental warming (**Figure 5**).

Gas Exchange Parameter Responses to Environmental Variables

While categorical gain score analysis of treatment and season only revealed photosynthetic thermal niche treatment effects, we did find significant responses to continuous environmental variables across plots. Overall, photosynthetic optimum temperatures and thermal niches increased for *P. brachiata* as vegetation became warmer, but *P. glabrescens* photosynthesis and stomatal conductance declined as temperatures rose. *P. brachiata* T_{opt} increased significantly with daily mean and maximum vegetation temperatures (**Supplementary Table S7**, **Figure 6A** and **Supplementary Figure S7A**). *P. glabrescens* T_{opt} showed no response with $T_{vegMEAN}$ or T_{vegMAX} (**Supplementary Table S7**, **Figure 6B**, and **Supplementary Figure S7B**). *P. brachiata* A_{opt} did not respond to surface vegetation temperature (T_{veg}; **Figure 6C** and **Supplementary Figure S7C**); although, A_{opt} intercept was higher during winter for $T_{vegMEAN}$ analysis but higher during summer for the T_{vegMAX} analysis (**Supplementary Table S7**). *P. glabrescens* A_{opt} declined as $T_{vegMEAN}$, but not T_{vegMAX}, increased (**Figure 6D** and **Supplementary Figure S7D**) and was higher during the summer (**Supplementary Table S7**). Thermal niche (**Ω**) broadened for *P. brachiata* as T_{veg} rose (**Figure 6E** and **Supplementary Figure S7E**), but *P. glabrescens* **Ω** did not respond to T_{veg} (**Figure 6F** and **Supplementary Figure S7F**). *P. brachiata* showed no relationship between g_{s_Opt} and T_{veg} (**Figure 6G** and **Supplementary Figure S7G**). *P. brachiata* g_{s_Opt} followed similar trends to A_{opt}, where g_{s_Opt} decreased as $T_{vegMEAN}$ increased (**Figure 6H**), however, the relationship was not significant for T_{vegMAX} (**Supplementary Table S7** and **Supplementary Figure S7H**).

Temperature sensitivity of respiration did not respond to vegetation temperatures for either species, while respiratory rates at a standard temperature showed evidence of down regulation only for *P. brachiata.* Neither *P. brachiata* nor *P. glabrescens* Q_{10} responded to temperature (**Figures 7A,B** and **Supplementary Figures S8A,B**). *P. brachiata* R_{25} decreased with increasing $T_{vegMEAN}$ during the winter months only (**Supplementary Table S7** and **Figure 7C**) and had no response to T_{vegMIN} (**Supplementary Figure S8C**). *P. glabrescens* R_{25} did not respond to $T_{vegMEAN}$ (**Figure 7D**) or T_{vegMIN} (**Supplementary Figure S8D**).

As soils dried, both species' optimum temperatures increased, and *P. brachiata* photosynthesis declined. *P. brachiata* and *P. glabrescens* T_{opt} rose as deeper (20–30 cm; VWC_{20}) but

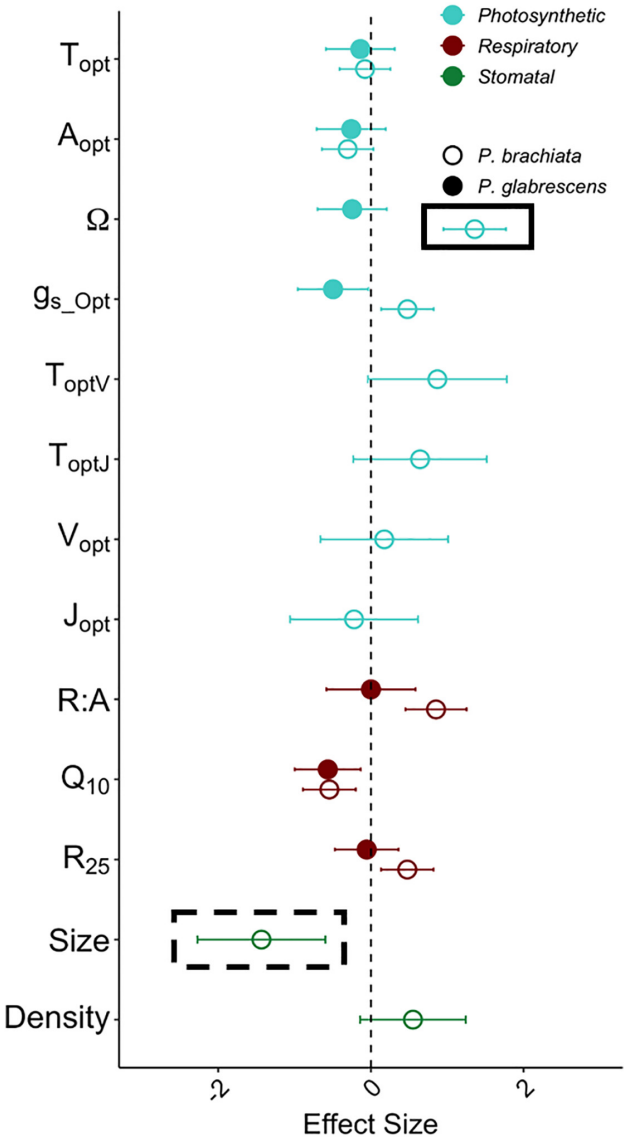

FIGURE 5 | Acclimation effect size with warming for the photosynthesis, respiration, and stomatal size and density variables. Variables represented are the optimum temperature of photosynthesis (T_{opt}) (°C), the photosynthetic rate at T_{opt} (A_{opt}) (μmol m^{-2} s^{-1}), the width of the photosynthetic – temperature response curve (**Ω**) (°C), the rate of stomatal conductance at T_{opt} (g_{s_Opt}) (mol m^{-2} s^{-1}), optimum temperature of the maximum rate of Rubisco carboxylation (T_{optV}) (°C), optimum temperature of the maximum photosynthetic electron transport (T_{optJ}) (°C), rate of the maximum rate of Rubisco carboxylation at the optimum temperature (V_{opt}) (μmol m^{-2} s^{-1}), rate of maximum photosynthetic electron transport at the optimum temperature (J_{opt}) (μmol m^{-2} s^{-1}), respiration increase with every 10°C (Q_{10}), the rate of leaf dark respiration at 25°C (R_{25}) (μmol m^{-2} s^{-1}), the ratio between R_{25} and photosynthesis at 25°C (*R:A*), stomatal density (Density) (m m^{-2}) and stomatal size (Size) (μm^2). Colors of data points depict the variable type, where light blue represents photosynthetic variables, dark red represents dark respiration variables, and green represents stomatal size and density. Symbols depict whether the sample is *Psychotria brachiata* (open) or *Piper glabrescens* (closed). Black boxes around *P. brachiata* **Ω** and stomatal size indicate significant (solid box) or marginally significant (dashed box) acclimation as calculated through the gain score analysis. Error bars depict variance of effect size as calculated from Gurevitch et al. (1992).

not shallow (0–10 cm; VWC_{10}) soils dried (**Supplementary Table S7**, **Figures 8A,B**, and **Supplementary Figures S9A,B**). *P. brachiata* A_{opt} declined as shallow soils dried during the summer but not during the winter (**Supplementary Figure S9C**) and declined with decreasing VWC_{20} (**Figure 8C**). *P. glabrescens* A_{opt} did not respond to VWC_{10} (**Supplementary Figure S9C**). As shown by the significant interaction (**Supplementary Table S7**), *P. glabrescens* A_{opt} declined as deep soils dried during the summer, however, A_{opt} was overall lower and did not respond to soil moisture during the winter (**Figure 8C**). **Ω** and g_{s_Opt} did not respond to soil moisture for either species (**Supplementary Table S7**, **Figures 7E–H**, and **Supplementary Figures S9E–H**).

Both species showed down-regulation of respiratory basal rates with drying soils. Neither species Q_{10} responded to soil moisture (**Supplementary Table S7**, **Figures 9A,B**, and **Supplementary Figures S10A,B**). *P. brachiata* R_{25} did not respond to VWC_{10} but R_{25} declined as the 20 cm soils dried (**Figure 9C** and **Supplementary Figure S10C**). *P. glabrescens* R_{25} decreased with decreasing VWC_{10} and VWC_{20} (**Figure 9D** and **Supplementary Figure S10D**).

Hierarchical partitioning revealed that most variation in photosynthesis and respiratory parameters was controlled, unexpectedly, by deeper soil moisture, rather than vegetation temperature. Variance in T_{opt}, A_{opt}, and g_{s_Opt} were all strongly controlled by VWC_{20} for both species (**Supplementary Figure S11**). Variance of thermal niche (**Ω**) for *P. brachiata* was strongly driven by VWC_{20} (**Supplementary Figure S11A**), however, *P. glabrescens* **Ω** variance was better explained by vegetation temperature (**Supplementary Figure S11B**). Q_{10} variance was relatively evenly explained by vegetation temperature and soil moisture (**Supplementary Figure S11**), particularly for *P. glabrescens,* while VWC_{20} explained most of the variance in R_{25} (**Supplementary Figure S11**).

DISCUSSION

Photosynthetic and Stomatal Responses to Temperature

Our hypothesis that tropical woody shrubs would not photosynthetically acclimate after 8 months of experimental warming was supported for *P. glabrescens*, but not *P. brachiata*. While we did not detect a warming treatment effect on the optimum temperature for photosynthesis (T_{opt}) from the gain score analysis, *P. brachiata* T_{opt} up-regulated as mean daily temperature increased (**Figure 6A**). *P. glabrescens* T_{opt} showed no acclimation to either experimental warming or daily temperature variations. Other studies have found that tropical species have some ability to photosynthetically acclimate to warmer temperatures (Cheesman and Winter, 2013; Slot and Winter, 2017; but see Fauset et al., 2019) or stimulate photosynthesis (Krause et al., 2013), however, acclimation was limited and had, until now, only been found in greenhouses or growth chambers. This emphasizes the importance of whole-plant *in situ* studies, such as this one, which may provide a more comprehensive representation of how plants will respond to climate warming.

Fewer warming studies investigate thermal niche acclimation, however, Slot and Winter (2017) found that thermal niche narrowed in experimentally warmed tropical seedlings where these plants shifted to maintain carbon gain under a wider temperature range. *P. brachiata* revealed a broadened photosynthetic thermal niche (**Ω**) following extended experimental warming (**Figure 5** and **Supplementary Figure S4**) and in response to warmer daily temperatures (**Figure 6E**). Acclimation to both the experimental treatment and daily temperature variation suggests that this species' thermal niche has a particularly plastic response to warming. Similar to T_{opt} results, *P. glabrescens* showed no thermal niche acclimation potential. *P. brachiata* thermal niche acclimation occurred alongside slightly declined stomatal size with prolonged warming (**Figure 5**). Warming can either increase (Hill et al., 2014; Becker et al., 2017; Jumrani et al., 2017; Shen et al., 2017) or decrease (Rodrigues et al., 2016; Shen et al., 2017) stomatal density or size. For example, Wu et al. (2018) found that subtropical tree species with smaller stomata are better able to maintain rates of stomatal conductance and photosynthesis under high temperature-induced water deficits. Within our study, smaller size potentially allowed *P. brachiata* stomata to lose less water as the apertures remain open under wider temperature ranges (i.e., broadened thermal niche). Due to sampling restriction, we were unable to assess alterations in stomatal size for *P. glabrescens*; therefore, we cannot speculate if a lack of stomatal plasticity limited acclimation for this species. The co-occurring acclimation toward a wider thermal niche and slightly smaller stomata may give *P. brachiata* a slight advantage under climate warming, however, with mean values above 17°C, both of these understory species already had relatively wide photosynthetic thermal niches (**Supplementary Table S5** and **Figure 3**).

Conversely, our hypothesis was supported for *P. glabrescens,* as this species showed no positive shift in photosynthetic temperature response with experimental warming (**Figure 5** and **Supplementary Figure S4**). Instead of acclimating, *P. glabrescens* experienced slightly declined photosynthesis with warmer daily temperatures (**Figure 6D**). The negative correlation between A_{opt} and vegetation temperature in *P. glabrescens* corresponded with a decline in stomatal conductance (g_s) at T_{opt} (**Figure 6H**). Many model simulations of tropical forests have predicted that temperature will negatively affect carbon gain through lowered g_s (Doughty and Goulden, 2008; Lloyd and Farquhar, 2008; Galbraith et al., 2010), rather than more direct effects to photosynthetic machinery. For our species, *P. glabrescens* experienced declines in g_s as vegetation warmed (**Figure 6H**), while *P. brachiata* did not (**Figure 6G**). *P. brachiata* leaves shifted toward lower stomatal size in the heated leaves (**Figure 5**), suggesting that *P. brachiata* may be able to more readily maintain plant water status. While we did not measure plot-level VPD during most of the physiological measurement campaigns, VPD was higher in the heated plots during late summer 2017 (**Supplementary Figure S3**). Higher temperatures increase VPD, further increasing transpirational drive, and the shift to smaller stomata may have allowed *P. brachiata* to lose less water during warmer days. Smaller size allows stomata to close more quickly (Aasamaa et al., 2001), allowing plants to have more

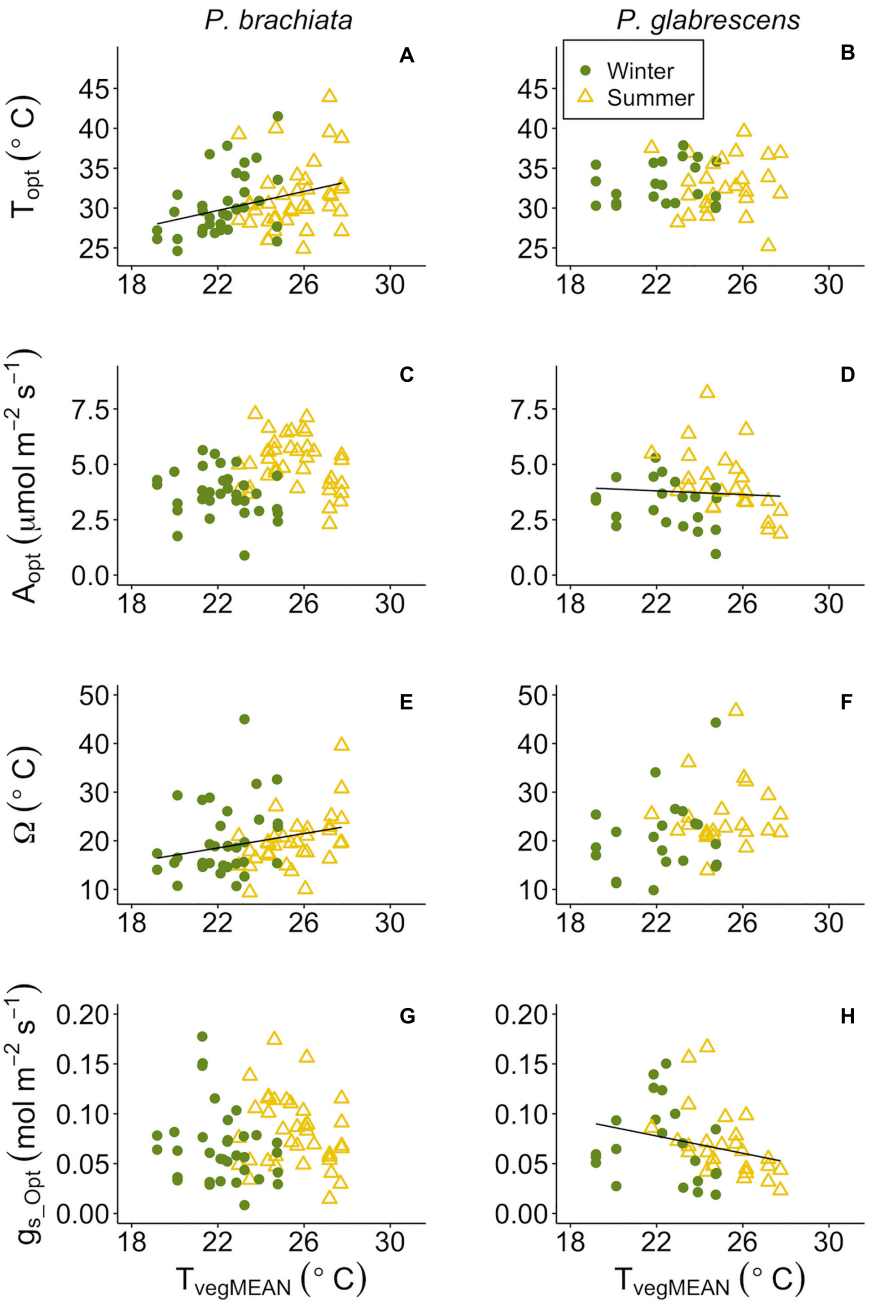

FIGURE 6 | Photosynthetic parameter responses to mean daily vegetation temperature ($T_{vegMEAN}$). **(A)** *Psychotria brachiata* optimum temperature of photosynthesis (T_{opt}) response to $T_{vegMEAN}$ of winter (green circles) and summer (yellow triangles), **(B)** *Piper glabrescens* T_{opt} response to $T_{vegMEAN}$, **(C)** *P. brachiata* rate of photosynthesis at T_{opt} (A_{opt}) response to $T_{vegMEAN}$, **(D)** *P. glabrescens* A_{opt} response to $T_{vegMEAN}$, **(E)** *P. brachiata* photosynthetic thermal niche (Ω) response to $T_{vegMEAN}$, **(F)** *P. glabrescens* Ω response to $T_{vegMEAN}$, **(G)** *P. brachiata* rate of stomatal conductance at T_{opt} (g_{s_Opt}) response to $T_{vegMEAN}$, and **(H)** *P. glabrescens* rate of stomatal conductance at T_{opt} (g_{s_Opt}) response to $T_{vegMEAN}$. Fit lines (green - winter; yellow – summer) indicate a significant interaction between $T_{vegMEAN}$ and season (**Supplementary Table S7**). A solid black line is fit when there is a significant $T_{vegMEAN}$ response but no interaction (**Supplementary Table S7**).

dynamic responses to environmental conditions (Hetherington and Woodward, 2003). This, in conjunction with overall lower water loss from smaller stomata, could further contribute to maintained photosynthesis with higher daily temperatures. Although we did find that *P. glabrescens* A_{opt} declined with increasing temperature, *P. glabrescens* A_{opt} was up-regulated during the warmer, wetter summer months, suggesting that this species does show some seasonal plasticity.

While we found indications of *P. brachiata* A_{net} acclimation potential, we did not detect evidence of thermal acclimation

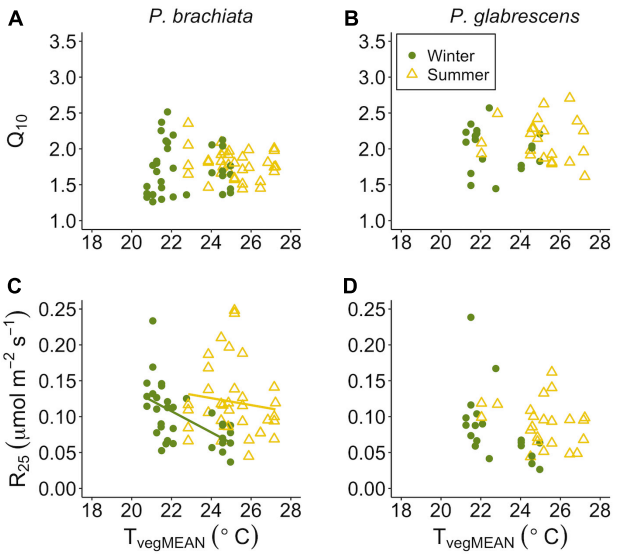

FIGURE 7 | Respiration parameter responses to mean daily vegetation temperature ($T_{vegMEAN}$). **(A)** *Psychotria brachiata* increase in respiration for every 10°C (Q_{10}) response to $T_{vegMEAN}$ of winter (green circles) and summer (yellow triangles), **(B)** *Piper glabrescens* Q_{10} response to $T_{vegMEAN}$ **(C)** *P. brachiata* rate of respiration at 25°C (R_{25}) response to $T_{vegMEAN}$, and **(D)** *P. glabrescens* R_{25} response to $T_{vegMEAN}$. Fit lines (green - winter; yellow – summer) indicate a significant interaction between $T_{vegMEAN}$ and season (**Supplementary Table S7**). A solid black line is fit when there is a significant $T_{vegMEAN}$ response but no interaction (**Supplementary Table S7**).

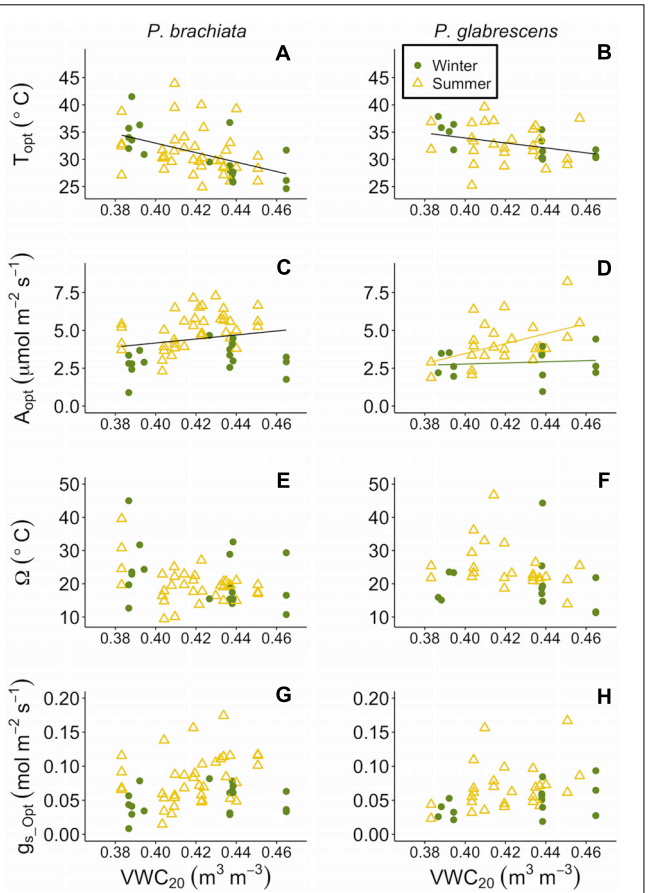

FIGURE 8 | Photosynthetic parameter responses to soil moisture at 20–30 cm depth (VWC_{20}). **(A)** *Psychotria brachiata* optimum temperature of photosynthesis (T_{opt}) response to VWC_{20} of winter (green circles) and summer (yellow triangles), **(B)** *Piper glabrescens* T_{opt} response to VWC_{20}, **(C)** *P. brachiata* rate of photosynthesis at T_{opt} (A_{opt}) response to VWC_{20}, **(D)** *P. glabrescens* A_{opt} response to VWC_{20}, **(E)** *P. brachiata* photosynthetic thermal niche (Ω) response to VWC_{20}, **(F)** *P. glabrescens* Ω response to VWC_{20}, **(G)** *P. brachiata* rate of stomatal conductance at T_{opt} (g_{s_Opt}) response to VWC_{20}, and **(H)** *P. glabrescens* rate of stomatal conductance at T_{opt} (g_{s_Opt}) response to VWC_{20}. Fit lines (green - winter; yellow – summer) indicate a significant interaction between VWC_{20} and season (**Supplementary Table S7**). A solid black line is fit when there is a significant VWC_{20} response but no interaction (**Supplementary Table S7**).

of the biochemical components of net photosynthesis (J_{max} and V_{cmax}). While both J_{max} and V_{cmax} have been found to acclimate within days (Smith and Dukes, 2017), it is possible that longer-term warming would be required to detect a shift of these processes within our study system or, perhaps, acclimation more readily occurs in the controlled environment of a growth chamber than for *in situ* studies (Gunderson et al., 2000). In addition, for both the photosynthetic and respiratory acclimation results, some of the study leaves were already fully developed prior to warming initiation. Leaf age, however, was not tracked, leading to uncertainty in whether leaves developed under the treatment (with the exception of the stomatal size and density measurements). Leaves that developed prior to initiation of warmer temperatures are less likely to acclimate (Loveys et al., 2003); therefore acclimation potential could have been limited for the fully developed leaves.

Our study site is in an area with frequent hurricanes, which can rapidly increase the light and temperature environment experienced by understory species. The higher plasticity in response to elevated temperature of *P. brachiata* may allow this species to respond more quickly to new environments (**Figures 6A,E**, **7C**). Early successional species such as *P. brachiata* are often associated with higher plasticity (Valladares et al., 2000, 2002). There is some evidence that thermal acclimation is more likely to occur in faster growing, early successional species (e.g., Slot and Winter, 2018), however, this is not consistent across all species (reviewed in Atkin et al., 2006). More shade tolerant species, such as *P. glabrescens*, are generally adapted to thrive in relatively stable environmental conditions (Valladares et al., 2002; Niinemets and Valladares, 2004), which is supported by *P. glabrescens*' wide thermal niches (**Supplementary Table S5** and **Figure 3**). As a result, these two species may respond differently to the greater hurricane intensity and frequency predicted to occur with climate change (Knutson et al., 2015; Bacmeister et al., 2018). While higher *P. brachiata* plasticity may allow quicker responses to both warming and disturbance, the wider thermal niches found in *P. glabrescens* could also potentially mitigate negative effects of climate warming.

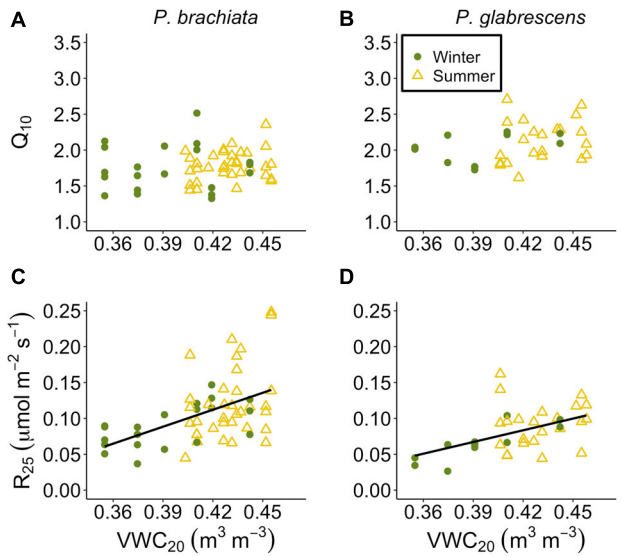

FIGURE 9 | Respiration parameter responses to soil moisture at 20–30 cm depth (VWC_{20}). **(A)** *Psychotria brachiata* increase in respiration for every 10°C (Q_{10}) response to VWC_{20} of winter (green circles) and summer (yellow triangles), **(B)** *Piper glabrescens* Q_{10} response to VWC_{20} **(C)** *P. brachiata* rate of respiration at 25°C (R_{25}) response to VWC_{20}, and **(D)** *P. glabrescens* R_{25} response to VWC_{20}. Fit lines (green - winter; yellow – summer) indicate a significant interaction between VWC_{20} and season (**Supplementary Table S7**). A solid black line is fit when there is a significant VWC_{20} response but no interaction (**Supplementary Table S7**).

Respiratory Responses to Temperature

There is currently a general consensus that, unlike photosynthesis, tropical plants will be able to acclimate their rates of respiration (Slot and Kitajima, 2015). Contrary to this expectation, we found little to no respiratory thermal acclimation in either species. *P. brachiata* showed no acclimation response to experimental warming, however, there was slight evidence for acclimation to daily environmental variables. *P. brachiata* showed physiological plasticity by down-regulating the basal rate of respiration (R_{25}) as vegetation warmed, but that trend only occurred during the cooler, drier winter months (**Figure 7C**). *P. brachiata* R_{25} decreased as soils dried (**Figure 9C**); therefore, R_{25} might have been more sensitive to warming temperatures, and the corresponding drier soils, during the drier winter season. *P. glabrescens*' respiration did not acclimate to daily changes in temperature or experimental warming (**Figure 5** and **Supplementary Figures S5, S7B,D**). While there are few studies to corroborate respiratory acclimation through *in situ* tropical warming studies, Slot et al. (2014) found that canopy leaves exposed to only one week of nighttime warming were able to acclimate through a down-regulation of basal respiration rate (R_{25}). Studies on juvenile tropical species have found evidence of both decreased slope (Cheesman and Winter, 2013; Krause et al., 2013) or both decreased basal rate and slope (Cheesman and Winter, 2013; Drake et al., 2015) of respiratory acclimation. Meta-analyses suggest that plants across all biomes will acclimate their rates of respiration in response to warmer temperatures (Way and Oren, 2010; Slot and Kitajima, 2015) and, our study adds an important set of results suggesting that respiratory acclimation might not be universal across tropical species.

There were no treatment differences in the ratio of respiration to photosynthesis (*R:A*; **Figure 5** and **Supplementary Figure S5E,F**). Because these species were operating well below their optimum temperatures for photosynthesis (**Supplementary Table S5**), +4°C of current conditions would likely not negatively affect leaf carbon balance for these two species. It is possible, however, that maximum vegetation temperatures inside the plots were underestimated (**Supplementary Table S5**). The infrared thermometer reads temperature over multiple surfaces; therefore, measured temperature was likely lower than the actual temperature experienced for some individual leaves if the thermometer was measuring multiple leaves experiencing different temperatures. Photosynthesis and respiration were measured on different days; therefore, we were unable to investigate variability in *R:A* with daily fluctuations of temperature and soil moisture.

Soil Moisture: A Stronger Driver Than Temperature

Our study aimed to investigate how plants specifically respond to elevated temperature, however, along with heating plant tissues, our warming treatment caused soil drying (**Supplementary Figure S2D**). Changing precipitation patterns and soil drying are predicted to have large effects on ecosystem carbon balance (Ciais et al., 2005; Phillips et al., 2009; Kao and Ganguly, 2011; Sherwood and Fu, 2014). Periodic drought and lowered soil moisture cause declines in tropical forest productivity (Santos et al., 2018; van Schaik et al., 2018). Importantly, hierarchical partitioning revealed that deeper soil moisture, even more so than vegetation temperature or shallow soil moisture, was the most influential climate variable determining variation in many gas exchange parameters (**Supplementary Figure S11**). Deeper, rather than shallow, soil moisture may have been a stronger driver because it was less variable in general (**Figure 2D**; Kimball et al., 2018) likely because of less surface evaporation and fewer roots present to rapidly draw water from that soil depth (Yaffar and Norby, 2020). T_{opt} increased as soil moisture decreased (**Figures 8A,B**), suggesting that neither species' T_{opt} will likely be negatively affected by a drying climate. T_{opt} increasing with drying soil in both of our species is somewhat surprising and the increase may not be a direct effect of soil drying. If increases in vegetation temperature (T_{veg}) coincided with soil drying, the negative relationship between T_{opt} and soil moisture could be due to the indirect influence of *higher* T_{veg}, however, T_{opt} only increased with T_{veg} for *P. brachiata*. We may lack the data to fully explain T_{opt} responses to soil moisture.

While drier soils may not negatively affect T_{opt}, we did observed decreased A_{opt} for *P. brachiata* as soils dried (**Figure 8C**). This negative association between photosynthesis and drier soil also occurred for *P. glabrescens* during the summer (**Figure 8D**), suggesting that drying soil has the potential to negatively affect both species' carbon uptake. Similarly, a long-term study found that photosynthesis declined as soil moisture decreased in 11 boreal and temperate species, likely due to

stomatal conductance restrictions (Reich et al., 2018). R_{25} also decreased as soil moisture decreased (**Figures 9C,D**), perhaps following the trend of A_{opt}, where decreased substrate may have limited the rate of respiration in drier soils. Soil drying often occurs with ecosystem-level warming experiments, and is also expected to occur with climate warming (e.g., Jarvi and Burton, 2013; Rich et al., 2015). Accordingly, the role soil moisture played in our study and the likelihood that, in the absence of precipitation changes, higher temperatures will result in reduced soil moisture, reinforces the importance of investigating how both temperature and moisture affect plant responses to climate change.

Assessing Physiological Responses by Treatment Versus Actual Environmental Conditions

We assessed thermal acclimation of physiological responses in two ways: (1) by assessing treatment effects using a binary comparison of control vs. warmed plots, and (2) by exploring responses to actual environmental conditions experienced by the plants in the day prior to each measurement. Although the experiment was initially designed to assess thermal acclimation through treatment effects, we detected stronger responses when looking at the responses to values of environmental variables across all treatments and time points. Several factors may have contributed to the disparity between the two assessments. First, *in situ* studies contend with many sources of variation across space and time. Gunderson et al. (2010) found a higher capacity for acclimation in seedlings grown in a growth chamber than saplings grown in the field. The authors suggest factors such as uncontrolled VPD and lower soil moisture could have limited acclimation capacity *in situ*.

The differences between plots prior to initiation of the warming treatment necessitated the gain score analysis comparing pre- and post- warming responses. This approach required all leaf-level measurements to be pooled at the plot level, thus dramatically reducing our statistical power compared to the regression-style analyses, which included plant-level data. We found no differences in temperature, soil moisture, or available nutrients between treatments that could easily explain pre-warming physiological variation between heated and control plots (Kimball et al., 2018; Reed et al., 2020). In January 2016, prior to initiation of the warming treatment, there were no differences in foliar nitrogen per unit leaf area for either *P. brachiata* (Student's *t* test, $p = 0.122$) nor *P. glabrescens* ($p = 0.520$). Our experience here highlights not only the value of pre-treatment measurements, but also the importance of high-resolution measurements of actual environmental conditions when designing large-scale *in situ* experiments.

CONCLUSION AND IMPLICATIONS

We assessed physiological acclimation potential of two Puerto Rican understory shrub species +4°C in an *in situ* field-scale warming experiment in a tropical forest and, overall, found different acclimation potential between species. Only one of our two study species, *P. brachiata*, acclimated to warmer temperatures through a wider photosynthetic thermal niche and higher photosynthetic optimum temperatures. In contrast, our other study species, *P. glabrescens,* showed no evidence photosynthetic acclimation, and in fact showed declines in both photosynthesis and stomatal conductance with warmer temperatures Surprisingly, we found little evidence for leaf respiratory acclimation, *P. brachiata* R_{25} decreased with increasing vegetation temperature during the drier winter season, but *P. glabrescens* showed no acclimation to experimental warming or daily temperature variations. These data provide important insight into how tropical understory plants respond to warming, as there are limited examples and, to our knowledge, no other large-scale *in situ* assessments of tropical forest understory plant physiological acclimation.

Expanding *in situ* experimental warming studies to include more species across different tropical forest types is essential, as a lack of acclimation could indicate altered tropical forest carbon uptake as global temperatures rise. Of our two study species, *P. brachiata* may be more resilient to climate warming due to higher plasticity in traits that conserve water and promote carbon gain. *P. glabrescens* experienced lower rates of photosynthesis at higher daily vegetation temperatures, perhaps due to reduced stomatal conductance. If a trend of higher physiological plasticity in early successional species and reduced photosynthesis with higher shade tolerance is conserved across more tropical understory species, we could see shifts in understory composition with climate warming. Soil moisture played an important role in determining the variation of many gas exchange variables and thus should be carefully considered *in situ* warming studies.

This study was conducted on understory species, yet upper canopy foliage may respond similarly to temperature as shaded layers (Slot et al., 2019) and, due to high heat stress, leaves in the canopy are *already* operating at or above thermal thresholds for photosynthesis (Doughty and Goulden, 2008; Mau et al., 2018). Thus, canopy foliage may not have the plasticity to up-regulate physiology to the same degree as understory plants. If so, the understory could become an even more dominant component of tropical forests' carbon cycle. In conclusion, our study addresses a critical gap in our understanding of how tropical plants may respond to warming and suggests that species' plasticity may play an important role in their ability to respond to climate change.

DATA AVAILABILITY STATEMENT

The raw data supporting the conclusions of this article doi: 10.2737/RDS-2020-0055.

AUTHOR CONTRIBUTIONS

MC, TW, and SR designed the TRACE experiment and acquired financial support for the overall study. KC and MC designed the physiological study. KC collected the photosynthesis, respiration, and leaf trait data. ES collected the stomatal size and density data. KC carried out all of the statistical analysis and wrote the first draft of the manuscript. MC provided additional advice and contributed to revisions of the text. All authors provided input and revisions to the final draft.

FUNDING

This research was funded by U.S. Department of Energy award numbers DE-SC-0012000, DE-SC-0011806, 89243018S-SC-000014, and DE-SC-0018942 awarded to MC, TW, and SR. This research was also funded by the National Science Foundation award DEB-1754713. SR was also supported by the U.S. Geological Survey Ecosystem Mission Area. The USDA Forest Service's International Institute of Tropical Forestry (IITF) and University of Puerto Rico-Río Piedras provided additional support. All research at IITF is done in collaboration with the University of Puerto Rico. ES was also funded by Michigan Technological University Ecosystem Science Center and a Summer Undergraduate Research Fellowship. KC was also funded by Michigan Technological Finishing Fellowship and Michigan Tech Ecosystem Science Center.

ACKNOWLEDGMENTS

We are very grateful to TRACE project managers Aura M. Alonso-Rodríguez and Megan Berberich for their logistical support. We are also grateful to Kaylie Butts, Benjamin Miller, Talia Anderson, Jamarys Torres, GraceAnna Schilz, Jack Zwart, and Brian Peacock for their excellent field and lab assistance. Reviewers gave critical feedback on an earlier manuscript version that we believe greatly enhanced the quality. We also thank Robert Froese, Andrew Burton, and Sarah Green for thoughtful discussions. A previous version of this manuscript was included in a Ph.D. dissertation (Carter, 2019). Any use of trade, firm, or product names is for descriptive purposes only and does not imply endorsement by the United States Government.

SUPPLEMENTARY MATERIAL

The Supplementary Material for this article can be found online at: https://www.frontiersin.org/articles/10.3389/ffgc.2020.576320/full#supplementary-material

Supplementary Figure 1 | A-C_i curves at different temperatures.

Supplementary Figure 2 | Gain score analysis of heated and control plot vegetation temperature and soil moisture.

Supplementary Figure 3 | VPD of heated and control plots during summer 2017.

Supplementary Figure 4 | Photosynthetic parameter gain scores between pre-warming and post-warming measurements.

Supplementary Figure 5 | Dark respiration parameter gain scores between pre-warming and post-warming measurements.

Supplementary Figure 6 | Biochemical parameter responses to leaf temperature.

Supplementary Figure 7 | Photosynthetic parameter responses to maximum daily vegetation temperature.

Supplementary Figure 8 | Respiratory parameter responses to minimum daily vegetation temperature.

Supplementary Figure 9 | Photosynthetic parameter responses to soil moisture at 0–10 cm depth.

Supplementary Figure 10 | Respiratory parameter responses to soil moisture at 0–10 cm depth.

Supplementary Figure 11 | Hierarchical partitioning results of gas exchange parameter variances explained by environmental variables.

Supplementary Table 1 | Mean daily vegetation temperature of the control plots, mean, minimum, and maximum daily air temperature and rainfall during each measurement campaign.

Supplementary Table 2 | Count of total individual trees and leaves measured for each campaign, species, treatment, and gas exchange measurement.

Supplementary Table 3 | P-values and degrees of freedom from ANOVA results of gain score of vegetation temperature and soil moisture.

Supplementary Table 4 | P-values and degrees of freedom from ANOVA results of gain score of leaf gas exchange variables.

Supplementary Table 5 | Mean daily maximum vegetation temperature and physiological parameter means of the heated and control plots for each species.

Supplementary Table 6 | Temperature response parameters estimated for the maximum rate of Rubisco carboxylation (V_{cmax}) and the maximum rate of electron transport (J_{max}).

Supplementary Table 7 | Summary of mixed effects model results of gas exchange parameter responses to environmental variables.

REFERENCES

Aasamaa, K., Sõber, A., and Rahi, M. (2001). Leaf anatomical characteristics associated with shoot hydraulic conductance, stomatal conductance and stomatal sensitivity to change in leaf water status in temperate deciduous trees. *Aust. J. Plant Physiol.* 28, 765–774. doi: 10.1071/pp00157

Arneth, A., Mercado, L., Kattge, J., and Booth, B. B. B. (2012). Future challenges of representing land-processes in studies on land-atmosphere interactions. *Biogeosciences* 9, 3587–3599. doi: 10.5194/bg-9-3587-2012

Aspinwall, M. J., Drake, J. E., Campany, C., Vårhammar, A., Ghannoum, O., Tissue, D. T., et al. (2016). Convergent acclimation of leaf photosynthesis and respiration to prevailing ambient temperatures under current and warmer climates in Eucalyptus tereticornis. *New Phytol.* 212, 354–367. doi: 10.1111/nph.14035

Atkin, O. K., Bruhn, D., Hurry, V. M., and Tjoelker, M. G. (2005). The hot and the cold: unravelling the variable response of plant respiration to temperature. *Funct. Plant Biol.* 32, 87–105. doi: 10.1071/FP03176

Atkin, O. K., Loveys, B. R., Atkinson, L. J., and Pons, T. L. (2006). Phenotypic plasticity and growth temperature: understanding interspecific variability. *J. Exp. Bot.* 57, 267–281. doi: 10.1093/jxb/erj029

Atkin, O. K., and Tjoelker, M. G. (2003). Thermal acclimation and the dynamic response of plant respiration to temperature. *Trends Plant Sci.* 8, 343–351. doi: 10.1016/S1360-1385(03)00136-5

Bacmeister, J. T., Reed, K. A., Hannay, C., Lawrence, P., Bates, S., Truesdale, J. E., et al. (2018). Projected changes in tropical cyclone activity under future warming scenarios using a high-resolution climate model. *Clim. Change* 146, 547–560. doi: 10.1007/s10584-016-1750-x

Bates, D., Meachler, M., Bolker, B., and Walker, S. (2015). Fitting linear mixed-effects models using lme4. *J. Stat. Softw* 67, 1–48. doi: 10.18637/jss.v067.i01

Becker, V. I., Goessling, J. W., Duarte, B., Cacador, I., Liu, F., Rosenqvist, E., et al. (2017). Combined effects of soil salinity and high temperature on photosynthesis and growth of quinoa plants (*Chenopodium quinoa*). *Funct. Plant Biol.* 44, 665–678. doi: 10.1071/FP16370

Beer, C., Reichstein, M., Tomelleri, E., Ciais, P., Jung, M., Carvalhais, N., et al. (2010). Terrestrial gross carbon dioxide uptake: global distribution and covariation with climate. *Science* 329, 834–839. doi: 10.1126/science.1184984

Berry, J., and Bjorkman, O. (1980). Photosynthetic response and adaptation to temperature in higher plants. *Annu. Rev. Plant Physiol.* 31, 491–543. doi: 10.1146/annurev.pp.31.060180.002423

Booth, B. B. B., Jones, C. D., Collins, M., Totterdell, I. J., Cox, P. M., Sitch, S., et al. (2012). High sensitivity of future global warming to land carbon cycle processes. *Environ. Res. Lett.* 7:024002. doi: 10.1088/1748-9326/7/2/024002

Carter, K. R. (2019). *Ecophysiological Responses of Tropical Woody Species to Ambient and Elevated Temperatures*. Ph.D. Dissertation, Michigan Technological University, Houghton, MI.

Cavaleri, M. A., Oberbauer, S. F., and Ryan, M. G. (2008). Foliar and ecosystem respiration in an old-growth tropical rain forest. *Plant, Cell Environ.* 31, 473–483. doi: 10.1111/j.1365-3040.2008.01775.x

Cavaleri, M. A., Reed, S. C., Smith, W. K., and Wood, T. E. (2015). Urgent need for warming experiments in tropical forests. *Glob. Chang. Biol.* 21, 2111–2121. doi: 10.1111/gcb.12860

Cernusak, L. A., Winter, K., Dalling, J. W., Holtum, J. A. M., Jaramillo, C., Körner, C., et al. (2013). Tropical forest responses to increasing atmospheric CO2: current knowledge and opportunities for future research. *Funct. Plant Biol.* 40, 531–551. doi: 10.1071/FP12309

Cheesman, A. W., and Winter, K. (2013). Growth response and acclimation of CO2 exchange characteristics to elevated temperatures in tropical tree seedlings. *J. Exp. Bot.* 64, 3817–3828. doi: 10.1093/jxb/ert211

Chen, J. M., Mo, G., Pisek, J., Liu, J., Deng, F., Ishizawa, M., et al. (2012). Effects of foliage clumping on the estimation of global terrestrial gross primary productivity. *Glob. Biogeochem. Cycles* 26:GB1019. doi: 10.1029/2010GB003996

Ciais, P., Reichstein, M., Viovy, N., Granier, A., Ogée, J., Allard, V., et al. (2005). Europe-wide reduction in primary productivity caused by the heat and drought in 2003. *Nature* 437, 529–533. doi: 10.1038/nature03972

Cox, P. M., Betts, R. A., Jones, C. D., Spall, S. A., and Totterdell, I. J. (2000). Acceleration of global warming due to carbon-cycle feedbacks in a coupled climate model. *Nature* 408, 184–187. doi: 10.1038/35041539

Crous, K. Y., Sharwood, E., Drake, J. E., Tjoelker, M. G., Aspinwall, M. J., and Ghannoum, O. (2018). Photosynthetic capacity and leaf nitrogen decline along a controlled climate gradient in provenances of two widely distributed Eucalyptus species. *Glob. Chang. Biol.* 24, 4626–4644. doi: 10.1111/gcb.14330

Cunningham, S. C., and Read, J. (2003). Do temperate rainforest trees have a greater ability to acclimate to changing temperatures than tropical rainforest trees? *New Phytol.* 157, 55–64. doi: 10.1046/j.1469-8137.2003.00652.x

Devoe, N. N. (1989). *Differential Seedling and Regerneration in Openings and Beneath Closed Canopy in Sub-Tropical Wet Forest*. Ph.D. thesis, Yale University, New Haven, CT.

Dewar, R. C., Medlyn, B. E., and Mcmurtrie, R. E. (1999). Acclimation of the respiration/photosynthesis ratio to temperature: insights from a model. *Glob. Chang. Biol.* 5, 615–622. doi: 10.1046/j.1365-2486.1999.00253.x

Diffenbaugh, N. S., and Scherer, M. (2011). Observational and model evidence of global emergence of permanent, unprecedented heat in the 20th and 21st centuries. *Clim. Change* 107, 615–624. doi: 10.1007/s10584-011-0112-y

Doughty, C. E. (2011). An in situ leaf and branch warming experiment in the Amazon. *Biotropica* 43, 658–665. doi: 10.1111/j.1744-7429.2010.00746.x

Doughty, C. E., and Goulden, M. L. (2008). Are tropical forests near a high temperature threshold? *J. Geophys. Res. Biogeosci.* 114, 1–12. doi: 10.1029/2007JG000632

Drake, J. E., Aspinwall, M. J., Pfautsch, S., Rymer, P. D., Reich, P. B., Smith, R. A., et al. (2015). The capacity to cope with climate warming declines from temperate to tropical latitudes in two widely distributed Eucalyptus species. *Glob. Chang. Biol.* 21, 459–472. doi: 10.1111/gcb.12729

Drake, J. E., Tjoelker, M. G., Aspinwall, M. J., Reich, P. B., Barton, C. V. M., Belinda, E., et al. (2016). Does physiological acclimation to climate warming stabilize the ratio of canopy respiration to photosynthesis? *New Phytol.* 211, 850–863. doi: 10.1111/nph.13978

Duursma, R. A. (2015). Plantecophys - An R package for analysing and modelling leaf gas exchange data. *PLoS One* 10:e0143346. doi: 10.1371/journal.pone.0143346

Ellsworth, D. S., and Reich, P. B. (1993). Canopy structure and vertical patterns of photosynthesis and related leaf traits in a deciduous forest. *Oecologia* 96, 169–178. doi: 10.1007/BF00317729

Farquhar, G. D., von Caemmerer, S., and Berry, J. A. (1980). A biochemical model of photosynthesis CO2 fixation in leaves of C3 species. *Planta* 149, 78–90. doi: 10.1007/bf00386231

Fauset, S., Oliveira, L., Buckeridge, M. S., Foyer, C. H., Galbraith, D., Tiwari, R., et al. (2019). Contrasting responses of stomatal conductance and photosynthetic capacity to warming and elevated CO2 in the tropical tree species Alchornea glandulosa under heatwave conditions. *Environ. Exp. Bot.* 158, 28–39. doi: 10.1016/j.envexpbot.2018.10.030

Fox, J., and Weisberg, S. (2011). *An {R} Companion to Applied Regression*, 2nd Edn. Thousand Oaks, CA: Sage.

Galbraith, D., Levy, P. E., Sitch, S., Huntingford, C., Cox, P., Williams, M., et al. (2010). Multiple mechanisms of Amazonian forest biomass losses in three dynamic global vegetation models under climate change. *New Phytol.* 187, 647–665. doi: 10.1111/j.1469-8137.2010.03350.x

Gunderson, C. A., Norby, R. J., and Wullschleger, S. D. (2000). Acclimation of photosynthesis and respiration to simulated climatic warming in northern and southern populations of Acer saccharum: laboratory and field evidence. *Tree Physiol.* 20, 87–96. doi: 10.1093/treephys/20.2.87

Gunderson, C. A., O'Hara, K. H., Campion, C. M., Walker, A. V., and Edwards, N. T. (2010). Thermal plasticity of photosynthesis: the role of acclimation in forest responses to a warming climate. *Glob. Chang. Biol.* 16, 2272–2286. doi: 10.1111/j.1365-2486.2009.02090.x

Gurevitch, J., Morrow, L. L., Wallace, A., and Walsh, J. S. (1992). A meta-analysis of competition in field experiments. *Am. Nat.* 140, 539–572. doi: 10.2307/2462913

Harris, N., Lugo, A., Brown, S., and Heartsill Scalley, T. (2012). *Luquillo Experimental Forest: Research History and Opportunities. EFR-1*. Washington, DC: U.S. Department of Agriculture, 152.

He, L., Chen, J. M., Gonsamo, A., Luo, X., Wang, R., Liu, Y., et al. (2018). Changes in the shadow: the shifting role of shaded leaves in global carbon and water cycles under climate change. *Geophys. Res. Lett.* 45, 5052–5061. doi: 10.1029/2018GL077560

Hedges, L. V., and Olkin, I. (1985). *Statistical Methods for Meta-Analysis*. New York, NY: Academic Press.

Heskel, M. A., O'Sullivan, O. S., Reich, P. B., Tjoelker, M. G., Weerasinghe, L. K., Penillard, A., et al. (2016). Convergence in the temperature response of leaf respiration across biomes and plant functional types. *Proc. Natl. Acad. Sci. U.S.A.* 113, 3832–3837. doi: 10.1073/pnas.1520282113

Hetherington, A. M., and Woodward, F. I. (2003). The role of stomata in sensing and driving environmental change. *Nature* 424, 901–908. doi: 10.1038/nature01843

Hill, K. E., Guerin, G. R., Hill, R. S., and Watling, J. R. (2014). Temperature influences stomatal density and maximum potential water loss through stomata of *Dodonaea viscosa* subsp. *angustissima* along a latitude gradient in southern Australia. *Aust. J. Bot.* 62, 657–665. doi: 10.1071/BT14204

Hubau, W., Lewis, S. L., Phillips, O. L., Affum-Baffoe, K., Beeckman, H., Cuní-Sanchez, A., et al. (2020). Asynchronous carbon sink saturation in African and Amazonian tropical forests. *Nature* 579, 80–87. doi: 10.1038/s41586-020-2035-0

Huntingford, C., Zelazowski, P., Galbraith, D., Mercado, L. M., Sitch, S., Fisher, R., et al. (2013). Simulated resilience of tropical rainforests to CO2 -induced climate change. *Nat. Geosci.* 6, 268–273. doi: 10.1038/ngeo1741

Janzen, D. H. (1967). Why mountain passes are higher in the tropics. *Am. Nat.* 101, 233–249. doi: 10.1086/282487

Jarvi, M. P., and Burton, A. J. (2013). Acclimation and soil moisture constrain sugar maple root respiration in experimentally warmed soil. *Tree Physiol.* 33, 949–959. doi: 10.1093/treephys/tpt068

Jumrani, K., Bhatia, V. S., and Pandey, G. P. (2017). Impact of elevated temperatures on specific leaf weight, stomatal density, photosynthesis and chlorophyll fluorescence in soybean. *Photosynth. Res.* 131, 333–350. doi: 10.1007/s11120-016-0326-y

June, T., Evans, J. R., and Farquhar, G. D. (2004). A simple new equation for the reversible temperature dependence of photosynthetic electron transport: a study on soybean leaf. *Funct. Plant Biol.* 31, 275–283. doi: 10.1071/FP03250

Kao, S. C., and Ganguly, A. R. (2011). Intensity, duration, and frequency of precipitation extremes under 21st-century warming scenarios. *J. Geophys. Res. Atmos.* 116, 1–14. doi: 10.1029/2010JD015529

Kattge, J., and Knorr, W. (2007). Temperature acclimation in a biochemical model of photosynthesis: a reanalysis of data from 36 species. *Plant Cell Environ.* 30, 1176–1190. doi: 10.1111/j.1365-3040.2007.01690.x

Kimball, B. A., Alonso-Rodríguez, A. M., Cavaleri, M. A., Reed, S. C., González, G., and Wood, T. E. (2018). Infrared heater system for warming tropical forest understory plants and soils. *Ecol. Evol.* 8, 1931–1944. doi: 10.1002/ece3.3780

Kirschbaum, M. U. F., and McMillan, A. M. S. (2018). Warming and elevated CO2 have opposing influences on transpiration. Which is more important? *Curr. For. Rep.* 4, 51–71. doi: 10.1007/s40725-018-0073-8

Knutson, T. R., Sirutis, J. J., Zhao, M., Tuleya, R. E., Bender, M., Vecchi, G. A., et al. (2015). Global projections of intense tropical cyclone activity for the late twenty-first century from dynamical downscaling of CMIP5/RCP4.5 *scenarios*. *J. Clim.* 28, 7203–7224. doi: 10.1175/JCLI-D-15-0129.1

Korner, C. (2004). Through enhanced tree dynamics carbon dioxide enrichment may cause tropical forests to lose carbon. *Philos. Trans. R. Soc. B Biol. Sci.* 359, 493–498. doi: 10.1098/rstb.2003.1429

Krause, G. H., Cheesman, A. W., Winter, K., Krause, B., and Virgo, A. (2013). Thermal tolerance, net CO2 exchange and growth of a tropical tree species, *Ficus insipida*, cultivated at elevated daytime and nighttime temperatures. *J. Plant Physiol.* 170, 822–827. doi: 10.1016/j.jplph.2013.01.005

Lloyd, J., and Farquhar, G. D. (2008). Effects of rising temperatures and [CO2] on the physiology of tropical forest trees. *Philos. Trans. R. Soc. Lond. B. Biol. Sci.* 363, 1811–1817. doi: 10.1098/rstb.2007.0032

Lombardozzi, D. L., Bonan, G. B., Smith, N. G., Dukes, J. S., and Fisher, R. A. (2015). Temperature acclimation of photosynthesis and respiration: a key uncertainty in the carbon cycle-climate feedback. *Geophys. Res. Lett.* 42, 8624–8631. doi: 10.1002/2015GL065934

Loveys, B., Atkinson, L., Sherlock, D., Roberts, R., Fitter, A., and Atkin, O. (2003). Thermal acclimation of leaf and root respiration: an investigation comparing inherently fast- and slow- growing plant species. *Glob. Chang. Biol.* 9, 895–910. doi: 10.1046/j.1365-2486.2003.00611.x

Mau, A., Reed, S., Wood, T., and Cavaleri, M. (2018). Temperate and tropical forest canopies are already functioning beyond their thermal thresholds for photosynthesis. *Forests* 9:47. doi: 10.3390/f9010047

Medlyn, B. E., Dreyer, E., Ellsworth, D., Forstreuter, M., Harley, P. C., Kirschbaum, M. U. F., et al. (2002). Temperature response of parameters of a biochemically based model of photosynthesis. II. A review of experimental data. *Plant Cell Environ.* 25, 1167–1179. doi: 10.1046/j.1365-3040.2002.00891.x

Mercado, L. M., Medlyn, B. E., Huntingford, C., Oliver, R. J., Clark, D. B., Sitch, S., et al. (2018). Large sensitivity in land carbon storage due to geographical and temporal variation in the thermal response of photosynthetic capacity. *New Phytol.* 218, 1462–1477. doi: 10.1111/nph.15100

Monteith, J. L., and Unsworth, M. H. (2008). *Principles of Environmental Physics*, 3rd Edn. New York, NY: Academic Press.

Mora, C., Frazier, A. G., Longman, R. J., Dacks, R. S., Walton, M. M., Tong, E. J., et al. (2013). The projected timing of climate departure from recent variability. *Nature* 502, 183–187. doi: 10.1038/nature12540

Myster, R. W., and Walker, L. R. (1997). Plant successional pathways on Puerto Rican landslides. *J. Trop. Ecol.* 13, 165–173. doi: 10.1017/S0266467400010397

Nicotra, A. B., Atkin, O. K., Bonser, S. P., Davidson, A. M., Finnegan, E. J., Mathesius, U., et al. (2010). Plant phenotypic plasticity in a changing climate. *Trends Plant Sci.* 15, 684–692. doi: 10.1016/j.tplants.2010.09.008

Niinemets, Ü, and Valladares, F. (2004). Photosynthetic acclimation to simultaneous and interacting environmental stresses along natural light gradients: optimality and constraints. *Plant Biol.* 6, 254–268. doi: 10.1055/s-2004-817881

O'Sullivan, O. S., Heskel, M. A., Reich, P. B., Tjoelker, M. G., Weerasinghe, L. K., Penillard, A., et al. (2017). Thermal limits of leaf metabolism across biomes. *Glob. Chang. Biol.* 23, 209–223. doi: 10.1111/gcb.13477

O'Sullivan, O. S., Weerasinghe, K. W. L. K., Evans, J. R., Egerton, J. J. G., Tjoelker, M. G., and Atkin, O. K. (2013). High-resolution temperature responses of leaf respiration in snow gum (*Eucalyptus pauciflora*) reveal high-temperature limits to respiratory function. *Plant Cell Environ.* 36, 1268–1284. doi: 10.1111/pce.12057

Pan, Y., Birdsey, R. A., Phillips, O. L., and Jackson, R. B. (2013). The structure, distribution, and biomass of the world's forests. *Annu. Rev. Ecol. Evol. Syst.* 44, 593–622. doi: 10.1146/annurev-ecolsys-110512-135914

Pau, S., Detto, M., Kim, Y., and Still, C. J. (2018). Tropical forest temperature thresholds for gross primary productivity. *Ecosphere* 9, 1–12. doi: 10.1002/ecs2.2311

Pearcy, R. W., Valladares, F., Wright, S. J., and De Paulis, E. L. (2004). A functional analysis of the crown architecture of tropical forest Psychotria species: Do species vary in light capture efficiency and consequently in carbon gain and growth? *Oecologia* 139, 163–177. doi: 10.1007/s00442-004-1496-4

Phillips, O. L., Lewis, S. L., Lloyd, J., López-González, G., Peacock, J., Quesada, C. A., et al. (2009). Drought sensitivity of the amazon rainforest. *Science* 323, 1344–1347. doi: 10.1126/science.1164033

Piersma, T., and Drent, J. (2003). Phenotypic flexibility and the evolution of organismal design. *Trends Ecol. Evol.* 18, 228–233. doi: 10.1016/S0169-5347(03)00036-3

R Core Team (2018). *R: A Language and Environment for Statistical Computing*. Vienna, Austria: R Foundation for Statical Computing.

Reed, S. C., Reibold, R., Cavaleri, M. A., Alonso-Rodríguez, A. M., Berberich, M. E., and Wood, T. E. (2020). Soil biogeochemical responses of a tropical forest to warming and hurricane disturbance. *Adv. Ecol. Res.* 62, 225–252. doi: 10.1016/bs.aecr.2020.01.007

Reich, P. B., Sendall, K. M., Stefanski, A., Rich, R. L., Hobbie, S. E., and Montgomery, R. A. (2018). Effects of climate warming on photosynthesis in boreal tree species depend on soil moisture. *Nature* 562, 263–267. doi: 10.1038/s41586-018-0582-4

Rich, R. L., Stefanski, A., Montgomery, R. A., Hobbie, S. E., Kimball, B. A., and Reich, P. B. (2015). Design and performance of combined infrared canopy and belowground warming in the B4WarmED (Boreal Forest Warming at an Ecotone in Danger) experiment. *Glob. Chang. Biol.* 21, 2334–2348. doi: 10.1111/gcb.12855

Rodrigues, W. P., Martins, M. Q., Fortunato, A. S., Rodrigues, A. P., Semedo, J. N., Simões-Costa, M. C., et al. (2016). Long-term elevated air [CO2] strengthens photosynthetic functioning and mitigates the impact of supra-optimal temperatures in tropical *Coffea arabica* and *C. canephora* species. *Glob. Chang. Biol.* 22, 415–431. doi: 10.1111/gcb.13088

Santos, V. A. H. F. D., Ferreira, M. J., Rodrigues, J. V. F. C., Garcia, M. N., Ceron, J. V. B., Nelson, B. W., et al. (2018). Causes of reduced leaf-level photosynthesis during strong El Niño drought in a Central Amazon forest. *Glob. Chang. Biol.* 24, 4266–4279. doi: 10.1111/gcb.14293

Scatena, F. (1989). *An Introduction to the Physiography and History of the Bisley Experimental Watersheds in the Luquillo Mountains of Puerto Rico. General Technical Report SO-72*. New Orleans, LA: United States Department of Agriculture Southern Forest Experimental Station, 22. doi: 10.2737/SO-GTR-72

Schimel, D., Pavlick, R., Fisher, J. B., Asner, G. P., Saatchi, S., Townsend, P., et al. (2015). Observing terrestrial ecosystems and the carbon cycle from space. *Glob. Chang. Biol.* 21, 1762–1776. doi: 10.1111/gcb.12822

Shen, H. F., Zhao, B., Xu, J. J., Liang, W., Huang, W. M., and Li, H. H. (2017). Effects of heat stress on changes in physiology and anatomy in two cultivars of Rhododendron. *S. Afr. J. Bot.* 112, 338–345. doi: 10.1016/j.sajb.2017.06.018

Sherwood, S., and Fu, Q. (2014). A drier future? *Science* 343, 737–739. doi: 10.1126/science.1247620

Slot, M., and Kitajima, K. (2015). General patterns of acclimation of leaf respiration to elevated temperatures across biomes and plant types. *Oecologia* 177, 885–900. doi: 10.1007/s00442-014-3159-4

Slot, M., Krause, G. H., Krause, B., Hernández, G. G., and Winter, K. (2019). Photosynthetic heat tolerance of shade and sun leaves of three tropical tree species. *Photosynth. Res.* 141, 119–130. doi: 10.1007/s11120-018-0563-3

Slot, M., Rey-Sánchez, C., Gerber, S., Lichstein, J. W., Winter, K., and Kitajima, K. (2014). Thermal acclimation of leaf respiration of tropical trees and lianas: response to experimental canopy warming, and consequences for tropical forest carbon balance. *Glob. Chang. Biol.* 20, 2915–2926. doi: 10.1111/gcb.12563

Slot, M., and Winter, K. (2017). Photosynthetic acclimation to warming in tropical forest tree seedlings. *J. Exp. Bot.* 68, 2275–2284. doi: 10.1093/jxb/erx071

Slot, M., and Winter, K. (2018). High tolerance of tropical sapling growth and gas exchange to moderate warming. *Funct. Ecol.* 32, 599–611. doi: 10.1111/1365-2435.13001

Smith, N. G., and Dukes, J. S. (2017). Short-term acclimation to warmer temperatures accelerates leaf carbon exchange processes across plant types. *Glob. Chang. Biol.* 4840–4853. doi: 10.1111/gcb.13735

Smith, N. G., Malyshev, S. L., Shevliakova, E., Kattge, J., and Dukes, J. S. (2016). Foliar temperature acclimation reduces simulated carbon sensitivity to climate. *Nat. Clim. Chang.* 6, 407–411. doi: 10.1038/nclimate2878

Valladares, F., Chico, J. M., Aranda, I., Balaguer, L., Dizengremel, P., Manrique, E., et al. (2002). The greater seedling high-light tolerance of *Quercus robur* over *Fagus sylvatica* is linked to a greater physiological plasticity. *Trends Ecol. Evol.* 16, 395–403. doi: 10.1007/s00468-002-0184-4

Valladares, F., Wright, S. J., Lasso, E., Kitajima, K., and Pearcy, R. W. (2000). Plastic phenotypic response to light of 16 congeneric shrubs from a Panamanian rainforest. *Ecology* 81, 1925–1936.

van Schaik, E., Killaars, L., Smith, N. E., Koren, G., Van Beek, L. P. H., Peters, W., et al. (2018). Changes in surface hydrology, soil moisture and gross primary production in the Amazon during the 2015/2016 El Niño. *Philos. Trans. R. Soc. B Biol. Sci.* 373:20180084. doi: 10.1098/rstb.2018.0084

von Caemmerer, S., and Farquhar, G. D. (1981). Some relationships between the biochemistry of photosynthesis and the gas exchange of leaves. *Planta* 153, 376–387. doi: 10.1007/BF00384257

Walsh, C., and Mac Nally, R. (2013). *hier.part: Hierarchical Partitioning. R package version 1.0-4*. Available online at: http://CRAN.R-project.org/package=hier.part (accessed September 15, 2013).

Way, D. A., and Oren, R. (2010). Differential responses to changes in growth temperature between trees from different functional groups and biomes: a review and synthesis of data. *Tree Physiol.* 30, 669–688. doi: 10.1093/treephys/tpq015

Way, D. A., and Yamori, W. (2014). Thermal acclimation of photosynthesis: on the importance of adjusting our definitions and accounting for thermal acclimation of respiration. *Photosynth. Res.* 119, 89–100. doi: 10.1007/s11120-013-9873-7

Wood, T. E., Cavaleri, M. A., Giardina, C. P., Khan, S., Mohan, J. E., Nottingham, A. T., et al. (2019). *Soil Warming Effects on Tropical Forests with Highly Weathered Soils*. Cambridge, MA: Academic Press. doi: 10.1016/b978-0-12-813493-1.00015-6

Wood, T. E., Cavaleri, M. A., and Reed, S. C. (2012). Tropical forest carbon balance in a warmer world: a critical review spanning microbial- to ecosystem-scale processes. *Biol. Rev.* 87, 912–927. doi: 10.1111/j.1469-185X.2012.00232.x

Wu, G., Liu, H., Hua, L., Luo, Q., Lin, Y., He, P., et al. (2018). Differential responses of stomata and photosynthesis to elevated temperature in two co-occurring subtropical forest tree species. *Front. Plant Sci.* 9:467. doi: 10.3389/fpls.2018.00467

Yaffar, D., and Norby, R. J. (2020). A historical and comparative review of 50 years of root data collection in Puerto Rico. *Biotropica* 52, 563–576. doi: 10.1111/btp.12771

Zhang, Y., Yu, G., Yang, J., Wimberly, M. C., Zhang, X., Tao, J., et al. (2014). Climate-driven global changes in carbon use efficiency. *Glob. Ecol. Biogeogr.* 23, 144–155. doi: 10.1111/geb.12086

Conflict of Interest: The authors declare that the research was conducted in the absence of any commercial or financial relationships that could be construed as a potential conflict of interest.

frontiers in Ecology and Evolution

ORIGINAL RESEARCH
published: 06 November 2020
doi: 10.3389/fevo.2020.576296

Coordination of Morpho-Physiological and Metabolic Traits of *Cistus incanus* L. to Overcome Heatwave-Associated Summer Drought: A Two-Year On-Site Field Study

Francesca Alderotti[1], Cecilia Brunetti[1,2], Giovanni Marino[2], Mauro Centritto[2], Francesco Ferrini[1,2], Cristiana Giordano[3], Massimiliano Tattini[2], Bárbara Baêsso Moura[1,4] and Antonella Gori[1,2]*

[1] Section Woody Plants, Department of Agriculture, Food, Environment and Forestry, University of Florence, Florence, Italy, [2] Institute for Sustainable Plant Protection, National Research Council of Italy, Sesto Fiorentino, Italy, [3] Institute for BioEconomy, National Research Council of Italy, Sesto Fiorentino, Italy, [4] Research Institute on Terrestrial Ecosystems, National Research Council of Italy, Sesto Fiorentino, Italy

OPEN ACCESS

Edited by:
Andrea Ghirardo,
Helmholtz Zentrum München,
Germany

Reviewed by:
Giacomo Puglielli,
Estonian University of Life Sciences,
Estonia
Carmen Arena,
University of Naples Federico II, Italy
Jürgen Kreuzwieser,
University of Freiburg, Germany

***Correspondence:**
Cecilia Brunetti
cecilia.brunetti@ipsp.cnr.it

Specialty section:
This article was submitted to Chemical Ecology, a section of the journal Frontiers in Ecology and Evolution

Received: 25 June 2020
Accepted: 12 October 2020
Published: 06 November 2020

Citation:
Alderotti F, Brunetti C, Marino G, Centritto M, Ferrini F, Giordano C, Tattini M, Moura BB and Gori A (2020) Coordination of Morpho-Physiological and Metabolic Traits of Cistus incanus L. to Overcome Heatwave-Associated Summer Drought: A Two-Year On-Site Field Study. Front. Ecol. Evol. 8:576296. doi: 10.3389/fevo.2020.576296

The shrub *Cistus incanus* L. is well-adapted to Mediterranean conditions thanks to its morpho-anatomical, physiological and biochemical traits. However, its distribution and survival in coastal dunes will be likely threatened by ongoing runaway climate change. We investigated how the harsh climatic conditions generated by the 2015 summer heat wave triggered specific anatomical, physiological, and biochemical responses of this species in its natural environment. These adjustments were compared to those measured in summer 2014. The drier and hotter conditions of summer 2015 determined an increment in leaf lamina thickness, due to a greater palisade parenchyma, thus leading to an increase in the whole leaf mass per area. These morphoanatomical adjustments enhanced leaf resistance against dehydration, optimized carbon assimilation, and delayed leaf senescence. In addition, the higher amount of secondary metabolites detected for 2015, in particular tannins and monoterpenes, contributed to the maintenance of physiological performances even under hotter and drier conditions, preventing oxidative stress through the consumption of excess reducing power. In conclusion, our study offers new evidence on the integration of morphophysiological and metabolic adjustments of this species growing in its natural habitat to cope with ongoing climate change.

Keywords: drought, flavonols, heat wave, leaf morpho-anatomical traits, Mediterranean maquis, monoterpenes, photosynthesis, tannins

INTRODUCTION

Mediterranean climate is characterized by mild and humid winters and hot and dry summers, with most of the rainfalls concentrated in the cold season (Lionello et al., 2006). Summer drought is considered the primary constraint affecting both productivity and distribution of Mediterranean vegetation due to a combination of high irradiance, high temperatures and water scarcity (Gratani et al., 2013; Flexas et al., 2014).

Mediterranean maquis vegetation mostly consists of evergreen sclerophylls with a deep root system and semi-deciduous shrubs, which reduce transpiring surface during stressful periods (Galmés et al., 2007; Medrano et al., 2009). Shrub species, in particular, are a widespread life form in the coastal ecosystem and their potential resilience to environmental change deserves special attentions (Arena et al., 2011; Galle et al., 2011; Puglielli et al., 2017a). Mediterranean shrubs display a vast array of strategies to cope with severe climatic constraints (Lefi et al., 2004; Sardans and Peñuelas, 2013), which may in part correlate with the large biological diversity encountered in Mediterranean areas suffering from most severe environmental pressures (Van Der Plas et al., 2016). Evergreen species usually display a conservative resource use strategy (David et al., 2007), characterized by low net photosynthesis and relative growth rate, and the utilization of the fresh assimilated carbon for leaf construction (Sardans and Peñuelas, 2013). By contrast, semi-deciduous species display a higher physiological plasticity compared to the evergreen counterparts, with a decline in photosynthetic performances during central hours in summer season, when high solar irradiance occurs in concomitance with severe reduction in soil water availability and excessive air temperature (Di Ferdinando et al., 2014).

Among these metabolic adjustments, the increase in polyphenol contents in stressed plants has been linked to improve photoinhibition tolerance and, in general, to the protection of photosynthetic organs from oxidative damages (Brunetti et al., 2015). Mediterranean shrubs also emit large amounts of biogenic volatile organic compounds (BVOCs), among which mono- and sesqui-terpenes are the most abundant. These compounds play prominent functions against biotic and abiotic stresses as well as in mediating ecological interactions (Loreto and Schnitzler, 2010; Niinemets et al., 2013; Loreto et al., 2014; Mu et al., 2018). Specifically, monoterpenes have been shown to protect leaves against oxidative and thermal damages, decreasing the rate of formation of reactive oxygen species (ROS) that can damage the photosynthetic apparatus (Loreto et al., 1998, 2014). It is known that water stress may result in increased monoterpene emission (Ormeño et al., 2007) or in a significant change in the blend composition of stored monoterpenes (Brilli et al., 2013).

Cistus L. is a genus of dicotyledonous plants colonizing open areas of stony and infertile soils (Papaefthimiou et al., 2014). Among *Cistus* spp., *Cistus* × *incanus* L. (pink rock-rose, hereby *C. incanus*) belongs to the autochthonous Tertiary Mediterranean flora (Quézel, 1985). This species is classified as a summer drought semi-deciduous species, shedding a high percentage of leaves and branches and increasing the mass investments per leaf area unit during drought (LMA, leaf mass per area) (Catoni et al., 2012; De Dato et al., 2013; Grant et al., 2015). The semi-deciduousness allows this species to be well-adapted to summer drought (Correia and Ascensao, 2016; Puglielli, 2019). In addition, also seasonal dimorphism, expressed both in the leaf morphoanatomical traits as well as in the wood properties, may be considered another important adaptation of this species to the Mediterranean harsh climate (Aronne and De Micco, 2001; De Micco and Aronne, 2009; Arena et al., 2013). Indeed, summer leaf anatomy is characterized by a crimped lamina partially rolled to form crypts in the lower surface and a thick palisade parenchyma in the mesophyll tissue (Aronne and De Micco, 2001; Rotondi et al., 2003).

Despite being well-adapted to multiple stress factors, *C. incanus* distribution and survival in coastal dune areas will be likely negatively affected by the ongoing climatic change conditions (Nogués et al., 2015; Gori et al., 2019). In this respect, very few field investigations have been conducted on the effects of drought and heat stress on this Mediterranean shrub (Gratani et al., 2008; De Micco and Aronne, 2009; Gratani et al., 2018; Parra and Moreno, 2018; Gori et al., 2019). Furthermore, morpho-physiological and metabolic responses of this species to extreme drought remain poorly investigated despite the increasing frequencies of heat waves hitting the Mediterranean region as a consequence of climate change.

In this context, the contrasting climatic conditions of the summers 2014 and 2015 provided an optimum opportunity to study the modifications in this maquis shrub behavior in response to ongoing climate change in its natural environment. In fact, the summer 2014 showed irregular rainfalls and moderate drought, while the summer 2015 was one of the driest and hottest in Europe in the last 70 years as a result of an extreme heatwave that lasted about 30 days until the end of July (Russo et al., 2015).

We took advantage of contrasting climatic conditions of summers 2014 and 2015 to test if changes in morpho-anatomical traits allow to maintain physiological performances and enhance the biosynthesis of secondary metabolites in *C. incanus*. We hypothesized that semi-deciduous Mediterranean shrubs species adapted to harsh environment, such as *C. incanus*, are able to face drought and heat stress thank to a coordination of morpho-anatomical, physiological and biochemical traits. We expected that higher temperature in 2015 may have promoted a major investment in leaf construction and boosted the production of secondary metabolites, thus reducing water loss and damages to photosynthetic apparatus caused by oxidative stress. Overall, this study provides the substantial contribution of secondary metabolites, both condensed tannins and monoterpenes, to the suite of traits conferring high plasticity to *C. incanus* and, consequently to its high resilience against extreme environmental pressures associated to climate change.

MATERIALS AND METHODS

Plant Material, Study Area, Sampling Design and Meteorological Data

In May 2014, eight healthy individuals of *C. incanus* were selected in the population previously described in Gori et al. (2019) and screened for size and uniformity. *C. incanus* plants were 0.6 ± 0.07 m height with a canopy area of around 0.6 ± 0.08 m^2. The study was performed over 2 consecutive years on cloudless days in summer 2014 and 2015 (8–9 July 2014 and 14–15 July 2015) on the coastal sand dunes located in Castiglione della Pescaia (GR, Italy, 42° 46′ N, 10° 53′ E).

The diurnal time courses of leaf water potential was monitored at five different sampling hours, at 4:00 (predawn, PD), 8:00,

12:00 (midday, MD), 15:00, and 18:00, while gas exchanges, chlorophyll fluorescence parameters, chlorophyll index and epidermal flavonol index at 8:00, 12:00, 15:00, and 18:00. Samples for polyphenol analysis and Biogenic Volatile Organic Compounds (BVOCs) were collected between 12:30 and 14:00. Air temperature (T), precipitation (P) and global irradiance (G_i) were recorded every hour by the weather station "Grosseto" (Italy) and provided from the regional archive of the LaMMA Consortium[1].

Water Relations

Two leaves per plant were collected in the field and transported to the laboratory in sealed zip-lock, tared plastic bags stored in a fridge bag. The leaves were weighed to determine fresh mass (FW) and then allowed to hydrate until saturation (constant weight) for 48 h in darkness to determine turgid mass (TW). Then, leaves were dried in an oven at 80°C for 48 h to determine dry mass (DW). Finally, Relative Water Content (RWC) was calculated using the following equation:

$$RWC(\%) = (FW - DW)/(TW - DW)$$

Leaf water potentials (Ψ_w) were directly measured in field, after the cut of two twigs per plant, using a Scholander-type pressure chamber (PMS Instruments, Corvallis, OR). The measurements of RWC and Ψ_w obtained from the same plant were combined to make an individual replicate.

Morphological and Anatomical Measurements

From the upper part of the canopy 10 adult leaves per plant were sampled at midday to measure LMA by the calculation of the dry mass (drying the leaves in oven at 80°C for 48 h) to leaf area ratio (mg cm^{-2}). One twig per plant was collected and transported to the laboratory for anatomical measurements. Light microscopy segments of leaf tissue were taken from the basal-mid-lamina regions of eight adult leaves and fixed for 2 h at room temperature in 0.2 M phosphate buffer (pH 7.2) with 2.5% glutaraldehyde (Sigma Aldrich). Then, they were washed twice in the same buffer and post-fixed in 2% osmium tetroxide (Sigma Aldrich) for additional 2 h. Following dehydration in a graded ethanol series (30, 40, 50, 60, 70, 80, 95, and 100%), the samples were gradually embedded in Spurr resin (Sigma Aldrich) and polymerized at 70°C for 24 h (Spurr, 1969). Semi-thin sections, 1–2 μm, were affixed to glass slides and observations were carried out in a Leica DM LB2 Light Microscope (Leica Microsystem, Germany).

Gas Exchanges and Chlorophyll Fluorescence

Measurements of gas exchanges and photosystem II maximum efficiency (Φ_{PSII}) were performed on two fully expanded and healthy leaves per plant, selected in the most illuminated part of the canopy, utilizing a LI-6400 portable photosynthesis system (Li-Cor, Lincoln, NE, United States) equipped with a cuvette of 2 cm^2. Photosynthesis (P_n), stomatal conductance (g_s), intercellular CO_2 concentration (C_i) and Φ_{PSII} were measured at (CO_2) of 400 μmol mol^{-1} and at the photosynthetic photon flux density recorded in the environment. The integral of daily photosynthesis (P_n), calculated using Sigma Plot 11.0 (Systat Software, Inc., San Jose, CA), has been employed to quantify the amount of carbon fixed during the day. Then, mesophyll conductance to CO_2 (g_m) was calculated using the variable *J* method (Harley et al., 1992) as follows:

$$g_m = \frac{Pn}{Ci - \frac{\Gamma^*[J_F + 8^*(Pn + R_d]}{J_F - 4^*(Pn + R_d)}}$$

where Γ, representing the CO_2 compensation point to photorespiration, was obtained from data reported in Galle et al. (2011), while light respiration (R_d) was calculated using the Kok method at PPFD steps of 150, 100, 80, 60, and 30 μmol $m^{-2}s^{-1}$ (Kok, 1948).

Electron transport rate (J_F) was calculated from chlorophyll fluorescence:

$$J_F = \Phi\ PSII^*\ PPFD^*\ \alpha^*\ \beta$$

where Φ_{PSII} is the actual photochemical efficiency of Photosystem II (Genty et al., 1989), the partitioning factor (β) between photosystems I and II was considered to be 0.5 and leaf absorbance (α) 0.84.

Moreover, we use the ratio J_F/P_n as an indicator of the excess of electron transport which can be diverted to other alternative electron sinks rather than photosynthesis (Arena and Vitale, 2018; Brunetti et al., 2018).

After gas exchanges, F_v/F_m was measured on the same leaves using a portable chlorophyll fluorescence system (Handy Pea, Hansatech, Norflolk, United Kingdom). Before measurements, leaves were adapted to the dark for 30 min. Gas exchange and chlorophyll fluorescence measurements obtained from the same plant were combined to make an individual replicate.

Biochemical Parameters

Non-destructive Determination of Chlorophyll and Epidermal Flavonols

At each daily sampling hour, four leaves per plant were measured with a Dualex® device (Dualex® Research, FORCE-A®, Orsay, France) on adaxial and abaxial side. Chlorophyll index (Chl_i) and epidermal Flavonol index ($Flav_i$) were obtained as described in Agati et al. (2016). In particular, the Chl_i was calculated as the average of the adaxial and abaxial measurements, while the $Flav_i$ was calculated as the sum of both measurements. All measurements obtained from the same plant were combined to make an individual replicate.

HPLC Quantification of Polyphenols

Two leaves per plant were collected, immediately frozen in liquid nitrogen, stored at −80°C and then lyophilized. In detail, lyophilized samples (150 mg of DW) were extracted twice with 5 mL of ethanol/water (75/25) adjusted at pH2.5 with formic acid and the supernatant partitioned with 3 × 5 mL of *n*-hexane. The ethanol fraction was reduced to dryness, and the residue

[1]http://lamma.rete.toscana.it

was rinsed with 1 mL of methanol/water (90/10). Aliquots of 10μL were injected into the Flexar liquid chromatography equipped with a quaternary 200Q/410 pump and an LC 200 diode array detector (DAD) (all from Perkin Elmer®, Bradford®, CT, United States). Identification and quantification of these metabolites was carried out using retention times and UV spectral characteristics of authentic standards, as well as based on literature data (Gori et al., 2016). The total polyphenols content (Pol_{Tot}) consists in the sum of individual polyphenols detected, namely tannins (Tan) and flavonols (Flav).

GC-MS Quantification of Biogenic Volatile Organic Compounds (BVOCs)

The emission of BVOCs was measured on the same leaves used for gas exchange analyses by partially diverting the outlet of the cuvette of the Li-Cor system described above into a silico-steel cartridge packed with 200 mg of Tenax (Agilent, Cernusco sul Naviglio, Italy). A volume of 4 dm^3 of air was pumped through the trap at a rate of 200 cm^3 min^{-1} utilizing an environmental air sampling equipment (A.P. BUCK, Inc., Orlando, FL). Prior to the first enclosure of the leaves, blank samples from the empty cuvettes were taken every sampling day. The cartridge was analyzed using a Perkin Elmer Clarus 580 gas chromatograph coupled with a Clarus 560 Mass-Selective-Detector and a thermal desorber TurboMatrix (Perkin Elmer Inc., Waltham, MA, United States) operating for 25 min at 250°C. The desorbed compounds were separated in a 30-m Elite-5-MS capillary column. The temperature of the column was first maintained at 40°C (5 min), then increased with a 5°C min^{-1} 175 ramp to 250°C, and maintained at 250°C for 2 min. BVOCs were identified using the NIST library provided with the GC/MS Turbomass software. The authentic standards of α-pinene, β-pinene and myrcene (Sigma Aldrich, Milan, Italy) were used to prepare calibration curves as well as to compare the peak retention time and the peak fragmentation of monoterpenes found in the samples. Authentic standards of other compounds collected in the traps (tujene, α-phellandrene, and β-phellandrene) were not available, therefore the amount of these compounds was calculated using the calibration curve of α-pinene. Total BVOC emission ($BVOCs_{Tot}$) consists in the sum of individual monoterpenes detected in the samples.

Statistical Analysis

Statistical analysis was performed using the SPSS software program (SPSS, Inc., Chicago, IL, United States). To test the daily trend of parameters, we performed a *two way* ANOVA followed by Tukey's *post-hoc* test. When a mean value was reported for each summer, Student's *t*-tests were performed to evaluate differences between the two years. Linear regression analyses were performed to determine the effect of air temperature on gas exchanges and chlorophyll fluorescence parameters (P_n, g_s, F_v/F_m and Φ_{PSII}) and water relations (Ψ_w and RWC) considering the data collected in four different sampling hours (8:00, 12:00, 15:00, and 18:00) and on total polyphenols content (Pol_{Tot}) and BVOCs emission considering the data collected at 12:00. The linear regression analysis was also applied to determine the differential contribution of the morpho-anatomical traits (upper and lower epidermis, palisade and spongy parenchyma) to the total leaf thickness (LT) and to the gas exchange and chlorophyll fluorescence parameters (P_n, g_s, F_v/F_m, and Φ_{PSII}). With the same set of data, a principal component analysis (PCA) was applied to gas exchange and chlorophyll fluorescence parameters (P_n, g_s, F_v/F_m, and Φ_{PSII}), water relations (RWC and Ψ_w) and morpho-anatomical (leaf thickness) or total polyphenols content (Pol_{Tot}), biogenic organic compounds (BVOCs) emission and morpho-anatomical (leaf thickness) in order to distinguish the trait syndromes between the year of sampling. The PCA was calculated based on a correlation matrix using OriginPro 2020 software.

RESULTS

Meteorological Data

In July 2014, the average maximum temperature (T_{max}) was 29°C, almost 5°C lower than that recorded in July 2015. Average minimum temperatures (T_{min}) were 17.7 and 21.1°C in July 2014 and 2015, respectively (**Table 1**). Hence, summer 2015 was unusually dry and hot as a consequence of a severe heat wave that hit the Mediterranean regions for about 30 days between the end of June and July (Russo et al., 2015). During the 2 months prior measurements cumulative rainfall was 84 mm in 2014 and 29 mm in 2015 (**Table 1**). During the days of measurements, temperatures (**Figure 1A**) and global irradiance (**Figure 1B**) had a typically daily trend, showing higher values during the central hours. The daily irradiance did not change between the two summers (**Figure 1B**). Whereas, in 2014 the daily time course of temperature was consistently lower than in 2015 (**Figure 1A**), with minimum and maximum temperatures of 18°C and 30°C in 2014, and 22°C, and 33°C in 2015, respectively (**Figure 1A**).

Morpho-Anatomical Leaf Traits

The microscopy analysis revealed significant variations among the samples collected in summer 2014 and 2015 (**Figure 2A** and **Table 2**). In both years, leaves showed a typical structure of a heliophylous plant: a dorso-ventral orientation, a high mesophyll density, with a well-developed palisade consisting of two/three layers of elongate-prismatic cells and a spongy parenchyma with a few airspaces (**Figure 2A**). In the leaves collected in 2015, the vacuolar accumulation of tannins, as evidenced through osmium staining, as spherical deposits or adjacent to the internal surface of the vacuolar membrane; condensed tannins fill almost completely the vacuoles of adaxial epidermis and palisade

TABLE 1 | Meteorological data of the two study years.

	T MAX (°C)	T min (°C)	Cumulative rainfall (mm)
	July	July	May–July
2014	29.0	17.7	84.0
2015	33.9	21.1	29.0

Average maximum and minimum temperatures (°C) and cumulative rainfall (mm) referred to May, June, and July prior the days of measurements. Data of the weather station "Grosseto" (Italy) from the regional archive of the LaMMA Consortium (http://lamma.rete.toscana.it).

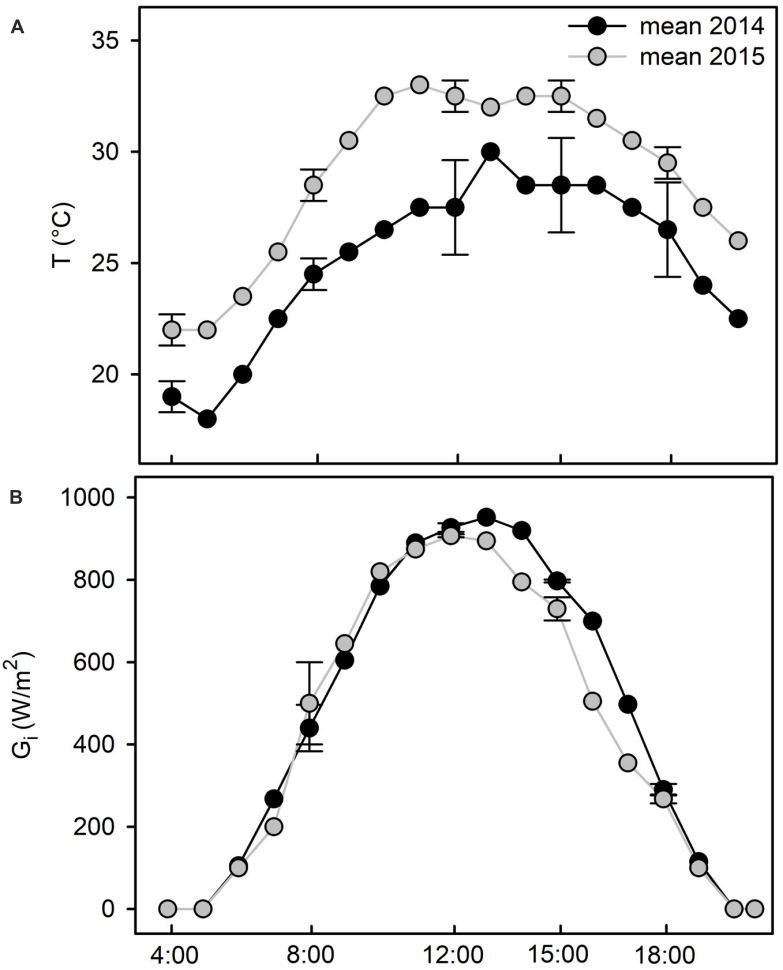

FIGURE 1 | Time course of average air temperatures (T,°C) **(A)** and of global irradiance (G_i, Wm^{-2}) **(B)** of the sampling days in July 2014 (black line) and July 2015 (gray line). Data of the weather station "Grosseto" (Italy) from the regional archive of the LaMMA Consortium (http://lamma.rete.toscana.it).

parenchyma cells, whereas occur in fewer cells or in smaller quantities in spongy and abaxial epidermis cells (**Figure 2A**). In addition, leaves collected in 2015 showed a significant increase in the thickness of almost all leaf tissues compared to those collected in 2014, i.e., increases of 44.2% (*t*-test; $p \leq 0.001$) in the palisade and of 28.2% (*t*-test; $p = 0.024$) in the lower epidermis (**Table 2**). A slight, but not significant increment, was observed also in the spongy parenchyma. The palisade parenchyma was the leaf tissue that mostly contributed to increase the leaf thickness in 2015 presenting a higher coefficient of determination ($R^2 = 0.66$) when compared to the other tissues (spongy mesophyll $R^2 = 0.35$, upper epidermis $R^2 = 0.44$ and lower epidermis = regression not significant) (**Figure 2B** and **Supplementary Table S1B**). A strong, significant increase in LMA (+34.5%) (*t*-test; $p = 0.002$) was observed in 2015, as LMA ranged from 11.2 mg cm^{-2} in July 2014 to 17.1 mg cm^{-2} in July 2015 (**Table 2**).

Water Relations and Gas Exchanges

Plants had a better water status in 2014 than in 2015, as shown by the significantly higher values of RWC recorded at all sampling hours (*two way* ANOVA; $p < 0.001$) (**Table 3**). As expected, RWC showed the maximum values at PD (∼70% in 2014 vs. ∼60% in 2015) in both years. In 2014, after 8:00 RWC decreased significantly (*two way* ANOVA; $p < 0.001$) never recovering to the morning value during the day. Similarly, in 2015, RWC declined significantly after 8:00 and, following the depression registered during the hottest hours of the day, showed a significant recovery to the morning values. A significant year-sampling time interaction was revealed for water potential (Ψ_w) (*two way* ANOVA; $p < 0.001$). Ψ_w was significant lower in 2015 than in 2014 (*two way* ANOVA; $p < 0.001$), except for the late-afternoon value 2014 (*two way* ANOVA; $p = 0.463$) (**Table 3**). This parameter followed a typically daily pattern, showing marked reduction during the central hours of the day in both years. It is worth noting that midday Ψ_w fell to a minimum of −4.8 MPa in 2015, compared to the 2014 value which reached −3.2 MPa (**Table 3**). Both parameters of water status (RWC and Ψ_w) presented a negative relation with the air temperatures (**Supplementary Table S1A**). A significant year-sampling time interaction was revealed for net photosynthetic

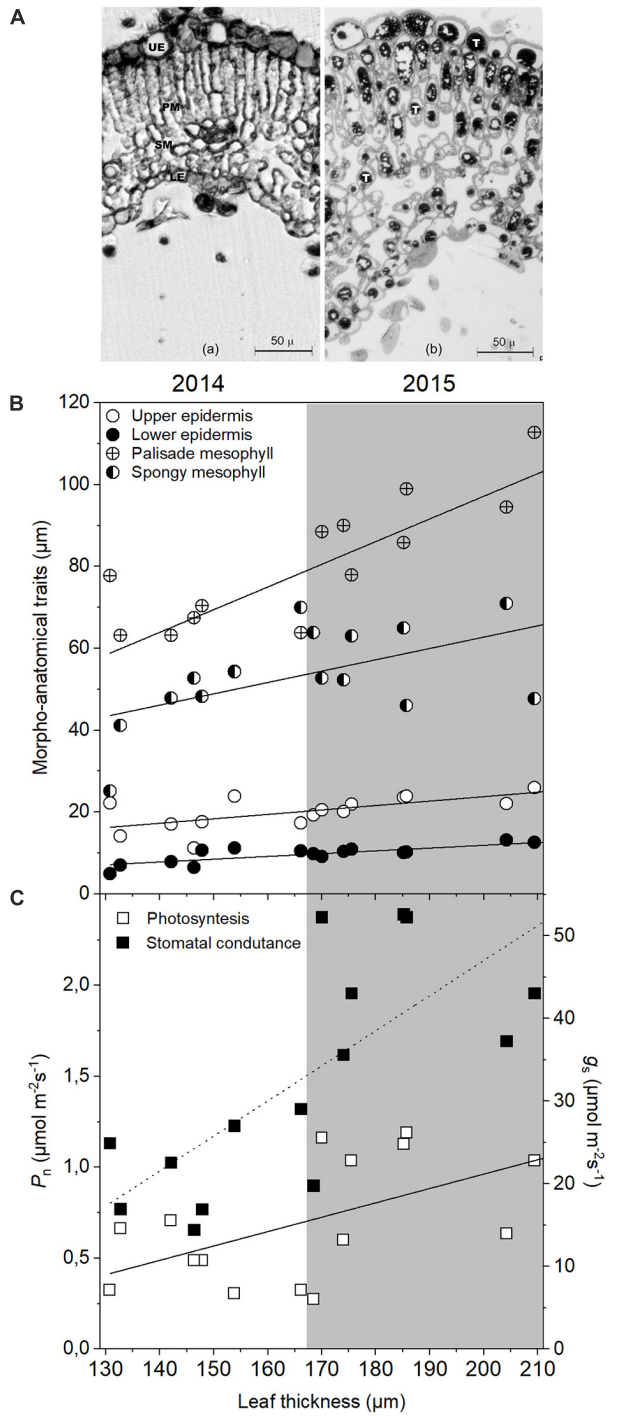

FIGURE 2 | Transverse cross sections of osmium-stained *C. incanus* leaves collected in July 2014 (a) and 2015 (b) illustrating the difference in in thickness of palisade parenchyma and epidermal cells between the plants collected in the two different years **(A)**. Condensed tannin deposits are shown in the vacuoles of cells. UE, upper epidermis; PM, palisade mesophyll; SM, spongy mesophyll; LE, lower epidermis; T, tannin. Bars = 50 µm. Linear regressions between leaf thickness and the other morpho-anatomical traits **(B)**. Linear regressions between leaf thickness and photosynthesis (P_n) and stomatal conductance (g_s) **(C)**. Detailed analysis is presented in **Supplementary Table S1**.

TABLE 2 | Morpho-anatomical traits of *C. incanus* leaves in July 2014 and 2015.

Parameters	2014		2015
UE (µm)	17.81 ± 7.1	*n.s.*	22.89 ± 2.5
PM (µm)	65.48 ± 10	***	94.47 ± 11
SM (µm)	50.36 ± 14	*n.s.*	57.89 ± 10
LE (µm)	8.52 ± 2.3	*	10.92 ± 1.4
PM/SM (%)	149.7 ± 79	*n.s.*	171.1 ± 52
LT (µm)	148.5 ± 14	***	189.5 ± 17
LMA (mg cm^{-2})	11.18 ± 1.7	**	17.07 ± 1.8

*UE, upper epidermis; PM, palisade mesophyll; SM, spongy mesophyll; LE, lower epidermis; PM/SM, palisade/spongy mesophyll ratio; LT, leaf thickness; LMA, leaf mass per area. Data are means ± SD (anatomical parameters n = 8; LMA n = 80). Asterisks represent differences between the two years, *($p \leq 0.05$), **($p \leq 0.01$), ***($p \leq 0.001$) based on t-test.*

rate (P_n) (*two way* ANOVA; $p < 0.001$). P_n dropped from morning to midday in 2015, ranging from 2.92 ± 0.80 µmol m^{-2} s^{-1} to 0.99 ± 0.24 µmol m^{-2} s^{-1} (-66% *two way* ANOVA; $p < 0.001$), while in 2014 it did not change in the same time slot (*two way* ANOVA; $p = 0.064$). Differences in P_n diurnal time courses emerged between the two summers after 12:00. In fact, while in 2014 P_n values increased from 12:00 to 15:00 (+85% *two way* ANOVA; $p < 0.001$) and subsequent decreased at 18:00 (-65% *two way* ANOVA; $p < 0.001$), in 2015, P_n did not change from 12:00 to late afternoon (*two way* ANOVA; $p > 0.05$) (**Figure 3A**). The daily integral of photosynthesis (P_n) did not show significant differences between the two summers (0.12 ± 0.03 g CO_2 d^{-1}m^{-2} in 2014 and 0.11 ± 0.01 g CO_2 d^{-1}m^{-2} in 2015) (*t*-test; $p = 0.55$) (**Figure 3B**). Stomatal conductance (g_s) was significantly lower in 2014 than in 2015 at all sampling hours (*two way* ANOVA; $p < 0.001$), except for values recorded at 18:00 (*two way* ANOVA; $p = 0.324$) (**Figure 4A**). However, g_s had a very similar trend in the two summers, with the highest values recorded at 8:00 and 15:00 and the lowest at 12:00 and 18:00 (**Figure 4A**). A significant linear regression between the leaf thickness and the P_n and g_s was observed (**Figure 2C** and **Supplementary Table S1A**) with g_s presenting the higher coefficient of determination ($R^2 = 0.59$) when comparing to P_n ($R^2 = 0.28$). However, the relationship between those parameters with the air temperature was only significant for the g_s (**Supplementary Table S1A**). Similarly to g_s, mesophyll conductance calculated at 12:00 (g_{mMD}), showed significantly higher values in 2015 than in 2014 (*t*-test; $p = 0.05$) (**Figure 4A**). In 2014, C_i did not change from morning to 12:00 in 2014, while a significant increment was observed for this parameter in 2015 (**Figure 4B**). Then while in 2014 C_i strongly dropped from 12:00 to 15:00 (-24% *two way* ANOVA; $p < 0.001$) and partially recovered in the late afternoon, in 2015 this parameter slowly returned to the morning value at 18:00 (**Figure 4B**). In addition, significant year-sampling time interaction was revealed for both C_i and J_F/P_n (*two way* ANOVA; $p < 0.001$). The morning and midday values of the J_F/P_n ratio were similar and did not change between the 2 years (*two way* ANOVA; $p > 0.05$) (**Figure 4C**). However, in 2015, the J_F/P_n ratio increased significantly during the afternoon and resulted 86 and 68% higher than in 2014 at 15:00 (*two*

TABLE 3 | Time course of relative water content (RWC) and of water potential (Ψ_w) of *C. incanus* plants in July 2014 and 2015.

	RWC (%)			Ψ_w (Mpa)		
	2014		**2015**	**2014**		**2015**
PD	71 ± 4 a	***	60 ± 3 a	−2.0 ± 0.18 a	**	−2.7 ± 0.58 a
08:00	68 ± 3 a	***	53 ± 3 ab	−2.7 ± 0.19 b	***	−3.9 ± 0.55 b
12:00	53 ± 5 b	**	45 ± 4 c	−3.2 ± 0.08 b	***	−4.6 ± 0.43 bc
15:00	55 ± 5 b	*	49 ± 5 cb	−3.0 ± 0.19 b	***	−4.8 ± 0.33 c
18:00	59 ± 3 b	*	54 ± 3 ab	−2.7 ± 0.25 b	*n.s.*	−2.9 ± 0.25 a
Significance	Hour***	Year***	Hour × Year *n.s.*	Hour***	Year***	Hour × Year***

*Two way ANOVA followed by Tukey's pairwise comparison was performed to compare data (means ± SD; n = 8). Letters indicate significant differences ($p \leq 0.05$) among sampling hours for each years, whereas asterisks represent significant differences among yeas for each sampling hour, *($p \leq 0.05$), **($p \leq 0.01$), ***($p \leq 0.001$). PD, predawn.*

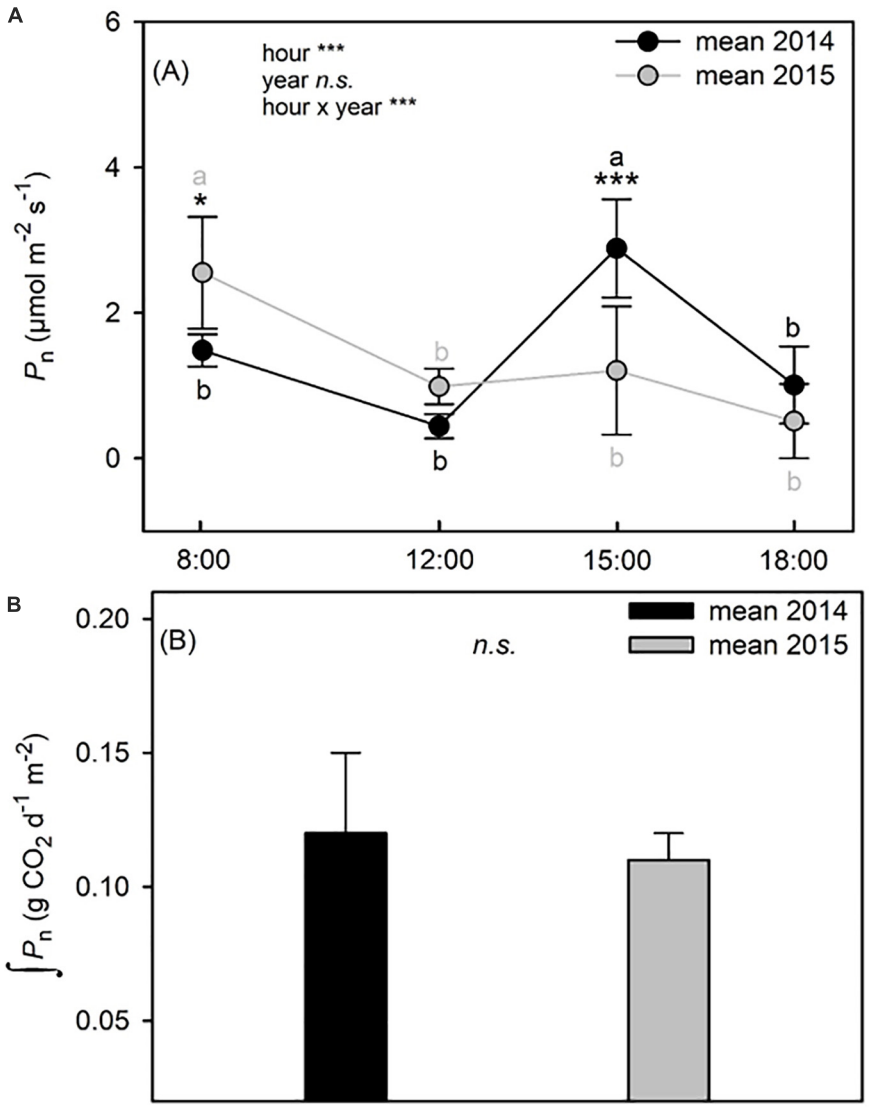

FIGURE 3 | Time course of net photosynthetic rate (P_n) **(A)** and integration of daily net photosynthetic rate (P_n) **(B)** of *C. incanus* leaves in July 2014 and 2015. *Two way* ANOVA followed by Tukey's pairwise comparison was performed to compare data (means ± SD; $n = 8$) in **(A)**. Letters indicate significant differences ($p \leq 0.05$) among sampling hour for each year, whereas asterisks represent significant differences among years for each sampling hour, *($p \leq 0.05$), **($p \leq 0.01$), ***($p \leq 0.001$). The statistic adopted in panel B was a Student's *t*-tests, asterisks represent differences between the two years, *($p \leq 0.05$), **($p \leq 0.01$), ***($p \leq 0.001$).

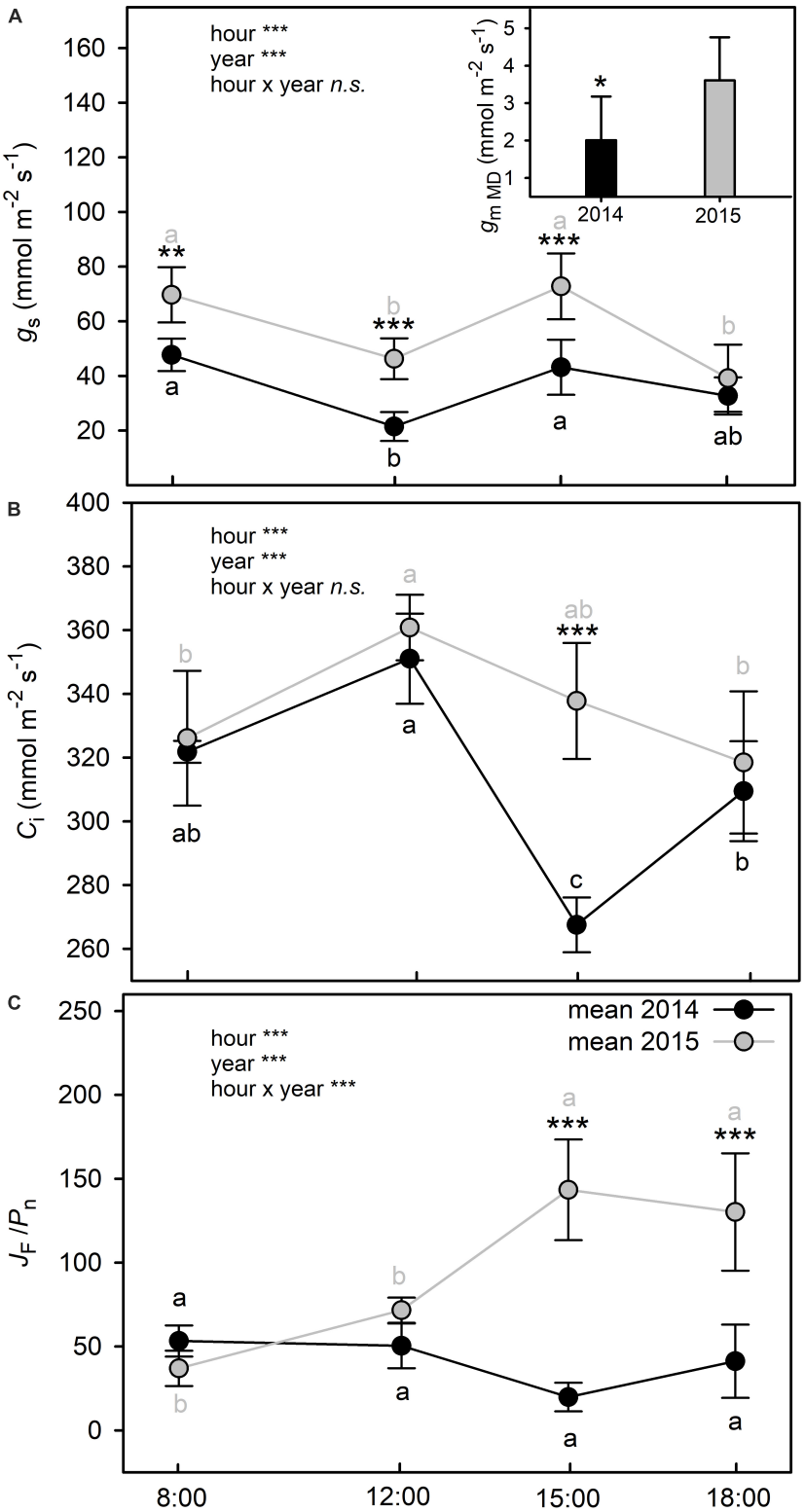

FIGURE 4 | Time course of stomatal conductance (g_s) **(A)**, intercellular CO_2 concentration (C_i) **(B)**, and electron transport rate (J_F) to net photosynthetic rate (P_n) ratio **(C)** of *C. incanus* leaves in July 2014 and 2015. Insert graph in **(A)** shows mesophyll conductance at *midday* (g_{mMD}) in July 2014 and 2015. *Two way* ANOVA followed by Tukey's pairwise comparison was performed to compare data (means ± SD; $n = 8$). Letters indicate significant differences ($p \leq 0.05$) among sampling hour for each year, whereas asterisks represent significant differences among years for each sampling hour, *($p \leq 0.05$), **($p \leq 0.01$), ***($p \leq 0.001$). The statistic adopted for the inclusion in **(A)** was a Student's *t*-test, asterisks represent differences between the two years, *($p \leq 0.05$), **($p \leq 0.01$), ***($p \leq 0.001$).

way ANOVA; $p < 0.001$) and at 18:00 (*two way* ANOVA; $p < 0.001$), respectively.

The PCA identified groups of plants with similar water relations, gas exchange and morpho-anatomical features, with the first two components of the PCA explaining 41.58 and 27.74% of the variances. In the biplot (**Supplementary Figure S1A**) samples collected in different years were segregated in distinct groups.

The samples collected in 2015 were mainly grouped at the negative score of PC1 presenting lower values of Ψw and RWC than samples collected in 2014 and grouped at the positive score of PC2 for g_s and leaf thickness (LT). The P_n vector contributed less for distinguishing both years.

Chlorophyll Fluorescence and Chlorophyll Index

Photosystem II maximum efficiency (F_v/F_m) showed a typical midday depression at 12:00 in both years (**Figure 5A**) (*two way* ANOVA; $p < 0.001$) with a negative correlation with air temperature along the day (**Supplementary Table S1A**). However, while in summer 2014 F_v/F_m recovered optimal values at 15:00, in 2015, this parameter fully recovered only at 18:00. In addition, F_v/F_m was significantly higher in 2014 than in 2015 at 8:00 (*two way* ANOVA; $p = 0.024$) and at 15:00 (*two way* ANOVA; $p < 0.001$) (**Figure 5A**). Photosystem II actual efficiency (Φ_{PSII}) differed between the 2 years, with significant lower values in 2014 than in 2015 (*two way* ANOVA; $p < 0.001$). The minimum values of Φ_{PSII} were observed from 12:00 to 15:00 in both summers (**Figure 5B**). The chlorophyll index (Chl_i) was significantly higher in 2014 than in 2015 at all sampling hours (*two way* ANOVA; $p < 0.001$) (**Figure 5C**). However, the daily trends of this parameter were similar in both years, with a reduction during the central hours of the day followed by a recovery at 18:00 (**Figure 5C**). The PCA identified groups of plant species with similar chlorophyll fluorescence and chlorophyll index as previously described for gas exchanges and water relations, with samples collected in different years segregated in distinct groups (**Supplementary Figure S1A**). According to the PCA analysis the samples collected in 2015 were mainly grouped at the negative score of PC1 presenting the lower values of F_v/F_m however, Φ_{PSII} vector contributed less for distinguishing both years.

Flavonol Index and Polyphenols

The Flavonol index ($Flav_i$) exhibited very similar values and daily trends in the two summers, increasing from 8:00 to 12:00 and then declining from 12:00 to 15:00 until 18:00 (**Figure 6A**). Moreover, at 12:00, the value of $Flav_i$ was significantly higher in summer 2014 than in 2015 (*two way* ANOVA; $p = 0.026$) (**Figure 6A**). Total polyphenols (Pol_{Tot}) were higher in 2015 than in 2014 (*t*-test; $p = 0.022$) (**Figure 6B**) with a positive relation with air temperature (**Supplementary Table S1**), because of the significant difference in the total content of tannins, passing from $\sim$ 51 μmol g^{-1} dw^{-1} in 2014 to ~70 μmol g^{-1} dw^{-1} in 2015 (*t*-test; $p = 0.002$) (**Figure 6C**). In contrast, the total content of flavonols did not change from 2014 to 2015 (*t*-test; $p = 0.183$) (**Figure 6C**).

Biogenic Volatile Organic Compounds

The total emission of BVOCs increased about fivefold in 2015 compared to 2014 (*t*-test; $p < 0.001$) (**Figure 7A**) presenting a positive relation with air temperature (**Supplementary Table S1**). All BVOCs detected in the study were monoterpenes. The most important monoterpenes emitted by *C. incanus* leaves were α- and β-pinene, their sum accounted for about 69% of the total emitted compounds in 2014 and for 60% in 2015 (**Figure 7B**). Other monoterpenes detected were: α-, β- phellandrene, thujene, and myrcene. In summer 2015, the emission of α-pinene, β-pinene and myrcene were about five times higher compared to summer 2014 (*t*-test; $p < 0.001$; $p = 0.013$; $p = 0.011$). The emissions of β-phellandrene and thujene increased three and nine times, respectively (*t*-test; $p = 0.005$; and $p < 0.001$), while α-phellandrene emission was about 15 times higher in July 2015 than July 2014 2014 (*t*-test; $p < 0.001$) (**Figure 7B**). The PCA identified groups of plant species with similar BVOCs (and also for Pol_{Tot}), with samples collected in different years segregated in distinct groups (**Supplementary Figure S1B**). The samples collected in 2015 were grouped at the positive score of PC1 (84.16% of the total variation), presenting the higher values for Pol_{Tot} and BVOCs as well as for the leaf thickness (LT).

DISCUSSION

Leaves of summer 2014 maintained a better water status compared to the drier and hotter summer 2015 (**Table 3**). In particular, the higher leaf dehydration observed during the heat wave in July 2015, as estimated by the lower RWC, led to a consequent drop in Ψ_w (**Table 3**). Leaf morpho-anatomical traits may have played an important role to avoid leaf shrinkage associated to dehydration during drought. Indeed, when water is a limiting factor, plants undergo anatomical alterations, particularly in their leaves, in which the transpiration flow is regulated by stomatal closure (Bosabalidis and Kofidis, 2002; Scoffoni et al., 2014). It has already been reported that the dimorphic *C. incanus* develops xerophytic leaves during summer (Puglielli and Varone, 2018; Puglielli, 2019). In our study, total lamina thickness was increased by 28% in 2015, as compared to 2014, mainly due to a higher palisade parenchyma (+44%) and to a greater epidermal thickness (+28%) (**Table 2** and **Supplementary Table S1B**). The smaller leaf size (**Supplementary Figure S2**) and the greater contribution of upper epidermis and of mesophyll tissues, in particular palisade parenchyma, to the whole leaf structure (**Figure 2B** and **Supplementary Table S1B**), could have been important to increase resistance against dehydration and cell collapsing induced by the drier conditions of summer 2015 (Bosabalidis and Kofidis, 2002; De Micco and Aronne, 2012; Mansoor et al., 2019). We hypothesize that accumulation of leaf condensed tannins, both in upper epidermis and mesophyll cells (**Figure 2A**), may have contributed to strengthen the leaf structure of *C. incanus* in 2015 as previously reported for other species grown in xeric environments (Grossoni et al., 1998; Gravano et al., 2000; Bussotti, 2008). We suggest that the increment in leaf condensed tannins and the higher LT observed in the drier

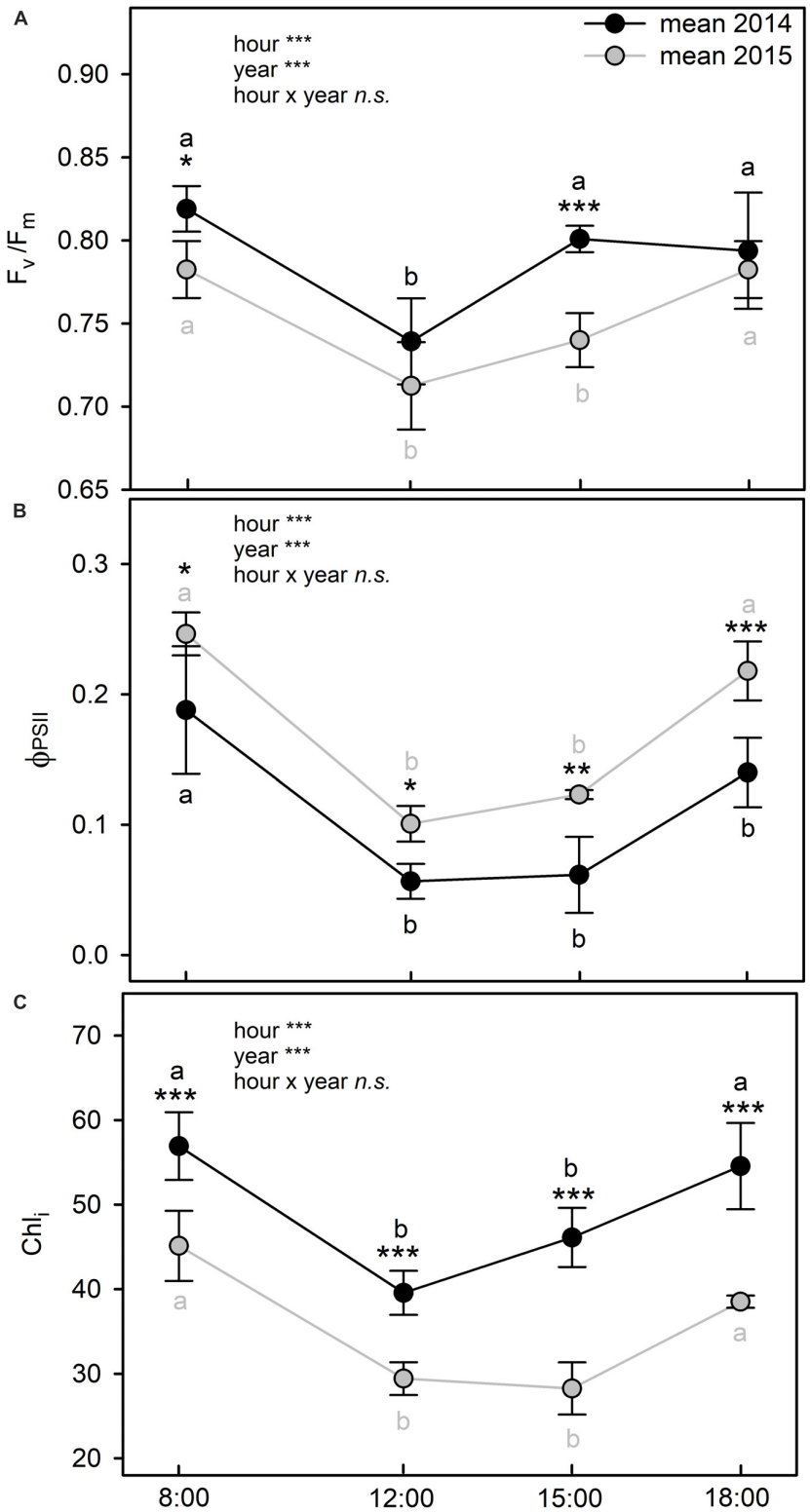

FIGURE 5 | Diurnal trends of maximal photochemical efficiency of PSII (F_v/F_m) **(A)**, actual efficiency of PSII (Φ_{PSII}) **(B)**, and Chlorophyll index (Chl_i) **(C)** of *C. incanus* leaves in July 2014 and 2015. *Two way* ANOVA followed by Tukey's pairwise comparison was performed to compare data (means ± SD; $n = 8$). Letters indicate significant differences ($p \leq 0.05$) among sampling hour for each year, whereas asterisks represent significant differences among years for each sampling hour, *($p \leq 0.05$), **($p \leq 0.01$), ***($p \leq 0.001$).

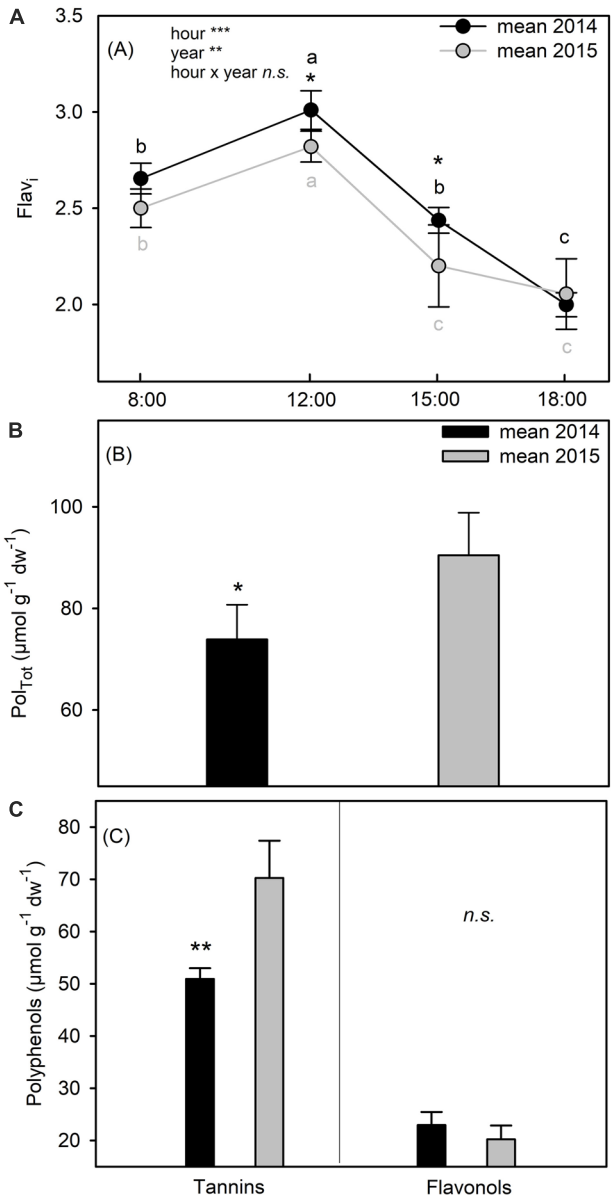

FIGURE 6 | Epidermal Flavonol index ($Flav_I$) **(A)**, total polyphenols content (Pol_{Tot}) **(B)**, condensed tannins (Tannins) and flavonols leaves content (Flavonols) **(C)** of *C. incanus* leaves in July 2014 and 2015. *Two way* ANOVA followed by Tukey's pairwise comparison was performed to compare data (means ± SD; $n = 8$). Letters indicate significant differences ($p \leq 0.05$) among sampling hour for each year, whereas asterisks represent significant differences among years for each sampling hour, *($p \leq 0.05$), **($p \leq 0.01$), ***($p \leq 0.001$).

and hotter summer 2015 resulted in a significant increase in LMA (+36%). Indeed, previous studies have clearly shown a positive relationship between LMA and LT (Puglielli et al., 2017c, 2019b; Gratani et al., 2018) and a possible contribution of soluble phenolics to LMA (Poorter et al., 2009). The higher LMA may have provided both a lower evaporative surface area and a lower light harvesting capability per unit of leaf mass (**Table 2**; Boughalleb and Hajlaoui, 2011; De Micco et al., 2011; Perez-Martin et al., 2014; De la Riva et al., 2016), enabling plants to tolerate lower Ψ_w without significant losses in leaf turgor (Munné-Bosch et al., 2003). LMA may have also an influence on leaf physiology by affecting the diffusion of CO_2 from substomatal cavities through intercellular air space to sites of carboxylation in the mesophyll tissues (Loreto and Centritto, 2008; Flexas et al., 2014; Peguero-Pina et al., 2017). In particular, several studies on non-stressed tree species have shown that a higher LMA constrains leaf mesophyll conductance (g_m), thus limiting photosynthetic assimilation rates (Syvertsen et al., 1995; Hassiotou et al., 2009). Nevertheless, recent evidences have shown that, when a higher LMA is accompanied to an increment in thickness of palisade parenchyma, this anatomical adaptation may be accompanied by a higher diffusion and availability of CO_2 across the leaf, facilitating the assimilation process (Evans, 1999; Milla-Moreno et al., 2016; Peguero-Pina et al., 2017). Similarly, in our study, the increment in LT and LMA in July 2015 may have led to a higher g_m and, in turn, resulted in a higher CO_2 uptake at midday compared to July 2014 (**Figure 3A** and **Table 3**). This result is in accordance with previous research on drought-acclimated plants, in which a positive relationship between g_m and mesophyll thickness was found, supporting the hypothesis that, under water stress, a thicker leaf increases the surface area of chloroplasts exposed to intercellular airspace per unit leaf area (Hanba et al., 1999; Terashima et al., 2001; De Micco et al., 2011; Galmés et al., 2013; Flexas et al., 2014). The higher LMA may have also contributed to lower leaf temperature in summer 2015 (Gratani and Varone, 2004), as similar daily leaf temperatures were observed between the 2 years (**Supplementary Figure S3**), despite the higher air temperatures caused by the heatwave in July 2015 (**Figure 1A**; Russo et al., 2015). In addition, the peculiar location of stomata inside epidermal crypts may have allowed the higher g_s values in 2015, which contributed to the regulation of leaf temperature and the maintenance of similar P_n between the 2 years (**Figure 3B** and **Supplementary Figure S1A**; Aronne and De Micco, 2001). We cannot exclude that other leaf morpho-anatomical adjustments (e.g., leaf rolling, variations in leaf angles and density in leaf pubescence) may have contributed to protect the photosynthetic apparatus under the drier and hotter conditions of July 2015 (**Figures 3A**, **4A** and **Supplementary Figure S2**; De Micco and Aronne, 2012; Arena et al., 2019). Particularly, paraheliotropism is an adaptative strategy of *C. incanus* to counteract the deleterious impact of high irradiance to protect leaves under stress condition, especially in summer, thus avoiding photoinhibition (Puglielli et al., 2017b; Pérez-Llorca et al., 2019). However, the P_n time course in 2015 (**Figure 3A**) showed the typical trend of a severe water-stressed plants, with a higher value in the morning followed by significant drop as the day progressed (Marino et al., 2014). In contrast, in 2014 at 15:00, the peak in P_n coupled with the drop of C_i (**Figures 3A**, **4B**) indicated the lack of significant biochemical limitations to photosynthesis (Lawlor and Cornic, 2002). Conversely, in summer 2015, C_i did not change significantly throughout the day with respect to the morning value, despite the significant drop in P_n. This result might be associated to leaf rolling and suggests that, despite

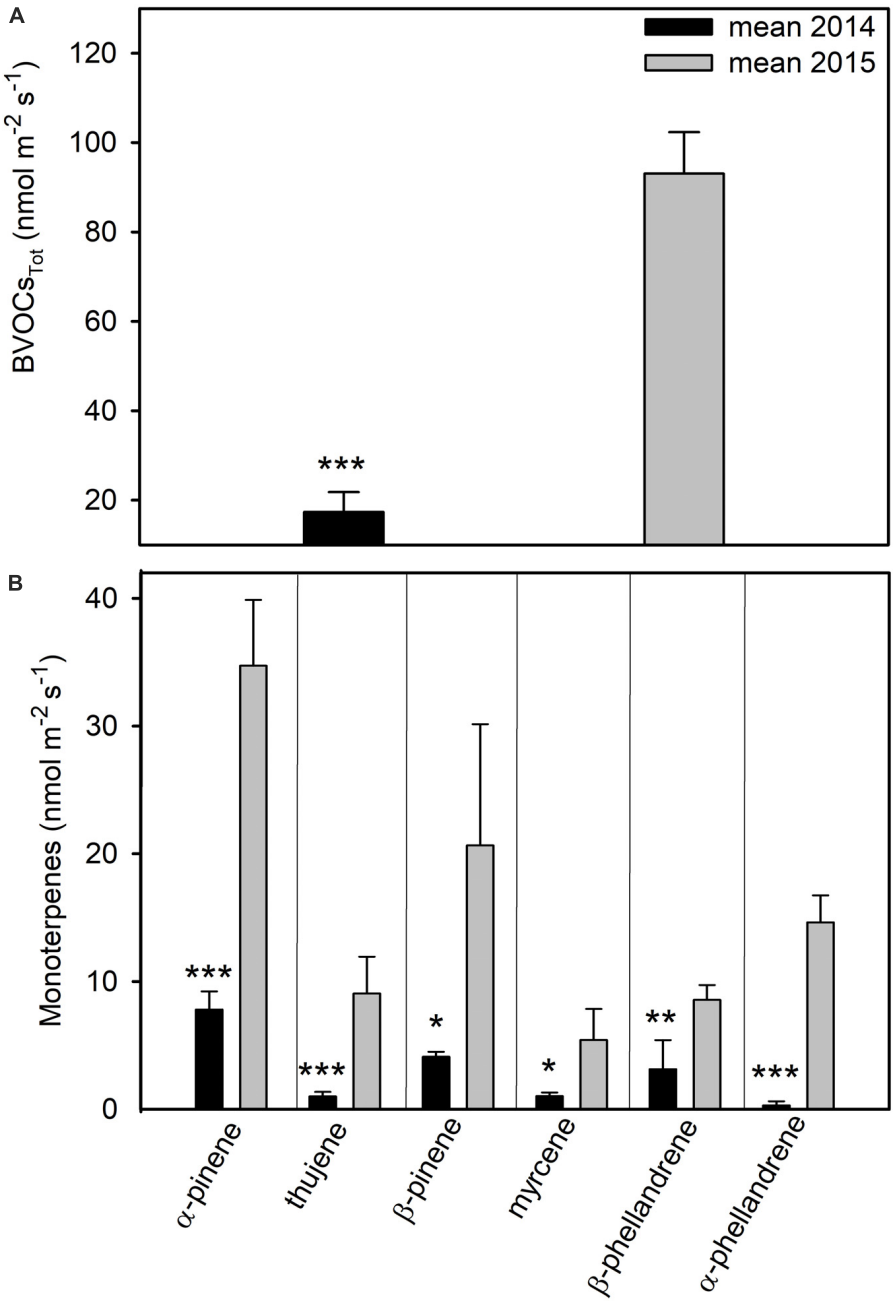

FIGURE 7 | Total biogenic volatile organic compound emission ($BVOC_{Tot}$) **(A)** and monoterpenes emitted **(B)** by *C. incanus* leaves in July 2014 and 2015. Data are means ± SD (n = 8). Asterisks represent differences between the two years, *($p \leq 0.05$), **($p \leq 0.01$), ***($p \leq 0.001$) based on t-test.

C. incanus leaf photochemistry is tolerant to extreme drought as well as different environmental conditions (Arena et al., 2011; Gori et al., 2019; Puglielli et al., 2019a), RUBP (ribulose 1, 5-bisphosphate) regeneration was partially impaired in July 2015, particularly during the hottest hours of the day, thus determining a P_n decline in 2015 when temperature was higher (Gratani et al., 2018). It is noteworthy that many studies have shown that enzymes involved in RUBP regeneration are impaired by water stress at g_s lower than 0.1 mol H_2O m^{-2} s^{-1} (Sharkey and Seemann, 1989; Sánchez-Rodríguez et al., 1997; Grassi and Magnani, 2005). In our case, even if g_s values were below this threshold in both years, we can hypothesize a significant metabolic impairment of P_n only in July 2015, especially during the hottest hours of the day (**Figure 4**). However, in *C. incanus* leaves, RUBP regeneration is likely not limited by a decrease in J_f and NADPH (nicotinamide adenine dinucleotide phosphate) synthesis (Flexas et al., 2004). In fact, the observed increase of J_f/P_n at 15:00 in July 2015 (**Figure 4C**) indicates an excess

of reducing power along the electron transport chain and a lower ability to use electrons for carbon assimilation (Sebastiani et al., 2019). In 2015, the excess of reducing power may have resulted in suboptimal F_v/F_m values (**Figure 5A**; Demmig and Björkman, 1987), which together with higher C_i (**Figure 4B**) and Φ_{PSII} (**Figure 5B**), may suggest higher utilization of alternative electron sinks (Grant et al., 2015; Puglielli et al., 2017b; Brunetti et al., 2018). At the same time, the daily down-regulation of Φ_{PSII} and the reduction of leaf chlorophyll content (**Figure 5C**) observed in both years may have worked as a photoprotection mechanism to dissipate the high amount of light intercepted during the central hours of the day (**Figure 1B**; Baquedano and Castillo, 2007; Gori et al., 2019). When the capacity of plants to use the radiant energy is severely constrained, the excess of reducing power may be utilized for the biosynthesis of secondary metabolites, such as isoprenoids and polyphenols (Niinemets et al., 2002a,b; Harrison et al., 2013; Tattini et al., 2015). Indeed, secondary metabolites have been suggested to act as alternative electron sinks by consuming trioses phosphate, ATP (adenosine triphosphate) and NADPH, thus playing a role as an energy escape valve (Hernández and Van Breusegem, 2010; Morfopoulos et al., 2013). Among secondary metabolites, polyphenols perform different functions depending on their location in the leaf, acting as both radiation screeners, quenchers of ROS and key molecules involved in the acclimation processes to diurnal changes in UV-B radiation (Agati and Tattini, 2010; Agati et al., 2012; Jansen et al., 2012; Barnes et al., 2016; Tohge and Fernie, 2017; Neugart and Schreiner, 2018). Indeed, the comparable trends of flavonol index ($Flav_i$) observed in both years (**Figure 6A**) could be related to similar diurnal changes in UV radiations (Stephanou and Manetas, 1997; Brossa et al., 2009). Furthermore, the reduction of chlorophyll content (**Figure 5C**), concomitantly with the increase in flavonols in the epidermis (**Figure 6A**) observed at 12:00 in both summers, may indicate that reversible changes in leaf biochemistry have helped *C. incanus* overcome stressful conditions on a daily basis (Mittler, 2006). Polyphenols of *C. incanus* leaves mainly belong to the classes of flavonols (quercetin and myricetin derivatives) and condensed tannins (Gori et al., 2016, 2020). Both classes of molecules possess antioxidant function and may have played a role in the inhibition of radical formation under severe stress conditions (**Figure 6C**; Hernández et al., 2004; Barbehenn et al., 2006; Sebastiani et al., 2019). In addition, flavonols may have contributed to both UV-B shielding and improve photo-protection at 12:00 (Burchard et al., 2000). As above mentioned, tannins may have helped increase leaf structure under the drier and hotter conditions of summer 2015 (**Figure 2** and **Supplementary Figure S1B**; Ishida et al., 2008; Tharayil et al., 2011; Sumbele et al., 2012; Top et al., 2017). In support of this hypothesis, we found a statistically significant correlation between total polyphenols, mainly constituted by tannins, and air temperature (**Table 2** and **Supplementary Table S1A**). The increase in tannin production observed in July 2015 could be also interpreted as a defense trait of *C. incanus* to protect the resources acquired during the growing season, thus contributing to retard leaf senescence and abscission and optimizing resource acquisition in nutrient-poor soils conditions (Mediavilla et al., 2001; Wright and Westoby, 2002; Poorter et al., 2009; Massad et al., 2014; Gratani et al., 2016; Puglielli et al., 2017a). Finally, the increment of the fiber-bound proportion of tannins in the leaf cell walls during leaf maturation may have contributed to the lignification process, thus protecting against pathogens and herbivores attack (Zucker, 1983; Bussotti et al., 1998). Another mechanism for counteracting leaf photo-oxidative damage under drought is the biosynthesis of BVOCs (Loreto and Schnitzler, 2010). The emission of monoterpenes is largely widespread among Mediterranean shrub vegetation exposed to concomitant stresses. In fact, these BOVCs have multiple protective functions (Rivoal et al., 2010; Fares et al., 2013; Fineschi et al., 2013; Llusià et al., 2016), ranging from antioxidant (Loreto et al., 2004; Llusià et al., 2006), protection against high temperatures (Owen et al., 2002; Haberstroh et al., 2018), defense against pathogens and herbivores to wound sealing after damage (Pichersky and Gershenzon, 2002). We observed a strong increment in monoterpene emissions in July 2015 compared to July 2014 (**Figure 7**), likely as a consequence of the higher air temperatures due to the 2015 heat wave (**Figure 1A** and **Supplementary Figure S1B**). This is because, being highly volatile, the higher air temperature in 2015 increased the monoterpene partial pressure gradient between leaf and the atmosphere (Niinemets et al., 2010), resulting in their higher emissions than in 2014 (**Supplementary Table S1A**). However, no qualitative differences in the blend of monoterpenes emerged between the two years. Our results are consistent with those of Owen et al. (2001, 2002) who found α-pinene as the major monoterpene produced by this species. In addition, α-pinene and β-pinene, β-myrcene and α-phellandrene emissions were already detected in others *Cistus* spp. (Ormeño et al., 2007; Rivoal et al., 2010; Haberstroh et al., 2018). A high production of these compounds has been shown to help the leaves to withstand drought, which supports the assumption that they improve membrane stability, thus conferring thermal protection (Loreto et al., 1998; Copolovici et al., 2005). Hence, the diverse blend of terpenes detected in the emissions of this species may likely contributes to the drought tolerance of *C. incanus* under field conditions.

CONCLUSION

In conclusion, the results of our study indicate that *C. incanus* is a climate resilient species able to tolerate different environmental conditions, including threats caused by extreme weather events, as revealed from the new evidence on its capacity to adjust morpho-physiological and biochemical traits. In particular, the major investment in leaf construction observed in the drier and hotter conditions caused by the summer 2015 heat wave helped avoid leaf shrinkage associated to dehydration. Interestingly, the stimulation of the biosynthesis of secondary metabolites, in particular of monoterpenes and tannins, may have increased leaf thermo-tolerance and may have counteracted photooxidative damage, thus protecting *C. incanus* photosynthetic apparatus and allowing the maintenance of carbon assimilation despite the severe water and temperature stresses. Therefore, our

results suggest that *C. incanus* might have greater potential to acclimate to climate change in its natural environment.

DATA AVAILABILITY STATEMENT

All datasets generated for this study are included in the article/**Supplementary Material**, further inquiries can be directed to the corresponding author.

AUTHOR CONTRIBUTIONS

AG and CB: conceptualization and validation. GM, CG, BM, and AG: data curation. GM and BM: formal analysis. MC and FF: funding acquisition. AG: investigation. CB: methodology. MC: supervision. FA, CB, and AG: writing – original draft. MC, FF, and MT: writing – review and editing. All authors contributed to the article and approved the submitted version.

FUNDING

This work was supported by funds from the Italian MIUR to CNR, project Economia Circolare (Green & Circular Economy-GECE) (FOE-2019, 436 DBA.AD003.139).

SUPPLEMENTARY MATERIAL

The Supplementary Material for this article can be found online at: https://www.frontiersin.org/articles/10.3389/fevo.2020.576296/full#supplementary-material

REFERENCES

Agati, G., Azzarello, E., Pollastri, S., and Tattini, M. (2012). Flavonoids as antioxidants in plants: location and functional significance. *Plant Sci.* 196, 67-76. doi: 10.1016/j.plantsci.2012.07.014

Agati, G., and Tattini, M. (2010). Multiple functional roles of flavonoids in photoprotection. *New Phytol.* 186, 786-793. doi: 10.1111/j.1469-8137.2010.03269.x

Agati, G., Tuccio, L., Kusznierewicz, B., Chmiel, T., Bartoszek, A., Kowalski, A., et al. (2016). Nondestructive optical sensing of flavonols and chlorophyll in white head cabbage (*Brassica oleracea* L. *var. capitata subvar. alba)* grown under different nitrogen regimens. *J. Agric. Food Chem.* 64, 85-94. doi: 10.1021/acs.jafc.5b04962

Arena, C., De Micco, V., De Maio, A., Mistretta, C., Aronne, G., and Vitale, L. (2013). Winter and summer leaves of *Cistus incanus*: differences in leaf morphofunctional traits, photosynthetic energy partitioning, and poly (ADP-ribose) polymerase (PARP) activity. *Botany* 91, 805-813.

Arena, C., Mistretta, C., Di Natale, E., Mennella, M. R. F., De Santo, A. V., and De Maio, A. (2011). Characterization and role of poly (ADP-ribosyl) ation in the Mediterranean species Cistus incanus L. *under different temperature conditions. Plant Physiol. Biochem.* 49, 435-440. doi: 10.1016/j.plaphy.2011.02.004

Arena, C., and Vitale, L. (2018). Chilling-induced reduction of photosynthesis is mitigated by exposure to elevated CO2 concentrations. *Photosynthetica* 56, 1259-1267. doi: 10.1007/s11099-018-0843-3

Arena, C., Vitale, L., Bianchi, A. R., Mistretta, C., Vitale, E., and Parisi, C., et al. (2019). The ageing process affects the antioxidant defences and the poly (ADPribosyl) ation activity in *Cistus incanus* L. leaves. *Antioxidants.* 8:528. doi: 10.3390/antiox8110528

Aronne, G., and De Micco, V. (2001). Seasonal dimorphism in the Mediterranean *Cistus incanus* L. *subsp. incanus*. *Ann. Bot.* 87, 789-794. doi: 10.1006/anbo.2001.1407

Baquedano, F. J., and Castillo, F. J. (2007). Drought tolerance in the Mediterranean species *Quercus coccifera*, *Quercus ilex*, *Pinus halepensis*, and *Juniperus phoenicea*. *Photosynthetica* 45, 229-238. doi: 10.1007/s11099-007-0037-x

Barbehenn, R. V., Jones, C. P., Hagerman, A. E., Karonen, M., and Salminen, J. P. (2006). Ellagitannins have greater oxidative activities than condensed tannins and galloyl glucoses at high pH: potential impact on caterpillars. *J. Chem. Ecol.* 32, 2253-2267. doi: 10.1007/s10886-006-9143-7

Barnes, P. W., Tobler, M. A., Keefover-Ring, K., Flint, S. D., Barkley, A. E., Ryel, R. J., et al. (2016). Rapid modulation of ultraviolet shielding in plants is influenced by solar ultraviolet radiation and linked to alterations in flavonoids. *Plant Cell Environ.* 39, 222-230. doi: 10.1111/pce.12609

Bosabalidis, A. M., and Kofidis, G. (2002). Comparative effects of drought stress on leaf anatomy of two olive cultivars. *Plant Sci.* 163, 375-379. doi: 10.1016/S0168-9452(02)00135-8

Boughalleb, F., and Hajlaoui, H. (2011). Physiological and anatomical changes induced by drought in two olive cultivars (cv Zalmati and Chemlali). *Acta Physiol Plant* 33, 53-65. doi: 10.1007/s11738-010-0516-8

Brilli, F., Tsonev, T., Mahmood, T., Velikova, V., Loreto, F., and Centritto, M. (2013). Ultradian variation of isoprene emission, photosynthesis, mesophyll conductance, and optimum temperature sensitivity for isoprene emission in water-stressed *Eucalyptus citriodora* saplings. *J. Exp. Bot.* 64, 519-528. doi: 10.1093/jxb/ers353

Brossa, R., Casals, I., Pintó-Marijuan, M., and Fleck, I. (2009). Leaf flavonoid content in *Quercus ilex* L. resprouts and its seasonal variation. *Trees* 23, 401-408. doi: 10.1007/s00468-008-0289-5

Brunetti, C., Guidi, L., Sebastiani, F., and Tattini, M. (2015). Isoprenoids and phenylpropanoids are key components of the antioxidant defense system of plants facing severe excess light stress. *Environ. Exp. Bot.* 119, 54-62. doi: 10.1016/j.envexpbot.2015.04.007

Brunetti, C., Loreto, F., Ferrini, F., Gori, A., Guidi, L., Remorini, D., et al. (2018). Metabolic plasticity in the hygrophyte *Moringa oleifera* exposed to water stress. *Tree Physiol.* 38, 1640-1654. doi: 10.1093/treephys/tpy089

Burchard, P., Bilger, W., and Weissenböck, G. (2000). Contribution of hydroxycinnamates and flavonoids to epidermal shielding of UV-A and UV-B radiation in developing rye primary leaves as assessed by ultraviolet-induced chlorophyll fluorescence measurements. *Plant Cell Environ.* 23, 1373-1380. doi: 10.1046/j.1365-3040.2000.00633.x

Bussotti, F. (2008). Functional leaf traits, plant communities and acclimation processes in relation to oxidative stress in trees: a critical overview. *Glob Chang Biol.* 14, 2727-2739. doi: 10.1111/j.1365-2486.2008.01677.x

Bussotti, F., Gravano, E., Grossoni, P., and Tani, C. (1998). Occurrence of tannins in leaves of beech trees (*Fagus sylvatica*) along an ecological gradient, detected by histochemical and ultrastructural analyses. *New Phytol.* 138, 469-479. doi: 10.1046/j.1469-8137.1998.00121.x

Catoni, R., Gratani, L., and Varone, L. (2012). Physiological, morphological and anatomical trait variations between winter and summer leaves of *Cistus species*. *Flora* 207, 442-449. doi: 10.1016/j.flora.2012.02.007

Copolovici, L. O., Filella, I., Llusià, J., Niinemets, Ü., and Peñuelas, J. (2005). The capacity for thermal protection of photosynthetic electron transport varies for different monoterpenes in *Quercus ilex*. *Plant Physiol.* 139, 485-496. doi: 10.1104/pp.105.065995

Correia, O., and Ascensao, L. (2016). "Summer semi-deciduous species of the Mediterranean landscape: a winning strategy of cistus species to face the predicted changes of the Mediterranean climate," in *Plant Biodiversity. Monitoring, Assessment and Conservation*, eds A. A. Ansari, S. S. Gill, Z. K. Abbas, and M. Naeem (Wallingford: CAB International), 195–217.

David, T. S., Henriques, M. O., Kurz-Besson, C., Nunes, J., Valente, F., and Vaz, M. et al. (2007). Water-use strategies in two co-occurring Mediterranean evergreen oaks: surviving the summer drought. *Tree Physiol.* 27, 793-803. doi: 10.1093/treephys/27.6.793

De Dato, G. D., Micali, M., Jaoudé, R. A., Liberati, D., and De Angelis, P. (2013). Earlier summer drought affects leaf functioning of the Mediterranean species *Cistus monspeliensis* L. *Environ. Exp. Bot.*93, 13-19. doi: 10.1016/j.envexpbot.2013.03.007

De la Riva, E. G., Olmo, M., Poorter, H., Ubera, J. L., and Villar, R. (2016). Leaf mass per area (LMA) and its relationship with leaf structure and anatomy in 34 Mediterranean woody species along a water availability gradient. *PLoS One* 11:e0148788. 10.1371/journal.pone.0148788

De Micco, V., Arena, C., Vitale, L., Aronne, G., and Virzo De Santo, A. (2011). Anatomy and photochemical behaviour of Mediterranean Cistus incanus winter leaves under natural outdoor and warmer indoor conditions. *Botany* 89, 677-688. doi: 10.1139/b11-059

De Micco, V., and Aronne, G. (2009). Seasonal dimorphism in wood anatomy of the Mediterranean *Cistus incanus* L. *subsp. incanus*. *Trees* 23, 981-989. doi: 10.1007/s00468-009-0340-1

De Micco, V., and Aronne, G. (2012). "Morpho-Anatomical traits for plant adaptation to drought," in *Plant Responses to Drought Stress: From Morphological to Molecular Features*, eds A. Ricardo (New York, NY: Springer), 37–61.

Demmig, B., and Björkman, O. (1987). Comparison of the effect of excessive light on chlorophyll fluorescence (77K) and photon yield of O2 evolution in leaves of higher plants. *Planta* 171, 171-184. doi: 10.1007/BF00391092

Di Ferdinando, M., Brunetti, C., Agati, G., and Tattini, M. (2014). Multiple functions of polyphenols in plants inhabiting unfavorable Mediterranean areas. *Environ. Exp. Bot.* 103, 107-116. doi: 10.1016/j.envexpbot.2013.09.012

Evans, J. R. (1999). Leaf anatomy enables more equal access to light and CO2 between chloroplasts. *New Phytol.* 143, 93-104. doi: 10.1046/j.1469-8137.1999.00440.x

Fares, S., Schnitzhofer, R., Jiang, X., Guenther, A., Hansel, A., and Loreto, F. (2013). Observations of diurnal to weekly variations of monoterpene-dominated fluxes of volatile organic compounds from mediterranean forests: implications for regional modeling. *Environ. Sci. Technol.* 47, 11073-11082. doi: 10.1021/es4022156

Fineschi, S., Loreto, F., Staudt, M., and Peñuelas, J. (2013). "Diversification of volatile isoprenoid emissions from trees: evolutionary and ecological perspectives" in *Biology, Controls and Models of Tree Volatile Organic Compound Emissions*, eds Ü. Niinemets, and R. K. Monson (Dordrecht, NL: Springer) 1–20.

Flexas, J., Bota, J., Loreto, F., Cornic, G., and Sharkey, T. D. (2004). Diffusive and metabolic limitations to photosynthesis under drought and salinity in C3 plants. *Plant Biol.* 6, 269-279. 10.1055/s-2004-820867

Flexas, J., Diaz-Espejo, A., Gago, J., Gallé, A., Galmés, J., Gulías, J., et al. (2014). Photosynthetic limitations in Mediterranean plants: a review. *Environ. Exp. Bot.* 103, 12-23. doi: 10.1016/j.envexpbot.2013.09.002

Galle, A., Florez-Sarasa, I., Aououad, H. E., and Flexas, J. (2011). The Mediterranean evergreen *Quercus ilex* and the semi-deciduous *Cistus albidus* differ in their leaf gas exchange regulation and acclimation to repeated drought and re-watering cycles. *J. Exp. Bot.*62, 5207-5216. doi: 10.1093/jxb/err233

Galmés, J., Abadía, A., Cifre, J., Medrano, H., and Flexas, J. (2007). Photoprotection processes under water stress and recovery in Mediterranean plants with different growth forms and leaf habits. *Physiol. Plant.* 130, 495-510. doi: 10.1111/j.1399-3054.2007.00919.x

Galmés, J., Ochogavía, J. M., Gago, J., Roldán, E. J., Cifre, J., and Conesa, M. À. (2013). Leaf responses to drought stress in Mediterranean accessions of *Solanum lycopersicum*: anatomical adaptations in relation to gas exchange parameters. *Plant Cell Environ.* 36, 920-935. doi: 10.1111/pce.12022

Genty, B., Briantais, J. M., and Baker, N. R. (1989). The relationship between the quantum yield of photosynthetic electron transport and quenching of chlorophyll fluorescence. *Biochim. Biophys. Acta* 990, 87-92. doi: 10.1016/S0304-4165(89)80016-9

Gori, A., Ferrini, F., Marzano, M. C., Tattini, M., Centritto, M., Baratto, M. C., et al. (2016). Characterisation and antioxidant activity of crude extract and polyphenolic rich fractions from *C. incanus leaves*. *Int. J. Mol. Sci.* 17:1344. doi: 10.3390/ijms17081344

Gori, A., Nascimento, L. B., Ferrini, F., Centritto, M., and Brunetti, C. (2020). Seasonal and diurnal variation in leaf phenolics of three medicinal mediterranean wild species: what is the best harvesting moment to obtain the richest and the most antioxidant extracts? *Molecules* 25:956. doi: 10.3390/molecules25040956

Gori, A., Tattini, M., Centritto, M., Ferrini, F., Marino, G., Mori, J., et al. (2019). Seasonal and daily variations in primary and secondary metabolism of three maquis shrubs unveil different adaptive responses to Mediterranean climate. *Conserv. Physiol.*7:coz070. doi: 10.1093/conphys/coz070

Grant, O. M., Tronina, Ł., García-Plazaola, J. I., Esteban, R., Pereira, J. S., and Chaves, M. M. (2015). Resilience of a semi-deciduous shrub, *Cistus salvifolius*, to severe summer drought and heat stress. *Funct. Plant Biol.* 42, 219-228. doi: 10.1071/FP14081

Grassi, G., and Magnani, F. (2005). Stomatal, mesophyll conductance and biochemical limitations to photosynthesis as affected by drought and leaf ontogeny in ash and oak trees. *Plant Cell Environ.* 28, 834-849. doi: 10.1111/j.1365-3040.2005.01333.x

Gratani, L., Catoni, R., and Varone, L. (2013). Morphological, anatomical and physiological leaf traits of *Q. ilex, P. latifolia, P. lentiscus, and M. communis* and their response to Mediterranean climate stress factors. *Bot Stud.* 54, 35-46. doi: 10.1186/1999-3110-54-35

Gratani, L., Catoni, R., and Varone, L. (2016). Evergreen species response to Mediterranean climate stress factors. *iForest* 9, 946-953. doi: 10.3832/ifor1848-009

Gratani, L., and Varone, L. (2004). Adaptive photosynthetic strategies of the Mediterranean maquis species according to their origin. *Photosynthetica* 42, 551-558. doi: 10.1007/S11099-005-0012-3

Gratani, L., Varone, L., and Catoni, R. (2008). Relationship between net photosynthesis and leaf respiration in Mediterranean evergreen species. *Photosynthetica* 46, 567-573. doi: 10.1007/s11099-008-0095-8

Gratani, L., Varone, L., Crescente, M. F., Catoni, R., Ricotta, C., and Puglielli, G. (2018). Leaf thickness and density drive the responsiveness of photosynthesis to air temperature in Mediterranean species according to their leaf habitus. *J. Arid Environ.* 150, 9-14. doi: 10.1016/j.jaridenv.2017.12.007

Gravano, E., Desotgiu, R., Tani, C., Bussotti, F., and Grossoni, P. (2000). Structural adaptations in leaves of two Mediterranean evergreen shrubs under. *JME* 1, 165–170.

Grossoni, P., Bussotti, F., Tani, C., Gravano, E., Antarelli, S., Bottacci, A., et al. (1998). Morpho-anatomical aterations in leaves of *Gagus vatica* L. and *Quercus ilex* L. in different environmental stress condition. *Chemosphere* 36, 919–924. doi: 10.1016/S0045-6535(97)10148-5

Haberstroh, S., Kreuzwieser, J., Lobo-do-Vale, R., Caldeira, M. C., Dubbert, M., and Werner, C. (2018). Terpenoid emissions of two Mediterranean woody species in response to drought stress. *Front. Plant Sci.*9, 1071-1087. doi: 10.3389/fpls.2018.01071

Hanba, Y. T., Miyazawa, S. I., and Terashima, I. (1999). The influence of leaf thickness on the CO2 transfer conductance and leaf stable carbon isotope ratio for some evergreen tree species in Japanese warm-temperate forests. *Funct. Ecol.* 13, 632-639. doi: 10.1046/j.1365-2435.1999.00364.x

Harley, P. C., Loreto, F., Di Marco, G., and Sharkey, T. D. (1992). Theoretical considerations when estimating the mesophyll conductance to CO2 flux by analysis of the response of photosynthesis to CO2. *Plant Physiol.* 98, 1429-1436. doi: 10.1104/pp.98.4.1429

Harrison, S. P., Morfopoulos, C., Dani, K. S., Prentice, I. C., Arneth, A., Atwell, B. J., et al. (2013). Volatile isoprenoid emissions from plastid to planet. *New Phytol.* 197, 49-57. doi: 10.1111/nph.12021

Hassiotou, F., Ludwig, M., Renton, M., Veneklaas, E. J., and Evans, J. R. (2009). Influence of leaf dry mass per area, CO2, and irradiance on mesophyll conductance in sclerophylls. *J. Exp Bot.* 60, 2303-2314. doi: 10.1093/jxb/erp021

Hernández, I., Alegre, L., and Munné-Bosch, S. (2004). Drought-induced changes in flavonoids and other low molecular weight antioxidants in *Cistus clusii* grown under Mediterranean field conditions. *Tree Physiol.* 24, 1303-1311. doi: 10.1093/treephys/24.11.1303

Hernández, I., and Van Breusegem, F. (2010). Opinion on the possible role of flavonoids as energy escape valves: novel tools for nature's Swiss army knife? *Plant Sci.* 179, 297-301. doi: 10.1016/j.plantsci.2010.06.001

Ishida, A., Nakano, T., Yazaki, K., Matsuki, S., Koike, N., Lauenstein, D. L., et al. (2008). Coordination between leaf and stem traits related to leaf carbon gain and hydraulics across 32 drought-tolerant angiosperms. *Oecologia* 156, 193-202. doi: 10.1007/s00442-008-0965-6

Jansen, M. A. K., Hideg, E., and Lidon, F. J. C. (2012). UV-B radiation: when does the stressor cause stress? *Emir. J. Food Agric*. 24, 1–3. doi: 10.9755/ejfa.v24i6.14663

Kok, B. (1948). A critical consideration of the quantum yield of Chlorella photosynthesis. *Enzymologia* 13, 1–56.

Lawlor, D. W., and Cornic G. (2002). Photosynthetic carbon assimilation and associated metabolism in relation to water deficits in higher plants. *Plant Cell Environ.* 25, 275-294. doi: 10.1046/j.0016-8025.2001.00814.x

Lefi, E., Medrano, H., and Cifre, J. (2004). Water uptake dynamics, photosynthesis and water use efficiency in field-grown *Medicago arborea* and *Medicago citrina* under prolonged Mediterranean drought conditions. *Ann. Appl. Biol.* 144, 299-307. doi: 10.1111/j.1744-7348.2004.tb00345.x

Lionello, P., Malanotte-Rizzoli, P., Boscolo, R., Alpert, P., Artale, V., Li, L., et al. (2006). "The Mediterranean climate: an overview of the main characteristics and issues," in *Mediterranean Climate Variability*, eds P. Lionello, P. Malanotte-Rizzoli, and R. Boscolo (Amsterdam, NL: Elviser), 1–26. doi: 10.1016/S1571-9197(06)80003-0

Llusià, J., Peñuelas, J., Alessio, G. A., and Estiarte, M. (2006). Seasonal contrasting changes of foliar concentrations of terpenes and other volatile organic compound in four dominant species of a Mediterranean shrubland submitted to a field experimental drought and warming. *Physiol Plant.* 127, 632-649. doi: 10.1111/j.1399-3054.2006.00693.x

Llusià, J., Roahtyn, S., Yakir, D., Rotenberg, E., Seco, R., Guenther, A., et al. (2016). Photosynthesis, stomatal conductance and terpene emission response to water availability in dry and mesic Mediterranean forests. *Trees* 30, 749-759. doi: 10.1007/s00468-015-1317-x

Loreto, F., Förster, A., Dürr, M., Csiky, O., and Seufert, G. (1998). On the monoterpene emission under heat stress and on the increased thermotolerance of leaves of *Quercus ilex* L. *fumigated with selected monoterpenes*. *Plant Cell Environ.* 21, 101-107. doi: 10.1046/j.1365-3040.1998.00268.x

Loreto, F., Pinelli, P., Manes, F., and Kollist, H. (2004). Impact of ozone on monoterpene emissions and evidence for an isoprene-like antioxidant action of monoterpenes emitted by *Quercus ilex* leaves. *Tree Physiol.* 24, 361-367. doi: 10.1093/treephys/24.4.361

Loreto, F., Pollastri, S., Fineschi, S., and Velikova, V. (2014). Volatile isoprenoids and their importance for protection against environmental constraints in the Mediterranean area. *Environ. Exp. Bot.* 103, 99-106. doi: 10.1016/j.envexpbot.2013.09.005

Loreto, F., and Schnitzler, J. P. (2010). Abiotic stresses and induced BVOCs. *Trends Plant Sci.* 15, 154-166. doi: 10.1016/j.tplants.2009.12.006

Loreto F., and Centritto M. (2008). Leaf carbon assimilation in a water-limited world. *Plant Biosyst.* 142, 154-161. doi: 10.1080/11263500701872937

Mansoor, U., Fatima, S., Hameed, M., Naseer, M., Ahmad, M. S. A., Ashraf, M., et al. (2019). Structural modifications for drought tolerance in stem and leaves of *Cenchrus ciliaris* L. *ecotypes from the Cholistan Desert*. *Flora* 261:151485. doi: 10.1016/j.flora.2019.151485

Marino, G., Pallozzi, E., Cocozza, C., Tognetti, R., Giovannelli, A., Cantini, C., et al. (2014). Assessing gas exchange, sap flow and water relations using tree canopy spectral reflectance indices in irrigated and rainfed *Olea europaea* L. *Environ. Exp. Bot.* 99, 43-52. doi: 10.1016/j.envexpbot.2013.10.008

Massad, T. J., Trumbore, S. E., Ganbat, G., Reichelt, M., Unsicker, S., Boeckler, A., et al. (2014). An optimal defense strategy for phenolic glycoside production in *Populus trichocarpa*–isotope labeling demonstrates secondary metabolite production in growing leaves. *New Phytol.* 203, 607-619. doi: 10.1111/nph.12811

Mediavilla, S., Escudero, A., and Heilmeier, H. (2001). Internal leaf anatomy and photosynthetic resource-use efficiency: interspecific and intraspecific comparisons. *Tree Physiol.* 21, 251-259. doi: 10.1093/treephys/21.4.251

Medrano, H., Flexas, J., and Galmés, J. (2009). Variability in water use efficiency at the leaf level among Mediterranean plants with different growth forms. *Plant Soil* 317, 17-29. doi: 10.1007/s11104-008-9785-z

Milla-Moreno, E. A., McKown, A. D., Guy, R. D., and Soolanayakanahally, R. Y. (2016). Leaf mass per area predicts palisade structural properties linked to mesophyll conductance in balsam poplar (*Populus balsamifera* L.). *Botany* 94, 225-239. doi: 10.1139/cjb-2015-0219

Mittler, R. (2006). Abiotic stress, the field environment and stress combination. *Trends Plant Sci.* 11, 15-19. doi: 10.1016/j.tplants.2005.11.002

Morfopoulos, C., Prentice, I. C., Keenan, T. F., Friedlingstein, P., Medlyn, B. E., Peñuelas, J., et al. (2013). Unifying conceptual model for the environmental responses of isoprene emissions from plants. *Ann. Bot.* 112, 1223-1238. doi: 10.1093/aob/mct206

Mu, Z., Llusià, J., Liu, D., Ogaya, R., Asensio, D., Zhang, C., et al. (2018). Seasonal and diurnal variations of plant isoprenoid emissions from two dominant species in Mediterranean shrubland and forest submitted to experimental drought. *Atmos Environ*. 191, 105-115. doi: 10.1016/j.atmosenv.2018.08.010

Munné-Bosch, S., Jubany-Marí, T., and Alegre, L. (2003). Enhanced photo-and antioxidative protection, and hydrogen peroxide accumulation in drought-stressed *Cistus clusii* and *Cistus albidus* plants. *Tree Physiol.* 23, 1-12. doi: 10.1093/treephys/23.1.1

Neugart, S., and Schreiner, M. (2018). UVB and UVA as eustressors in horticultural and agricultural crops. *Sci. Hortic.* 234, 370-381. doi: 10.1016/j.scienta.2018.02.021

Niinemets, Ü., Arneth, A., Kuhn, U., Monson, R. K., Peñuelas, J., and Staudt, M. (2010). The emission factor of volatile isoprenoids: stress, acclimation, and developmental responses. *Biogeosciences* 7, 2203–2223. doi: 10.5194/bg-7-2203-2010

Niinemets, Ü., Hauff, K., Bertin, N., Tenhunen, J. D., Steinbrecher, R., and Seufert, G. (2002a). Monoterpene emissions in relation to foliar photosynthetic and structural variables in Mediterranean evergreen *Quercus* species. *New Phytol.* 153, 243-256. doi: 10.1046/j.0028-646X.2001.00323.x

Niinemets, Ü., Kännaste, A., and Copolovici, L. (2013). Quantitative patterns between plant volatile emissions induced by biotic stresses and the degree of damage. *Front. Plant Sci.* 4:276. doi: 10.3389/fpls.2013.00262

Niinemets, Ü., Seufert, G., Steinbrecher, R., and Tenhunen, J. D. (2002b). A model coupling foliar monoterpene emissions to leaf photosynthetic characteristics in Mediterranean evergreen *Quercus* species. *New Phytol.* 153, 257-275. doi: 10.1046/j.0028-646X.2001.00324.x

Nogués, I., Medori, M., and Calfapietra, C. (2015). Limitations of monoterpene emissions and their antioxidant role in *Cistus* sp. under mild and severe treatments of drought and warming. *Environ. Exp. Bot.*119, 76-86. doi: 10.1016/j.envexpbot.2015.06.001

Ormeño, E., Mevy, J. P., Vila, B., Bousquet-Mélou, A., Greff, S., Bonin, G., et al. (2007). Water deficit stress induces different monoterpene and sesquiterpene emission changes in Mediterranean species. Relationship between terpene emissions and plant water potential. *Chemosphere*67, 276-284. doi: 10.1016/j.chemosphere.2006.10.029

Owen, S. M., Boissard, C., and Hewitt, C. N. (2001). Volatile organic compounds (VOCs) emitted from 40 Mediterranean plant species: VOC speciation and extrapolation to habitat scale. *Atmos. Environ.* 35, 5393-5409. doi: 10.1016/S1352-2310(01)00302-8

Owen, S. M., Harley, P., Guenther, A., and Hewitt, C. N. (2002). Light dependency of VOC emissions from selected Mediterranean plant species. *Atmos Environ.* 36, 3147-3159. doi: 10.1016/S1352-2310(02)00235-2

Papaefthimiou, D., Papanikolaou, A., Falara, V., Givanoudi, S., Kostas, S., and Kanellis, A. K. (2014). Genus *Cistus*: a model for exploring labdane-type diterpenes' biosynthesis and a natural source of high value products with biological, aromatic, and pharmacological properties. *Front. Chem.*2:35. doi: 10.3389/fchem.2014.00035

Parra, A., and Moreno, J. M. (2018). Drought differentially affects the post-fire dynamics of seeders and resprouters in a Mediterranean shrubland. *Sci. Total Environ.*626, 1219-1229. doi: 10.1016/j.scitotenv.2018.01.174

Peguero-Pina, J. J., Sisó, S., Flexas, J., Galmés, J., García-Nogales, A., Niinemets, Ü., et al. (2017). Cell-level anatomical characteristics explain high mesophyll conductance and photosynthetic capacity in sclerophyllous Mediterranean oaks. *New Phytol.* 214, 585-596. doi: 10.1111/nph.14406

Pérez-Llorca, M., Casadesús, A., Müller, M., and Munné-Bosch, S. (2019). Leaf orientation as part of the leaf developmental program in the semi-deciduous shrub, *Cistus albidus* L.: diurnal, positional and photoprotective effects during winter. *Front. Plant Sci.* .10:767. doi: 10.3389/fpls.2019.00767

Perez-Martin, A., Michelazzo, C., Torres-Ruiz, J. M., Flexas, J., Fernández, J. E., Sebastiani, L., et al. (2014). Regulation of photosynthesis and stomatal and mesophyll conductance under water stress and recovery in olive trees: correlation with gene expression of carbonic anhydrase and aquaporins. *J. Exp. Bot.* 65, 3143-3156. doi: 10.1093/jxb/eru160

Pichersky, E., and Gershenzon, J. (2002). The formation and function of plant volatiles: perfumes for pollinator attraction and defense. *Curr. Opin. Plant Biol.* 5, 237-243. doi: 10.1016/S1369-5266(02)00251-0

Poorter, H., Niinemets, Ü., Poorter, L., Wright, I. J., and Villar, R. (2009). Causes and consequences of variation in leaf mass per area (LMA): a meta-analysis. *New Phytol.* 182, 565-588. doi: 10.1111/j.1469-8137.2009.02830.x

Puglielli, G. (2019). Beyond the concept of winter-summer leaves of mediterranean seasonal dimorphic species. *Front. Plant Sci.* 10:696. doi: 10.3389/fpls.2019.00696

Puglielli, G., Catoni, R., Spoletini, A., Varone, L., and Gratani, L. (2017a). Short-term physiological plasticity: trade-off between drought and recovery responses in three Mediterranean *Cistus* species. *Ecol. Evol.* 7, 10880-10889. doi: 10.1002/ece3.3484

Puglielli, G., Gratani, L., and Varone, L. (2019a). Leaf rolling as indicator of water stress in Cistus incanus from different provenances. *Photosynthetica* 57, 202-208. doi: 10.32615/ps.2019.014

Puglielli, G., Redondo-Gómez, S., Gratani, L., and Mateos-Naranjo, E. (2017b). Highlighting the differential role of leaf paraheliotropism in two Mediterranean *Cistus* species under drought stress and well-watered conditions. *J. Plant Physiol.* 213, 199-208. doi: 10.1016/j.jplph.2017.02.015

Puglielli, G., and Varone, L. (2018). Inherent variation of functional traits in winter and summer leaves of Mediterranean seasonal dimorphic species: evidence of a 'within leaf cohort'spectrum. *AoB Plants* 10:ply027.doi: 10.1093/aobpla/ply027

Puglielli, G., Varone, L., and Gratani, L. (2019b). Diachronic adjustments of functional traits scaling relationships to track environmental changes: revisiting *Cistus* species leaf cohort classification. *Flora* 254, 173-180. doi: 10.1016/j.flora.2018.08.010

Puglielli, G., Varone, L., Gratani, L., and Catoni, R. (2017c). Specific leaf area variations drive acclimation of *Cistus salvifolius* in different light environments. *Photosynthetica* 55, 31-40. doi: 10.1007/s11099-016-0235-5

Quézel, P. (1985). "Definition of the Mediterranean region and the origin of its flora," in *Plant Conservation in the Mediterranean Area*, eds C. Gòmez Campo (Dordrecht,NL: Spinger), 9–24.

Rivoal, A., Fernandez, C., Lavoir, A. V., Olivier, R., Lecareux, C., Greff, S. et al. (2010). Environmental control of terpene emissions from *Cistus monspeliensis* L. *in natural Mediterranean shrublands*. *Chemosphere* 78, 942-949. doi: 10.1016/j.chemosphere.2009.12.047

Rotondi, A., Rossi, F., Asunis, C., and Cesaraccio, C. (2003). Leaf xeromorphic adaptations of some plants of a coastal Mediterranean macchia ecosystem. *JME* 4, 25–36.

Russo, S., Sillmann, J., and Fischer, E. M. (2015). Top ten European heatwaves since 1950 and their occurrence in the coming decades. *Environ. Res. Lett.* 10:124003.

Sánchez-Rodríguez, J., Martinez-Carrasco, R., and Pérez, P. (1997). Photosynthetic electron transport and carbon-reduction-cycle enzyme activities under long-term drought stress in *Casuarina equisetifolia Forst. & Forst*. *Photosyn. Res.* 52, 255-262. doi: 10.1023/A:1005878307607

Sardans, J., and Peñuelas, J. (2013). Plant-soil interactions in Mediterranean forest and shrublands: impacts of climatic change. *Plant Soil* 365, 1-33. doi: 10.1007/s11104-013-1591-6

Scoffoni, C., Vuong, C., Diep, S., Cochard, H., and Sack, L. (2014). Leaf shrinkage with dehydration: coordination with hydraulic vulnerability and drought tolerance. *Plant Physiol.* 164, 1772-1788. doi: 10.1104/pp.113.221424

Sebastiani, F., Torre, S., Gori, A., Brunetti, C., Centritto, M., Ferrini, F., et al. (2019). Dissecting adaptation mechanisms to contrasting solar irradiance in the mediterranean shrub *Cistus incanus*. *Int. J. Mol. Sci.*20:3599. doi: 10.3390/ijms20143599

Sharkey, T. D., and Seemann, J. R. (1989). Mild water stress effects on carbon-reduction-cycle intermediates, ribulose bisphosphate carboxylase activity, and spatial homogeneity of photosynthesis in intact leaves. *Plant Physiol.* 89, 1060-1065. doi: 10.1104/pp.89.4.1060

Spurr, A. R. (1969). A low-viscosity epoxy resin embedding medium for electron microscopy. *J. Ultrastruct. Res.* 26, 31–43.

Stephanou, M., and Manetas, Y. (1997). The effects of seasons, exposure, enhanced UV-B radiation, and water stress on leaf epicuticular and internal UV-B absorbing capacity of *Cistus creticus*: a Mediterranean field study. *J. Exp. Bot.* 48, 1977-1985. doi: 10.1093/jxb/48.11.1977

Sumbele, S., Fotelli, M. N., Nikolopoulos, D., Tooulakou, G., Liakoura, V., Liakopoulos, G., et al. (2012). Photosynthetic capacity is negatively correlated with the concentration of leaf phenolic compounds across a range of different species. *AoB Plants*. 2012:pls25. doi: 10.1093/aobpla/pls025

Syvertsen, J. P., Lloyd, J., McConchie, C., Kriedemann, P. E., and Farquhar, G. D. (1995). On the relationship between leaf anatomy and CO2 diffusion through the mesophyll of hypostomatous leaves. *Plant Cell Environ.* 18, 149-157. doi: 10.1111/j.1365-3040.1995.tb00348.x

Tattini, M., Loreto, F., Fini, A., Guidi, L., Brunetti, C., Velikova, V., et al. (2015). Isoprenoids and phenylpropanoids are part of the antioxidant defense orchestrated daily by drought-stressed *Platanus× acerifolia* plants during Mediterranean summers. *New Phytol.* 207, 613-626. doi: 10.1111/nph.13380

Terashima, I., Miyazawa, S. I., and Hanba, Y. T. (2001). Why are sun leaves thicker than shade leaves? Consideration based on analyses of CO2 diffusion in the leaf. *J. Plant Res.* 114, 93-105. doi: 10.1007/PL00013972

Tharayil, N., Suseela, V., Triebwasser, D. J., Preston, C. M., Gerard, P. D., and Dukes, J. S. (2011). Changes in the structural composition and reactivity of *Acer rubrum* leaf litter tannins exposed to warming and altered precipitation: climatic stress-induced tannins are more reactive. *New Phytol.* 191, 132-145. doi: 10.1111/j.1469-8137.2011.03667.x

Tohge, T., and Fernie, A. R. (2017). An overview of compounds derived from the shikimate and phenylpropanoid pathways and their medicinal importance. *Mini Rev Med Chem.* 17, 1013-1027. doi: 10.2174/1389557516666160624123425

Top, S. M., Preston, C. M., Dukes, J. S., and Tharayil, N. (2017). Climate influences the content and chemical composition of foliar tannins in green and senesced tissues of *Quercus rubra*. *Front. Plant Sci.* 8:423. doi: 10.3389/fpls.2017.00423

Van Der Plas, F., Manning, P., Allan, E., Scherer-Lorenzen, M., Verheyen, K., Wirth, C., et al., (2016). Jack-of-all-trades effects drive biodiversity–ecosystem multifunctionality relationships in European forests. *Nat. Commun.* 7, 1-11. doi: 10.1038/ncomms11109

Wright, I. J., and Westoby, M. (2002). Leaves at low versus high rainfall: coordination of structure, lifespan and physiology. *New Phytol.* 155, 403-416. doi: 10.1046/j.1469-8137.2002.00479.x

Zucker, W. V. (1983). Tannins: does structure determine function? An ecological perspective. *Am. Nat.* 121, 335-365. doi: 10.1086/2840

Conflict of Interest: The authors declare that the research was conducted in the absence of any commercial or financial relationships that could be construed as a potential conflict of interest.

frontiers in Forests and Global Change

OPINION
published: 06 April 2021
doi: 10.3389/ffgc.2021.654032

Plant Defense Proteins as Potential Markers for Early Detection of Forest Damage and Diseases

Tetyana Nosenko[1], Manuel Hanke-Uhe[2], Philip Alexander Heine[3], Afsheen Shahid[4], Stefan Dübel[3], Heinz Rennenberg[4,5], Jörg Schumacher[2], Jana Barbro Winkler[1], Jörg-Peter Schnitzler[1], Robert Hänsch[5,6]* and David Kaufholdt[6]*

[1] Research Unit Environmental Simulation (EUS), Institute for Biochemical Plant Pathology, Helmholtz Zentrum München, Neuherberg, Germany, [2] Faculty for Forest and Environment, Eberswalde University for Sustainable Development, Eberswalde, Germany, [3] Department of Biotechnology, Technische Universität Braunschweig, Braunschweig, Germany, [4] Institute of Forest Sciences, Chair of Tree Physiology, Albert-Ludwigs-University Freiburg, Freiburg, Germany, [5] Center of Molecular Ecophysiology (CMEP), College of Resources and Environment, Southwest University, Chongqing, China, [6] Institute of Plant Biology, Technische Universität Braunschweig, Braunschweig, Germany

Keywords: forest disease diagnostic, molecular markers, antimicrobial peptides, defensins, plant defense

OPEN ACCESS

Edited by:
Raffaella Balestrini, Institute for Sustainable Plant Protection, National Research Council (CNR), Italy

Reviewed by:
Franco Faoro, University of Milan, Italy
Walter Chitarra, Council for Agricultural and Economics Research (CREA), Italy

****Correspondence:***
Tetyana Nosenko
tetiana.nosenko@helmholtz-muenchen.de
Robert Hänsch
rhaensch@tu-braunschweig.de

Specialty section:
This article was submitted to Forest Ecophysiology, a section of the journal Frontiers in Forests and Global Change

Received: *15 January 2021*
Accepted: *15 March 2021*
Published: *06 April 2021*

Citation:
Nosenko T, Hanke-Uhe M, Heine PA, Shahid A, Dübel S, Rennenberg H, Schumacher J, Winkler JB, Schnitzler J-P, Hänsch R and Kaufholdt D (2021) Plant Defense Proteins as Potential Markers for Early Detection of Forest Damage and Diseases. Front. For. Glob. Change 4:654032. doi: 10.3389/ffgc.2021.654032

ADDRESSING THE PROBLEM—WHY FORESTRY NEEDS DIAGNOSTIC TOOLS?

Over the last two decades, European forest ecosystems have been exposed to increasing stress associated with an increasing number, duration and severity of extreme events triggered by climate change (Dyderski et al., 2018). For forest plants, the concomitant stresses are not limited to direct detrimental effects of rising temperatures, drought and heavy rainfall, but also include enhanced virulence of native plant pathogens and herbivores and the introduction of new pests (Stenlid and Oliva, 2016). The detection of forest diseases at an early stage, when visible symptoms cannot yet be observed, is a crucial prerequisite to counteract regional spreading of pathogens. However, the effective monitoring of forest damage and diseases requires reliable and easy-to-use portable test systems.

CURRENT METHODS FOR DETECTION AND DIAGNOSIS OF FOREST DAMAGE AND DISEASES IN AN ASYMPTOMATIC STAGE

For the detection and asymptomatic diagnosis of plant diseases, currently, a wide variety of biochemical molecular methods is applied. These approaches include well-established methods such as polymerase chain reaction, immunofluorescence, fluorescence *in situ* hybridization, enzyme immunosorbent assay and flow cytometry, and the use of portable sensors developed on the basis of the above-mentioned laboratory techniques. For a detailed description of the principles, advantages, and disadvantages of these methods we recommend several recently published review articles by Fang and Ramasamy (2015), Lau and Botella (2017), and Luchi et al. (2020). A common feature of most molecular biology techniques is that they are based on the recognition of pathogen DNA, RNA, or protein molecules present in the sampled plant tissue and often assume an advanced stage of the infection, which has spread over a large part of the tree. Such molecular markers are often highly specific for a particular pathogen and are therefore susceptible to false negative results in diseases caused by non-indigenous pathogens (i.e., invasive species) or species with high genetic diversity (Luchi et al., 2020). Therefore, other types of molecular markers are required for the detection of disease by different types of stress in forest populations at the early, asymptomatic stage.

Several advanced techniques have been applied to monitor stress conditions in agricultural land and forests, including biophysical methods such as thermographic, hyperspectral reflectance, and advanced fluorescence imaging techniques, as well as metabolome analyses such as profiling of volatile organic compounds or plant hormones (Martinelli et al., 2015). However, the interpretation of the results obtained with these methods depends on the availability of large amounts of data that would allow to distinguish between normal seasonal and diurnal variations of the measured parameters and their pathological profiles, and on appropriate data processing and analytical techniques. Both data collection and data analysis require special experience and are not field applicable.

To overcome these disadvantages, the development of a new test system based on host immune responses could be a promising strategy. We hypothesize that new host-derived markers, in combination with serological techniques already well-established for forest disease diagnosis, will provide a promising tool for the detection of forest damage and diseases at their early asymptomatic stage. Such a prospective technology will be an antibody-based Lateral-Flow-Test (LFT) targeting a particular stress-induced plant defense protein (**Figure 1A**).

PREREQUISITES OF GENE- OR PROTEIN-BIOMARKERS FOR THE EARLY DETECTION OF DISEASES

First of all, we have to keep in mind that the purpose of such markers is not to detect a particular species of plant pathogens or herbivores but rather to identify a general problem resulted from a predefined range of causative agents. Therefore, good host-derived markers should respond to a broad spectrum of stressors. In addition to the broad target range, potential markers are expected to exhibit specific spatio-temporal expression pattern. Disease-causing agents trigger two types of reactions in plants: a local reaction restricted to the attacked tissue and systemic reactions including biochemical and biophysical changes in tissues and organs distal to the affected locus (Eyles et al., 2010). Only genes or proteins involved in systemic reactions constitute potential markers for the early disease detection. Finally, in order to have an unrestricted time for sampling, a reliable marker should be rapidly upregulated and maintain a high expression level during a particular stress with negligible diurnal variation.

ANTIMICROBIAL PEPTIDES AS POTENTIAL MARKERS FOR THE EARLY DETECTION OF FOREST DISEASES

Are there any proteins in plants that fulfill the above criteria? To answer this question, we present here the relevant current knowledge about a large group of proteins of innate plant immunity, the antimicrobial peptides (AMPs), with special emphasis on the defensins as the best-studied class of AMPs. These peptides comprise a diverse group of short, cysteine-rich proteins, some of which are also known as Pathogenesis-Related (PR) proteins. AMPs, which are ubiquitous in higher plants, are characterized by a remarkable primary sequence variation and high stability of their three-dimensional protein structure maintained by disulfide bonds formed by highly conserved cysteine residues (Campos et al., 2018; Kovaleva et al., 2020). Based on their tertiary structure, AMPs are classified into defensins, thionins, lipid-transfer proteins, heveins, and other multigene families. Depending on the species, each family consists of dozens to hundreds of genes. AMPs are secreted mainly in the apoplastic space of peripheral cell layers and act as the plant's first line of defense against pathogenic fungi, bacteria, viruses, and herbivores (Lazzaro et al., 2020).

Spectra of the AMP Antimicrobial Activities

The majority of AMPs are positively charged at their surface and cause broad-spectrum antimicrobial activity by interacting with negatively charged microbial membranes. This interaction leads to a change in membrane structure, followed by cell death or, in some cases, to an intrusion of AMPs into the pathogen interior, where they interact with specific intracellular targets (van der Weerden et al., 2008). Other known AMP mechanisms of function include interaction of AMPs with specific lipid, protein, or oligosaccharide molecules of bacterial or fungal cell walls (Thevissen et al., 2000), inhibition of fungal phytopathogenic proteins (Slavokhotova et al., 2014), induction of systemic iron deficiency (Hsiao et al., 2017), and inhibition of digestive enzymes of insects (Major and Constabel, 2008). Each particular mechanism determines the spectrum of antimicrobial activities and spatiotemporal expression patterns of individual AMPs.

The specificity of antimicrobial activity and target range of individual AMPs vary widely within and between species. The type I defensins AtPDF1.1 and AtPDF1.2 from *Arabidopsis thaliana* are probably the best studied AMPs involved in non-specific plant resistance to a wide range of biotic and abiotic challenges such as necrotrophic fungi, bacteria, herbivorous insects, and an excess of heavy metals (Nguyen et al., 2014; Hsiao et al., 2017). Many AMPs are known to possess a more specific antimicrobial activity with their target range limited to a particular taxonomical group of plant pathogens. These limitations are due to the aforementioned ability of some AMPs to attach to membrane or cell wall molecules specific to certain groups of microorganisms such as fungi-specific sphingolipids or digestive enzymes of insects (Thevissen et al., 2000; Wijaya et al., 2000; Medeiros and Pockman, 2011). The most striking example of extreme functional specialization are defensin-like peptides involved in the regulation of plant-bacterial symbiosis. These AMPs are able to differentiate even between different strains of a symbiotic bacterium (Simsek et al., 2013).

Spatio-Temporal Patterns of Antimicrobial Peptide Formation Under Stress

Similar to their target ranges, plant AMPs show a great heterogeneity in tissue specificity and longevity after onset of the stress response. Many functionally promiscuous AMPs are known to be tightly integrated into general immune signaling networks and therefore form an integral part of the plant's systemic response to infection or environmental stress. For example, the aforementioned broad-spectrum defensins

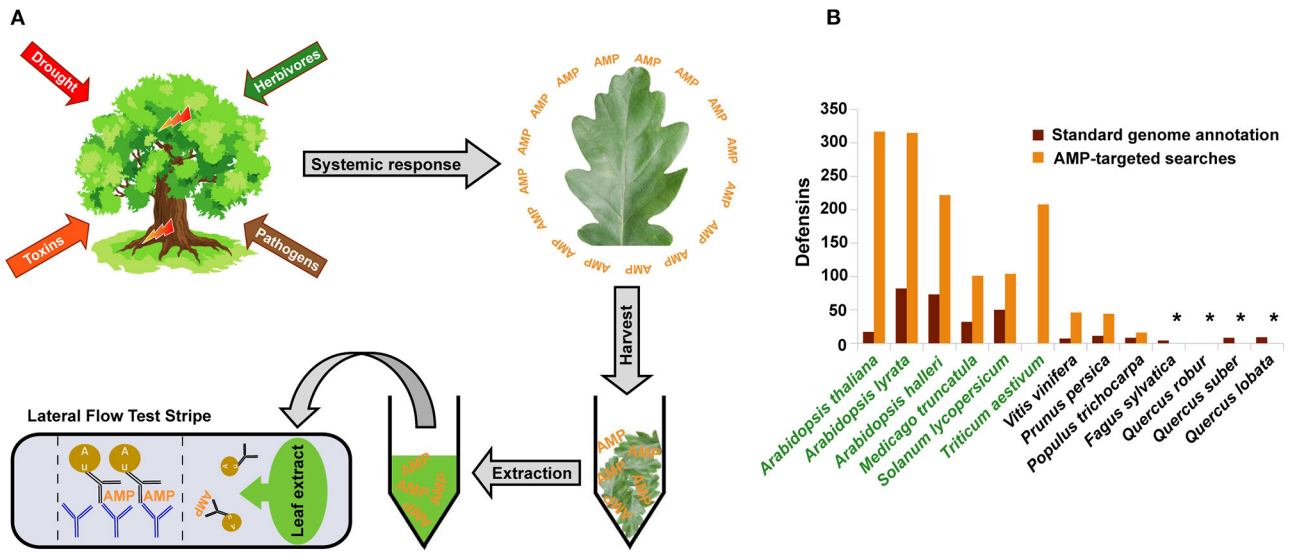

FIGURE 1 | Plant defense proteins as potential markers for an early detection of forest diseases. **(A)** Schematic representation of a plant proteins-based test system. In trees, visible symptoms often appear years after disease induction. At molecular level, plants develop a systemic defense response from hours to days after onset of infection or stress. Plant defense proteins, such as antimicrobial peptides (AMP), can be detected in leaf extracts using Lateral-Flow-Test (LFT) with two specific antibodies. The first anti-AMP antibody forms a mobile complex with an AMP molecule and flows in the direction of the stripe region containing an immobilized second anti-AMP antibody capturing this complex. If AMPs are present, the color of the corresponding stripe region changes because of macroscopic gold particles bound to the mobile anti-AMP antibody. Using LFTs, tree diseases can be detected at an early asymptomatic stage. In addition, more detailed results are conceivable with a multiple-readout test stripe containing multiple test lines with two antibody pairs against different antigens, e.g., one antibody pair against a general stress-marker and another against an AMP characterized by a narrow spectrum of antimicrobial activity. More technical details of LFTs are described elsewhere (Yetisen et al., 2013). **(B)** Current state of knowledge on defense proteins in woody plants: The case of defensins. Total number of defensin and defensin-like genes predicted using standard homology-based genome annotation (brown) and AMP-targeted (orange) pipelines are given for selected herbaceous and woody plant species (species names in green and black, respectively). Information about the number of genes identified using the AMP-specific approaches is available for *A. thaliana*, *A. halleri,* and *A. lyrata* (Silverstein et al., 2005), *M. truncatula* (de Bang et al., 2017), *T. aestivum* (International Wheat Genome Sequencing, 2018), *V. vinifera* (Giacomelli et al., 2012), *S. lycopersicum*, *P. persica,* and *P. trichocarpa* (Liu et al., 2017). Stars indicate species, for which corresponding information is not available.

AtPDF1.1 and AtPDF1.2 are known to be part of the plant's immune response triggered by the phytohormones ethylene and jasmonic acid. In response to infestation with necrotrophic fungi and bacteria, these AMPs are upregulated both locally at the inoculation site and systemically in tissues distal to the infection site as early as 6 h after the infection and remain detectable during at least the following 3 days (Hsiao et al., 2017). A broad-spectrum defensin PtDef from *Populus trichocarpa* showed a graduate increase of its expression levels in response to abiotic stresses, such as drought and cold, during seven days of the experiment (Wei et al., 2020). Further examples of systemic AMPs involved in either hormone-mediated or reactive oxygen species-activated MAPK signaling cascades are described in the review by Bolouri Moghaddam et al. (2016). In contrast, defensin-like nodular peptides exhibit a very high tissue specificity: they are not only expressed exclusively in root nodules, but also differentiate between several nodular zones (Roux et al., 2014); their temporal expression patterns are fine-tuned to the developmental stages of bacterial symbionts (Marx et al., 2016).

Some of the examples presented above suggest that AMP markers are applicable for the early detection of plant diseases. Depending on the task, the test-system may utilize either general-stress response, or more specific (e.g., fungal infection) AMP markers, or both (i.e., a dual-readout LFT; Gong et al., 2018). However, along with advantages, we have to consider challenges for developing a test-system for the early detection of plant diseases.

How Much Do We Know About AMPs in Perennial Woody Plants?

Currently, the greatest obstacle to the selection of host-derived markers for early detection of forest diseases is our limited knowledge on defense mechanisms in trees. The plant immune system has been studied primarily in the model organism *Arabidopsis* and several important crop species. These studies show an incredible between-species variation of gene copy number and biological functions of plant defense proteins, even between closely related species (Hanks et al., 2005; Mondragon-Palomino et al., 2017). Because of this variation, it is impossible to extrapolate findings derived from short-lived herbaceous plants directly to long-lived woody plants. As they are at the forefront of the host-parasite arms race, defense genes are subject to rapid diversification, which hinders their identification using homology-based techniques (Liu et al., 2017). To overcome such obstacles, specific computational approaches have been developed for the identification of genes involved in plant

defense. In the case of AMPs, gene identification methods are based on the conserved patterns of cysteine residues and presence of N-terminal signal peptides. In **Figure 1B**, we show that the number of genes annotated in plant genomes as AMPs varies considerably depending on the identification method applied. So far only very few genomes of perennial woody plants have been screened using specific AMP-targeting approaches. In addition, only very few studies have addressed the functions of AMPs in trees [e.g., *Pinus sylvestris* (Hrunyk et al., 2017; Khairutdinov et al., 2017), *Picea glauca* (Picart et al., 2012), and *P. trichocarpa* (Major and Constabel, 2008; Wei et al., 2020)]. Nevertheless, the results of these studies support the following statements: (a) There is a high diversity of AMPs in long-living woody plants. (b) Similar to herbaceous species, AMPs in tree species are involved in the development of resistance to a variety of biotic and abiotic stresses. (c) The target range and mechanisms of antimicrobial activity of individual AMPs of woody plants are species-specific.

CONCLUDING REMARKS

Defensins and other AMPs are promising candidates for early detection of plant diseases independent of a stress-factor in general. An AMP-dependent test-system can be designed for the tree species dominant in particular regions and used as a part of the regional forest monitoring program. Engineering highly specific antibodies is challenging but possible with modern techniques for the monoclonal antibody production like phage display (Bradbury et al., 2011). Unfortunately, the knowledge on immune responses in woody plants is rudimentary and needs further investigations. Advances in DNA and RNA sequencing technologies make it possible to generate whole genome and transcriptome sequence data for ecologically important forest tree species such as English oak and beech (Mishra et al., 2018; Plomion et al., 2018). This increasing availability of data can partially compensate for the lack of experimental evidence on the diversity, expression type, and tissue specificity of defense proteins of woody plants, information that can be used for the pre-selection of protein markers for developing an antibody-based LFT stripe for early detection of diseases in these species.

AUTHOR CONTRIBUTIONS

RH, HR, JS, and J-PS conceived the work. TN, DK, RH, and J-PS wrote the manuscript. MH-U, PH, AS, SD, and JW participated in discussions and made intellectual contribution to the manuscript. All authors commented on the manuscript and approved it for publication.

FUNDING

This work has been supported by a grant (WKF-WF04-22WB41300/1-4) from the German Federal Ministry of Food and Agriculture (BMEL) and Federal Ministry for the Environment, Nature Conservation and Nuclear Safety (BMU) in the frame or the Waldklimafonds Program.

REFERENCES

Bolouri Moghaddam, M. R., Vilcinskas, A., and Rahnamaeian, M. (2016). Cooperative interaction of antimicrobial peptides with the interrelated immune pathways in plants. *Mol. Plant Pathol.* 17, 464–471. doi: 10.1111/mpp.12299

Bradbury, A., Sidhu, S., Dübel, S., and McCafferty, J. (2011). Beyond natural antibodies: the power of in vitro display technologies. *Nat. Biotechnol.* 29, 245–254. doi: 10.1038/nbt.1791

Campos, M. L., Liao, L. M., Alves, E. S. F., Migliolo, L., Dias, S. C., and Franco, O. L. (2018). A structural perspective of plant antimicrobial peptides. *Biochem. J.* 475, 3359–3375. doi: 10.1042/BCJ20180213

de Bang, T. C., Lundquist, P. K., Dai, X., Boschiero, C., Zhuang, Z., Pant, P., et al. (2017). Genome-wide identification of *Medicago* peptides involved in macronutrient responses and nodulation. *Plant Physiol.* 175, 1669–1689. doi: 10.1104/pp.17.01096

Dyderski, M. K., Paz, S., Frelich, L. E., and Jagodzinski, A. M. (2018). How much does climate change threaten European forest tree species distributions? *Glob. Chang. Biol.* 24, 1150–1163. doi: 10.1111/gcb.13925

Eyles, A., Bonello, P., Ganley, R., and Mohammed, C. (2010). Induced resistance to pests and pathogens in trees. *New Phytol.* 185, 893–908. doi: 10.1111/j.1469-8137.2009.03127.x

Fang, Y., and Ramasamy, R. P. (2015). Current and prospective methods for plant disease detection. *Biosensors* 5, 537–561. doi: 10.3390/bios5030537

Giacomelli, L., Nanni, V., Lenzi, L., Zhuang, J., Dalla Serra, M., Banfield, M. J., et al. (2012). Identification and characterization of the defensin-like gene family of grapevine. *Mol. Plant Microbe Interact.* 25, 1118–1131. doi: 10.1094/MPMI-12-11-0323

Gong, X., Zhang, B., Piao, J., Zhao, Q., Gao, W., Peng, W., et al. (2018). High sensitive and multiple detection of acute myocardial infarction biomarkers based on a dual-readout immunochromatography test strip. *Nanomed. Nanotechnol. Biol. Med.* 14, 1257–1266. doi: 10.1016/j.nano.2018.02.013

Hanks, J. N., Snyder, A. K., Graham, M. A., Shah, R. K., Blaylock, L. A., Harrison, M. J., et al. (2005). Defensin gene family in *Medicago truncatula*: structure, expression and induction by signal molecules. *Plant Mol. Biol.* 58, 385–399. doi: 10.1007/s11103-005-5567-7

Hrunyk, N., Gout, R., and Kovaleva, V. (2017). Regulation of gene expression for defensins and lipid transfer protein in Scots pine seedlings by necrotrophic pathogen *Alternaria alternata* (Fr.). *Folia For. Pol.* 59, 152–158. doi: 10.1515/ffp-2017-0015

Hsiao, P. Y., Cheng, C. P., Koh, K. W., and Chan, M. T. (2017). The *Arabidopsis* defensin gene, AtPDF1.1, mediates defence against *Pectobacterium carotovorum* subsp. *carotovorum via an iron-withholding defence system. Sci Rep.* 7:9175. doi: 10.1038/s41598-017-08497-7

International Wheat Genome Sequencing (2018). Shifting the limits in wheat research and breeding using a fully annotated reference genome. *Science* 361:eaar7191. doi: 10.1126/science.aar7191

Khairutdinov, B. I., Ermakova, E. A., Yusypovych, Y. M., Bessolicina, E. K., Tarasova, N. B., Toporkova, Y. Y., et al. (2017). NMR structure, conformational dynamics, and biological activity of PsDef1 defensin from *Pinus sylvestris. Biochim. Biophys. Acta Proteins Proteom* 1865, 1085–1094. doi: 10.1016/j.bbapap.2017.05.012

Kovaleva, V., Bukhteeva, I., Kit, O. Y., and Nesmelova, I. V. (2020). Plant defensins from a structural perspective. *Int. J. Mol. Sci.* 21:5307. doi: 10.3390/ijms21155307

Lau, H. Y., and Botella, J. R. (2017). Advanced DNA-based point-of-care diagnostic methods for plant diseases detection. *Front. Plant Sci.* 8:2016. doi: 10.3389/fpls.2017.02016

Lazzaro, B. P., Zasloff, M., and Rolff, J. (2020). Antimicrobial peptides: application informed by evolution. *Science* 368:aau5480. doi: 10.1126/science.aau5480

Liu, X., Zhang, H., Jiao, H., Li, L., Qiao, X., Fabrice, M. R., et al. (2017). Expansion and evolutionary patterns of cysteine-rich peptides in plants. *BMC Genomics* 18:610. doi: 10.1186/s12864-017-3948-3

Luchi, N., Ioos, R., and Santini, A. (2020). Fast and reliable molecular methods to detect fungal pathogens in woody plants. *Appl. Microbiol. Biotechnol.* 104, 2453–2468. doi: 10.1007/s00253-020-10395-4

Major, I. T., and Constabel, C. P. (2008). Functional analysis of the Kunitz trypsin inhibitor family in poplar reveals biochemical diversity and multiplicity in defense against herbivores. *Plant Physiol.* 146, 888–903. doi: 10.1104/pp.107.106229

Martinelli, F., Scalenghe, R., Davino, S., Panno, S., Scuderi, G., Ruisi, P., et al. (2015). Advanced methods of plant disease detection. A review. *Agron. Sustain. Dev.* 35, 1–25. doi: 10.1007/s13593-014-0246-1

Marx, H., Minogue, C. E., Jayaraman, D., Richards, A. L., Kwiecien, N. W., Siahpirani, A. F., et al. (2016). A proteomic atlas of the legume *Medicago truncatula* and its nitrogen-fixing endosymbiont *Sinorhizobium meliloti*. *Nat. Biotechnol.* 34, 1198–1205. doi: 10.1038/nbt.3681

Medeiros, J. S., and Pockman, W. T. (2011). Drought increases freezing tolerance of both leaves and xylem of *Larrea tridentata*. *Plant Cell Environ.* 34, 43–51. doi: 10.1111/j.1365-3040.2010.02224.x

Mishra, B., Gupta, D. K., Pfenninger, M., Hickler, T., Langer, E., and Nam, B. (2018). A reference genome of the European beech (*Fagus sylvatica* L.). *Gigascience* 7:giy063. doi: 10.1093/gigascience/giy063

Mondragon-Palomino, M., John-Arputharaj, A., Pallmann, M., and Dresselhaus, T. (2017). Similarities between reproductive and immune pistil transcriptomes of *Arabidopsis* species. *Plant Physiol.* 174, 1559–1575. doi: 10.1104/pp.17.00390

Nguyen, N. N., Ranwez, V., Vile, D., Soulie, M. C., Dellagi, A., Expert, D., et al. (2014). Evolutionary tinkering of the expression of PDF1s suggests their joint effect on zinc tolerance and the response to pathogen attack. *Front. Plant Sci.* 5:70. doi: 10.3389/fpls.2014.00070

Picart, P., Pirttila, A. M., Raventos, D., Kristensen, H. H., and Sahl, H. G. (2012). Identification of defensin-encoding genes of *Picea glauca*: characterization of PgD5, a conserved spruce defensin with strong antifungal activity. *BMC Plant Biol.* 12:180. doi: 10.1186/1471-2229-12-180

Plomion, C., Aury, J. M., Amselem, J., Leroy, T., Murat, F., Duplessis, S., et al. (2018). Oak genome reveals facets of long lifespan. *Nat Plants* 4, 440–452. doi: 10.1038/s41477-018-0172-3

Roux, B., Rodde, N., Jardinaud, M. F., Timmers, T., Sauviac, L., Cottret, L., et al. (2014). An integrated analysis of plant and bacterial gene expression in symbiotic root nodules using laser-capture microdissection coupled to RNA sequencing. *Plant J.* 77, 817–837. doi: 10.1111/tpj.12442

Silverstein, K. A., Graham, M. A., Paape, T. D., and Vandenbosch, K. A. (2005). Genome organization of more than 300 defensin-like genes in *Arabidopsis*. *Plant Physiol.* 138, 600–610. doi: 10.1104/pp.105.060079

Simsek, S., Wood, K., and Reuhs, B. L. (2013). Structural analysis of succinoglycan oligosaccharides from *Sinorhizobium meliloti* strains with different host compatibility phenotypes. *J. Bacteriol.* 195, 2032–2038. doi: 10.1128/JB.00009-13

Slavokhotova, A. A., Naumann, T. A., Price, N. P., Rogozhin, E. A., Andreev, Y. A., Vassilevski, A. A., et al. (2014). Novel mode of action of plant defense peptides - hevein-like antimicrobial peptides from wheat inhibit fungal metalloproteases. *FEBS J.* 281, 4754–4764. doi: 10.1111/febs.13015

Stenlid, J., and Oliva, J. (2016). Phenotypic interactions between tree hosts and invasive forest pathogens in the light of globalization and climate change. *Philos. Trans. R. Soc. Lond. B Biol. Sci.* 371:455. doi: 10.1098/rstb.2015.0455

Thevissen, K., Cammue, B. P., Lemaire, K., Winderickx, J., Dickson, R. C., Lester, R. L., et al. (2000). A gene encoding a sphingolipid biosynthesis enzyme determines the sensitivity of *Saccharomyces cerevisiae* to an antifungal plant defensin from dahlia (*Dahlia merckii*). *Proc. Natl. Acad. Sci. U.S.A.* 97, 9531–9536. doi: 10.1073/pnas.160077797

van der Weerden, N. L., Lay, F. T., and Anderson, M. A. (2008). The plant defensin, NaD1, enters the cytoplasm of *Fusarium oxysporum* hyphae. *J. Biol. Chem.* 283, 14445–14452. doi: 10.1074/jbc.M709867200

Wei, H., Movahedi, A., Xu, C., Sun, W., Wang, P., Li, D., et al. (2020). Characterization, expression profiling, and functional analysis of PtDef, a defensin-encoding gene from *Populus trichocarpa*. *Front. Microbiol.* 11:106. doi: 10.3389/fmicb.2020.00106

Wijaya, R., Neumann, G. M., Condron, R., Hughes, A. B., and Polya, G. M. (2000). Defense proteins from seed of *Cassia fistula* include a lipid transfer protein homologue and a protease inhibitory plant defensin. *Plant Sci.* 159, 243–255. doi: 10.1016/S0168-9452(00)00348-4

Yetisen, A. K., Akram, M. S., and Lowe, C. R. (2013). Paper-based microfluidic point-of-care diagnostic devices. *Lab Chip* 13, 2210–2251. doi: 10.1039/c3lc50169h

Conflict of Interest: The authors declare that the research was conducted in the absence of any commercial or financial relationships that could be construed as a potential conflict of interest.

The handling editor RB declared a past co-authorship with one of the authors J-PS.

frontiers in Forests and Global Change

ORIGINAL RESEARCH
published: 29 April 2021
doi: 10.3389/ffgc.2021.663327

Evapotranspiration Intensification Over Unchanged Temperate Vegetation in the Baltic Countries Is Being Driven by Climate Shifts

Bruno Montibeller†, Jaak Jaagus†, Ülo Mander† and Evelyn Uuemaa†*

Department of Geography, Institute of Ecology and Earth Sciences, University of Tartu, Tartu, Estonia

OPEN ACCESS

Edited by:
James Blande, University of Eastern Finland, Finland

Reviewed by:
Sanjiv Kumar, Auburn University, United States
Miguel Portillo-Estrada, University of Antwerp, Belgium

***Correspondence:**
Bruno Montibeller
bruno.montibeller@ut.ee

†ORCID:
Bruno Montibeller
0000-0002-5250-8450
Jaak Jaagus
0000-0002-6617-9125
Ülo Mander
0000-0003-2340-6989
Evelyn Uuemaa
0000-0002-0782-6740

Specialty section:
This article was submitted to Forests and the Atmosphere, a section of the journal Frontiers in Forests and Global Change

Received: *02 February 2021*
Accepted: *06 April 2021*
Published: *29 April 2021*

Citation:
Montibeller B, Jaagus J, Mander Ü and Uuemaa E (2021) Evapotranspiration Intensification Over Unchanged Temperate Vegetation in the Baltic Countries Is Being Driven by Climate Shifts. Front. For. Glob. Change 4:663327. doi: 10.3389/ffgc.2021.663327

Shifts in climate driven by anthropogenic land use and land cover change are expected to alter various land–atmosphere interactions. Evapotranspiration (ET) is one of these processes and plays a fundamental role in the hydrologic cycle. Using gridded reanalysis and remote sensing data, we investigated the spatiotemporal trends of precipitation, temperature, and ET for areas in the Baltic countries Lithuania, Latvia and Estonia where the land cover type had not changed from 2000 to 2018. We focused on ET but investigated the spatiotemporal trends for the three variables at monthly, seasonal, and annual time scales during this period to quantify trade-offs among months and seasons. We used the Mann-Kendall test and Sen's slope to calculate the trends and rate of change for the three variables. Although precipitation showed fewer statistically significant increasing and decreasing trends due to its high variability, temperature showed only increasing trends. The trends were concentrated in late spring (May, +0.14°C annually), summer (June and August, +0.10°C), and early autumn (September, +0.13°C). For unchanged forest and cropland areas, we found no statistically significant ET trends. However, Sen's slope indicated increasing ET in April, May, June, and September for forest areas and in May and June for cropland. Our results indicate that during the study period, the temperature changes may have lengthened the growing season, which affected the ET patterns of forest and cropland areas. The results also provide important insights into the regional water balance and complement the findings of other studies.

Keywords: Baltic region, climate change, evapotranspiration, remote sensing, land use and land cover change

INTRODUCTION

Changes in precipitation and temperature regimes differ among the world's climatic regions. Previous studies have demonstrated changes or high variability in the patterns of two key climate variables, precipitation and temperature, in recent years in a range of climatic regions (Van den Besselaar et al., 2013; Silva Junior et al., 2018; Haghtalab et al., 2019; Krauskopf and Huth, 2020). The impact of these changes, which varies among the climatic regions, is exemplified by an

increased number of extreme events, such as heat waves, intense rainfall, or long-term droughts (Sena et al., 2012). In addition, according to the Intergovernmental Panel on Climate Change (IPCC) (Seneviratne et al., 2012), the frequency and magnitude of these extreme events and the climate variability are expected to increase in the future.

Among the factors responsible for the changing climate, anthropogenic land use and land cover (LULC) change is a main factor (Pielke, 2005; Ceccherini et al., 2020; Sy and Quesada, 2020), and is having a stronger impact than was assumed in previous studies (Seneviratne et al., 2012). Depending on the extent and intensity of the LULC change, climate variables can be affected at local, regional, and global scales (Hale et al., 2006; Mahmood et al., 2014; Cao et al., 2015; Chen and Dirmeyer, 2017; Findell et al., 2017). In Eastern India, for instance, 25 to 50% of the overall temperature increase of ∼0.3°C from 1981 to 2010 could be explained by local LULC change (Gogoi et al., 2019). In the Amazon, Llopart et al. (2018) analyzed how the spread of deforestation affected the regional climate using simulated scenarios and climate models. They reported that deforestation caused a dipole pattern in response to the region's precipitation, with increased precipitation in the eastern Amazon (+8.3%) and decreased precipitation in the west (−7.9%). At a global scale, Lawrence and Chase (2010) found that anthropogenic land cover change imposed a warming trend in the near surface atmosphere and reducing precipitation regionally, and both climate factors varied greatly between regions of the world.

In most cases, the impact of LULC change on climate results from changes in the biophysical and biogeochemical processes that regulate the complex land–atmosphere interactions (Pongratz et al., 2010; Alkama and Cescatti, 2016; Perugini et al., 2017). Evapotranspiration (ET) is one of the processes affected by climate and LULC change, and it plays an important role in balancing the hydrological cycle (Zhang et al., 2016). In temperate forest regions, for example, ET returns 71% of the precipitation to the atmosphere (Miralles et al., 2011). Using ET data derived from remote sensing or modeling, studies have been exploring the consequences of climate and LULC change on the dynamics of ET (Dias et al., 2015; Spera et al., 2016; Poon and Kinoshita, 2018; Paca et al., 2019; Qu and Zhuang, 2019; dos Santos et al., 2020). Wang et al. (2019) analyzed the spatiotemporal variability of ET over a Chinese catchment that has experienced strong climate and LULC changes. They found that the annual mean ET increased by nearly 14 mm as the result of a warming and drying trend combined with increasing areas of forest, grassland, water bodies, and urban land. Using a water-balance approach (i.e., the difference between precipitation and stream discharge) to estimate ET, Hamilton et al. (2018) found that ET is resilient in temperate humid catchments that have been experiencing climate and LULC change; that is, ET remained relatively stable. They attributed this resilience to field measurements that showed the ET rates did not differ greatly between rain-fed annual crops and perennial vegetation, and to the fact that these LULC types showed the biggest changes in area during the study period. However, this approach was limited because the ET was only calculated for the entire catchment and not independently for the different LULC types.

Even though several studies have provided spatiotemporal analysis of the combined effects of climate and LULC changes on ET (Mao et al., 2015; Li et al., 2017; Teuling et al., 2019), fewer studies have investigated the changes in ET in areas where LULC has not changed (Gaertner et al., 2019), where changes in ET are most likely driven by changes in climate variables. The limited number of studies that have investigated ET changes in areas where LULC has not changed, such as many forested areas, have reported different patterns for different climate regions. For semi-deciduous tropical forests, Vourlitis et al. (2014) showed that ET has decreased, whereas for temperate forests, Gaertner et al., 2019) reported that ET increased due to the longer growing season. Most of these studies evaluated annual ET changes, and restricted the assessment of the trade-offs between monthly and seasonal time scales (e.g., increasing ET in spring can be offset by an ET decrease in summer). Moreover, the studies did not account simultaneously for spatial variation and changes over time. Therefore, they did not produce a clear understanding on how ET changes spatially and temporally at different time scales (e.g., monthly, seasonally, and annually) in areas with stable LULC. Studies of ET in this context of stability are important because they help us to understand how stable LULC types such as forest and agricultural areas have been adapting to the new climate conditions and reveal the importance of these areas as a long-term solution to minimize climate change by stabilizing water cycles and sequestering carbon (Funk et al., 2019).

Given the abovementioned limitations of existing research and the lack of understanding of how ET rates change spatially and temporally at large scales, we designed the present study to investigate the changes in ET over areas with stable forest and cropland areas. We focused our analysis on three Baltic countries (Estonia, Latvia, and Lithuania). We used a newly developed gap-filled ET remote sensing dataset (Running et al., 2019) that provided data from 2000 to 2018. We chose these countries because the region has seen a clear shift in its climate from 1951 to 2015, with gradual warming and a slight trend of increasing precipitation (Jaagus et al., 2017). In addition, most of the region has not shown significant LULC changes during the study period, and no similar study has been performed in these three countries.

We defined unchanged forest as areas that showed no significant disturbance caused by anthropogenic activities such as clear-cut or selective logging during the study period. We defined unchanged cropland as cultivated land that remained cultivated throughout the study period but did not consider the effects of crop changes (e.g., from winter wheat to corn) to represent an LULC change. We chose forest and cropland areas for our analysis because these LULC types cover the majority of Estonia, Latvia, and Lithuania, and both types show large continuous patches of unchanged LULC. We also explored the spatiotemporal patterns of the two key factors that affect ET (i.e., precipitation and temperature) using gridded reanalysis data to better understand the driving forces for the changes in ET.

We posed two questions: (i) What are the spatial and temporal patterns of temperature, precipitation, and ET throughout the Baltic countries? (ii) How has ET of unchanged forest and cropland areas changed in this region? We hypothesized that

even though the region has not experienced intense LULC change since 2000, the overall ET rates of forest and croplands have changed to adapt to the observed shifts in the climate regime in response to large-scale atmospheric circulation patterns (Jaagus et al., 2003). Note that although climate *change* is the terminology adopted by most similar studies, we decided to use the term climate *shift* because our study period is shorter than the period (at least 30 years) recommended for climate change studies (Seneviratne et al., 2012).

MATERIALS AND METHODS

Study Area

The study area encompasses 175 × 10^3 km^2 of the three Baltic countries in north-eastern Europe. The region's climate is characterized as humid continental Dfb according to the Köppen climate classification, with mean annual temperature ranging between 5.5 and 6.5°C and mean annual precipitation ranging between 600 and 750 mm. In the westernmost part of the study region, which lies on the coast of the Baltic Sea, winters are much milder and the Köppen climate type changes to Cfb. However, parts of the region have shown shifts in the precipitation and temperature trends. The precipitation has increased during the cold months of the year (November to March) and in June, but the annual mean temperature has increased by 0.3 to 0.4 K per decade from 1951 to 2015 (Jaagus et al., 2017).

Data

Precipitation and Temperature Data

We used the gridded daily precipitation and daily mean temperature products from version v20.0e of the European Climate Assessment and Dataset, which is called E-OBS (Cornes et al., 2018). E-OBS was developed by interpolating climate data between weather stations based on data provided by the national meteorological agencies of the European countries. The product is available as a regular grid with a resolution of 0.1 or 0.25°, and covers the period since 1950. We used the 0.1°-resolution dataset, which represents a resolution of about 10 km. E-OBS has been applied in climate monitoring studies (Nastos et al., 2013; Van Der Schrier et al., 2013) and for validation of climate products (Katsanos et al., 2016; Domínguez-Castro et al., 2020). The reported shortcoming of this dataset is the uneven distribution of weather stations, which compromises the interpolation of E-OBS precipitation and temperature estimates (Hofstra et al., 2010). However, this limitation is less problematic in our study region, which has a higher weather station density (Navarro et al., 2019) than in other areas of Europe.

Even though the E-OBS grid was developed from national quality-controlled data, we checked for potential errors (e.g., missing or extreme low and high values) in the gridded precipitation and temperature datasets. We found no errors. To perform our analysis, we aggregated the gridded 0.1° daily precipitation and temperature data into monthly, seasonal, and annual temporal scales. We defined the seasons using the standard periods used for northern hemisphere climatology (Jaagus et al., 2017), with spring comprising March, April, and May; summer, June, July and August; autumn, September, October, and November; and winter, December, January, and February. For precipitation, we summed all total daily values for each month, season, and year, but for temperature, we calculated the mean for each temporal scale.

Evapotranspiration Data

To perform the ET analysis, we used the relatively recently developed MODIS MOD16A2GF product that comprises gap-filled 8-day composite images produced at 0.00416° pixel resolution (∼500 m) (Running et al., 2019). The gap-filled data is generated by mainly removing contaminated FPAR/LAI input data. For the cases where the pixel of FPAR/LAI pixels did not meet the quality criteria, the value is determined by linear interpolation between the previous period's value (Running et al., 2019). The MODIS ET pixels represent the sum of ET (kg/m^2) for 8-day periods. The product is an improvement of the MOD16A2 product that eliminates poor-quality pixels (e.g., pixels contaminated by cloud cover or aerosols). The MOD16A2 product provides almost real time estimates of ET using the Penman-Monteith equation, and has been used in several studies (Spera et al., 2016; Moura et al., 2019). We acquired 8-day composite MOD16A2GF images from January 2000 until December 2018.

Before analysis, we removed MODIS ET pixels with values ranging from 32,761 to 32,767 by assigning those values of *NoData* (the coding used by the R and QGis software). These pixels are flagged in the original dataset as non-vegetated areas, and therefore, no ET rate was calculated (Running et al., 2019). Moreover, we removed all pixels that showed negative values. In this way, we only used pixels that had plausible values during the entire period of analysis (2000 to 2018). Because of the pixel-removal process, our ET analysis covered 70% of the total Baltic countries territory (∼120 × 10^3 km^2). To retrieve the monthly ET rates, we calculated the mean of the 8-day composites images within the respective month for each pixel. The mean value was then divided by eight to obtain daily values, which were finally multiplied by the number of days of each month. We used this approach to retrieve the monthly ET rates because April, May, October, and November had different number of 8-day composite images in leap years. The seasonal and annual ET rates were calculated by aggregating the monthly values. We did not analyze the winter season for four reasons: (i) No data was available in January and February of 2016. (ii) The winter months of other years showed many pixels with negative values, and this would have resulted in the exclusion of a large number of pixels since we worked only with pixels that had plausible values for the whole period. (iii) ET rates in winter are low and the values are negligible, therefore studies have mainly used only the months of the growing season (Gaertner et al., 2019; Niu et al., 2019; Ruiz-Pérez and Vico, 2020). (iv) The ET analysis was not stratified by forest type and as deciduous and evergreen forest are present in the region, the ET rates analysis would be bias since some forest types loses or maintain the leaves. Although the original unit for the ET rates was kg/m^2, we decided to convert this to mm (at a rate of 1 kg/m^2 for 1 mm), to align with the units used in previous studies.

Land Use and Land Cover Data

For LULC data, we used version 2.0.7 of the (CCI Land Cover product[1]). This product consists of annual time series of consistent global land cover maps with 300-m spatial resolution from 1992 to 2018. We used the product data from 2000, 2005, 2010, 2015, and 2018. For 2018, we used version 2.1.1 of the product, which is consistent with v2.0.7. The advantage of the newer dataset is its consistency over time. We reclassified the original 22 LULC types into 6 main classes based on the IPCC class definitions (ESA, 2017 Land Cover CCI Product user guide version 2.0, 2017) (**Supplementary Table 1**). The final LULC types were cropland, forest, grassland, urban, wetland, and other. We identified the pixels of forest and cropland that remained as these classes throughout the study period to extract the unchanged forest and cropland areas. The map was only created for forest and cropland because these two LULC types covered more than 87% of the entire study region. Moreover, these LULC types also showed large continuous areas in which the LULC did not change, unlike in the other LULC types, and this lets us test our research hypothesis.

Analysis

First, we examined the monthly, seasonal, and annual spatial and temporal trends for temperature and precipitation for the entire region using the E-OBS data, and the MOD16A2GF data for ET. We examined the trends at a pixel level, with a spatial resolution of 0.00416°. Second, we assessed the monthly, seasonal, and annual ET for unchanged forest and cropland areas using the MOD16A2GF data. We used the Mann-Kendall test to detect significant increasing or decreasing trends.

Spatial Analysis

To analyze ET over forested and cropland areas, we calculated the vegetation cover of forest and cropland within the MODIS ET pixels that were overlapped by these LULC types. The MODIS ET pixels were defined as forest or cropland pixels if, during the entire study period, these LULC types covered >50% of the pixel area. The MODIS pixels that showed <50% of its area as forest or cropland during the study period were considered to have changed, and were excluded from this analysis. In this way, we could investigate the MODIS ET pixels that showed a decrease, increase, or no trend during the study period for areas that had forest or cropland as the major (>50%) LULC type.

To obtain the most representative ET values for unchanged forested and cropland areas, we created a buffer that extended 1 km inward from the edge of the unchanged area and extracted only those pixels that were completely within the unchanged area. This removed the potential bias due to the edge effect for the border pixels. After these procedures, we retrieved 15,359 pixels of forest and 899 pixels of croplands as the most representative MODIS ET pixels of these LULC types. We averaged the monthly, seasonal and annual ET values of these pixels for the trend analysis.

[1]https://www.esa-landcover-cci.org/?q=node/164

Trend Analysis

We used the non-parametric Mann-Kendall test (Mann, 1945; Kendall, 1957; Khambhammettu, 2005) to identify pixels with significant temporal trends (significant increase or decrease, or no significant trend) for the three variables (precipitation, temperature, and ET). The Mann-Kendall test has been widely applied for trend analysis of time series of meteorological (Jaagus, 2006; Almeida et al., 2017; Atta-ur and Dawood, 2017) and hydrological data (Hamed, 2008; Dinpashoh et al., 2011; Jaagus et al., 2017). However, the Mann-Kendall test has been shown to be sensitive to autocorrelation in the input data (Kumar et al., 2009). Therefore, before applying the Mann-Kendall test, we calculated the lag 1 coefficient of correlation test for serial correlation (Bari et al., 2016; Gao et al., 2020) in the time series of precipitation, temperature and ET for all time scales of the analysis. The calculation indicated that an average of <3% of all pixels analyzed showed significant autocorrelation in all-time series. Thus, we decided not to apply any correction and to use the Mann-Kendall test on the original data. We used a confidence level of 95% to define significant decreases and increases in the time series for each pixel ($p < 0.05$).

To estimate the magnitude of the trend, we used the non-parametric Sen's slope value (*SS*) method (Sen, 1968). The magnitude of the change is given by the median slope value for all pairwise points in the time series. Negative values of *SS* indicate a decreasing trend, whereas positive slopes indicate an increase. To calculate the Mann-Kendall trend and *SSs*, we used the package "wql" (Jassby and Cloern, 2017) implemented in version 3.6.1 of the R software. We calculated the trends as well as the SS values for all pixels at monthly, seasonal, and annual scales. We calculated SS values even for those pixels that did not show significant trends according to MK test.

RESULTS

Land Use and Land Cover Change

In 2000, 53.1% of the Baltic countries were covered by forest, followed by cropland (36.7%) and grassland (5.2%) (**Supplementary Table 2**). Urban, wetland and other land together totaled 5.0% of the region (**Supplementary Table 2**). By 2018, forest area had decreased by 0.4% and cropland had increased by 0.4% (**Supplementary Table 2**). Although the total change in the area of LULC types was negligible, the changes of areas of cropland and forest to other classes were noticeable (**Figure 1**). For example, 2,532.1 km^2 of forest was converted into cropland and 801 km^2 into grassland from 2000 to 2018. At the same time 2,300.8 km^2 of cropland was converted into forest (**Figure 1**). Despite these changes, 72.8% of the forest area and 73.2% of the cropland area in 2000 remained completely unchanged throughout the study period (**Supplementary Table 3**).

Spatiotemporal Precipitation Analysis

Our spatial and temporal analyses of the monthly precipitation at a pixel level indicated that half of the months showed no significant trend in the 2,557 pixels analyzed between

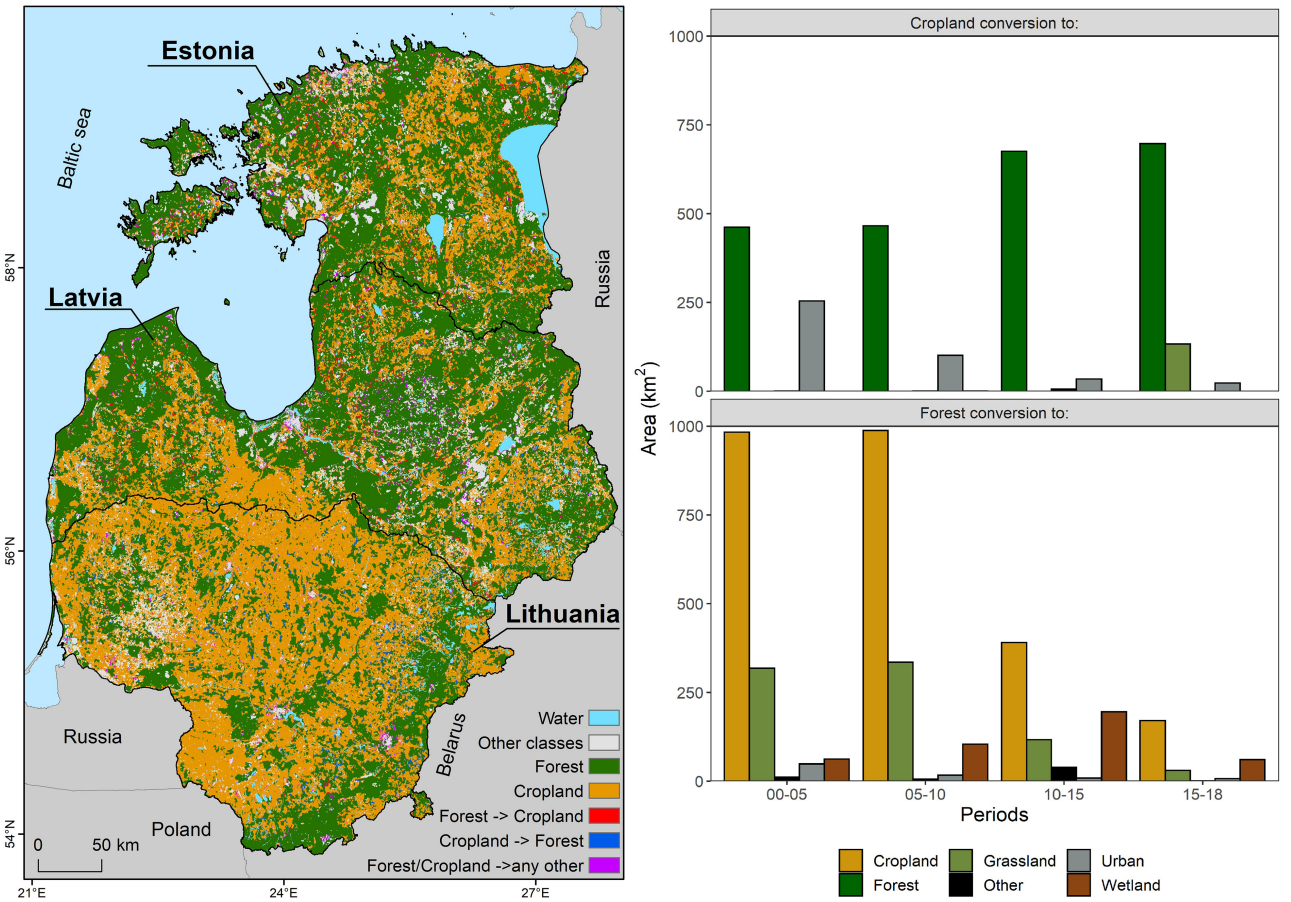

FIGURE 1 | Changes in the areas of forest and cropland in the Baltic countries from 2000 to 2018.

2000 and 2018 (**Figure 2A**). April, September, and December showed a significant increase in 13.6, 3.1, and 8.1% of the total pixels (**Supplementary Table 4**), respectively. March, June, and July presented significant decreasing trends in a small proportion of the pixels (0.8, 1.4, and 0.2% of the total, respectively). Spatially, it is interesting to note that the pixels with the significant decreasing trend were mainly concentrated in the south-west of Lithuania (in March and June), whereas the increase in precipitation was not only in the south and southwest of Lithuania and Latvia but also in the northeast of Estonia (**Figure 2A**). The *SS* values (**Figure 2B**) revealed the magnitude of the change for the pixels with a significant trend ($p < 0.05$) and without a significant trend ($p > 0.05$). September showed an average *SS* value of 2.37 ± 0.29 mm per year (mean ± SD) for the pixels with a significant increase, for a total increase of 45 mm per pixel for the whole study period. The pixels with an increasing trend in April and December showed an average *SS* increase of 1.60 ± 0.26 and 1.31 ± 0.32 mm per year, respectively (**Supplementary Table 4**). Similar *SS* values were observed for the pixels with a significant decreasing trend in March, June, and July, with average *SS* decreases of 1.66, 2.33, and 2.22 mm per year, respectively (**Supplementary Table 4**).

Although the trend analysis for seasonal precipitation (**Supplementary Figure 1**) showed that spring had only four pixels with a significant increasing trend and 31 pixels with a significant decreasing trend, the average SS reveals an overall increase trend of 0.32 ± 1 mm per year (mean ± SD) in the region. The pixels with an increasing trend in spring had an average *SS* value of 1.40 ± 0.24 mm per year, versus −1.34 mm per year for pixels with a decreasing trend (**Supplementary Table 5**). Winter pixels with an increasing trend (7 piels) had a higher average *SS* value (5.63 mm per year) than the spring pixels with an increasing trend (1.4 mm per year). Autumn and summer showed no pixel with significant trends. Despite the lack of significant trends, summer was the only season that showed a decrease in precipitation for the pixels that showed no significant trend (mean $SS = -0.91$ mm per year). The annual analysis revealed no significant trend for any pixel (**Supplementary Figure 2** and **Supplementary Table 6**).

Spatial and Temporal Temperature Analysis

Analysis of the monthly mean temperature showed that 8 months presented no significant ($p < 0.05$) trend in any pixel (**Figure 3A**).

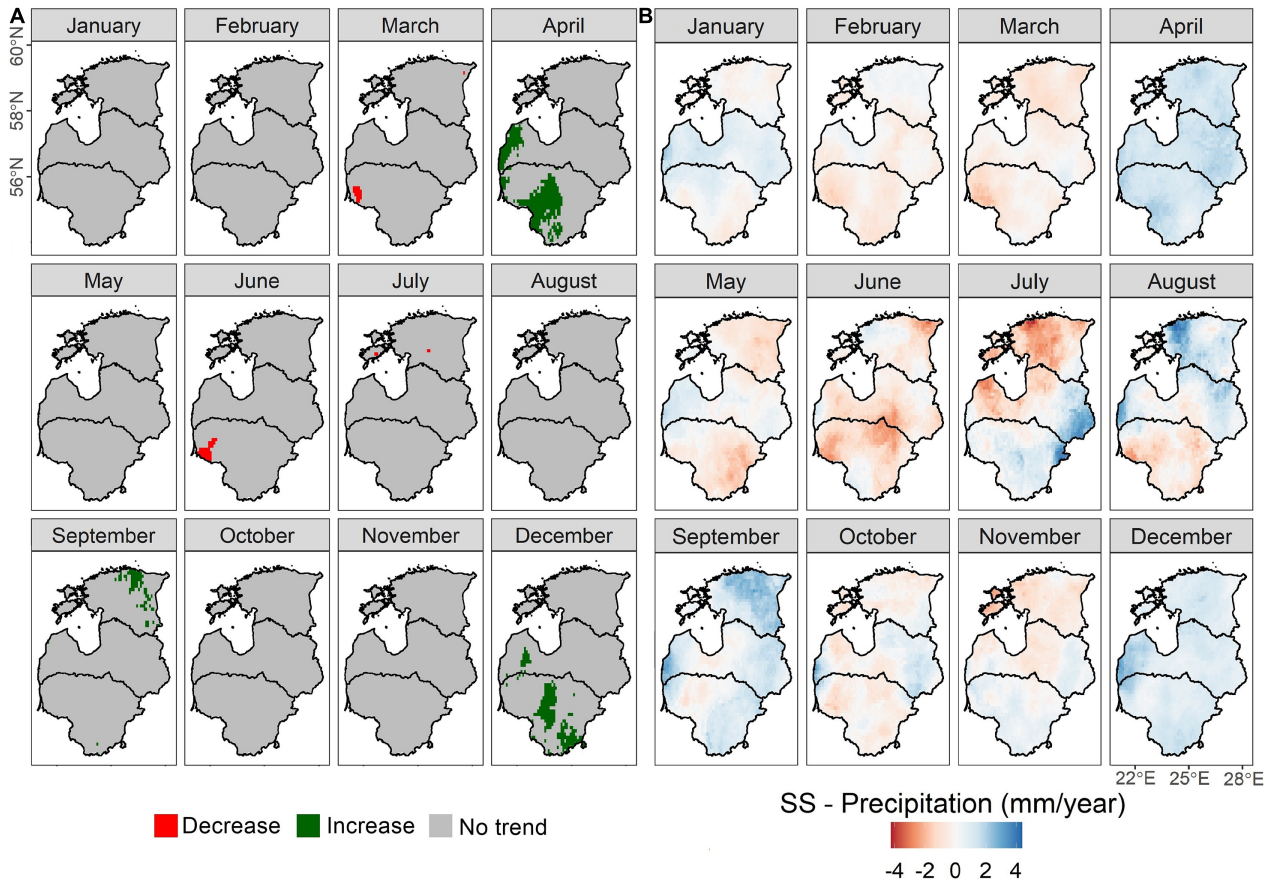

FIGURE 2 | (A) The results of the Mann-Kendall test for statistically significant ($p < 0.05$) trends in monthly precipitation at the pixel level. **(B)** Sen's slope (SS) values for changes in precipitation. Positive values represent increasing and negative values represent decreasing precipitation.

Moreover, no pixel with a significant decreasing trend was observed in any month. Pixels with significant increasing trends were identified in May (6.2% of the 2,557 pixels), June (4.6%), August (16.6%) and September (89.3%). In September, the pixels with a significant increasing trend covered almost the entire region. However, in May, June and August, the pixels with an increasing trend were clustered into a few areas in northern and western Estonia and eastern Latvia and Lithuania. The average *SS* values of the pixels with a significant increasing trend (**Figure 3B**) were 0.14 ± 0.14°C per year in May (mean ± SD), 0.10 ± 0.01°C per year in June and August, and 0.13 ± 0.02°C per year in September (**Supplementary Table 7**).

In the seasonal analysis, only autumn had pixels with significant increasing trends (6.6% of the pixels), and these pixels were located in the west of Lithuania and Latvia (**Supplementary Figure 4**). The pixels with an increasing trend in autumn had *SS* values that showed an average increase of 0.11 ± 0.01°C per year (**Supplementary Table 8**). Among the pixels with no significant trend in the other seasons, winter presented the highest average *SS* (0.07°C per year) with values ranging from 0.14 to −0.02°C per year (**Supplementary Table 8**). The annual analysis showed that 31.8% (813 out of 2557) of the pixels presented increasing trends (**Supplementary Figure 5**) and they are clustered in the west and east regions of Latvia and Lithuania, and in a smaller area in northern Estonia. The average *SS* of the pixels with an increase was 0.07°C per year, with values ranging from 0.04 to 0.09°C per year, versus 0.05°C per year for pixels with no trend and values ranging from 0.02 to 0.08°C per year (**Supplementary Table 9**).

Spatial and Temporal ET Analysis From 2000 to 2018

Pixels with significant ($p < 0.05$) increasing and decreasing trends for ET (**Figure 4A**) were more scattered compared to pixels with significant temperature and precipitation trends (**Figure 3A**). In May, June, and September, 23.2, 9.1, and 15.2% of the pixels (from a total of from 1 423 312) showed increasing ET trends, with mean *SS* values of 1.41 ± 0.50 (mean ± SD), 1.69 ± 0.67, and 0.65 ± 0.31 mm per year (**Figure 4B**), respectively. Interestingly, the mean *SS* values for the pixels with a decreasing trend in May, June, and September were much less common (0.1, 0.2, and 0.1%, respectively), showed *SS* values similar to those of the pixels with an increasing trend (**Supplementary Table 10**). August showed spatial segregation, with pixels that showed an increasing trend (9.3% of pixels) in the eastern part of the

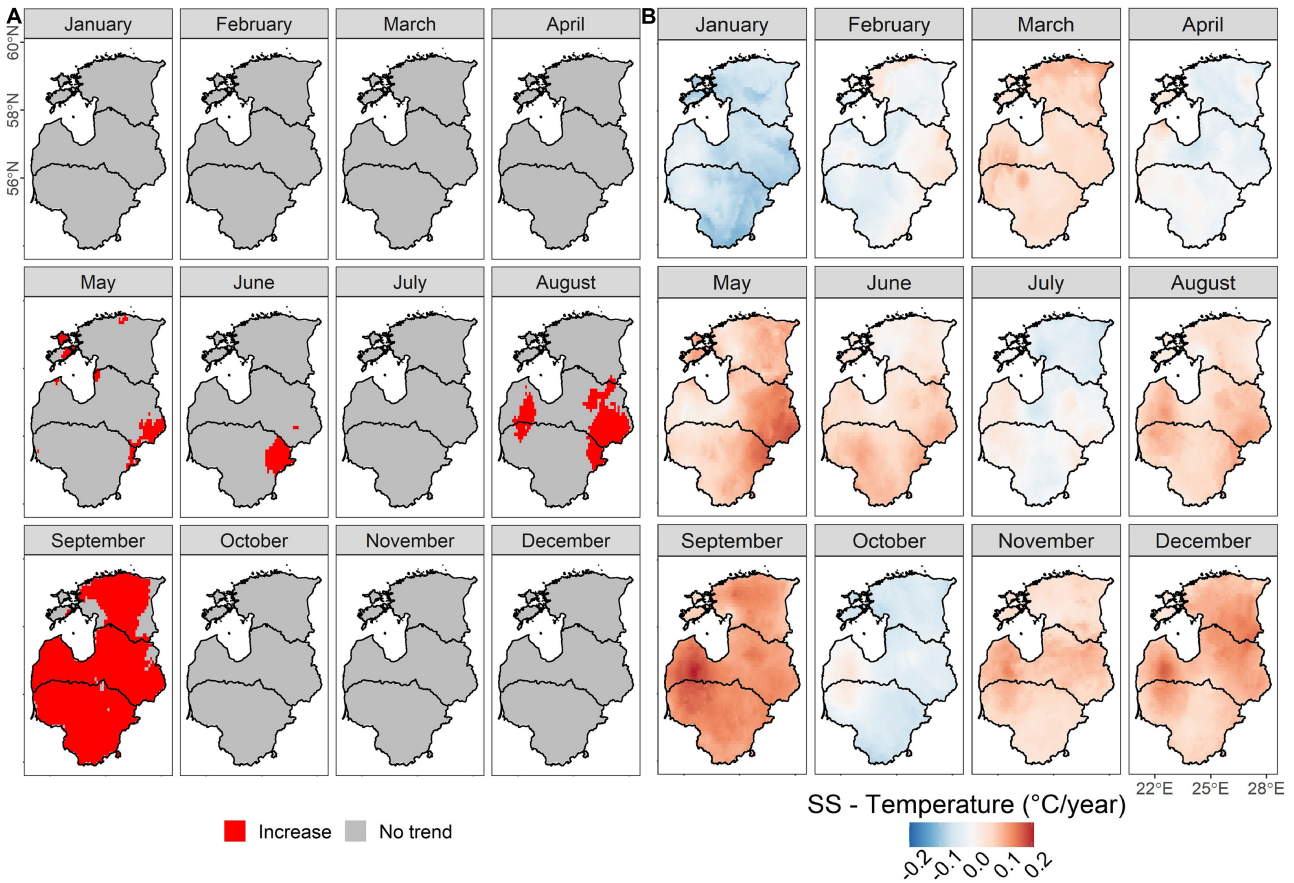

FIGURE 3 | (A) Mann-Kendall trend analysis for monthly mean air temperature at a pixel level. **(B)** Sen's slope values for monthly mean air temperature. Positive values represent a temperature increase, and negative values represent a decrease.

region and decreasing trends (3%) in the western part of the region (**Figure 4A**). November showed the biggest percentage of pixels with a decreasing trend for ET (9.5% of the total pixels; **Supplementary Table 10**). However, the mean *SS* values were smaller than the values for pixels with an increasing trend (**Supplementary Table 10**). March, April, July, and October showed <2.5% of the pixels with either increasing or decreasing trend. For these months (except July), the pixels with no significant trend revealed an average increase in the ET rates (**Supplementary Table 10**).

By analysing the ET trends seasonally, we found that 13% of the pixels in autumn (**Supplementary Table 11**) and 13.5% in spring presented a significant increasing trend, which is more than the proportion in summer (10%). All seasons had fewer than 1% of the pixels showing a decreasing trend (**Supplementary Table 11**). The pixels with a decreasing trend were spread throughout the Baltic countries during summer and autumn (**Supplementary Figure 6**). We also observed the latter spatial pattern for pixels with an increasing trend in all three seasons. On an annual basis, the spatiotemporal analysis revealed that 34.9% of the pixels had a significant increasing trend and only 0.3% showed a significant decreasing trend (**Supplementary Figure 7** and **Supplementary Table 12**).

We found that 83.5% of the MODIS ET pixels had forest (48.1%) and cropland (35.4%) as the major LULC type (with these types accounting for >50% of the MODIS ET pixel area). Hereafter, we refer to these as forest and cropland pixels. Most of these pixels (>77%) had no significant trend in ET in any month. Few forest and cropland pixels (<10%) showed a significant decreasing trend, with August showing the highest percentage (5.76%) for forest pixels (**Figure 4C**). For pixels with increasing trends, pixels of both LULC types showed similar percentages for March, April, October, and November (<2%). However, the difference between crop and forest pixels with an increasing trend was <4 percentage points in May, June, July, and August, September had a difference of 7.3 percentage points (11.2% of forest pixels and 3.8% of crop pixels; **Figure 4C**).

Evapotranspiration Over Unchanged Forest and Cropland Areas

We extracted the monthly ET of 10 949 MODIS ET pixels dominated by unchanged forest and 377 pixels dominated by unchanged cropland. Using the average monthly ET of these pixels, the Mann-Kendall trend analysis revealed that neither forest nor cropland showed a significant increasing or decreasing

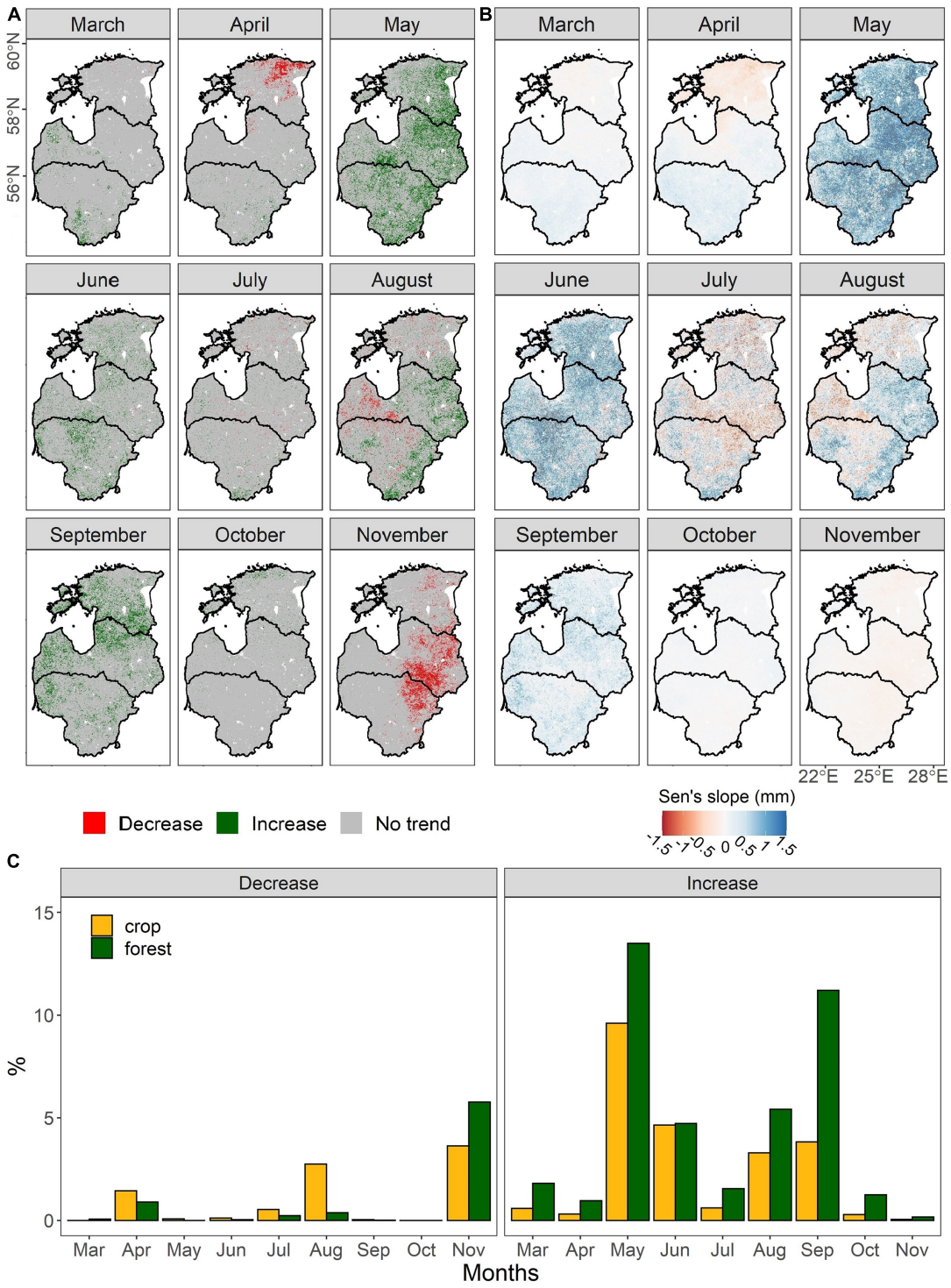

FIGURE 4 | (A) Mann-Kendall trend analysis for evapotranspiration at a pixel scale for each month, with $p < 0.05$ for significant trends. **(B)** Sen's slope values for evapotranspiration in each month. Positive values represent an increase, and negative values a decrease. **(C)** Percentage of forest and cropland pixels (>50% of the MODIS ET pixel area) that showed decreasing and increasing trends in each month.

trend in any month. However, the *SS* values (**Figure 5** and **Supplementary Table 13**) indicated that forest had an ET increase in most month (except July, August, and November) with May (0.7 mm per year), June (0.55 mm per year), and September (0.35 mm per year) showing the highest increasing values (**Supplementary Table 13**). At the same time, *SS* values

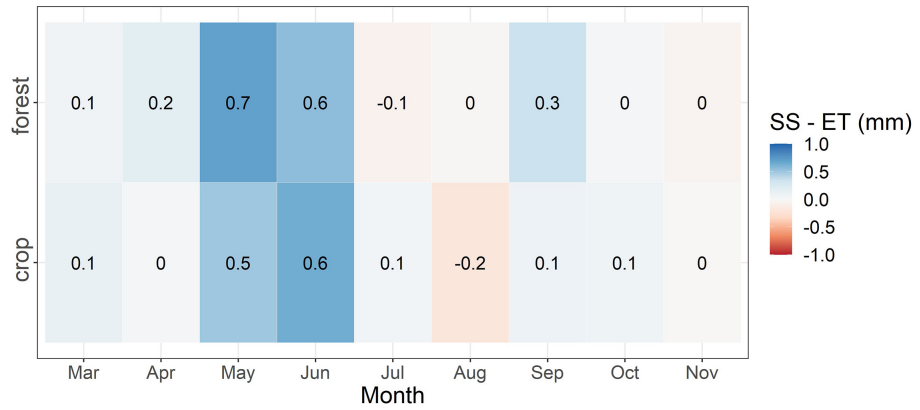

FIGURE 5 | Sen's slope (SS) values of evapotranspiration (ET mm) for forest and croplands in each month.

for cropland also showed increase for most months, except August (−0.2 mm per year) and November (−0.01 mm per year). Crop ET in June presented the highest value (0.64 mm per year), followed by May (0.50 mm per year). On a seasonal basis, forest showed a significant increasing trend in autumn ($SS = 0.46$ mm per year). Moreover, forest showed higher *SS* values than cropland in all seasons (**Supplementary Table 14**). At an annual scale, only forest had significant increasing trend (3.46 mm per year).

DISCUSSION

Precipitation and Temperature

In general, our results agreed with those of previous studies (Kriauciuniene et al., 2012; Jaagus et al., 2014, 2017), which also identified shifts in precipitation and temperature at monthly, seasonal, and annual temporal scales using weather station data. However, our study advanced these studies of climate shifts by analysing them both spatially (i.e., using a gridded dataset for the whole region) and at three temporal scales. The monthly analysis provided new insights that analysis with a coarser temporal resolution (i.e., seasonal and annual) would have not provided. For instance, the *SS* values for the overall summer season showed a reduction in precipitation. However, the monthly analysis showed that June and July had areas with statistically significant decreasing trends for precipitation and negative mean *SS* values for the pixels with non-significant trends, whereas August showed positive *SS* values. Therefore, the negative *SS* values of the summer season were influenced mostly by decreased June and July precipitation but not by August changes. This highlights the necessity of evaluating trends at a monthly level, as this more clearly reveals differences between the months within a season. Moreover, the spatial analysis using the monthly time scale provided an overview of the reduction in precipitation, which was more spatially dispersed in June and more clustered in July and August. Similar observations can be done for spring. March and May (the beginning and end of spring) showed reduced precipitation (negative *SS* values), whereas April (in the middle of the spring) showed an increase in precipitation, although with no significant trend. This dispersion of statistically significant trends at monthly and seasonal level was also reported by Jaagus et al. (2017), who investigated precipitation trends in Estonia using weather station data. They suggested that large-scale atmospheric circulation patterns were the main factor for the high spatiotemporal variability in the precipitation over the region (**Supplementary Figure 3**).

As was the case in other temperate regions (Zhang et al., 2017; Oishi et al., 2018), our results also indicated that the Baltic countries are experiencing a warming shift in most months, in all seasons (although only autumn showed a significant increasing trend), and in the mean annual temperature. Most of the statistically significant increase in temperature at a monthly scale was detected at the end of spring (May), at the beginning (June) and end of summer (August), and at the beginning of autumn (September). Similar findings were reported by Kriauciuniene et al. (2012), although these authors analyzed a longer time series record (from 1922 to 2007) for Lithuania, Latvia and Estonia.

By combining the temperature and the precipitation analysis, we found critical periods. For example, at the end of spring (May) and beginning of summer (June), the temperature showed statistically significant increasing trends, whereas the precipitation during the same period showed statistically significant decreasing trends. This can limit soil water availability during the spring warming period, and this will have several consequences for plant development, especially during the growing season. According to Grillakis (2019), soil moisture droughts events are expected to increase in frequency and spatial extent, and eastern Europe is likely to be most strongly affected. Similarly, Samaniego et al. (2018) reported that up to 40% of European soils will be affected by soil drought caused by anthropogenic warming if the temperature increases by 3°C compared to the pre-industrial period.

Evapotranspiration

Based on the ET trends and the LULC change analysis, we confirmed that the changes in ET rates over the Baltic

countries are most likely driven more by shifts in the climatic variables than by LULC change. This assumption agrees with the results of Li et al. (2017), who demonstrated a more significant impact of climate change than LULC change on ET throughout China. These changes in ET have an impact on the regional water balance. As highlighted by Teuling et al. (2019), the reduction in precipitation combined with an increase in ET to reduce streamflow. For example, by analysing precipitation, temperature and river discharge trends from 1991 to 2007, Kriauciuniene et al. (2012) found a significant decrease in river discharge in the western part of the Baltic region during the spring, a decrease in the whole region during the autumn, and an increase throughout the region during winter. Our results for ET showed statistically significant increases for most months that showed a reduction in river discharge in the same study area, and this partially explains the decrease in the river discharge. However, the reduction in the number of days and depth of snow cover (Rimkus et al., 2018) between 1961 and 2015 also affected the regional water balance, especially by limiting the amount of snowmelt water and groundwater, which are the major water sources for several rivers (Kriauciuniene et al., 2012). Moreover, our monthly ET analysis indicated that May, June, and July are critical months, since ET exceeds precipitation, on average, in 77% (+31.1 mm), 74.3% (+52.5 mm), and 50.7% (+36.3 mm), respectively (**Supplementary Figure 8**). This can potentially result in a reduction of soil moisture and groundwater availability if the water transported into the atmosphere by ET is not returning to the soil as precipitation, especially in June and July, when precipitation was decreasing. This type of seasonal hydrological shift was reported as a factor for summer drought in temperate forests (Parida and Buermann, 2014).

The changes in ET for croplands and forested areas are potentially a consequence of the lengthening growing season in the study region. Gaertner et al. (2019) found that an increase of ∼22 days in the growing season since 1982 until 2012 resulted in an increase of 12 mm in ET in the temperate forest region. They reported that temperature, vapor pressure deficit, wind, and humidity are important climatic variable for the change of the growing season. In addition, precipitation has been reported as an important factor for increasing growing season length (Dragoni and Rahman, 2012), since higher growing-season precipitation allows the vegetation to remain active over a longer period (Hussain et al., 2019). Therefore, the trends of increasing precipitation in April, August, and September (significant and not significant) combined with the temperature trends in May, August, and September that we observed, have likely driven the longer growing season. A longer growing season has been already reported for the study area using analysis of daily mean air temperature (Linderholm and Walther, 2008). According to the authors, the growing season increased between 11.5 and 12.2 days mainly due to an earlier starting of ∼10 days and a later ending of ∼2 days. Considering the findings of Gaertner et al. (2019), that a longer growing season result in an increase of ET, we can suggest that the forested ET rate increase in April and September (**Figure 5**) and the croplands ET rate increase in May (**Figure 5**) are likely caused by the changes in the growing season duration over the study area. We found that May and June showed reductions in precipitation and increases in temperature. This combination can potentially affect crop development, resulting in a soil moisture decrease that can cause drought during the early stages of crop development, and this can potentially result in significant yield reductions. For instance, the combination of decreased precipitation with decreased soil moisture can reduce crop yield (for wheat, canola, and barley) by 25 to 45% in a dry growing season (Madadgar et al., 2017).

For the forested areas, on the other hand, the reduction of ET during June and July, although not statistically significant, can be related to the decreased precipitation during these months. As a consequence, the forested areas can become more vulnerable to fires (Donis et al., 2017). One of the reasons that the decreases in ET over forested areas in June and July were not significant, and were lower than the decrease over the cropland, is that the forest can recycle more moisture due to its deeper roots (Zha et al., 2010). Lian et al. (2020) found that spring and summer soil moisture in the northern hemisphere has decreased from 1982 to 2011 due to earlier vegetation greening. They observed that this process was driven by an increase in ET rather than increased precipitation. Our observations for forest and cropland areas also agree with the results of Rimkus et al. (2017), who used the normalized-difference vegetation index, the vegetation condition index, and the standard precipitation index to study drought in the Baltic countries, concluded that cropland was affected more strongly than forest by precipitation deficits.

There are certain limitations of our study. First, our observations for unchanged cropland areas are limited by the small size of the patches of this LULC class, which did not allow us to sample <1.2% of MODIS ET pixels. To better estimate the changes in such small patches, future studies would benefit from higher resolution ET and climate datasets (Ruiz-Pérez and Vico, 2020). The datasets could be created using modeling (e.g., for ET, using the Penman-Monteith or Priestley-Taylor models). By using a higher spatial resolution, we could expand our analysis to include other LULC classes. For example, although we consolidated all forest types into a single forest class and all cropland types into a single cropland class, forests with different species or degrees of vegetation cover and different crops have different ET characteristics. In future research, these differences should be accounted for in our analysis. Another shortcoming is the lack of an uncertainty assessment for the MODIS ET data over the study region. However, several studies have pointed out the reliability of this data (Aguilar et al., 2018; Sriwongsitanon et al., 2020), with very good results over forested areas (Paca et al., 2019) and cropland areas (Velpuri et al., 2013). Future studies should also investigate the relationship or combined effect of precipitation and temperature change on ET rates at different time scales. Furthermore, it would be interesting to utilize water balance models to investigate how the changes in ET are affecting the water balance of the region (Kumar and Merwade, 2011).

DATA AVAILABILITY STATEMENT

The original contributions presented in the study are included in the article/**Supplementary Material**, further inquiries can be directed to the corresponding author/s.

AUTHOR CONTRIBUTIONS

BM and EU conceived the study and wrote the manuscript. BM performed the data analysis, with support from EU, JJ, and ÜM. All authors approved the manuscript for submission.

FUNDING

This research was funded by Mobilitas+ programme grant nos. MOBERC34 and PRG352 from the Estonian Research Council, NUTIKAS programme of the Archimedes foundation and European Regional Development Fund (EcolChange Centre of Excellence).

ACKNOWLEDGMENTS

We thank Geoff Hart for language editing and the reviewers for the useful comments that helped to improve our manuscript significantly.

SUPPLEMENTARY MATERIAL

The Supplementary Material for this article can be found online at: https://www.frontiersin.org/articles/10.3389/ffgc.2021.663327/full#supplementary-material

REFERENCES

Aguilar, A. L., Flores, H., Crespo, G., Marín, M. I., Campos, I., and Calera, A. (2018). Performance assessment of MOD16 in evapotranspiration evaluation in Northwestern Mexico. *Water* 10:901. doi: 10.3390/w10070901

Alkama, R., and Cescatti, A. (2016). Biophysical climate impacts of recent changes in global forest cover. *Science* 351, 600–604. doi: 10.1126/science.aac8083

Almeida, C. T., Oliveira-Júnior, J. F., Delgado, R. C., Cubo, P., and Ramos, M. C. (2017). Spatiotemporal rainfall and temperature trends throughout the Brazilian Legal Amazon, 1973–2013. *Int. J. Climatol.* 37, 2013–2026. doi: 10.1002/joc.4831

Atta-ur, R., and Dawood, M. (2017). Spatio-statistical analysis of temperature fluctuation using Mann–Kendall and Sen's slope approach. *Clim. Dyn.* 48, 783–797. doi: 10.1007/s00382-016-3110-y

Bari, S. H., Rahman, M. T. U., Hoque, M. A., and Hussain, M. M. (2016). Analysis of seasonal and annual rainfall trends in the northern region of Bangladesh. *Atmos. Res.* 176–177, 148–158. doi: 10.1016/j.atmosres.2016.02.008

Cao, Q., Yu, D., Georgescu, M., Han, Z., and Wu, J. (2015). Impacts of land use and land cover change on regional climate: a case study in the agro-pastoral transitional zone of China. *Environ. Res. Lett.* 10:124025. doi: 10.1088/1748-9326/10/12/124025

Ceccherini, G., Duveiller, G., Grassi, G., Lemoine, G., and Avitabile, V. (2020). Abrupt increase in forest harvested area over Europe After 2015. *Nature* 583, 72–77. doi: 10.1038/s41586-020-2438-y

Chen, L., and Dirmeyer, P. A. (2017). Impacts of land-use/land-cover change on afternoon precipitation over North America. *J. Clim.* 30, 2121–2140. doi: 10.1175/JCLI-D-16-0589.1

Cornes, R. C., van der Schrier, G., van den Besselaar, E. J. M., and Jones, P. D. (2018). An ensemble version of the E-OBS temperature and precipitation data sets. *J. Geophys. Res. Atmos.* 123, 9391–9409. doi: 10.1029/2017JD028200

Dias, L. C. P., Macedo, M. N., Costa, M. H., Coe, M. T., and Neill, C. (2015). Effects of land cover change on evapotranspiration and streamflow of small catchments in the Upper Xingu River Basin, Central Brazil. *J. Hydrol. Reg. Stud.* 4, 108–122. doi: 10.1016/j.ejrh.2015.05.010

Dinpashoh, Y., Jhajharia, D., Fakheri-Fard, A., Singh, V. P., and Kahya, E. (2011). Trends in reference crop evapotranspiration over Iran. *J. Hydrol.* 399, 422–433. doi: 10.1016/j.jhydrol.2011.01.021

Domínguez-Castro, F., Reig, F., Vicente-Serrano, S. M., Aguilar, E., Peña-Angulo, D., Noguera, I., et al. (2020). A multidecadal assessment of climate indices over Europe. *Sci. Data* 7:125. doi: 10.1038/s41597-020-0464-0

Donis, J., Kitenberga, M., Snepsts, G., Matisons, R., Zarins, J., and Jansons, A. (2017). The forest fire regime in Latvia during 1922–2014. *Silva Fenn* 51, 1–15. doi: 10.14214/sf.7746

dos Santos, C. A. C., Mariano, D. A., das Chagas, A., do Nascimento, F., Fabiane, F. R., de Oliveira, G., et al. (2020). Spatio-temporal patterns of energy exchange and evapotranspiration during an intense drought for drylands in Brazil. *Int. J. Appl. Earth Obs. Geoinf.* 85:101982. doi: 10.1016/j.jag.2019.101982

Dragoni, D., and Rahman, A. F. (2012). Trends in fall phenology across the deciduous forests of the Eastern USA. *Agric. For. Meteorol.* 157, 96–105. doi: 10.1016/j.agrformet.2012.01.019

ESA (2017). Land Cover CCI Product User Guide Version 2.0.

Findell, K. L., Berg, A., Gentine, P., Krasting, J. P., Lintner, B. R., Malyshev, S., et al. (2017). The impact of anthropogenic land use and land cover change on regional climate extremes. *Nat. Commun.* 8, 1–9. doi: 10.1038/s41467-017-01038-w

Funk, J. M., Aguilar-Amuchastegui, N., Baldwin-Cantello, W., Busch, J., Chuvasov, E., Evans, T., et al. (2019). Securing the climate benefits of stable forests. *Clim. Policy* 19, 845–860. doi: 10.1080/14693062.2019.1598838

Gaertner, B. A., Zegre, N., Warner, T., Fernandez, R., He, Y., and Merriam, E. R. (2019). Climate, forest growing season, and evapotranspiration changes in the central appalachian mountains. USA. *Sci. Total Environ.* 650, 1371–1381. doi: 10.1016/j.scitotenv.2018.09.129

Gao, F., Wang, Y., Chen, X., and Yang, W. (2020). Trend analysis of rainfall time series in Shanxi province, Northern China (1957-2019). *Water* 12, 1–22. doi: 10.3390/W12092335

Gogoi, P. P., Vinoj, V., Swain, D., Roberts, G., Dash, J., and Tripathy, S. (2019). Land use and land cover change effect on surface temperature over Eastern India. *Sci. Rep.* 9, 1–10. doi: 10.1038/s41598-019-45213-z

Grillakis, M. G. (2019). Increase in severe and extreme soil moisture droughts for Europe under climate change. *Sci. Total Environ.* 660, 1245–1255. doi: 10.1016/j.scitotenv.2019.01.001

Haghtalab, N., Moore, N., and Ngongondo, C. (2019). Spatio-temporal analysis of rainfall variability and seasonality in Malawi. *Reg. Environ. Chang.* 19, 2041–2054. doi: 10.1007/s10113-019-01535-2

Hale, R. C., Gallo, K. P., Owen, T. W., and Loveland, T. R. (2006). Land use/land cover change effects on temperature trends at U.S. Climate Normals stations. *Geophys. Res. Lett.* 33, 2–5. doi: 10.1029/2006GL026358

Hamed, K. H. (2008). Trend detection in hydrologic data: the mann-kendall trend test under the scaling hypothesis. *J. Hydrol.* 349, 350–363. doi: 10.1016/j.jhydrol.2007.11.009

Hamilton, S. K., Hussain, M. Z., Lowrie, C., Basso, B., and Robertson, G. P. (2018). Evapotranspiration is resilient in the face of land cover and climate change in a humid temperate catchment. *Hydrol. Process.* 32, 655–663. doi: 10.1002/hyp.11447

Hofstra, N., New, M., and McSweeney, C. (2010). The influence of interpolation and station network density on the distributions and trends of climate variables in gridded daily data. *Clim. Dyn.* 35, 841–858. doi: 10.1007/s00382-009-0698-1

Hussain, M. Z., Hamilton, S. K., Bhardwaj, A. K., Basso, B., Thelen, K. D., and Robertson, G. P. (2019). Evapotranspiration and water use efficiency of

continuous maize and maize and soybean in rotation in the upper Midwest U.S. *Agric. Water Manag.* 221, 92–98. doi: 10.1016/j.agwat.2019.02.049

Jaagus, J. (2006). Climatic changes in Estonia during the second half of the 20th century in relationship with changes in large-scale atmospheric circulation. *Theor. Appl. Climatol.* 83, 77–88. doi: 10.1007/s00704-005-0161-0

Jaagus, J., Briede, A., Rimkus, E., and Remm, K. (2014). Variability and trends in daily minimum and maximum temperatures and in the diurnal temperature range in Lithuania, Latvia and Estonia in 1951–2010. *Theor. Appl. Climatol.* 118, 57–68. doi: 10.1007/s00704-013-1041-7

Jaagus, J., Sepp, M., Tamm, T., Järvet, A., and Mõisja, K. (2017). Trends and regime shifts in climatic conditions and river runoff in Estonia during 1951–2015. *Earth Syst. Dyn.* 8, 963–976. doi: 10.5194/esd-8-963-2017

Jaagus, J., Truu, J., Ahas, R., and Aasa, A. (2003). Spatial and temporal variability of climatic seasons on the East European Plain in relation to large-scale atmospheric circulation. *Clim. Res.* 23, 111–129. doi: 10.3354/cr023111

Jassby, A. D., and Cloern, J. E. (2017). *wq: Exploring Water Quality Monitoring Data. R Package*. Available online at: https://cran.r-project.org/package=wq (accessed February 18, 2020).

Katsanos, D., Retalis, A., and Michaelides, S. (2016). Validation of a high-resolution precipitation database (CHIRPS) over Cyprus for a 30-year period. *Atmos. Res.* 169, 459–464. doi: 10.1016/j.atmosres.2015.05.015

Kendall, M. G. (1957). Rank correlation methods. *Biometrika* 44:298. doi: 10.2307/2333282

Khambhammettu, P. (2005). Mann-kendall analysis for the fort ord site. *HydroGeoLogic* 1, 1–7.

Krauskopf, T., and Huth, R. (2020). Temperature trends in Europe: comparison of different data sources. *Theor. Appl. Climatol.* 139, 1305–1316. doi: 10.1007/s00704-019-03038-w

Kriauciuniene, J., Meilutyte-Barauskiene, D., Reihan, A., Koltsova, T., Lizuma, L., and Sarauskiene, D. (2012). Variability in temperature, precipitation and river discharge in the Baltic States. *Boreal Environ. Res.* 17, 150–162.

Kumar, S., and Merwade, V. (2011). Evaluation of NARR and CLM3.5 outputs for surface water and energy budgets in the Mississippi River Basin. *J. Geophys. Res. Atmos.* 116, 1–21. doi: 10.1029/2010JD014909

Kumar, S., Merwade, V., Kam, J., and Thurner, K. (2009). Streamflow trends in Indiana: Effects of long term persistence, precipitation and subsurface drains. *J. Hydrol.* 374, 171–183. doi: 10.1016/j.jhydrol.2009.06.012

Lawrence, P. J., and Chase, T. N. (2010). Investigating the climate impacts of global land cover change in the community climate system model. *Int. J. Climatol.* 30, 2066–2087. doi: 10.1002/joc.2061

Li, G., Zhang, F., Jing, Y., Liu, Y., and Sun, G. (2017). Response of evapotranspiration to changes in land use and land cover and climate in China during 2001–2013. *Sci. Total Environ.* 596–597, 256–265. doi: 10.1016/j.scitotenv.2017.04.080

Lian, X., Piao, S., Li, L. Z. X., Li, Y., Huntingford, C., Ciais, P., et al. (2020). Summer soil drying exacerbated by earlier spring greening of northern vegetation. *Sci. Adv.* 6, 1–12. doi: 10.1126/sciadv.aax0255

Linderholm, H. W., and Walther, A. (2008). Twentieth-century trends in the thermal growing season in the Greater Baltic Area. *Clim. Chang.* 87, 405–419. doi: 10.1007/s10584-007-9327-3

Llopart, M., Reboita, M. S., Coppola, E., Giorgi, F., da Rocha, R. P., and de Souza, D. O. (2018). Land use change over the Amazon forest and its impact on the local climate. *Water* 10:149. doi: 10.3390/w10020149

Madadgar, S., AghaKouchak, A., Farahmand, A., and Davis, S. J. (2017). Probabilistic estimates of drought impacts on agricultural production. *Geophys. Res. Lett.* 44, 7799–7807. doi: 10.1002/2017GL073606

Mahmood, R., Pielke, R. A., Hubbard, K. G., Niyogi, D., Dirmeyer, P. A., Mcalpine, C., et al. (2014). Land cover changes and their biogeophysical effects on climate. *Int. J. Climatol.* 34, 929–953. doi: 10.1002/joc.3736

Mann, H. B. (1945). Non-parametric test against trend. *Econometrica* 13, 245–259.

Mao, J., Fu, W., Shi, X., Ricciuto, D. M., Fisher, J. B., Dickinson, R. E., et al. (2015). Disentangling climatic and anthropogenic controls on global terrestrial evapotranspiration trends. *Environ. Res. Lett.* 10:094008. doi: 10.1088/1748-9326/10/9/094008

Miralles, D. G., De Jeu, R. A. M., Gash, J. H., Holmes, T. R. H., and Dolman, A. J. (2011). Magnitude and variability of land evaporation and its components at the global scale. *Hydrol. Earth Syst. Sci.* 15, 967–981. doi: 10.5194/hess-15-967-2011

Moura, M. M., dos Santos, A. R., Pezzopane, J. E. M., Alexandre, R. S., da Silva, S. F., Pimentel, S. M., et al. (2019). Relation of El Niño and La Niña phenomena to precipitation, evapotranspiration and temperature in the Amazon basin. *Sci. Total Environ.* 651, 1639–1651. doi: 10.1016/j.scitotenv.2018.09.242

Nastos, P. T., Kapsomenakis, J., and Douvis, K. C. (2013). Analysis of precipitation extremes based on satellite and high-resolution gridded data set over Mediterranean basin. *Atmos. Res.* 131, 46–59. doi: 10.1016/j.atmosres.2013.04.009

Navarro, A., García-Ortega, E., Merino, A., Sánchez, J. L., Kummerow, C., and Tapiador, F. J. (2019). Assessment of IMERG precipitation estimates over Europe. *Remote Sens.* 11:2470. doi: 10.3390/rs11212470

Niu, Z., He, H., Zhu, G., Ren, X., Zhang, L., Zhang, K., et al. (2019). An increasing trend in the ratio of transpiration to total terrestrial evapotranspiration in China from 1982 to 2015 caused by greening and warming. *Agric. For. Meteorol.* 279:107701. doi: 10.1016/j.agrformet.2019.107701

Oishi, A. C., Miniat, C. F., Novick, K. A., Brantley, S. T., Vose, J. M., and Walker, J. T. (2018). Warmer temperatures reduce net carbon uptake, but do not affect water use, in a mature southern Appalachian forest. *Agric. For. Meteorol.* 252, 269–282. doi: 10.1016/j.agrformet.2018.01.011

Paca, V. H. D. M., Espinoza-Dávalos, G. E., Hessels, T. M., Moreira, D. M., Comair, G. F., and Bastiaanssen, W. G. M. (2019). The spatial variability of actual evapotranspiration across the Amazon river basin based on remote sensing products validated with flux towers. *Ecol. Process* 8:6. doi: 10.1186/s13717-019-0158-8

Parida, B. R., and Buermann, W. (2014). Increasing summer drying in North American ecosystems in response to longer nonfrozen periods. *Geophys. Res. Lett.* 41, 5476–5483. doi: 10.1002/2014GL060495

Perugini, L., Caporaso, L., Marconi, S., Cescatti, A., Quesada, B., De Noblet-Ducoudré, N., et al. (2017). Biophysical effects on temperature and precipitation due to land cover change. *Environ. Res. Lett.* 12:053002. doi: 10.1088/1748-9326/aa6b3f

Pielke, R. A. (2005). Land use and climate change. *Science* 310, 1625–1626. doi: 10.1126/science.1120529

Pongratz, J., Reick, C. H., Raddatz, T., and Claussen, M. (2010). Biogeophysical versus biogeochemical climate response to historical anthropogenic land cover change. *Geophys. Res. Lett.* 37, 1–5. doi: 10.1029/2010GL043010

Poon, P. K., and Kinoshita, A. M. (2018). Spatial and temporal evapotranspiration trends after wildfire in semi-arid landscapes. *J. Hydrol.* 559, 71–83. doi: 10.1016/j.jhydrol.2018.02.023

Qu, Y., and Zhuang, Q. (2019). Evapotranspiration in North America: implications for water resources in a changing climate. *Mitig. Adapt. Strateg. Glob. Chang.* 25, 205–220. doi: 10.1007/s11027-019-09865-6

Rimkus, E., Briede, A., Jaagus, J., Stonevicius, E., Kilpys, J., and Viru, B. (2018). Snow-cover regime in Lithuania, Latvia and Estonia and its relationship to climatic and geographical factors in 1961-2015. *Boreal Environ. Res.* 23, 193–208.

Rimkus, E., Stonevicius, E., Kilpys, J., MacIulyte, V., and Valiukas, D. (2017). Drought identification in the eastern Baltic region using NDVI. *Earth Syst. Dyn.* 8, 627–637. doi: 10.5194/esd-8-627-2017

Ruiz-Pérez, G., and Vico, G. (2020). Effects of temperature and water availability on Northern European Boreal Forests. *Front. For. Glob. Chang.* 3:34. doi: 10.3389/ffgc.2020.00034

Running, S., Mu, Q., Zhao, M., and Moreno, A. (2019). *MOD16A2GF MODIS/Terra Net Evapotranspiration Gap-Filled 8-Day L4 Global 500 m SIN Grid V006 [Data set]. NASA EOSDIS Land Processes DAAC*. Available online at: https://doi.org/10.5067/MODIS/MOD16A2GF.006 (accessed March 30, 2020).

Samaniego, L., Thober, S., Kumar, R., Wanders, N., Rakovec, O., Pan, M., et al. (2018). Anthropogenic warming exacerbates European soil moisture droughts. *Nat. Clim. Chang.* 8, 421–426. doi: 10.1038/s41558-018-0138-5

Sen, P. K. (1968). Estimates of the regression coefficient based on kendall's tau. *J. Am. Stat. Assoc.* 63, 1379–1389.

Sena, J. A., de Deus, L. A. B., Freitas, M. A. V., and Costa, L. (2012). Extreme events of droughts and floods in amazonia: 2005 and 2009. *Water Resour. Manag.* 26, 1665–1676. doi: 10.1007/s11269-012-9978-3

Seneviratne, S. I., Nicholls, N., Easterling, D., Goodess, C. M., Kanae, S., Kossin, J., et al. (2012). Changes in climate extremes and their impacts on the natural physical environment. *Manag. Risks Extrem. Events Disasters Adv. Clim. Chang.*

Adapt. Spec. Rep. Intergov. Panel Clim. Chang. 9781107025, 109–230. doi: 10.1017/CBO9781139177245.006

Silva Junior, C. H. L., Almeida, C. T., Santos, J. R. N., Anderson, L. O., Aragão, L. E. O. C., and Silva, F. B. (2018). Spatiotemporal rainfall trends in the Brazilian legal Amazon between the years 1998 and 2015. *Water*10, 1–16. doi: 10.3390/w10091220

Spera, S. A., Galford, G. L., Coe, M. T., Macedo, M. N., and Mustard, J. F. (2016). Land-use change affects water recycling in Brazil's last agricultural frontier. *Glob. Chang. Biol.* 22, 3405–3413. doi: 10.1111/gcb.13298

Sriwongsitanon, N., Suwawong, T., Thianpopirug, S., Williams, J., Jia, L., and Bastiaanssen, W. (2020). Validation of seven global remotely sensed ET products across Thailand using water balance measurements and land use classifications. *J. Hydrol. Reg. Stud.* 30:100709. doi: 10.1016/j.ejrh.2020.100709

Sy, S., and Quesada, B. (2020). Anthropogenic land cover change impact on climate extremes during the 21st century. *Environ. Res. Lett.* 15:034002. doi: 10.1088/1748-9326/ab702c

Teuling, A. J., De Badts, E. A. G., Jansen, F. A., Fuchs, R., Buitink, J., Van Dijke, A. J. H., et al. (2019). Climate change, reforestation/afforestation, and urbanization impacts on evapotranspiration and streamflow in Europe. *Hydrol. Earth Syst. Sci.* 23, 3631–3652. doi: 10.5194/hess-23-3631-2019

Van den Besselaar, E. J. M., Klein Tank, A. M. G., and Buishand, T. A. (2013). Trends in European precipitation extremes over 1951-2010. *Int. J. Climatol.* 33, 2682–2689. doi: 10.1002/joc.3619

Van Der Schrier, G., Van Den Besselaar, E. J. M., Klein Tank, A. M. G., and Verver, G. (2013). Monitoring European average temperature based on the E-OBS gridded data set. *J. Geophys. Res. Atmos.* 118, 5120–5135. doi: 10.1002/jgrd.50444

Velpuri, N. M., Senay, G. B., Singh, R. K., Bohms, S., and Verdin, J. P. (2013). A comprehensive evaluation of two MODIS evapotranspiration products over the conterminous United States: Using point and gridded FLUXNET and water balance ET. *Remote Sens. Environ.* 139, 35–49. doi: 10.1016/j.rse.2013.07.013

Vourlitis, G. L., de Souza Nogueira, J., de Almeida Lobo, F., and Pinto, O. B. (2014). Variations in evapotranspiration and climate for an Amazonian semi-deciduous forest over seasonal, annual, and El Niño cycles. *Int. J. Biometeorol.* 59, 217–230. doi: 10.1007/s00484-014-0837-1

Wang, H., Xiao, W., Zhao, Y., Wang, Y., Hou, B., Zhou, Y., et al. (2019). The spatiotemporal variability of evapotranspiration and its response to climate change and land use/land cover change in the three gorges reservoir. *Water* 11:1739. doi: 10.3390/w11091739

Zha, T., Barr, A. G., van der Kamp, G., Black, T. A., McCaughey, J. H., and Flanagan, L. B. (2010). Interannual variation of evapotranspiration from forest and grassland ecosystems in western canada in relation to drought. *Agric. For. Meteorol.* 150, 1476–1484. doi: 10.1016/j.agrformet.2010.08.003

Zhang, Y., Peña-Arancibia, J. L., McVicar, T. R., Chiew, F. H. S., Vaze, J., Liu, C., et al. (2016). Multi-decadal trends in global terrestrial evapotranspiration and its components. *Sci. Rep.* 6, 1–12. doi: 10.1038/srep19124

Zhang, Z., Zhang, R., Cescatti, A., Wohlfahrt, G., Buchmann, N., Zhu, J., et al. (2017). Effect of climate warming on the annual terrestrial net ecosystem CO2 exchange globally in the boreal and temperate regions. *Sci. Rep.* 7, 1–11. doi: 10.1038/s41598-017-03386-5

Conflict of Interest: The authors declare that the research was conducted in the absence of any commercial or financial relationships that could be construed as a potential conflict of interest.

frontiers in Forests and Global Change

MINI REVIEW
published: 10 May 2021
doi: 10.3389/ffgc.2021.682512

Birch as a Model Species for the Acclimation and Adaptation of Northern Forest Ecosystem to Changing Environment

*Elina Oksanen**

Department of Environmental and Biological Sciences, University of Eastern Finland, Joensuu, Finland

Northern forest ecosystems are exposed to rapid climate change, i.e., climate warming, extended growing seasons, increasing greenhouse gases, and changes in precipitation and water availability, accompanied by increasing pressure of herbivores and pathogens. Silver birch (*Betula pendula* Roth) is an important deciduous trees species in the boreal zone, with extensive distribution across Eurasia. Silver birch is an excellent model system for the adaptation of northern trees to climate change due to recent advances in genomics, high genetic variation, and intensive studies with different abiotic and biotic stress factors. In this paper, the current understanding about the responses and acclimation mechanisms of birch to changing environment is presented, based on Fennoscandian studies. Several complementary experiments in laboratory, semi-field and natural field conditions have shown that warming climate and increasing CO_2 is expected to increase the growth and biomass of birch, but the risk of herbivore damage will increase with negative impact on carbon sink strength. Deleterious impacts of high humidity, soil drought and increasing ozone has been clearly demonstrated. All these environmental changes have led to metabolic shifts or changes in carbon/nutrient balance which may have further ecological impacts. However, high plasticity and genotypic variation predict excellent acclimation capacity in rapidly changing environment and a rich genetic pool for sustainable forestry. Because the trees and forest ecosystems are exposed to multiple environmental factors simultaneously, it is necessary to continue research with multiple-stress interaction studies.

Keywords: birch, warming, air humidity, water stress, CO_2, ozone

OPEN ACCESS

Edited by:
Andrea Ghirardo, Helmholtz Zentrum München, Helmholtz-Gemeinschaft Deutscher Forschungszentren (HZ), Germany

Reviewed by:
Hilke Schroeder, Thünen Institute of Forest Genetics, Germany
Michael Eisenring, Swiss Federal Institute for Forest, Snow and Landscape Research (WSL), Switzerland

***Correspondence:**
Elina Oksanen
elina.oksanen@uef.fi

Specialty section:
This article was submitted to Forest Ecophysiology, a section of the journal Frontiers in Forests and Global Change

Received: *18 March 2021*
Accepted: *16 April 2021*
Published: *10 May 2021*

Citation:
Oksanen E (2021) Birch as a Model Species for the Acclimation and Adaptation of Northern Forest Ecosystem to Changing Environment. Front. For. Glob. Change 4:682512. doi: 10.3389/ffgc.2021.682512

INTRODUCTION

White birches (*Betula* sp.) are among the key species in the northern ecosystems which are strongly affected by current climate warming, increased pests and pathogen damage, land-use changes and forest fragmentation (Gauthier et al., 2015; IPCC, 2019). These factors may reduce genetic diversity and make forests more fragile and sensitive to other threats. *Betula pendula* (silver birch) and *B. pubescens* (downy birch) are the most common broad-leaved tree species in Fennoscandia and found in most other parts of Europe (Kuuluvainen et al., 2017). *B. pendula* is economically important in plywood, fiber and furniture production particularly in Finland due to fast growth and

good stem form (Verkasalo, 2002; Hynynen et al., 2010; Dubois et al., 2020). Besides the development of industrial potential in wider areas of Europe, the ecological and societal (aesthetic and recreational) value of *B. pendula* and *B. pubescens* has been recognized and evaluated (Dubois et al., 2020). Due to efficient seed propagation, birches are strong pioneer species in colonizing forest gaps in diverse climates and soils, enhancing biodiversity and soil functioning and improving the forest resilience e.g., against climate change, forest fires, and wind and herbivore damage (Mauer and Palatova, 2003; Kanerva and Smolander, 2007; Ascoli and Bovio, 2010; Rosenvald et al., 2011; Lehnert et al., 2013; Dubois et al., 2020). Besides many opportunities, high sensitivity to wood rot, crown competition and aero-allergenic properties of birches must not be ignored (Panula et al., 2009; Hynynen et al., 2010; Vanhellemont et al., 2016; Dubois et al., 2020).

Silver birch (*B. pendula*) is an excellent model system for the adaptation of northern trees to climate change due to recent advances in birch genomics (Salojärvi et al., 2017), intensive long-term studies e.g., for herbivory resistance, nitrogen economy, photosynthetic efficiency and phenology, and high genetic variation (Heimonen et al., 2016; Silfver et al., 2020; Tenkanen et al., 2020). In general, northern tree species of the boreal zone are adapted to cool climate with four seasons. Therefore, rapid climate warming is expected to strongly modify the function, phenology and development of these species. In addition to warming, changes in precipitation, drought and increasing greenhouse gases, and increasing herbivore and pathogen pressure are the most important factors affecting the boreal and subarctic forest trees and ecosystems (IPCC, 2019; Oksanen et al., 2019). The aim of this review is to present and discuss what we have learned about the impacts of these environmental factors on birch species growing in northern parts of Europe.

RESPONSES TO WARMING

Heating Experiments

Artificial heating experiments with infra-red heaters have provided basic knowledge about the direct physiological and biochemical responses and mechanisms of plants to warming environment (Mäenpää et al., 2011; Silfver et al., 2020). Field experiments using infra-red heaters with silver birch saplings revealed that elevated temperature (ambient +1.2°C) increased whole-plant photosynthesis, leaf area, specific leaf area (SLA), biomass, stem height and delayed autumnal leaf abscission, while stomatal conductance was declined (Riikonen et al., 2009; Mäenpää et al., 2011). Gas exchange profiles along the vertical axis of the saplings showed that the leaves near the top of the plant were the most responsive to warming (Mäenpää et al., 2011). Improved defence capacity of birch due to warming was demonstrated by higher total antioxidant capacity and redox state of ascorbate (Riikonen et al., 2009). Elevation of night-time temperature in the growth chamber conditions increased the leaf level respiration and shifted the metabolic profiles, depending strongly on the genotypes (Mäenpää et al., 2013). The most clear responses were seen as increased concentrations of triperpenoids, hydrolysable tannins, certain phenolic compounds such as DHPPG (3,4′-dihydroxypropiophenone-3-ß-D-glucopyranoside) and fructose (Mäenpää et al., 2013). Metabolic shifts were also observed in VOC emissions, with the clearest increases in homoterpene DMNT and several sesquiterpenes (SQT) (Ibrahim et al., 2010). Higher emissions of certain volatile compounds were related to improved thermotolerance (Ibrahim et al., 2010).

Another open-air warming experiment using infra-red heaters in Subarctic area demonstrated the positive impacts of warming (2.3 and 1.2°C increases in air and soil temperature, respectively) on four native *Betula* species (silver birch, *B. pendula*; downy birch, *B. pubescens*, dwarf birch, *B. nana*; and mountain birch, *B. pubescens* subsp. *Czerepanovii*) (Silfver et al., 2020). Warming treatment increased the plant height growth, leaf chlorophyll concentration, CO_2 uptake potential, and advanced the bud break. When the warming was combined with insecticide treatment reducing the pressure from insect feeding, the carbon sink strength of birches was even stronger, indicating the counteractive and negative impact of herbivores on carbon fluxes (Silfver et al., 2020). It is therefore expected that birch populations in the northern boreal and subarctic areas are vulnerable to climate warming and increasing herbivore pressure, as predicted earlier e.g., by Pöyry et al. (2011). Further, competition with the more southern genotypes can affect the genetic structure of the northern silver birch populations.

Translocation Experiments

A recent translocation experiment with 26 different silver birch genotypes simulating rapid climate warming across Finland has provided ecologically relevant information about the acclimation traits and capacity of birch as well as interactions with the other biotic and abiotic factors, such as herbivorous insect communities and nutrient availability (Heimonen et al., 2015a,b, 2016; Tenkanen et al., 2020, 2021). The results of herbivory studies show that climate warming can change the composition of herbivorous insect communities on birch, many herbivores can feed on novel host plant genotypes and the herbivory community composition is dependent on the physical size of plants and the phenological pattern of the genotypes (Heimonen et al., 2015a,b, 2016). Most severe herbivore damage was found in the small-size (height, leaf area) genotypes characterized by late bud burst and early growth cessation, and originating from high-latitude provenances (Heimonen et al., 2016).

Long-term field experiments have shown that Finnish silver birch populations can be divided into northern and southern groups according to several physiological traits, reflecting the evolutionary history of this species (Salojärvi et al., 2017; Tenkanen et al., 2020). Northern birch genotypes showed higher stomatal conductance (g_s) rates but lower water-use efficiency (WUE) accompanied by more efficient N acquisition compared to southern genotypes (Ruhanen, 2018; Tenkanen et al., 2020). Clear differences in the chemical profiles of the leaves have been confirmed between the northern and southern groups (Deepak et al., 2018). Complementary laboratory studies in equal growth conditions revealed also different biomass

accumulation strategies between the northern and southern birch origins (Tenkanen et al., 2021): while southern trees invest in canopy biomass and leaves, northern trees show more efficient photosynthetic capacity per leaf area (higher gas exchange, higher Fv/Fm) and relatively more investment in the below-ground fraction of the plant, but have a shorter total growth period. High root biomass is assumed to be an adaptation to better exploit and store the scarce nutrients and water resources in poor northern and arctic soils, safeguarding the leaf burst in the spring (Tenkanen et al., 2021). On the other hand, high soil N availability seems to increase the survival of silver birch plantlets, and growth and phenology may be adapted to soil N and day length rather than to temperature (Possen et al., 2014, 2021). Therefore, it is expected that the role of root compartment and root processes will be more important for birches in rapidly changing environment. Transfer of silver birch provenances in field experiments has, however, produced mixed results for fitness and survival and more research is needed for resistance traits. Viherä-Aarnio et al. (2013) indicated that long transfers (>2 latitudes) lead to a sharp decrease in survival and growth, while successful long-distance transfers of Finnish birches have been reported in North America and South Korea (Han et al., 1985; Rousi et al., 2012).

RESPONSES TO WATER STRESS

Soil Drought and Wetness

Impacts of soil drought on ozone-sensitive and ozone-tolerant silver birch genotypes have been studied in short-term and high-stress chamber experiment and long-term and mild-stress open-field experiment together with the ozone fumigation (Pääkkönen et al., 1998a,b). In both experiments, reduced leaf area, dry mass of leaves, stem and roots, gas exchange, transpiration rate, the number of stomata and starch was observed, accompanied by the higher contents or activity of Rubisco and chlorophyll, depending on the genotype (Pääkkönen et al., 1998a,b). Improved water-use-efficiency (WUE) developed in the open-field conditions (Pääkkönen et al., 1998a,b), while the induction of transcript levels for stress-protein PR-10 occurred in the chamber study (Pääkkönen et al., 1998c). Drought treatment mitigated the negative ozone effects in the acute chamber study, whereas negative interaction on the two stresses was detected in the open-field study (Pääkkönen et al., 1998a,b). Accordingly, high plasticity and a substantial variation in physiological and morphological responses, particularly in stomatal conductance, net photosynthesis, WUE, leaf carbon isotope composition, leaf osmotic potentials, leaf area indicators, root-to-shoot ratio and fine root growth have been detected among the silver birch clones exposed to drought in a common garden experiment by Aspelmeier and Leuschner (2004, 2006).

A semi-field experiment with three silver birch genotypes exposed to three soil moisture conditions (wet-control-dry) showed that drought stress reduced the growth, biomass, shoot-to-root ratio and gas exchange, while the wet treatment has opposite effects (Possen et al., 2011). Although there was a clear variation between the genotypes, the maintenance of the foliar processes as increasing number of leaves and high SLA during the stress treatments was observed for all genotypes (Possen et al., 2011). Silver birch seedlings have been also investigated for the impacts of waterlogging and soil freezing throughout the year, showing better tolerance against waterlogging during the winter dormancy compared to growing season (Repo et al., 2021). However, without the proper insulating snow cover, the downy birch seedlings suffered from the impaired growth and carbohydrate metabolism during the next following season (Domisch et al., 2019).

High Humidity

Responses of silver birch under long-term exposure to high humidity (low VPD) have been studied with the Free Air Humidity Manipulation (FAHM) facility in Estonia (Lihavainen et al., 2016b; Sellin et al., 2016; Oksanen et al., 2019). The results show that atmospheric humidity is an important climatic factor for birch trees affecting metabolism, physiology, water and nutrient cycling and balance, structure and development of leaf, roots and stem and growth properties (Sellin et al., 2016; Oksanen et al., 2019). At the whole-tree level, high humidity reduced the above-ground growth, total leaf area, leaf biomass, sap flux, slenderness, bud size, LAI (leaf area index) and soil respiration, delayed leaf fall and enhanced spring-term bud break, while increases in root biomass was detected concomitant with the higher number of root tips, increased fine root biomass, hydraulic conductance and hydrophilic ectomycorrhiza (Sellin et al., 2016; Oksanen et al., 2019). At the leaf level, high humidity increased starch, antioxidants (ascorbate metabolites, tocopherols), phenolic compounds and SLA, while glandular trichome density, N and P contents, leaf size, dark respiration, photosynthetic capacity and hydraulic conductance were declined (Lihavainen et al., 2016b; Sellin et al., 2016; Oksanen et al., 2019). In the stem, N and P contents and number of living parenchyma cells were increased, while wood density was reduced and wood chemistry altered (Sellin et al., 2016).

Short-term complementary laboratory experiments with high humidity (low VPD) provided more detailed information about metabolic responses and nutrient cycling of silver birch (Lihavainen et al., 2016a). In addition to starch, high humidity increased the foliar concentrations of quercetin glycosides, raffinose and glutamate, whereas the levels of amino acids alanine and valine, several citric acid cycle intermediates, glutamine-to-glutamate ratio, shikimic acid, ribonic acid, nutrient concentrations (N in particular) and glandular trichome density were reduced (Lihavainen et al., 2016a). This metabolic adjustment and limited nutrient availability shifted the balance towards carbohydrates and phenolics. Leaf surface wax composition shifted towards less hydrophobic waxes, with lower alkane and hydrophobic flavonoid contents, but the responses were mitigated by high N availability (Lihavainen et al., 2017). The two different experimental approaches revealed also some differences in plant responses between the field and laboratory studies (Lihavainen et al., 2016a). For instance, the transient increase in biomass, height, leaf number, whole-plant leaf area, stem diameter and root growth was observed in the laboratory, along with the higher

stomatal conductance rates, while antioxidants were unaffected (Lihavainen et al., 2016a; Oksanen et al., 2019). Increasing leaf wettability was considered predisposing the leaves to pathogen and pest damage (Lihavainen et al., 2017).

RESPONSES TO GREENHOUSE GASES

Increasing CO_2

Impacts of increasing CO_2 level has been studied in young in silver birch trees growing in open-top-chambers and in paper birch (*Betula papyrifera*) growing in the Aspen FACE site (Riikonen et al., 2004, 2005; Kontunen-Soppela et al., 2010a,b). High CO_2 (2 × ambient) increased biomass, growth and leaf area of the trees and lengthened the duration of the green leaves at the end of the season (Riikonen et al., 2004). Responses of net photosynthesis rates varied from considerable increase measured at high-CO_2 environment to decline measured at the ambient-CO_2 level, accompanied by reduced leaf N content, lower activity and amount of Rubisco and accumulation of starch (Riikonen et al., 2005). Genetic studies have supported these physiological and biochemical results and revealed the CO_2 caused down-regulation of the expression of several genes relating to the light reactions of the photosynthesis (Oksanen et al., 2005; Kontunen-Soppela et al., 2010a,b). Shift in secondary compound profiles due to high CO_2 was observed as increased phenolic acid and decreased flavonone aglycon and DHPPG contents (Peltonen et al., 2005). At the leaf structural level, increased size of starch grains and chloroplasts and higher number of mitochondria was observed at high CO_2 treatment, while SLA was reduced (Oksanen et al., 2005). Further, leaf chemistry was altered, reflecting lower nutrient contents, and cell wall composition was affected, containing a higher proportion of hemicellulose but lower proportion of a-cellulose, uronic acids, acid-soluble lignin and acetone-soluble extractives (Oksanen et al., 2005). As a whole, high CO_2 was considered strengthening the oxidative stress tolerance of silver birch trees through increased carbon pool for phenolic compounds, detoxification and cell wall structural modifications, but also exposing the trees to nutrient imbalance (Oksanen et al., 2005; Riikonen et al., 2005; Kontunen-Soppela et al., 2010a,b).

Increasing Ozone

Responses of silver birch to increasing tropospheric ozone, alone and in combination with other environmental factors such as CO_2, warming, soil nitrogen and drought, have been extensively investigated (e.g., Oksanen et al., 2007 and references therein). Harmful impacts of ozone has been reported as impaired growth and photosynthesis, declined Rubisco and chlorophyll content, altered shoot-to-root ratio at the expense of roots, visible leaf injuries, H_2O_2 accumulation (indicating oxidative stress) and related ultrastructural injuries particularly in the chloroplasts, altered cell wall chemistry, and disturbed nutrient

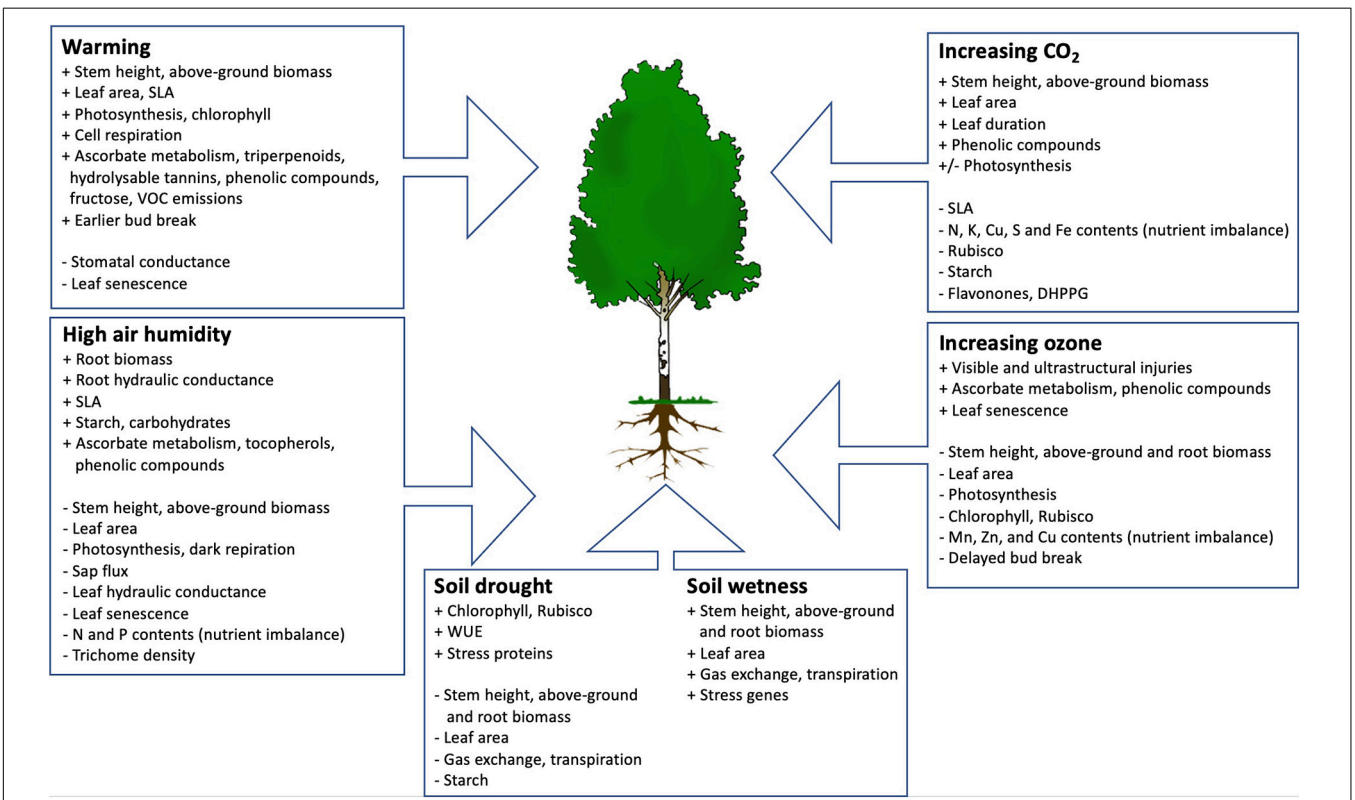

FIGURE 1 | The impacts of warming, high air humidity, soil drought and wetness, increasing CO_2 and ozone on birch. Positive responses are indicated with (+), negative responses with (–) and variable (both positive and negative) with (±). 'Above-ground biomass' includes stem and leaf biomass.

cycling and phenology through slower bud break and earlier leaf senescence (Oksanen et al., 2005, 2007; Oksanen and Kontunen-Soppela, 2021). These changes have been accompanied by shifted metabolic profiles towards phenolic compounds and increased antioxidative capacity through ascorbate metabolism (Yamaji et al., 2003; Kontunen-Soppela et al., 2007; Riikonen et al., 2009). Genetic variation in ozone responses is large, allowing the identification of ozone sensitive and ozone tolerant genotypes (Oksanen et al., 2007). Similar ozone responses have been reported also for paper birch growing in the Aspen FACE site in the temperate zone of the United States (Oksanen et al., 2003; Kontunen-Soppela et al., 2010b).

DISCUSSION

The present understanding about the impacts of warming, high air humidity, soil drought and wetness, increasing CO_2 and ozone on birch is shown in **Figure 1**, based on Fennoscandian studies. Warming climate is expected to increase the growth and biomass of birch, but the risk of herbivore damage will increase with negative impact on carbon sink strength (Mäenpää et al., 2011; Heimonen et al., 2015a,b, 2016; Silfver et al., 2020; **Figure 1**). Deleterious impacts of high humidity, soil drought and increasing ozone on birch has been clearly demonstrated (Pääkkönen et al., 1998a,b; Oksanen et al., 2007; Possen et al., 2011; Lihavainen et al., 2016b, 2017; **Figure 1**), as well as the positive impact of increasing CO_2 on growth (Riikonen et al., 2004). All these environmental changes have led to metabolic shifts which have been regarded as stress protection mechanisms, or changes in carbon/nutrient balance which may have further ecological impacts (Peltonen et al., 2005; Kontunen-Soppela et al., 2007; Mäenpää et al., 2013; Lihavainen et al., 2016a). Practically all experiments described above have shown high plasticity and genotypic variation in silver birch, predicting excellent acclimation capacity in rapidly changing environment and a rich genetic pool for sustainable forestry (Possen et al., 2015, 2021; Deepak et al., 2018; Tenkanen et al., 2020, 2021). High net assimilation rate, investment in leaf mass and high shoot-to-root ratio could be related to the fast growth rate of young birch trees (Possen et al., 2015), while high soil fertility (N content in particular) promoted the survival of birch in rapidly changing conditions (Possen et al., 2021).

An increasing body of literature underlines the value of birch as a model system for understanding how northern tree respond to climate change. To date, most studies on European birch species explore tree responses to changes in a single environmental variable. Yet, in the face of climate change trees and forest ecosystems will be exposed to multiple environmental factors simultaneously. However, the effects of multiple, interacting environmental factors on tree traits cannot be reliably assessed based on single factor analyses (Niinemets, 2010). Therefore, it is important to increasingly explore the multiple interactions, as done e.g., by Pääkkönen et al. (1998a, 1998b), Oksanen et al. (2005); Riikonen et al. (2005), and Kontunen-Soppela et al. (2010a,b) finding that ozone injuries were mitigated when birch trees were jointly exposed to drought, elevated CO_2, and increased nitrogen availability. More research is needed particularly for increasing CO_2 × water stress (drought, wetness, humidity) interactions, and for below-ground processes.

Finally, this review implies that birch with its rapid growth rate combined with a relatively high herbivore resistance, its ability to adapt to climatic changes and its recolonization traits possesses large potential in future silviculture. This is particularly true for mixed tree stands and reforestation areas. Therefore, birch deserves more attention in European tree breeding programms and silvicultural strategies.

DATA AVAILABILITY STATEMENT

The datasets presented in this study can be found in online repositories. The names of the repository/repositories and accession number(s) can be found in the article/supplementary material.

AUTHOR CONTRIBUTIONS

EO wrote all parts of the manuscript and made the Figure.

FUNDING

The work was funded by the University of Eastern Finland and The Finnish Cultural Foundation (project 00210798).

REFERENCES

Ascoli, D., and Bovio, G. (2010). Tree encroachment dynamics in heathlands of Northwest Italy: the fire regime hypothesis. *iForest* 3, 137–143. doi: 10.3832/ifor0548-003

Aspelmeier, S., and Leuschner, C. (2004). Genotypic variation in drought response of silver birch (*Betula pendula*): Leaf water status and carbon gain. *Tree Physiol.* 24, 517–528. doi: 10.1093/treephys/24.5.517

Aspelmeier, S., and Leuschner, C. (2006). Genotypic variation in drought response of silver birch (*Betula pendula* Roth): leaf and root morphology and carbon partitioning. *Trees* 20, 42–52. doi: 10.1007/s00468-005-0011-9

Deepak, M., Lihavainen, J., Keski-Saari, S., Kontunen-Soppela, S., Tenkanen, A., Oksanen, E., et al. (2018). Genotypic variation and provenance-related clinal patterns in leaf surface secondary compounds of silver birch. *J. Can. For. Res.* 48, 494–505. doi: 10.1139/cjfr-2017-0456

Domisch, T., Martz, F., Repo, T., and Rautio, P. (2019). Let it snow! winter conditions affect growth of birch seedlings during the following growing season. *Tree Phys.* 39, 544–555. doi: 10.1093/treephys/tpy128

Dubois, H., Verkasalo, E., and Claessens, H. (2020). Potential of birch (*Betula pendula* Roth and B. pubescens Ehrh.) for forestry and forest-based industry sector within the changing climatic and socio-economic context of Western Europe. *Forests* 11:336. doi: 10.3390/f11030336

Gauthier, S., Bernier, P., Kuuluvainen, T., Shvidenko, A. Z., and Schepaschenko, D. G. (2015). Boreal forest health and global change. *Science* 349, 819-822. doi: 10.1126/science.aaa9092

Han, Y., Lee, Y., Ryu, K., and Park, M. (1985). *Growth of European white birch (Betula pendula Roth) introduced from Finland at age 11 in Korea (No. Research Report 21)*. Suwon: Institute of Forest Genetics.

Heimonen, K., Valtonen, A., Kontunen-Soppela, S., Keski-Saari, S., Rousi, M., Oksanen, E., et al. (2015a). Colonization of a host tree by herbivorous insects under a changing climate. *Oikos* 124, 1013–1022. doi: 10.1111/oik.01986

Heimonen, K., Valtonen, A., Kontunen-Soppela, S., Keski-Saari, S., Rousi, M., Oksanen, E., et al. (2015b). Insect herbivore damage on latitudinally translocated silver birch (*Betula pendula*) – predicting the effects of climate change. *Clim. Change* 131, 245–257. doi: 10.1007/s10584-015-1392-4

Heimonen, K., Valtonen, A., Kontunen-Soppela, S., Keski-Saari, S., Rousi, M., Oksanen, E., et al. (2016). Susceptibility of silver birch (*Betula pendula*) to herbivorous insects is associated with size and phenology of birch– implications for climate warming. *Scan. J. For. Res.* 32, 95–104. doi: 10.1080/02827581.2016.1195867

Hynynen, J., Niemistö, P., Viherä-Aarnio, A., Brunner, A., Hein, S., and Velling, P. (2010). Silviculture of birch (*Betula pendula* Roth and *Betula pubescens* Ehrh.) in northern Europe. *Forestry* 83, 103–119. doi: 10.1093/forestry/cpp035

Ibrahim, M. A., Mäenpää, M., Hassinen, V., Kontunen-Soppela, S., Malec, L., Rousi, M., et al. (2010). Elevation of night-time temperature increases terpenoid emissions from *Betula pendula* and *Populus tremula*. *J. Exp. Bot.* 61, 1583–1595. doi: 10.1093/jxb/erq034

IPCC (2019). *Climate Change and Land, Report 2019*. Available online at: https://www.ipcc.ch/site/assets/uploads/2019/08/2c.-Chapter-2_FINAL.pdf (accessed February 15, 2021).

Kanerva, S., and Smolander, A. (2007). Microbial activities in forest floor layers under silver birch, Norway spruce and Scots pine. *Soil Biol. Biochem.* 39, 1459–1467. doi: 10.1016/j.soilbio.2007.01.002

Kontunen-Soppela, S., Ossipov, V., Ossipova, S., and Oksanen, E. (2007). Shift in birch leaf metabolome and carbon allocation during long-term open-field ozone exposure. *Glob. Change Biol.* 13, 1053–1067. doi: 10.1111/j.1365-2486.2007.01332.x

Kontunen-Soppela, S., Riikonen, J., Ruhanen, H., Brosché, M., Peltonen, P., Kangasjärvi, J., et al. (2010a). Differential gene expression in senescing leaves of two silver birch genotypes in response to elevated CO2 and tropospheric ozone. *Plant Cell Environ.* 33, 1016–1028. doi: 10.1111/j.1365-3040.2010.02123.x

Kontunen-Soppela, S., Parviainen, J., Brosché, M., Keinänen, M., Kolehmainen, M., Kangasjärvi, J., et al. (2010b). Gene expression responses of paper birch (*Betula papyrifera*) to elevated CO2 and O3 during leaf maturation and senescence. *Environ. Poll.* 158, 959–968. doi: 10.1016/j.envpol.2009.10.008

Kuuluvainen, T., Hofgaard, A., Aakala, T., and Jonsson, B. G. (2017). North Fennoscandian mountain forests: history, composition, disturbance dynamics and the unpredictable future. *For. Ecol. Manag.* 385, 140–149. doi: 10.1016/j.foreco.2016.11.031

Lehnert, L. W., Bassler, C., Brandl, R., Burton, P. J., and Muller, J. (2013). Conservation value of forests attacked by bark beetles: Highest number of indicator species is found in early successional stages. *J. Nat. Conserv.* 21, 97–104. doi: 10.1016/j.jnc.2012.11.003

Lihavainen, J., Ahonen, V., Keski-Saari, S., Kontunen-Soppela, S., Sober, A., Oksanen, E., et al. (2016a). Low vapour pressure affects nitrogen nutrition and foliar metabolites of silver birch. *J. Exp. Bot.* 67, 4353–4365. doi: 10.1093/jxb/erw218

Lihavainen, J., Ahonen, V., Keski-Saari, S., Sober, A., Oksanen, E., and Keinänen, M. (2017). Low vapor pressure deficit reduces glandular trichome density and modifies the chemical composition of cuticular waxes in silver birch leaves. *Tree Phys.* 28, 1–16. doi: 10.1093/treephys/tpx045

Lihavainen, J., Keinänen, M., Keski-Saari, S., Kontunen-Soppela, S., Sober, A., and Oksanen, E. (2016b). Artificially decreased VPD in field conditions modifies foliar metabolite profiles of birch and aspen. *J. Exp. Bot.* 67, 4367–4378. doi: 10.1093/jxb/erw219

Mäenpää, M., Ossipov, V., Kontunen-Soppela, S., Keinänen, M., Rousi, M., and Oksanen, E. (2013). Biochemical and growth acclimation of birch to night-time temperatures: genotypic similarities and differences. *Plant Biol.* 15, 36–43. doi: 10.1111/j.1438-8677.2012.00609.x

Mäenpää, M., Riikonen, J., Kontunen-Soppela, S., Rousi, M., and Oksanen, E. (2011). Vertical profiles reveal impact of ozone and temperature on carbon assimilation of *Betula pendula* and *Populus tremula*. *Tree Phys.* 31, 819–830. doi: 10.1093/treephys/tpr075

Mauer, O., and Palatova, E. (2003). The role of root system in silver birch (Betula pendula Roth) dieback in the air-polluted area of Krušné hory Mts. *J. For. Sci.* 49, 191–199. doi: 10.17221/4693-JFS

Niinemets, Ü (2010). Responses of forest trees to single and multiple environmental stresses from seedlings to mature plants: Past stress history, stress interactions, tolerance and acclimation. *For. Ecol. Manag.* 260, 1623–1639. doi: 10.1016/j.foreco.2010.07.054

Oksanen, E., Häikiö, E., Sober, J., and Karnosky, D. (2003). Ozone-induced H2O2 accumulation in field-grown aspen and birch is linked to foliar ultrastructure and peroxisomal activity. *New Phytol.* 161, 791–800. doi: 10.1111/j.1469-8137.2003.00981.x

Oksanen, E., and Kontunen-Soppela, S. (2021). Plants have different strategies to defend against air pollutants. *Curr. Opin. Env. Sci. Health* 19:100222. doi: 10.1016/j.coesh.2020.10.010

Oksanen, E., Kontunen-Soppela, S., Riikonen, J., Uddling, J., and Vapaavuori, E. (2007). Northern environment predisposes birches to ozone damage. *Plant Biol.* 9, 191–196. doi: 10.1055/s-2006-924176

Oksanen, E., Lihavainen, J., Keinänen, M., Kontunen-Soppela, S., Keski-Saari, S., Sellin, A., et al. (2019). "Northern forest trees under increasing atmospheric humidity," in *Progress in Botany ISBN 978-3-030-10760-4*, Vol. 80, eds U. Lüttge, F. M. Canovas, R. Matyssek, and H. Pretzsch (Cham: Springer Nature), 317–336. doi: 10.1007/124_2017_15

Oksanen, E., Riikonen, J., Kaakinen, S., Holopainen, T., and Vapaavuori, E. (2005). Structural characteristics and chemical composition of birch (*Betula pendula*) leaves are modified by increasing and CO2 and ozone. *Glob. Change Biol.* 11, 732–748. doi: 10.1111/j.1365-2486.2005.00938.x

Pääkkönen, E., Vahala, J., Holopainen, T., and Kärenlampi, L. (1998a). Physiological and ultrastructural responses of birch clones exposed to ozone and drought stress. *Chemosphere* 36, 679–684. doi: 10.1016/S0045-6535(97)10107-2

Pääkkönen, E., Vahala, J., Pohjola, M., Holopainen, T., and Kärenlampi, L. (1998b). Physiological, stomatal and ultrastructural ozone responses in birch (*Betula pendula* Roth) are modified by water stress. *Plant Cell Env.* 21, 671–684. doi: 10.1046/j.1365-3040.1998.00303.x

Pääkkönen, E., Seppänen, S., Holopainen, T., Kärenlampi, S., Kärenlampi, L., and Kangasjärvi, J. (1998c). Induction of genes for the stress proteins PR-10 and PAL in relation to growth, visible injuries and stomatal responses in ozone and drought exposed birch (*Betula pendula*) clones. *New Phytol.* 138, 295–305. doi: 10.1046/j.1469-8137.1998.00898.x

Panula, E. Y., Fekedulegn, D. B., Green, B. J., and Ranta, H. (2009). Analysis of airborne Betula pollen in Finland; a 31-year perspective. *Int. J. Environ. Res. Public Health* 6, 1706–1723. doi: 10.3390/ijerph6061706

Peltonen, P. A., Vapaavuori, E., and Julkunen-Tiitto, R. (2005). Accumulation of phenolic compounds in birch leaves is changed by elevated carbon dioxide and ozone. *Glob. Change Biol.* 11, 1305–1324. doi: 10.1111/j.1365-2486.2005.00979.x

Possen, B. J. H. M., Heinonen ,J., Anttonen, M., Rousi, M., Kontunen-Soppela, S., Oksanen, E., et al. (2015). Trait syndromes underlying stand-level differences in growth and acclimation in 10 silver birch (Betula pendula Roth) genotypes. *For. Ecol. Manag.* 343, 123–135. doi: 10.1016/j.foreco.2015.02.004

Possen, B. J. H. M., Oksanen, E., Rousi, M., Ruhanen, H., Ahonen, V., Tervahauta, A., et al. (2011). Adaptability of birch (*Betula pendula* Roth) and aspen (*Populus tremula* L.) genotypes to different soil moisture conditions. *For. Ecol. Manag.* 262, 1387–1399. doi: 10.1016/j.foreco.2011.06.035

Possen, B. J. H. M., Rousi, M., Keski-Saari, S., Kontunen-Soppela, S., Oksanen, E., and Mikola, J. (2021). New evidence for the importance of soil nitrogen on the survival and adaptation of birch to climate warming. *Ecosphere*

Possen, B. J. H. M., Rousi, M., Silfver, T., Anttonen, M., Ruotsalainen, S., Oksanen, E., et al. (2014). Within-stand variation in silver birch (*Betula pendula* Roth) phenology. *Trees* 28, 1801–1812. doi: 10.1007/s00468-014-1087-x

Pöyry, J., Leinonen, R., Söderman, G., Nieminen, M., Heikkinen, R. K., and Carter, T. R. (2011). Climate-induced increase of moth multivoltinism in boreal regions. *Glob. Ecol. Biogeogr.* 20, 289–298. doi: 10.1111/j.1466-8238.2010.00597.x

Repo, T., Domisch, T., Roitto, M., Kilpeläinen, J., Wang, A.-F., Piirainen, S., et al. (2021). Dynamics of above- and belowground responses of silver birch saplings and soil gases to soil freezing and waterlogging during dormancy. *Tree Phys.* tab002. doi: 10.1093/treephys/tpab002

Riikonen, J., Holopainen, T., Oksanen, E., and Vapaavuori, E. (2005). Leaf photosynthetic characteristics of silver birch during three years of exposure to elevated CO2 and O3 in the field. *Tree Phys.* 25, 621–632. doi: 10.1093/treephys/25.5.621

Riikonen, J., Lindsberg, M.-M., Holopainen, T., Oksanen, E., Peltonen, P., Lappi, J., et al. (2004). Silver birch and climate change: Variable growth and carbon allocation responses to elevated concentrations of carbon dioxide and ozone. *Tree Phys.* 24, 1227–1237. doi: 10.1093/treephys/24.11.1227

Riikonen, J., Mäenpää, M., Alavillamo, M., Silfver, T., and Oksanen, E. (2009). Interactive effects of elevated temperature and O3 on antioxidant capacity and gas exchange in *Betula pendula* saplings. *Planta* 230, 419–427. doi: 10.1007/s00425-009-0957-8

Rosenvald, K., Ostonen, I., Truu, M., Truu, J., Uri, V., Vares, A., et al. (2011). Fine-root rhizosphere and morphological adaptations to site conditions in interaction with tree mineral nutrition in young silver birch (*Betula pendula* Roth.) stands. *Eur. J. For. Res.* 130, 1055–1066. doi: 10.1007/s10342-011-0492-6

Rousi, M., Possen, B., Hagqvist, R., and Thomas, B. (2012). From the Arctic circle to the Canadian prairies - a case study of silver birch acclimation capacity. *Silva Fenn.* 46, 355–364. doi: 10.14214/sf.46

Ruhanen, H. (2018). *Effects of Soil, Birch Origin and Genotype on Growth and Physiology of Silver Birch and Downy birch.* Ph.D. Thesis. Joensuu: University of Eastern Finland.

Salojärvi, J., Smolander, O.-P., Nieminen, K., Rajaraman, S., Safronov, O., Safdari, P., et al. (2017). Genome sequencing and population genomic analyses provide insights into the adaptive landscape of silver birch. *Nat. Gen.* 49, 904–912. doi: 10.1038/ng.3862

Sellin, A., Alber, M., Keinänen, M., Kupper, P., Lihavainen, J., Lõhmus, K., et al. (2016). Growth of northern deciduous trees under increasing atmospheric humidity: possible mechanisms behind the growth retardation. *Reg. Env. Change* 17, 2135–2148. doi: 10.1007/s10113-016-1042-z

Silfver, T., Heiskanen, L., Aurela, M., Myller, K., Karhu, K., Meyer, N., et al. (2020). Insect herbivory control of Subarctic ecosystem CO2 exchange in present and future climates. *Nature Commun.* 11:2529. doi: 10.1038/s41467-020-16404-4

Tenkanen, A., Keski-Saari, S., Salojärvi, J., Oksanen, E., Keinänen, M., and Kontunen-Soppela, S. (2020). Differences in growth and gas exchange between southern and northern provenances of silver birch (*Betula pendula*) in northern Europe. *Tree Phys.* 40, 198–214. doi: 10.1093/treephys/tpz124

Tenkanen, A., Suprun, S., Oksanen, E., Keinänen, M., Keski-Saari, S., and Kontunen-Soppela, S. (2021). Strategy by latitude? Higher photosynthetic capacity and root mass fraction in northern than southern silver birch (*Betula pendula* Roth) in uniform growing conditions. *Tree Phys.* tpaa148. doi: 10.1093/treephys/tpaa148

Vanhellemont, M., Van Acker, J., and Verheyen, K. (2016). Exploring life growth patterns in birch (*Betula pendula*). *Scand. J. For. Res.* 31:7. doi: 10.1080/02827581.2016.1141978

Verkasalo, E. (2002). "Properties of domestic birch, aspen and alder and their utilisation in mechanical wood processing," in *Proceedings of the Finnish Forest Cluster Research Programme WOOD WISDOM (1998-2001).* Final report, Helsinki, 215–229.

Viherä-Aarnio, A., Kostiainen, K., Piispanen, R., Saranpää, P., and Vapaavuori, E. (2013). Effects of seed transfers on yield and stem defects of silver birch (*Betula pendula* Roth). *For. Ecol. Manag.* 289, 133–142. doi: 10.1016/j.foreco.2012.10.030

Yamaji, K., Julkunen-Tiitto, R., Rousi, M., Freiwald, V., and Oksanen, E. (2003). Ozone exposure over two growing seasons alters root to shoot ratio and chemical composition of birch (*Betula pendula* Roth). *Glob. Change Biol.* 9, 1363–1377. doi: 10.1046/j.1365-2486.2003.00669.x

Conflict of Interest: The author declares that the research was conducted in the absence of any commercial or financial relationships that could be construed as a potential conflict of interest.

frontiers in Forests and Global Change

ORIGINAL RESEARCH
published: 03 June 2021
doi: 10.3389/ffgc.2021.688534

Autumn Warming Delays the Downregulation of Photosynthesis and Does Not Increase the Risk of Freezing Damage in Interior and Coastal Douglas-fir

*Devin Noordermeer[1,2], Vera Marjorie Elauria Velasco[1] and Ingo Ensminger[1,2,3]**

[1] Department of Biology, University of Toronto Mississauga, Mississauaga, ON, Canada, [2] Graduate Department of Cell and Systems Biology, University of Toronto, Toronto, ON, Canada, [3] Graduate Department of Ecology and Evolutionary Biology, University of Toronto, Toronto, ON, Canada

During autumn, evergreen conifers utilize the decrease in daylength and temperature as environmental signals to trigger cold acclimation, a process that involves the downregulation of photosynthesis, upregulation of photoprotection, and development of cold hardiness. Global warming will delay the occurrence of autumn low temperatures while daylength remains unaffected. The impact of autumn warming on cold acclimation and the length of the carbon uptake period of species with ranges that encompass diverse climates, such as Douglas-fir (*Pseudotsuga menziesii*), remains unclear. Our study investigated intraspecific variation in the effects of autumn warming on photosynthetic activity, photosynthetic pigments, and freezing tolerance in two interior (var. *glauca*) and two coastal (var. *menziesii*) Douglas-fir provenances. Following growth under simulated summer conditions with long days (16 h photoperiod) and summer temperatures (22/13°C day/night), Douglas-fir seedlings were acclimated to simulated autumn conditions with short days (8 h photoperiod) and either low temperatures (cool autumn, CA; 4/−4°C day/night) or elevated temperatures (warm autumn, WA; 19/11°C day/night). Exposure to low temperatures in the CA treatment induced the downregulation of photosynthetic carbon assimilation and photosystem II efficiency, increased the size and de-epoxidation of the xanthophyll cycle pigment pool, and caused the development of sustained nonphotochemical quenching (NPQ). Seedlings in the WA treatment exhibited no downregulation of photosynthesis, no change in xanthophyll cycle pigment de-epoxidation, and no development of sustained NPQ. Albeit these changes, freezing tolerance was not impaired under WA conditions compared with CA conditions. Interior Douglas-fir seedlings developed greater freezing tolerance than coastal seedlings. Our findings suggest that autumn warming, i.e., short photoperiod alone, does not induce the downregulation of photosynthesis in Douglas-fir. Although autumn warming delays the downregulation of photosynthesis, the prolonged period of photosynthetic activity does not bear a trade-off of impaired freezing tolerance.

Keywords: ***Pseudotsuga menziesii*, autumn cold acclimation, intraspecific variation, photosynthesis, photoprotection, freezing tolerance, climate change, autumn warming**

OPEN ACCESS

Edited by:
James Blande,
University of Eastern Finland, Finland

Reviewed by:
Rongzhou Man,
Ontario Ministry of Natural Resources and Forestry, Canada
José Javier Peguero-Pina,
Aragon Agrifood Research and Technology Center (CITA), Spain

***Correspondence:**
Ingo Ensminger
ingo.ensminger@utoronto.ca

Specialty section:
This article was submitted to Forest Ecophysiology, a section of the journal Frontiers in Forests and Global Change

Received: *31 March 2021*
Accepted: *23 April 2021*
Published: *03 June 2021*

Citation:
Noordermeer D, Velasco VME and Ensminger I (2021) Autumn Warming Delays the Downregulation of Photosynthesis and Does Not Increase the Risk of Freezing Damage in Interior and Coastal Douglas-fir. Front. For. Glob. Change 4:688534. doi: 10.3389/ffgc.2021.688534

INTRODUCTION

Climate change is projected to increase global average surface temperatures by 2.5–5°C by the end of the century (IPCC, 2014). Even larger increases are projected for the middle to high latitudes of the Northern Hemisphere, which are dominated by temperate and boreal forests. In these forests, evergreen conifers undergo cold acclimation during autumn to protect their overwintering tissues (Chang et al., 2020). This cold acclimation process involves the cessation of growth, downregulation of photosynthesis, upregulation of photoprotection, and development of cold hardiness (Öquist and Hüner, 2003; Chang et al., 2020). Evergreen conifers rely upon decreases in temperature and photoperiod during autumn as signals to trigger these physiological changes (Welling et al., 2002; Rossi et al., 2008; Singh et al., 2017). Autumn warming will delay the low temperature signal while the short photoperiod signal will remain unaffected; this desynchronization has the potential to disrupt the cold acclimation process (Hänninen, 2016; Chang et al., 2020). Thus, the impact of projected autumn warming on evergreen conifer species will be strongly influenced by the importance of photoperiod versus temperature for the induction of the physiological changes that constitute cold acclimation (Way and Montgomery, 2015).

Evergreen conifer cold acclimation begins during late summer and early autumn with the initiation of growth cessation (Repo et al., 2000; Hamilton et al., 2016) and bud formation (Chen et al., 2012; Maurya and Bhalerao, 2017). Most evergreen conifers utilize short photoperiod as the dominant signal for initiation of growth cessation (Rossi et al., 2006). In these species, growth cessation likely involves a preemptive redirection of photoassimilates from sink tissues to storage tissues in early autumn (Oleksyn et al., 2000; Palacio et al., 2014). During late autumn, low temperatures begin to limit cell division, cell differentiation, and carbon allocation (Rossi et al., 2008). These changes decrease metabolic sink capacity and further cease growth. Photosynthesis continues to fuel the cold acclimation process (Wong et al., 2019; Fréchette et al., 2020); however, the combined effects of growth cessation and low temperatures eventually induce a downregulation of photosynthetic activity (Öquist and Hüner, 2003; Chang et al., 2020). This downregulation is due to limitation of the rates of photosynthetic electron transport and the Calvin cycle (Kingston-Smith et al., 1997; Öquist and Hüner, 2003; Crosatti et al., 2013). Comparatively, the rates of the primary photophysical and photochemical reactions of photosystem II (PSII) are largely temperature independent (Hüner et al., 1998; Ensminger et al., 2006). This disparity in temperature sensitivities creates potential for the accumulation of excess light energy during late autumn and winter (Öquist and Hüner, 2003; Hüner et al., 2013). Excess light energy can lead to the generation of reactive oxygen species (ROS) that cause photooxidative damage to PSII (Barber and Andersson, 1992; Apel and Hirt, 2004). This is especially threatening since low temperatures also inhibit the repair of damaged PSII subunits, such as the reaction center protein D1 (Ottander et al., 1995; Ensminger et al., 2006).

To protect against the harmful effects of low temperatures, evergreen conifers reorganize their photosynthetic apparatus into large aggregates that exhibit downregulated photosynthesis and upregulated photoprotection (Ottander et al., 1995; Savitch et al., 2002; Chang et al., 2020). In Scots pine (*Pinus sylvestris*), the downregulation of photosynthetic activity involves the moderate degradation of chlorophyll pigments and reaction center proteins, which causes a decrease in the size of PSII light-harvesting complexes (LHCs; Ottander et al., 1995; Porcar-Castell et al., 2008). The upregulation of photoprotective capacity usually involves the accumulation of carotenoid pigments that perform ROS scavenging, such as β-carotene, neoxanthin, and lutein (Krieger-Liszkay et al., 2008; Jahns and Holzwarth, 2012; Chang et al., 2015). It also involves the accumulation of carotenoid pigments that contribute to nonphotochemical quenching (NPQ), particularly xanthophyll pigments (Demmig-Adams and Adams, 1992; Ensminger et al., 2006; Verhoeven, 2014). In response to excess light energy, light-harvesting violaxanthin is de-epoxidated to form antheraxanthin, which is further de-epoxidated to form energy quenching zeaxanthin (Müller et al., 2001; Horton et al., 2008). During the growing season, these reactions occur in a fast and reversible process called the xanthophyll cycle, which provides a dynamic mechanism of NPQ in response to short-term stress (Demmig-Adams et al., 2012; Janka et al., 2015). During winter, the pigment quantity (VAZ) and de-epoxidation state (DEPS) of the xanthophyll cycle are increased, providing a sustained mechanism of NPQ in response to long-term stress (Sveshnikov et al., 2006; Demmig-Adams et al., 2012).

Cold acclimation also involves the development of cold hardiness, which is initiated during early autumn in response to decreasing photoperiod and evolves during late autumn in response to the combination of short photoperiod and low temperature (Chang et al., 2015; Strimbeck et al., 2015). Freezing temperatures can induce the formation of extracellular ice crystals that impose mechanical and osmotic stresses, causing tissue damage and cellular dehydration (Sutinen et al., 2001; Crosatti et al., 2013). Freezing and thawing in leaves can also disrupt the integrity of plasma and thylakoid membranes, resulting in leakage of solutes and collapse of cells and chloroplasts (Steponkus, 1984). To protect against this, evergreen conifers, such as Siberian spruce (*Picea obovata*), undergo large changes in lipid and carbohydrate metabolism during the development of cold hardiness (Angelcheva et al., 2014). These metabolic changes help maintain membrane fluidity (Moellering et al., 2010; Crosatti et al., 2013) and provide cellular osmo- and cryoprotection (Angelcheva et al., 2014; Chang et al., 2015). In addition, specific dehydrin proteins that have osmo- and cryoprotective functions are expressed (Close, 1997; Chang et al., 2015, 2016). Together, these cold hardening processes provide evergreen conifers, such as Douglas-fir, with tolerance to prolonged exposure to winter temperatures below −40°C (Strimbeck et al., 2015).

Several studies have investigated the effects of autumn warming on cold acclimation in evergreen conifers in order to assess the impact of climate change on temperate and boreal forests. Growth chamber experiments employing elevated

temperatures ranging from +5 to +15°C have demonstrated delayed downregulation of photosynthesis in seedlings of white pine (*Pinus strobus*; Chang et al., 2016; Fréchette et al., 2016) and white spruce (*Picea glauca*; Hamilton et al., 2016; Stinziano and Way, 2017). These findings are consistent with those of open-top chamber field experiments on mature Scots pine (Wang, 1996). Delayed development of freezing tolerance due to autumn warming has also been demonstrated in both growth chamber and open-top chamber experiments (Repo et al., 1996; Guak et al., 1998; Chang et al., 2016). However, a +15/+13°C (day/night) autumn warming treatment caused the downregulation of photosynthetic carbon assimilation but not PSII efficiency in jack pine seedlings (*Pinus banksiana*) (Busch et al., 2007). These seedlings responded to the resulting excess light energy *via* enhanced dynamic NPQ and increased quantities of ROS-scavenging β-carotene. In addition, the development of freezing tolerance in white spruce seedlings was unaffected under a +14/+12°C autumn warming treatment (Hamilton et al., 2016). These contrasting results highlight the variation among evergreen conifer species in the photoperiod sensitivity of the different cold acclimation processes.

Responses to shorter photoperiod and lower temperature during late summer and autumn can also vary within species and among populations originating from different geographical areas (i.e., provenances) (Savolainen et al., 2007). Fréchette et al. (2020) observed in white pine that the timing of the downregulation of photosynthesis in response to shorter photoperiod was delayed in southern provenances compared with northern provenances. In the same field experiment, Fréchette et al. (2020) also simulated autumn warming (+1.5°C above ambient during the day and +3°C above ambient during the night) and observed that warming caused a larger delay in the downregulation of photosynthesis in southern provenances than in northern provenances. Beuker et al. (1998) observed that northern provenances of Scots pine and Norway spruce (*Picea abies*) initiated the development of freezing tolerance in response to shorter photoperiods. These examples of intraspecific variation emerge from selective pressure for local adaptation to climate (Aitken et al., 2008). Local adaptation often results in patterns of trait variability that follow latitudinal and elevational gradients across the ranges of evergreen conifer species (Howe et al., 2003; Savolainen et al., 2007; Rehfeldt et al., 2014). However, local adaptation in many populations is lagging behind the shifts in climate caused by rapid warming (Carter, 1996; Corlett and Westcott, 2013; Gray and Hamann, 2013). As sessile species with long generation times, evergreen conifers are limited in their capacity to migrate and adapt in response to these shifts (Savolainen et al., 2007; Aitken et al., 2008). Thus, their capacity for phenotypic plasticity will be a major factor determining their ability to avoid maladaptation to autumn warming.

Douglas-fir (*Pseudotsuga menziesii*) has been used in many studies to demonstrate local adaptation (Eckert et al., 2009; Eilmann et al., 2013) and phenotypic plasticity (Isaac-Renton et al., 2014; Hess et al., 2016). It is a dominant and economically valuable evergreen conifer in western North America with a range that encompasses diverse climates (Howe et al., 2006; Mullin et al., 2011). In British Columbia specifically, mean annual temperature can vary as much as 6°C among Douglas-fir provenances (Wang et al., 2012). High levels of intraspecific variation in growth cessation and freezing tolerance development have been observed across its latitudinal and elevational gradients (Bansal et al., 2015; Ford et al., 2017). Intraspecific variation in the response of photosynthetic and photoprotective mechanisms to photoperiod and temperature is thus expected as well. The coastal Douglas-fir variety (var. *menziesii*) generally originates from low- to mid-elevation environments with milder climates, whereas the interior variety (var. g*lauca*) generally originates from mid- to high-elevation environments with colder climates and larger daily temperature ranges (Howe et al., 2006). Adaptation of these varieties in part reflects trade-offs between traits that improve vigor in milder climates and traits that improve tolerance to early frost (St Clair et al., 2005). However, selection pressures are changing rapidly; an increase in average autumn temperature of up to 6°C is projected in British Columbia by the end of the century (Arora et al., 2011; Wang et al., 2012). The impact that this will have on the physiological mechanisms that regulate the autumn cold acclimation process in Douglas-fir remains unclear.

In this study, we assessed the effects of simulated autumn warming on cold acclimation in two interior and two coastal provenances of Douglas-fir seedlings. We aimed to characterize the intraspecific variation in (1) the autumn cold acclimation process as well as (2) the plasticity of this process in response to warming. We hypothesized that (1) the autumn cold acclimation process requires both low temperature and short photoperiod signals in Douglas-fir. Autumn warming therefore delays the downregulation of photosynthesis and the corresponding upregulation of photoprotection, which causes an extension of the carbon uptake period at the cost of impairment of the development of freezing tolerance. We further hypothesized that (2) interior Douglas-fir is maladapted to warm autumn (WA) temperatures at lower latitudes and elevations, whereas coastal Douglas-fir is maladapted to frost risk at higher latitudes and elevations.

MATERIALS AND METHODS

Plant Materials and Experimental Conditions

Seeds of interior and coastal Douglas-fir provenances (*P. menziesii* var. *glauca* and var. *menziesii*, respectively) in British Columbia were obtained from the Tree Seed Centre (Surrey, British Columbia, Canada). Interior Douglas-fir seeds originated from Little Elk Creek (LIT; 50°32′24.0″N, 115°37′12.0″W, 1,525 m) and Meldrum Creek (MEL; 52°02′24.0″N, 122°19′48.0″W, 900 m), and coastal Douglas-fir seeds originated from Pemberton (PEM; 50°19′12.0″N, 122°43′48.0″W, 550 m) and Tsowwin River (TSO; 49°46′48.0″N, 126°37′48.0″W, 225 m) (**Figure 1**). These four provenances were selected because they represent a wide scope of the geographic and climatic conditions present across Douglas-fir's range in British Columbia (**Table 1**).

Seeds were soaked for 24 h in distilled water at room temperature, surface-sterilized for 5 h in 30 ml of 3% hydrogen peroxide, and stratified for 3 weeks in the dark at 4°C. pH 4.5 potting soil was prepared with 21.6% (v/v) silica sand

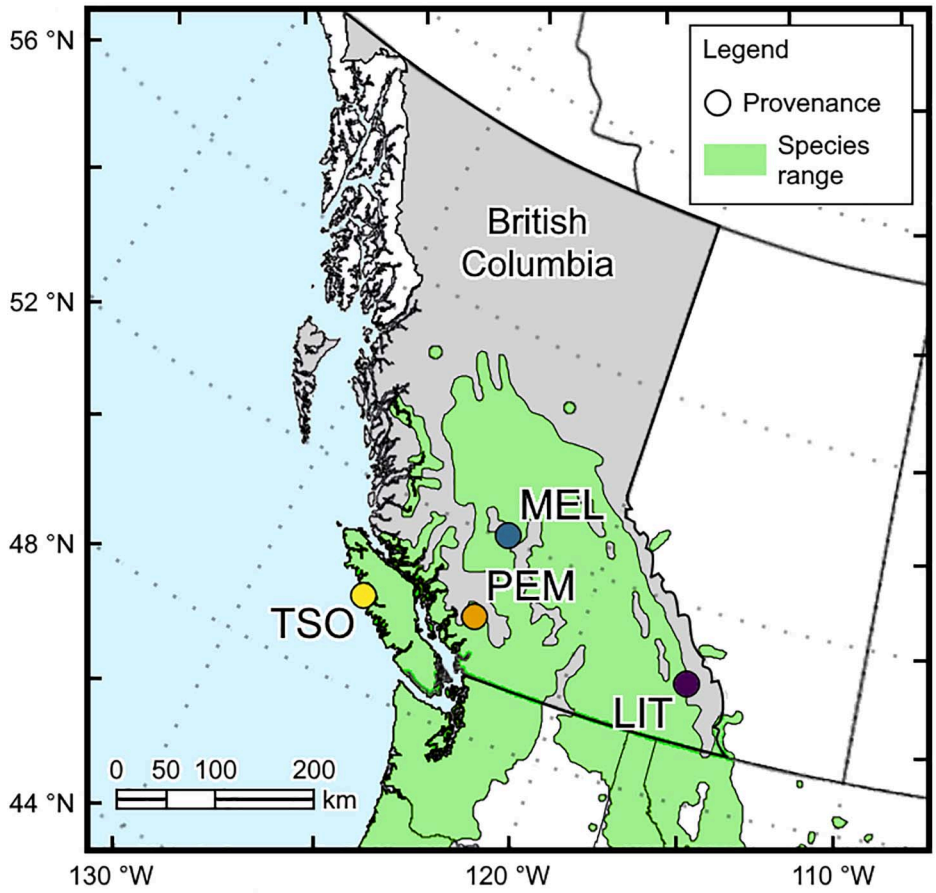

FIGURE 1 | Locations of the interior (LIT, MEL) and coastal (PEM, TSO) Douglas-fir provenances used in this experiment.

(Cat. No. 1240s; Bell & Mackenzie, Hamilton, ON, Canada), 13.5% (v/v) sphagnum peatmoss (Premier Tech, Rivière-du-Loup, PQ, Canada), 10.8% (v/v) Turface (PROFILE, Buffalo Grove, IL, United States), 7.6% (v/v) coarse perlite (Therm-O-Rock, New Eagle, PA, United States), 3.2% (v/v) medium vermiculite (Therm-O-Rock), 0.1% (v/v) dolomitic limestone (National Lime & Stone, Findlay, OH, United States), and 43.2% (v/v) distilled water. Seeds were planted in 168 ml cones lightly packed with potting soil and covered with 5 mm of silica sand. Seeds were germinated for 4 weeks in greenhouse under 17 h photoperiod and 25/17°C day/night, 400–1,200 μmol photos m^{-2} s^{-1} of photosynthetically active radiation, and 55% relative humidity (RH). At 4 weeks after planting, seedlings were transplanted into 25 l square pots containing one seedling from

TABLE 1 | Historical and projected autumn climate of the Douglas-fir provenances used in this experiment.

Var	Prov	Lat	Long	Elev	Historical (1961–1990)					Projected (2085)				
		(°N)	(°E)	(m)	T_{max} (°C)	T_{min} (°C)	T_{ave} (°C)	P (mm)	RH (%)	T_{max} (°C)	T_{min} (°C)	T_{ave} (°C)	P (mm)	RH (%)
Int	LIT	50.54	−115.62	1525	7.9	−3.7	2.1	134	59	14.3	2.9	8.6	174	63
	MEL	52.04	−122.33	900	10.1	−1.5	4.3	104	61	16.7	5.1	10.9	126	64
Cst	PEM	50.32	−122.73	550	10.9	1.6	6.2	320	69	17.4	7.8	12.6	363	71
	TSO	49.78	−126.63	225	12.8	5.2	9	1343	75	18.5	10.7	14.6	1464	76

Climate data were obtained from the ClimateWNA software; predictions for 2085 were based on the CanESM2 model RCP 8.5 scenario (Arora et al., 2011; Wang et al., 2012). Var, seed lot variety; Int, interior variety; Cst, coastal variety; Prov, provenance; Lat, latitudinal coordinates; Long, longitudinal coordinates; Elev, elevation above sea level; T_{max}, mean maximum autumn temperature; T_{min}, mean minimum autumn temperature; T_{ave}, mean average autumn temperature; P, mean total autumn precipitation; RH, mean autumn relative humidity.

each provenance. Seedlings were grown for 6 months under 18 h photoperiod and a temperature regime based on Wang et al. (2016). Following this growth phase, seedlings were transferred to growth chambers (BioChambers, Winnipeg, MB, Canada) and chilled for 2 months under 8 h photoperiod, 8/4°C day/night, and 50–300 μmol photons m^{-2} s^{-1}. This was followed by a second 6-month-long growth phase in greenhouse. During growth phases, seedlings were watered once per week and fertilized twice per week according to Wenny and Dumroese (1992).

At the start of the experiment, 2-year-old seedlings were transferred to four growth chambers and acclimated to simulated summer control (SC) conditions. This SC treatment consisted of long days and average summer temperatures (16 h photoperiod; 22/13°C day/night). Following 6 weeks of acclimation, sampling and measurements were performed for the SC treatment. Seedlings were then shifted to simulated WA or cool autumn (CA) conditions (two growth chambers per treatment). The WA treatment consisted of short days and elevated temperature (8 h photoperiod; 19/11°C day/night), designed to simulate the projected autumn temperature range for Tsowwin River in 2085 (Wang et al., 2012) according to the representative concentration pathway (RCP) 8.5 climate change scenario of the CanESM2 climate model (Arora et al., 2011). The CA treatment consisted of short days and low temperatures (8 h photoperiod; 4/-4°C day/night), designed to reproduce the average autumn temperature range for Little Elk Creek from 1961 to 1990. Following 6 weeks of acclimation, sampling and measurements were performed for the WA and CA treatments. Ten seedlings per treatment and provenance were randomly selected for sampling and measurements. All analyses were performed on 2-year-old needles. Seedlings were rotated within each growth chamber once per week. Photosynthetically active radiation (PAR) was maintained at 1,200 μmol photons m^{-2} s^{-1} midday and 400 μmol photons m^{-2} s^{-1} during the first and last hours of each day. Light was provided using metal halide and high-pressure sodium bulbs. RH was set to 55%.

Photosynthetic Gas Exchange and Chlorophyll Fluorescence

Photosynthetic gas exchange was measured using a GFS-3000 portable gas exchange system with a standard cuvette and a 3056-FL PAM-Fluorometer (Walz, Effeltrich, Germany). Measurements were started at least 1 h after growth lights were turned on. The measuring cuvette settings were: 400 ml min^{-1} flow rate; 400 ppm CO_2; 22 (SC treatment), 19 (WA treatment), or 4°C (CA treatment); and 55% RH. Dark respiration (R_d) was measured after 40 min of dark adaptation. Net photosynthetic carbon assimilation (A_{net}) and stomatal conductance (g_s) were measured during steady-state assimilation at 1,500 μmol m^{-2} s^{-1} PAR after at least 3 min of exposure. Gas exchange measurements were normalized to leaf surface area measurements estimated using WinSEEDLE Pro v.2011b (Regent Instruments, Québec City, QC, Canada).

Chlorophyll fluorescence was measured simultaneously with photosynthetic gas exchange. Dark adapted minimum PSII fluorescence (F_o) and maximum PSII fluorescence (F_m) were measured after 40 min of dark adaptation. This was followed by measurement of light-adapted minimum PSII fluorescence (F_o'), maximum PSII fluorescence (F_m'), and transient PSII fluorescence (F_t) at 1,500 μmol m^{-2} s^{-1} PAR after at least 3 min of exposure. Maximum quantum yield of PSII (F_v/F_m) was calculated as according to Genty et al. (1989).

$$\frac{F_v}{F_m} = \frac{F_m - F_o}{F_m} \quad (1)$$

Light energy partitioning was calculated using the parameters Φ_{PSII}, Φ_{NPQ}, and $\Phi_{f,D}$ (Hendrickson et al., 2004).

$$\Phi_{PSII} = 1 - \frac{F_t}{F'_m} \quad (2)$$

$$\Phi_{NPQ} = \frac{F_t}{F'_m} - \frac{F_t}{F_m} \quad (3)$$

$$\Phi_{f,D} = \frac{F_t}{F_m} \quad (4)$$

Photosynthetic Pigments

Photosynthetic pigments were extracted according to Junker and Ensminger (2016). Samples were flash-frozen in liquid nitrogen and stored at −80°C. Frozen samples were transferred to a pre-cooled mortar and pestle filled with liquid nitrogen and homogenized to a fine powder. Approximately 50–60 mg of homogenized frozen needle tissue was then transferred to a 2 ml amber vial, and pigments were then extracted for 2 h at 4°C in 98% methanol buffered with 2% 0.5 M ammonium acetate in the dark. The extract was centrifuged for 5 min at 4°C at 14,000 rpm, the supernatant was collected, and the pellet was washed with 100% methanol. This step was repeated twice. The supernatants were combined and filtered using 0.2 μm pore PTFE syringe filters (Thermo Scientific, Rockwood, TN, United States). Photosynthetic pigments were separated using a reverse-phase C30 column (5 μm, 250 × 4.6 mm; YMC Co., Ltd., Kyoto, Japan) and analyzed with a 1260 Infinity high performance liquid chromatography (HPLC) system equipped with a UV-diode array detector (Agilent Technologies, Santa Clara, CA, United States). Pigments were eluted using a mobile phase with a gradient of methanol, water buffered with 0.2% ammonium acetate, and methyl tert-butyl ether. Elution was performed at a flow rate of 1 ml min^{-1} and a column temperature of 25°C. Calibration was performed using standards for chlorophyll *a* and chlorophyll *b* (St. Louis, MO, United States) and antheraxanthin, α-carotene, β-carotene, lutein, neoxanthin, violaxanthin, and zeaxanthin from DHI Lab (Hørsholm, Denmark). Peak detection and pigment quantification were performed using ChemStation (Agilent Technologies).

Total chlorophyll content (Chl) was calculated as the sum of chlorophyll *a* and *b* contents per gram of fresh weight. Total carotenoid content (Car) was calculated as the sum of violaxanthin (Vio), antheraxanthin (Ant), zeaxanthin (Zea), neoxanthin (Neo), lutein (Lut), α-carotene (α-Car), and β-carotene (β-Car), normalized to Chl. Total xanthophyll cycle pigment content (VAZ) was calculated as the sum of Vio, Ant, and Zea. DEPS of xanthophyll cycle pigments was calculated according to Thayer and Bjorkman (1990).

$$DEPS = \frac{(0.5Ant + Zea)}{(Vio + Ant + Zea)} \quad (5)$$

Freezing Tolerance

Cold hardiness was assessed by measuring chlorophyll fluorescence to determine leaf freezing tolerance, following a modified protocol after Chang et al. (2016). Samples were taken after 9 weeks of exposure to WA or CA treatments. Needles were excised and placed proximal-end-down within 1.5 ml microcentrifuge tubes containing 0.10 ml of distilled water. Needles were exposed to a range of freezing temperatures at 5°C intervals from 0 to −40°C using a Thermotron SM-16-8200 environmental test chamber (Thermotron Industries, Holland, MI, USA). The initial decrease from 0 to −1°C occurred over 1 h, followed by a maximum cooling rate of −5°C per h to reach target temperature. Each target temperature was held for 10–12 h. After each freezing interval, needles were transferred to thaw in a stepwise manner: −20°C refrigeration for 24 h (if target temperature was >30°C), 4°C refrigeration for 24 h, and room temperature for 24 h. Following recovery, needles were exposed to 800 μmol photons m^{-2} s^{-1} for 1 h. Needles were then dark-adapted for 40 min, and F_v/F_m was assessed. The temperature corresponding to a 50% reduction in post-recovery F_v/F_m (LT_{50}) was used as a proxy for freezing tolerance of the photosynthetic apparatus. LT_{50} was calculated using the midpoints of sigmoidal vulnerability curves constructed using a modified generalized logistic function.

Statistical Analysis

All statistical tests were performed in R v3.5.2 (R Development Core Team, 2010). For all photosynthetic gas exchange, chlorophyll fluorescence, and photosynthetic pigment parameters, the effects of treatment, provenance, and the interaction thereof were assessed *via* two-way mixed-design ANOVA models using the *lmerTEST* package (Kuznetsova et al., 2017), where treatment and provenance represented categorical fixed factors, and chamber and pot represented random factors. For each parameter, the best-fit model was chosen according to lowest Akaike information criterion (AIC; Akaike, 1998). Following the determination of estimated marginal means between provenances for all parameters where provenance was significant, using the *emmeans* package (Lenth, 2016), significance of pairwise differences between provenances was assessed *via* Tukey's HSD test. Freezing tolerance was compared between treatments and provenances *via* Satterthwaite's approximate F test using the *drc* package (Ritz et al., 2015). Normality of distributions and equality of variances (homoscedasticity) for model residuals were assessed *via* Shapiro–Wilk test and Levene's test, respectively.

RESULTS

Photosynthetic Gas Exchange

Under simulated SC conditions, net photosynthetic carbon assimilation (A_{net}) was similar in seedlings of the provenances MEL, PEM, and TSO (**Figure 2A**). The lowest A_{net} was observed in the interior provenance LIT, which exhibited levels that were significantly lower than those in the interior provenance MEL ($P < 0.05$). After 6 weeks of acclimation to WA conditions, there were no significant changes in A_{net}. In contrast, after 6 weeks of acclimation to CA conditions, A_{net} significantly decreased by 85–95% ($P < 0.001$). This trend of treatment effects was also observed for stomatal conductance (g_s) (**Figure 2B**). Under SC, dark respiration (R_d) was significantly higher (approximately 50–60%) in seedlings of the interior provenances LIT and MEL than in those of the coastal provenances PEM and TSO ($P < 0.001$; **Figure 2C**). After acclimation to WA, only MEL seedlings exhibited a strong decrease in R_d. After acclimation to CA, LIT, MEL, and TSO seedlings all exhibited strong decreases in R_d. For LIT seedlings in particular, R_d significantly decreased by almost 50% under CA ($P < 0.001$).

Chlorophyll Fluorescence

Analysis of the maximum quantum yield of PSII (F_v/F_m) revealed values of approximately 0.81 in seedlings of all provenances under SC conditions (**Figure 3**). Acclimation to WA did not significantly affect F_v/F_m. However, F_v/F_m was approximately 75–85% lower under CA conditions than under SC and WA conditions ($P < 0.001$). There were no significant differences in F_v/F_m between provenances under any treatment (**Table 2**). Analysis of the proportion of absorbed light energy used for photochemistry (Φ_{PSII}), dynamic NPQ (Φ_{NPQ}), and the sum of fluorescence and sustained NPQ ($\Phi_{f,D}$) revealed that, under SC conditions, decreases in Φ_{PSII} under increasing light intensity were compensated for *via* increases in Φ_{NPQ} (**Figure 4** and **Supplementary Figure 2**). Acclimation to WA did not significantly alter this pattern of light energy partitioning (**Table 2**). However, acclimation to CA caused an almost fivefold increase in quenching of excess light energy *via* $\Phi_{f,D}$ ($P < 0.001$). This shift in light energy partitioning primarily replaced Φ_{NPQ}. LIT seedlings exhibited significantly higher Φ_{PSII} and lower Φ_{NPQ} than seedlings of other provenances ($P < 0.001$; **Figure 4**).

Photosynthetic Pigments

After acclimation to WA and CA, there were no significant changes in total chlorophylls (Chl) (**Table 2**). However, there were small but significant decreases in the ratio of chlorophyll *a* to chlorophyll *b* (Chl *a*/*b*) for all provenances under WA and CA ($P < 0.01$; **Figure 5B**). In contrast, acclimation to WA and CA caused increases in total carotenoids (Car), lutein (Lut), and total xanthophyll cycle pigments (VAZ) (**Figures 5C–E**). After acclimation to WA, Car, Lut, and VAZ increased in seedlings of the interior provenances only. After acclimation to CA, however, they increased in seedlings of both the interior and coastal provenances. Under CA compared with SC and WA, VAZ was significantly higher (approximately 40–50%) in seedlings of all provenances ($P < 0.01$; **Figure 5E**). The DEPS of the xanthophyll cycle increased only in response to CA conditions (**Figure 5F**). Under CA compared with SC and WA, DEPS was 3.5–5 times higher in seedlings of all provenances ($P < 0.01$).

Freezing Tolerance

The freezing temperature corresponding to 50% reduction in F_v/F_m (LT_{50}) did not significantly differ between seedlings

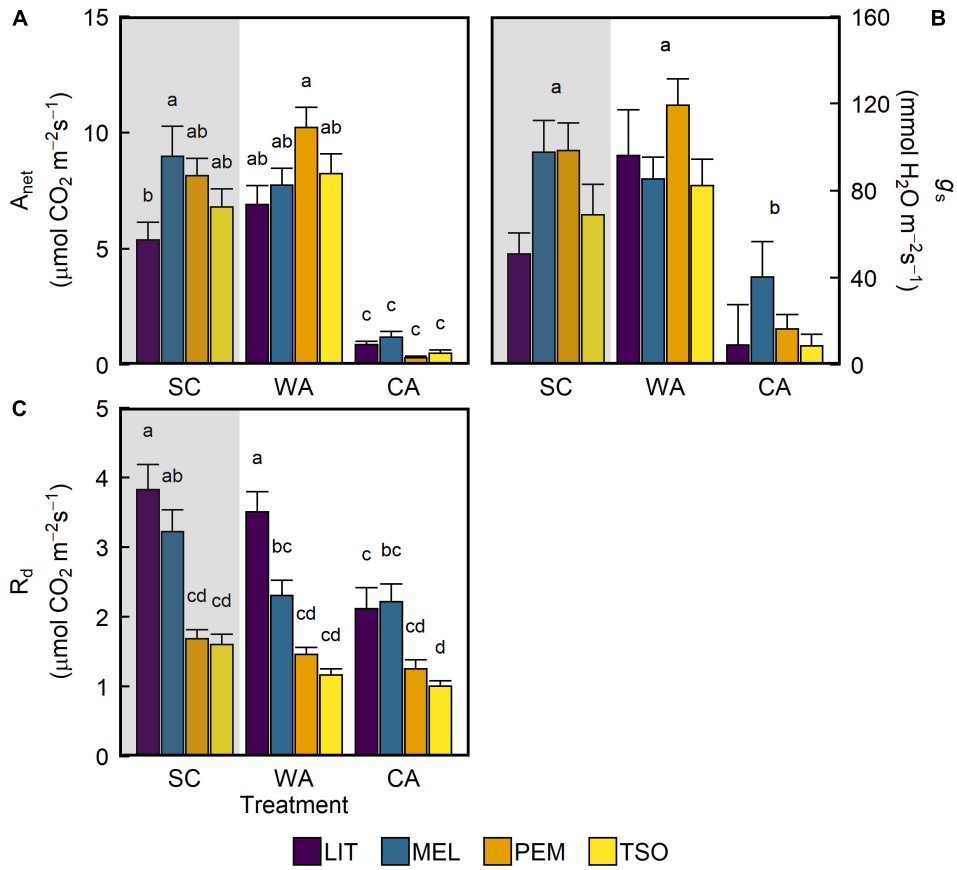

FIGURE 2 | Response of photosynthetic gas exchange of interior (LIT, MEL) and coastal (PEM, TSO) Douglas-fir seedlings to summer control (SC), warm autumn (WA), and cool autumn (CA) conditions. **(A)** Net photosynthetic carbon assimilation (A_{net}); **(B)** stomatal conductance (g_s); **(C)** dark respiration (R_d). Gray background indicates long photoperiod (summer); white background indicates short photoperiod (autumn). Measurements for A_{net} and g_s were taken at 1,500 µmol m^{-2} s^{-1} light intensity under growth conditions. Bars represent the mean of n = 7–10 ± SE. Letters where present indicate statistically different groups ($P < 0.05$) as determined by Tukey's HSD test.

acclimated to WA and seedlings acclimated to CA (**Figure 6**). However, LT_{50} of the interior provenances LIT and MEL was approximately 8–9°C higher than that of the coastal provenances PEM and TSO ($P < 0.01$).

DISCUSSION

Downregulation of Photosynthesis and Upregulation of Photoprotection in Response to CA Conditions

The transition from simulated SC conditions to simulated CA conditions caused substantial decreases in photosynthetic carbon assimilation (**Figure 2A**) and PSII efficiency (**Figure 3**). These changes are indicative of the downregulation of photosynthesis that is expected in evergreen conifers undergoing cold acclimation during autumn (Wong et al., 2019; Chang et al., 2020). The near-zero levels of A_{net} and F_v/F_m in our seedlings after 6 weeks of acclimation to CA were comparable with those observed in mature interior Douglas-fir growing under field conditions during mid-winter (Adams et al., 2002). Unlike in other evergreen conifer species, such as white pine (Chang et al., 2016; Fréchette et al., 2016) and Scots pine (Ottander et al., 1995; Ensminger et al., 2004), we did not observe that the degradation of chlorophyll pigments contributed to the downregulation of photosynthesis in our Douglas-fir seedlings following acclimation to low temperatures (**Figure 5A**). However, it is likely that the degradation of the PSII protein D1 contributed to the observed downregulation of photosynthesis, as has been demonstrated in field-grown white pine (Verhoeven et al., 2009) and Douglas-fir (Ebbert et al., 2005). The additional reduction of R_d in all provenances except PEM under CA conditions suggests a general downregulation in metabolic processes in these seedlings. While counterintuitive, the higher levels of R_d observed in the interior provenances LIT and MEL compared with the coastal provenances PEM and TSO are consistent with studies that report a general trend of higher R_d in trees originating from colder, high-elevation environments (Mitchell et al., 1999). This trend has been found to persist even in common growing environments similar to our own (Reich et al., 1996; Oleksyn et al., 1998).

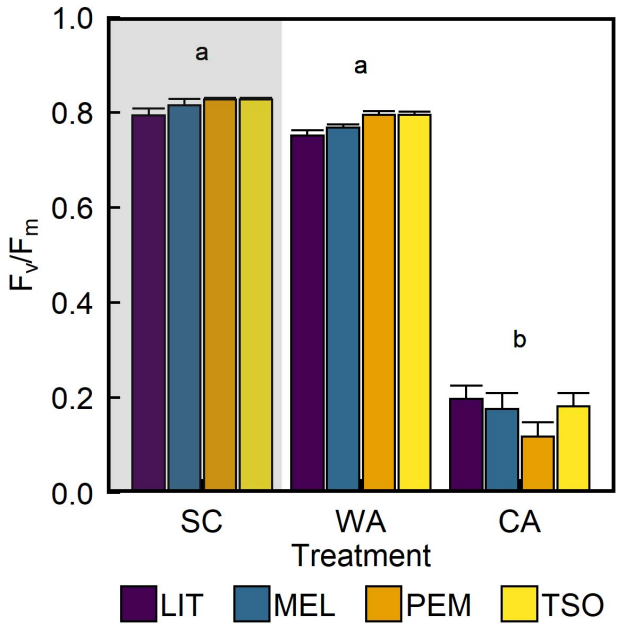

FIGURE 3 | Response of maximum quantum efficiency of photosystem II (F_v/F_m) of interior (LIT, MEL) and coastal (PEM, TSO) Douglas-fir seedlings to summer control (SC), warm autumn (WA), and cool autumn (CA) conditions. Gray background indicates long photoperiod (summer); white background indicates short photoperiod (autumn). Bars represent the mean of $n = 10 \pm$ SE. Letters where present indicate statistically different groups ($P < 0.05$) as determined by Tukey's HSD test.

The low F_v/F_m observed in our CA seedlings indicates photoinhibition of PSII caused by excess light energy, which was likely caused by the combination of light and low temperature (Ensminger et al., 2006). The transition from simulated summer conditions to simulated CA conditions caused a substantial shift in the quenching of excess light energy from dynamic NPQ to sustained NPQ (**Figure 4**). Levels of $\Phi_{f,D}$ in our seedlings after 6 weeks of acclimation to CA were comparable with those observed in field-grown white spruce seedlings during mid-winter (D'Odorico et al., 2020). This change in energy partitioning corresponded with increased quantities of the photoprotective xanthophyll carotenoids lutein, violaxanthin, antheraxanthin, and zeaxanthin (**Figures 5D,E**). Increased lutein content indicates an increased capacity for quenching of chlorophyll triplet states that generate photodamaging ROS (Dall'Osto et al., 2006; Jahns and Holzwarth, 2012). Increased violaxanthin, antheraxanthin, and zeaxanthin contents imply a general upregulation of xanthophyll cycle-dependent NPQ mechanisms. However, the increased xanthophyll cycle DEPS (**Figure 5F**) reflects a longer retention of energy quenching zeaxanthin, which indicates an upregulation of a sustained mechanism of zeaxanthin-dependent thermal energy dissipation (Demmig-Adams and Adams, 2006; Verhoeven, 2014). Similar to the findings of Fréchette et al. (2016), our Douglas-fir seedlings also retained some dynamic NPQ functionality under CA conditions. Φ_{NPQ} increased in response to increasing light intensity (**Supplementary Figure 1**), highlighting its continued importance as a short-term response to light stress even under low temperatures.

Warm Temperature Delays the Downregulation of Photosynthesis and Development of Sustained NPQ in Seedlings Growing Under Short Autumn Photoperiod

In contrast to CA, the transition from simulated summer conditions to conditions where we simulated the anticipated future warmer autumn did not affect photosynthetic carbon assimilation (**Figure 2A**) or PSII efficiency (**Figure 3**). Even after 6 weeks of exposure to short photoperiod, A_{net} and F_v/F_m remained largely unchanged under WA temperature. This suggests that short photoperiod alone does not trigger the downregulation of photosynthesis in Douglas-fir seedlings. This is in contrast to previous findings in white pine (Fréchette et al., 2016, 2020), jack pine (*P. banksiana*; Busch et al., 2007), and Scots pine (Vogg et al., 1998). The downregulation of photosynthesis has been linked to reduced metabolic sink capacity due to short photoperiod-induced growth cessation (Savitch et al., 2002; Busch et al., 2007; Hamilton et al., 2016). We did not measure growth cessation or bud formation, so it is unclear to what degree growth acted as a metabolic sink in our WA seedlings. Ford et al. (2017) used a modeling approach to determine that growth cessation is primarily induced by short photoperiod in provenances originating from low elevations that are adapted to warmer autumn temperatures compared with provenances originating from higher elevations that are adapted to colder autumn temperatures. The lack of downregulation of photosynthesis under WA conditions in our warmer low-elevation coastal provenances suggests that growth cessation may not be a major factor influencing the downregulation of photosynthesis in Douglas-fir. Photoassimilates produced during continued photosynthesis under WA were likely used to drive the metabolically expensive alterations that contribute to the accumulation of photoprotective carotenoid pigments and the development of cold hardiness (discussed below). Distribution of carbon through roots to soil organisms has been demonstrated to increase substantially at the end of the growing season in Scots pine forests (Högberg et al., 2010), presenting another potential sink for photoassimilates produced during autumn under warm temperatures.

In Interior Seedlings, Warm Temperature Does Not Impair the Accumulation of Photoprotective Carotenoid Pigments That Is Observed During Cold Acclimation and Growth Under Short Autumn Photoperiod

Following the transition from simulated summer conditions to simulated WA conditions, absorbed light energy that was in excess of the capacity for photochemistry and required safe dissipation was primarily quenched *via* dynamic NPQ (**Figure 4**). This indicates that the development of sustained NPQ during

TABLE 2 | Effect of treatment and provenance on photosynthetic gas exchange, chlorophyll fluorescence, photosynthetic pigments, and freezing tolerance.

Category	Parameter	Best-fit model	Treatment		Provenance		Treatment × Provenance	
			F	P	F	P	F	P
Photosynthetic gas exchange	A_{net}	Treatment × Provenance	117.937	**<0.001**	4.002	**0.009**	2.536	**0.024**
	R_d	Treatment × Provenance	19.170	**<0.001**	52.116	**<0.001**	2.800	**0.014**
	g_s	Treatment	32.967	**<0.001**	NA	NA	NA	NA
Chlorophyll fluorescence	F_v/F_m	Treatment	1221.000	**<0.001**	NA	NA	NA	NA
	Φ_{PSII}	Treatment + Provenance	12.025	**<0.001**	26.918	**<0.001**	NA	NA
	Φ_{NPQ}	Treatment + Provenance	2343.621	**<0.001**	11.421	**<0.001**	NA	NA
	$\Phi_{f,D}$	Treatment	3532.800	**<0.001**	NA	NA	NA	NA
Photosynthetic pigments	Chl	Treatment + Provenance	2.5150	0.089	2.796	**0.048**	NA	NA
	Chl a/b	Treatment	12.998	**<0.001**	NA	NA	NA	NA
	Car/Chl	Treatment × Provenance	34.076	**<0.001**	23.486	**<0.001**	2.965	**0.013**
	VAZ/Chl	Treatment × Provenance	85.374	**<0.001**	14.172	**<0.001**	2.731	**0.022**
	DEPS	Treatment	824.440	**<0.001**	NA	NA	NA	NA
	Vio/Chl	Treatment × Provenance	459.446	**<0.001**	13.372	**<0.001**	2.597	**0.026**
	Ant/Chl	Treatment + Provenance	109.424	**<0.001**	5.910	**0.001331**	NA	NA
	Zea/Chl	Treatment	338.190	**<0.001**	NA	NA	NA	NA
	Neo/Chl	Treatment + Provenance	3.402	**0.045**	2.668	0.057	NA	NA
	Lut/Chl	Treatment × Provenance	28.786	**<0.001**	18.486	**<0.001**	4.265	**0.001**
	α-Car/Chl	Treatment × Provenance	23.820	**<0.001**	3.110	**0.034**	7.613	**<0.001**
	β-Car/Chl	–	NA	NA	NA	NA	NA	NA

For each parameter, the best-fit model including treatment, provenance, week, and interactions thereof was chosen according to AIC. NA is used to denote that a factor was not included in the best-fit model. Effects of treatment, provenance, and week were assessed by pairwise comparison of models with and without each factor using a log-likelihood ratio test. P-values are bolded to denote statistical significance ($P < 0.05$). A_{net}, net photosynthetic carbon assimilation; g_s, stomatal conductance; R_d, dark respiration; F_m, maximum quantum yield of PSII; Φ_{PSII}, fraction of light energy quenched via photochemistry (i.e., effective quantum yield of photosystem II); Φ_{NPQ}, fraction of light energy quenched via dynamic nonphotochemical quenching; $\Phi_{f,D}$, fraction of light energy quenched via fluorescence and sustained nonphotochemical quenching; Chl, chlorophylls; Chl a/b, ratio of chlorophyll a to chlorophyll b; Car, carotenoids; VAZ, total xanthophyll cycle pigments; DEPS, de-epoxidation state of the xanthophyll cycle; Vio, violaxanthin; Ant, antheraxanthin; Zea, zeaxanthin; Neo, neoxanthin; and Lut, lutein; α-Car, α-carotene; β-Car, β-carotene.

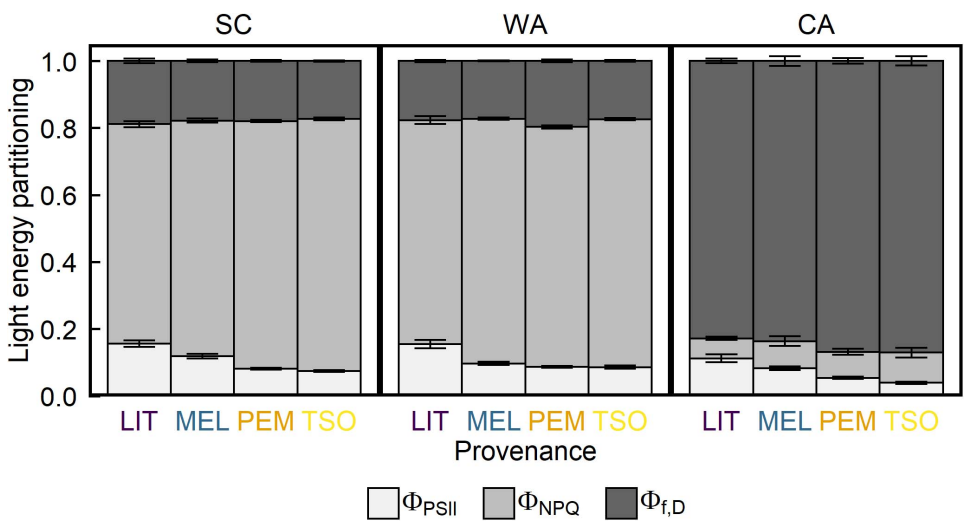

FIGURE 4 | Response of light energy partitioning of interior (LIT, MEL) and coastal (PEM, TSO) Douglas-fir seedlings to summer control (SC), warm autumn (WA), and cool autumn (CA) conditions. Off-white represents Φ_{PSII}, the fraction of absorbed light used for photochemistry; light gray represents Φ_{NPQ}, dynamic NPQ; and dark gray represents $\Phi_{f,D}$, the sum of fluorescence and sustained NPQ. Measurements were taken at 1,500 μmol m^{-2} s^{-1} light intensity under growth conditions. Bars represent the mean of $n = 10 \pm$ SE.

autumn cold acclimation requires low temperature in Douglas-fir, which is consistent with recent findings in white pine (Chang et al., 2016; Fréchette et al., 2016). Accordingly, the DEPS of the photoprotective xanthophyll cycle also remained unchanged under WA conditions (**Figure 5F**). Interestingly, the interior provenances LIT and MEL increased their photoprotective

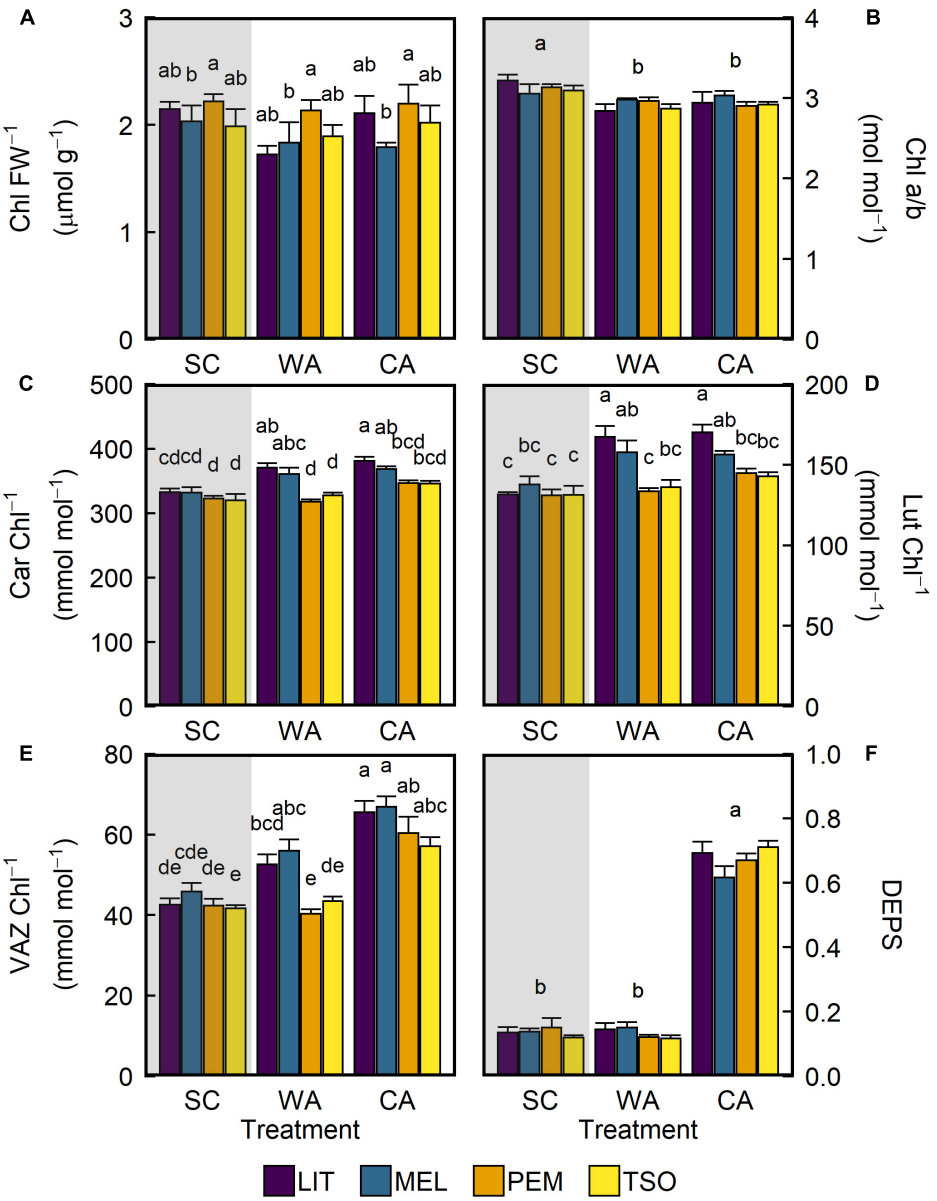

FIGURE 5 | Response of photosynthetic leaf pigments of interior (LIT, MEL) and coastal (PEM, TSO) Douglas-fir seedlings to summer control (SC), warm autumn (WA), and cool autumn (CA) conditions. **(A)** Total chlorophylls per fresh weight (Chl); **(B)** ratio of chlorophyll *a* to chlorophyll *b* (Chl *a*/*b*); **(C)** total carotenoids per Chl (Car); **(D)** amount of lutein per Chl (Lut); **(E)** total xanthophyll cycle pigments per Chl (VAZ); **(F)** de-epoxidation state of the xanthophyll cycle (DEPS). Gray background indicates long photoperiod (summer); white background indicates short photoperiod (autumn). Bars represent the mean of $n = 5 \pm$ SE. Letters where present indicate statistically different groups ($P < 0.05$) as determined by Tukey's HSD test.

capacity during WA through increases in carotenoid pigments (**Figure 5C**). The increased levels of lutein under WA were identical to those under CA (**Figure 5D**), suggesting that lutein accumulates only in response to short photoperiod in these provenances. The increase in xanthophyll cycle pigments in LIT and MEL under WA is surprising (**Figure 5E**) considering that there were no corresponding increases in dynamic or sustained NPQ (**Figure 4**). The short photoperiod sensitivity of these metabolic changes may reflect an adaptation to the sub-zero temperatures that colder high elevation provenances, such as LIT and MEL, experience during autumn (**Table 1**). Since temperature is a less reliable signal during the summer–autumn transition (Way and Montgomery, 2015), these seedlings may utilize shortening photoperiod to initiate changes in photoprotective pigments prior to low temperature exposure that causes excess light stress. Xanthophyll cycle activity can be rapidly induced by exposure to low temperature under controlled conditions in white pine (Chang et al., 2016; Fréchette et al., 2016). If this is also true in Douglas-fir under field conditions, the short photoperiod sensitivity of carotenoid accumulation in

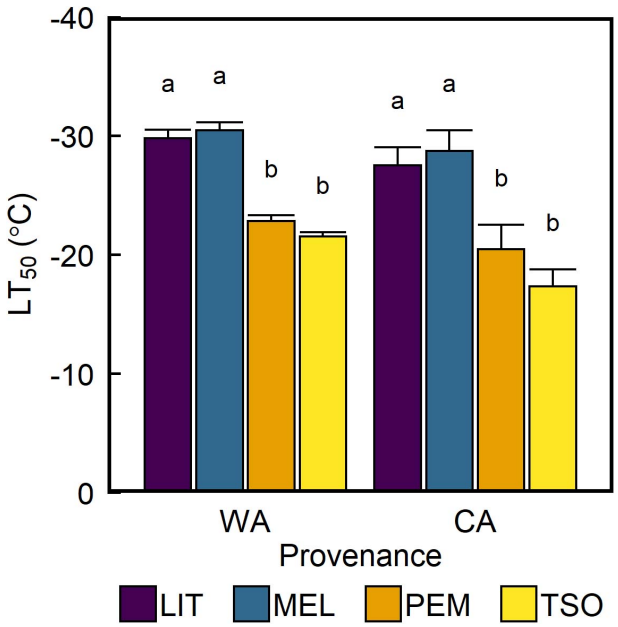

FIGURE 6 | Response of leaf freezing tolerance of interior (LIT, MEL) and coastal (PEM, TSO) Douglas-fir seedlings to warm autumn (WA) and cool autumn (CA) conditions. Bars represent the mean LT_{50} of $n = 5 \pm$ SE, estimated using sigmoidal vulnerability curves fit to the data (**Supplementary Figure 3**). Different letters where present indicate statistically different groups ($P < 0.05$) as determined by log-likelihood ratio test.

interior Douglas-fir may actually provide better photoprotection during sporadic cold exposure in future warmer autumns.

Warm Temperature Does Not Impair the Development of Freezing Tolerance in Seedlings Growing Under Short Autumn Photoperiod

Levels of freezing tolerance in our seedlings after 6 weeks of acclimation to CA (**Figure 6**) were consistent with those exhibited by Douglas-fir seedlings under late autumn field conditions in a coastal site (Guak et al., 1998) as well as by mature Douglas-fir under mid-autumn field conditions in a mountain site (Bansal et al., 2016). In field-grown white pine seedlings, the development of freezing tolerance begins in response to shortening photoperiod and rapidly increases following exposure to sub-zero temperatures (Chang et al., 2016). Field experiments employing elevated temperatures of approximately +1.5/+3°C day/night have shown no change in freezing tolerance development compared with ambient autumn conditions (Riikonen et al., 2012; Chang et al., 2015). However, chamber experiments using larger temperature increases in the same range as the one used in our experiment have demonstrated delayed development of freezing tolerance under autumn warming (Repo et al., 1996; Guak et al., 1998; Chang et al., 2016). Guak et al. (1998) observed delayed development of freezing tolerance in Douglas-fir seedlings in response to only +4°C of warming applied continuously year round in open-top chambers. In contrast to this experiment and our expectations, we observed no difference in freezing tolerance between seedlings acclimated to CA and WA conditions. We also observed higher freezing tolerance in seedlings of the interior provenances versus coastal provenances, which is consistent with the observations of Bansal et al. (2016) that indicated provenances with colder autumn climates develop greater freezing tolerance. Nevertheless, WA conditions induced in all seedlings the development of freezing tolerance sufficient for the winter temperature minimums projected across the range of Douglas-fir in British Columbia (Arora et al., 2011; Wang et al., 2012), even under the highest emissions scenario. These results suggest that Douglas-fir possesses a degree of short photoperiod sensitivity that will help conserve their freezing tolerance development under future warmer climates.

CONCLUSION

Our findings indicate that low temperature is the dominant signal for the downregulation of photosynthesis and upregulation of photoprotection in Douglas-fir seedlings during autumn. As we hypothesized, warming disrupts these key components of the autumn cold acclimation process, resulting in prolonged photosynthetic activity. Interior Douglas-fir does not appear to be maladapted to WA temperatures compared with coastal Douglas-fir. They exhibited unique accumulation of photoprotective carotenoid pigments in response to short photoperiod, which may be a benefit during low temperature events in future warmer autumns. Contrary to our hypothesis, the development of freezing tolerance does not appear to require both low temperature and short photoperiod signals in Douglas-fir. The short photoperiod sensitivity of the development of freezing tolerance appears to provide a degree of frost resistance that is sufficient for winter temperatures projected across Douglas-fir's range. Thus, even coastal Douglas-fir appears to be adapted to frost risk at higher latitudes and elevations. Based on our findings, Douglas-fir from interior and coastal origin may benefit from an extended carbon uptake period resulting from autumn warming due to changing climate, without the costs associated with the disruption of cold acclimation. This distinguishes Douglas-fir from species of pine assessed in similar studies, which have demonstrated both limitation of photosynthesis under short autumn photoperiod and limitation of cold hardiness under warm autumn temperature (Repo et al., 1996; Vogg et al., 1998; Chang et al., 2016; Fréchette et al., 2016, 2020). While our study focused on the effects of warming, rising CO_2 and episodes of drought are concurrent with rising temperature under natural climate conditions. Elevated CO_2 was demonstrated to additionally delay the downregulation of photosynthesis in white pine (Chang et al., 2016) and Scots pine (Wang, 1996). If this pattern holds for Douglas-fir, rising CO_2 may further prolong the period of photosynthetic activity under future climate. Albeit the potential carbon gains caused by elevated CO_2 and warming during autumn, it is crucial to emphasize that these carbon gains might be offset by loss in carbon uptake resulting from water stress and drought due to climate warming (Spittlehouse, 2003).

DATA AVAILABILITY STATEMENT

The raw data supporting the conclusions of this article will be made available by the authors, without undue reservation.

AUTHOR CONTRIBUTIONS

DN performed all experiments and collected the experimental data. DN and VV analyzed the data with input from IE. DN and IE wrote the manuscript. All authors designed the experiments, and reviewed, and edited the final manuscript.

FUNDING

IE acknowledges support by the NSERC (RGPIN-2020-06928), the Canadian Foundation for Innovation (CFI) (grant no. 27330), and the Ontario Ministry of Research and Innovation (grant no. ER10-07-015). Funding for the CoAdapTree project is provided by Genome Canada (241REF), Genome British Columbia, and 16 other sponsors (https://coadaptree.forestry.ubc.ca/sponsors/).

ACKNOWLEDGMENTS

We would like to thank the CoAdapTree project seed contributors (https://coadaptree.forestry.ubc.ca/seed-contributors/). We are grateful to Chris Wong for his expertise and assistance with photosynthetic pigment analysis, as well as Sepideh Torabi, Tomoyuki Sen, and Annika Elimelech for their assistance with growing the plants used for this study.

SUPPLEMENTARY MATERIAL

The Supplementary Material for this article can be found online at: https://www.frontiersin.org/articles/10.3389/ffgc.2021.688534/full#supplementary-material

REFERENCES

Adams, W. W. III, Demmig-Adams, B., Rosenstiel, T. N., Brightwell, A. K., and Ebbert, V. (2002). Photosynthesis and photoprotection in overwintering plants. *Plant Biol.* 4, 545–557. doi: 10.1055/s-2002-35434

Aitken, S. N., Yeaman, S., Holliday, J. A., Wang, T., and Curtis-McLane, S. (2008). Adaptation, migration or extirpation: climate change outcomes for tree populations. *Evol. Appl.* 1, 95–111. doi: 10.1111/j.1752-4571.2007.00013.x

Akaike, H. (1998). "Information theory and an extension of the maximum likelihood principle," in *Selected Papers of Hirotugu Akaike Springer Series in Statistics (Perspectives in Statistics)*, eds E. Parzen, K. Tanabe, and G. Kitagawa (New York, NY: Springer), 199–213. doi: 10.1007/978-1-4612-1694-0_15

Angelcheva, L., Mishra, Y., Antti, H., Kjellsen, T. D., Funk, C., Strimbeck, R. G., et al. (2014). Metabolomic analysis of extreme freezing tolerance in Siberian spruce (*Picea obovata*). *New Phytol.* 204, 545–555. doi: 10.1111/nph.12950

Apel, K., and Hirt, H. (2004). Reactive oxygen species: metabolism, oxidative stress, and signal transduction. *Annu. Rev. Plant Biol.* 55, 373–399. doi: 10.1146/annurev.arplant.55.031903.141701

Arora, V. K., Scinocca, J. F., Boer, G. J., Christian, J. R., Denman, K. L., Flato, G. M., et al. (2011). Carbon emission limits required to satisfy future representative concentration pathways of greenhouse gases. *Geophys. Res. Lett.* 38:L05805. doi: 10.1029/2010GL046270

Bansal, S., Harrington, C. A., Gould, P. J., and St.Clair, J. B. (2015). Climate-related genetic variation in drought-resistance of Douglas-fir (*Pseudotsuga menziesii*). *Glob. Change Biol.* 21, 947–958. doi: 10.1111/gcb.12719

Bansal, S., Harrington, C. A., and St.Clair, J. B. (2016). Tolerance to multiple climate stressors: a case study of Douglas-fir drought and cold hardiness. *Ecol. Evol.* 6, 2074–2083. doi: 10.1002/ece3.2007

Barber, J., and Andersson, B. (1992). Too much of a good thing: light can be bad for photosynthesis. *Trends Biochem. Sci.* 17, 61–66. doi: 10.1016/0968-0004(92)90503-2

Beuker, E., Valtonen, E., and Repo, T. (1998). Seasonal variation in the frost hardiness of Scots pine and Norway spruce in old provenance experiments in Finland. *For. Ecol. Manage.* 107, 87–98. doi: 10.1016/S0378-1127(97)00344-7

Busch, F., Hüner, N. P. A., and Ensminger, I. (2007). Increased air temperature during simulated autumn conditions does not increase photosynthetic carbon gain but affects the dissipation of excess energy in seedlings of the evergreen conifer jack pine. *Plant Physiol.* 143, 1242–1251. doi: 10.1104/pp.106.092312

Carter, K. K. (1996). Provenance tests as indicators of growth response to climate change in 10 north temperate tree species. *Can. J. For. Res.* 26, 1089–1095. doi: 10.1139/x26-120

Chang, C. Y., Bräutigam, K., Hüner, N. P. A., and Ensminger, I. (2020). Champions of winter survival: cold acclimation and molecular regulation of cold hardiness in evergreen conifers. *New Phytol.* 229, 675–691. doi: 10.1111/nph.16904

Chang, C. Y., Unda, F., Zubilewich, A., Mansfield, S. D., and Ensminger, I. (2015). Sensitivity of cold acclimation to elevated autumn temperature in field-grown *Pinus strobus* seedlings. *Front. Plant Sci.* 6:165. doi: 10.3389/fpls.2015.00165

Chang, C. Y.-Y., Fréchette, E., Unda, F., Mansfield, S. D., and Ensminger, I. (2016). Elevated temperature and CO_2 stimulate late season photosynthesis but impair cold hardening in pine. *Plant Physiol.* 172, 802–818. doi: 10.1104/pp.16.00753

Chen, J., Källman, T., Ma, X., Gyllenstrand, N., Zaina, G., Morgante, M., et al. (2012). Disentangling the roles of history and local selection in shaping clinal variation of allele frequencies and gene expression in Norway spruce (*Picea abies*). *Genetics* 191, 865–881. doi: 10.1534/genetics.112.140749

Close, T. J. (1997). Dehydrins: a commonalty in the response of plants to dehydration and low temperature. *Physiol. Plant.* 100, 291–296. doi: 10.1111/j.1399-3054.1997.tb04785.x

Corlett, R. T., and Westcott, D. A. (2013). Will plant movements keep up with climate change? *Trends Ecol. Evol.* 28, 482–488. doi: 10.1016/j.tree.2013.04.003

Crosatti, C., Rizza, F., Badeck, F. W., Mazzucotelli, E., and Cattivelli, L. (2013). Harden the chloroplast to protect the plant. *Physiol. Plant.* 147, 55–63. doi: 10.1111/j.1399-3054.2012.01689.x

Dall'Osto, L., Lico, C., Alric, J., Giuliano, G., Havaux, M., and Bassi, R. (2006). Lutein is needed for efficient chlorophyll triplet quenching in the major LHCII antenna complex of higher plants and effective photoprotection *in vivo* under strong light. *BMC Plant Biol.* 6:32. doi: 10.1186/1471-2229-6-32

Demmig-Adams, B., and Adams, W. W. (1992). Photoprotection and other responses of plants to high light stress. *Annu. Rev. Plant Physiol. Plant Mol. Biol.* 43, 599–626. doi: 10.1146/annurev.pp.43.060192.003123

Demmig-Adams, B., and Adams, W. W. (2006). Photoprotection in an ecological context: the remarkable complexity of thermal energy dissipation. *New Phytol.* 172, 11–21. doi: 10.1111/j.1469-8137.2006.01835.x

Demmig-Adams, B., Cohu, C. M., Muller, O., and Adams, W. W. (2012). Modulation of photosynthetic energy conversion efficiency in nature: from seconds to seasons. *Photosynth. Res.* 113, 75–88. doi: 10.1007/s11120-012-9761-6

D'Odorico, P., Besik, A., Wong, C. Y. S., Isabel, N., and Ensminger, I. (2020). High-throughput drone-based remote sensing reliably tracks phenology in thousands of conifer seedlings. *New Phytol.* 226, 1667–1681. doi: 10.1111/nph.16488

Ebbert, V., Adams Iii, W. W., Mattoo, A. K., Sokolenko, A., and Demmig-Adams, B. (2005). Up-regulation of a photosystem II core protein phosphatase inhibitor and sustained D1 phosphorylation in zeaxanthin-retaining, photoinhibited needles of overwintering Douglas fir. *Plant Cell Environ.* 28, 232–240. doi: 10.1111/j.1365-3040.2004.01267.x

Eckert, A. J., Bower, A. D., Wegrzyn, J. L., Pande, B., Jermstad, K. D., Krutovsky, K. V., et al. (2009). Association genetics of coastal Douglas fir (*Pseudotsuga menziesii* var. *menziesii*, Pinaceae). I. Cold-hardiness related traits. *Genetics* 182, 1289–1302. doi: 10.1534/genetics.109.102350

Eilmann, B., de Vries, S. M. G., den Ouden, J., Mohren, G. M. J., Sauren, P., and Sass-Klaassen, U. (2013). Origin matters! Difference in drought tolerance and productivity of coastal Douglas-fir (*Pseudotsuga menziesii* (Mirb.)) provenances. *For. Ecol. Manage.* 302, 133–143. doi: 10.1016/j.foreco.2013.03.031

Ensminger, I., Busch, F., and Huner, N. P. A. (2006). Photostasis and cold acclimation: sensing low temperature through photosynthesis. *Physiol. Plant.* 126, 28–44. doi: 10.1111/j.1399-3054.2006.00627.x

Ensminger, I., Sveshnikov, D., Campbell, D. A., Funk, C., Jansson, S., Lloyd, J., et al. (2004). Intermittent low temperatures constrain spring recovery of photosynthesis in boreal Scots pine forests. *Glob. Change Biol.* 10, 995–1008. doi: 10.1111/j.1365-2486.2004.00781.x

Ford, K. R., Harrington, C. A., and St.Clair, J. B. (2017). Photoperiod cues and patterns of genetic variation limit phenological responses to climate change in warm parts of species' range: Modeling diameter-growth cessation in coast Douglas-fir. *Glob. Change Biol.* 23, 3348–3362. doi: 10.1111/gcb.13690

Fréchette, E., Chang, C. Y., and Ensminger, I. (2020). Variation in the phenology of photosynthesis among eastern white pine provenances in response to warming. *Glob. Change Biol.* 26, 5217–5234. doi: 10.1111/gcb.15150

Fréchette, E., Chang, C. Y.-Y., and Ensminger, I. (2016). Photoperiod and temperature constraints on the relationship between the photochemical reflectance index and the light use efficiency of photosynthesis in *Pinus strobus*. *Tree Physiol.* 36, 311–324. doi: 10.1093/treephys/tpv143

Genty, B., Briantais, J.-M., and Baker, N. R. (1989). The relationship between the quantum yield of photosynthetic electron transport and quenching of chlorophyll fluorescence. *Biochim. Biophys. Acta (BBA) Gen. Subjects* 990, 87–92. doi: 10.1016/S0304-4165(89)80016-9

Gray, L. K., and Hamann, A. (2013). Tracking suitable habitat for tree populations under climate change in western North America. *Clim. Change* 117, 289–303. doi: 10.1007/s10584-012-0548-8

Guak, S., Olsyzk, D. M., Fuchigami, L. H., and Tingey, D. T. (1998). Effects of elevated CO_2 and temperature on cold hardiness and spring bud burst and growth in Douglas-fir (*Pseudotsuga menziesii*). *Tree Physiol.* 18, 671–679. doi: 10.1093/treephys/18.10.671

Hamilton, J. A., El Kayal, W., Hart, A. T., Runcie, D. E., Arango-Velez, A., and Cooke, J. E. K. (2016). The joint influence of photoperiod and temperature during growth cessation and development of dormancy in white spruce (*Picea glauca*). *Tree Physiol.* 36, 1432–1448. doi: 10.1093/treephys/tpw061

Hänninen, H. (2016). *Boreal and Temperate Trees in a Changing Climate*. Dordrecht: Springer, doi: 10.1007/978-94-017-7549-6

Hendrickson, L., Furbank, R. T., and Chow, W. S. (2004). A simple alternative approach to assessing the fate of absorbed light energy using chlorophyll fluorescence. *Photosynth. Res.* 82, 73–81. doi: 10.1023/B:PRES.0000040446.87305.f4

Hess, M., Wildhagen, H., Junker, L. V., and Ensminger, I. (2016). Transcriptome responses to temperature, water availability and photoperiod are conserved among mature trees of two divergent Douglas-fir provenances from a coastal and an interior habitat. *BMC Genomics* 17:780. doi: 10.1186/s12864-016-3022-6

Högberg, M. N., Briones, M. J. I., Keel, S. G., Metcalfe, D. B., Campbell, C., Midwood, A. J., et al. (2010). Quantification of effects of season and nitrogen supply on tree below-ground carbon transfer to ectomycorrhizal fungi and other soil organisms in a boreal pine forest. *New Phytol.* 187, 485–493. doi: 10.1111/j.1469-8137.2010.03274.x

Horton, P., Johnson, M. P., Perez-Bueno, M. L., Kiss, A. Z., and Ruban, A. V. (2008). Photosynthetic acclimation: Does the dynamic structure and macro-organisation of photosystem II in higher plant grana membranes regulate light harvesting states? *FEBS J.* 275, 1069–1079. doi: 10.1111/j.1742-4658.2008.06263.x

Howe, G., Jayawickrama, K., and Cherry, M. (2006). "Breeding douglas-fir," in *Plant Breeding Reviews*, ed. J. Janick (Hoboken, NJ: John Wiley & Sons), 245–353. doi: 10.1002/9780470650349.ch6

Howe, G. T., Aitken, S. N., Neale, D. B., Jermstad, K. D., Wheeler, N. C., and Chen, T. H. (2003). From genotype to phenotype: unraveling the complexities of cold adaptation in forest trees. *Can. J. Bot.* 81, 1247–1266. doi: 10.1139/b03-141

Hüner, N. P. A., Bode, R., Dahal, K., Busch, F. A., Possmayer, M., Szyszka, B., et al. (2013). Shedding some light on cold acclimation, cold adaptation, and phenotypic plasticity. *Botany* 91, 127–136. doi: 10.1139/cjb-2012-0174

Hüner, N. P. A., Öquist, G., and Sarhan, F. (1998). Energy balance and acclimation to light and cold. *Trends Plant Sci.* 3, 224–230. doi: 10.1016/S1360-1385(98)01248-5

IPCC (2014). in *Climate Change 2014: Synthesis Report. Contribution of Working Groups I, II and III to the Fifth Assessment Report of the Intergovernmental Panel on Climate Change*, eds Core Writing Team, R. K. Pachauri, and L. E. Mayer (Geneva: IPCC). doi: 10.1016/s1360-1385(98)01248-5

Isaac-Renton, M. G., Roberts, D. R., Hamann, A., and Spiecker, H. (2014). Douglas-fir plantations in Europe: a retrospective test of assisted migration to address climate change. *Glob. Change Biol.* 20, 2607–2617. doi: 10.1111/gcb.12604

Jahns, P., and Holzwarth, A. R. (2012). The role of the xanthophyll cycle and of lutein in photoprotection of photosystem II. *Biochim. Biophys. Acta (BBA) Bioenerg.* 1817, 182–193. doi: 10.1016/j.bbabio.2011.04.012

Janka, E., Körner, O., Rosenqvist, E., and Ottosen, C.-O. (2015). Using the quantum yields of photosystem II and the rate of net photosynthesis to monitor high irradiance and temperature stress in chrysanthemum (*Dendranthema grandiflora*). *Plant Physiol. Biochem.* 90, 14–22. doi: 10.1016/j.plaphy.2015.02.019

Junker, L. V., and Ensminger, I. (2016). Fast detection of leaf pigments and isoprenoids for ecophysiological studies, plant phenotyping and validating remote-sensing of vegetation. *Physiol. Plant.* 158, 369–381. doi: 10.1111/ppl.12512

Kingston-Smith, A. H., Harbinson, J., Williams, J., and Foyer, C. H. (1997). Effect of chilling on carbon assimilation, enzyme activation, and photosynthetic electron transport in the absence of photoinhibition in maize leaves. *Plant Physiol.* 114, 1039–1046. doi: 10.1104/pp.114.3.1039

Krieger-Liszkay, A., Fufezan, C., and Trebst, A. (2008). Singlet oxygen production in photosystem II and related protection mechanism. *Photosynth. Res.* 98, 551–564. doi: 10.1007/s11120-008-9349-3

Kuznetsova, A., Brockhoff, P. B., and Christensen, R. H. B. (2017). lmerTest package: tests in linear mixed effects models. *J. Stat. Softw.* 82:26. doi: 10.18637/jss.v082.i13

Lenth, R. V. (2016). Least-squares means: the R package lsmeans. *J. Stat. Softw.* 69, 1–33. doi: 10.18637/jss.v069.i01

Maurya, J. P., and Bhalerao, R. P. (2017). Photoperiod- and temperature-mediated control of growth cessation and dormancy in trees: a molecular perspective. *Ann. Bot.* 120, 351–360. doi: 10.1093/aob/mcx061

Mitchell, K. A., Bolstad, P. V., and Vose, J. M. (1999). Interspecific and environmentally induced variation in foliar dark respiration among eighteen southeastern deciduous tree species. *Tree Physiol.* 19, 861–870. doi: 10.1093/treephys/19.13.861

Moellering, E. R., Muthan, B., and Benning, C. (2010). Freezing tolerance in plants requires lipid remodeling at the outer chloroplast membrane. *Science* 330, 226–228. doi: 10.1126/science.1191803

Müller, P., Li, X.-P., and Niyogi, K. K. (2001). Non-photochemical quenching. A response to excess light energy. *Plant Physiol.* 125, 1558–1566. doi: 10.1104/pp.125.4.1558

Mullin, T., Andersson, B., Bastien, J., Beaulieu, J., Burdon, R., Dvorak, W., et al. (2011). "Economic importance, breeding objectives and achievements," in *Genetics, Genomics and Breeding of Conifers*, ed. C. Kole (Enfield, NH: Science Publishers), doi: 10.1201/b11075-3

Oleksyn, J., Modrzynski, J., Tjoelker, M. G., Z.ytkowiak, R., Reich, P. B., and Karolewski, P. (1998). Growth and physiology of *Picea abies* populations from elevational transects: common garden evidence for altitudinal ecotypes and cold adaptation. *Funct. Ecol.* 12, 573–590. doi: 10.1046/j.1365-2435.1998.00236.x

Oleksyn, J., Zytkowiak, R., Karolewski, P., Reich, P. B., and Tjoelker, M. G. (2000). Genetic and environmental control of seasonal carbohydrate dynamics in trees of diverse *Pinus sylvestris* populations. *Tree Physiol.* 20, 837–847. doi: 10.1093/treephys/20.12.837

Öquist, G., and Hüner, N. P. A. (2003). Photosynthesis of overwintering evergreen plants. *Annu. Rev. Plant Biol.* 54, 329–355. doi: 10.1146/annurev.arplant.54.072402.115741

Ottander, C., Campbell, D., and Oquist, G. (1995). Seasonal changes in photosystem II organisation and pigment composition in *Pinus syivestris*. *Planta* 197, 176–183.

Palacio, S., Hoch, G., Sala, A., Körner, C., and Millard, P. (2014). Does carbon storage limit tree growth? *New Phytol.* 201, 1096–1100. doi: 10.1111/nph.12602

Porcar-Castell, A., Juurola, E., Ensminger, I., Berninger, F., Hari, P., and Nikinmaa, E. (2008). Seasonal acclimation of photosystem II in *Pinus sylvestris*. II. Using the rate constants of sustained thermal energy dissipation and photochemistry to study the effect of the light environment. *Tree Physiol.* 28, 1483–1491. doi: 10.1093/treephys/28.10.1483

R Development Core Team (2010). *R: A Language and Environment for Statistical Computing*. Vienna: R Core Team.

Rehfeldt, G. E., Leites, L. P., St Clair, J. B., Jaquish, B. C., Sáenz-Romero, C., López-Upton, J., et al. (2014). Comparative genetic responses to climate in the varieties of *Pinus ponderosa* and *Pseudotsuga menziesii*: Clines in growth potential. *For. Ecol. Manage.* 324, 138–146. doi: 10.1016/j.foreco.2014.02.041

Reich, P. B., Oleksyn, J., and Tjoelker, M. G. (1996). Needle respiration and nitrogen concentration in Scots pine populations from a broad latitudinal range: a common garden test with field-grown trees. *Funct. Ecol.* 10, 768–776. doi: 10.2307/2390512

Repo, T., Hanninen, H., and Kellomaki, S. (1996). The effects of long-term elevation of air temperature and CO_2 on the frost hardiness of Scots pine. *Plant Cell Environ.* 19, 209–216. doi: 10.1111/j.1365-3040.1996.tb00242.x

Repo, T., Zhang, G., Ryyppö, A., Rikala, R., and Vuorinen, M. (2000). The relation between growth cessation and frost hardening in Scots pines of different origins. *Trees* 14, 456–464. doi: 10.1007/s004680000059

Riikonen, J., Kontunen-Soppela, S., Ossipov, V., Tervahauta, A., Tuomainen, M., Oksanen, E., et al. (2012). Needle metabolome, freezing tolerance and gas exchange in Norway spruce seedlings exposed to elevated temperature and ozone concentration. *Tree Physiol.* 32, 1102–1112. doi: 10.1093/treephys/tps072

Ritz, C., Baty, F., Streibig, J. C., and Gerhard, D. (2015). Dose-response analysis using R. *PLoS One* 10:e0146021. doi: 10.1371/journal.pone.0146021

Rossi, S., Deslauriers, A., Anfodillo, T., Morin, H., Saracino, A., Motta, R., et al. (2006). Conifers in cold environments synchronize maximum growth rate of tree-ring formation with day length. *New Phytol.* 170, 301–310. doi: 10.1111/j.1469-8137.2006.01660.x

Rossi, S., Deslauriers, A., Griçar, J., Seo, J.-W., Rathgeber, C. B., Anfodillo, T., et al. (2008). Critical temperatures for xylogenesis in conifers of cold climates. *Glob. Ecol. Biogeogr.* 17, 696–707. doi: 10.1111/j.1466-8238.2008.00417.x

Savitch, L. V., Leonardos, E. D., Krol, M., Jansson, S., Grodzinski, B., Huner, N. P. A., et al. (2002). Two different strategies for light utilization in photosynthesis in relation to growth and cold acclimation. *Plant Cell Environ.* 25, 761–771. doi: 10.1046/j.1365-3040.2002.00861.x

Savolainen, O., Pyhäjärvi, T., and Knürr, T. (2007). Gene flow and local adaptation in trees. *Annu. Rev. Ecol. Evol. Syst.* 38, 595–619. doi: 10.1146/annurev.ecolsys.38.091206.095646

Singh, R. K., Svystun, T., AlDahmash, B., Jönsson, A. M., and Bhalerao, R. P. (2017). Photoperiod- and temperature-mediated control of phenology in trees–a molecular perspective. *New Phytol.* 213, 511–524. doi: 10.1111/nph.14346

Spittlehouse, D. L. (2003). Water availability, climate change and the growth of Douglas-Fir in the Georgia Basin. *Can. Water Resour. J. Rev. Can. Ressour. Hydriques* 28, 673–688. doi: 10.4296/cwrj2804673

St Clair, J. B., Mandel, N. L., and Vance-Borland, K. W. (2005). Genecology of douglas fir in Western Oregon and Washington. *Ann. Bot.* 96, 1199–1214. doi: 10.1093/aob/mci278

Steponkus, P. L. (1984). Role of the plasma membrane in freezing injury and cold acclimation. *Annu. Rev. Plant Physiol.* 35, 543–584. doi: 10.1146/annurev.pp.35.060184.002551

Stinziano, J. R., and Way, D. A. (2017). Autumn photosynthetic decline and growth cessation in seedlings of white spruce are decoupled under warming and photoperiod manipulations. *Plant Cell Environ.* 40, 1296–1316. doi: 10.1111/pce.12917

Strimbeck, G. R., Schaberg, P. G., Fossdal, C. G., Schröder, W. P., and Kjellsen, T. D. (2015). Extreme low temperature tolerance in woody plants. *Front. Plant Sci.* 6:884. doi: 10.3389/fpls.2015.00884

Sutinen, M.-L., Arora, R., Wisniewski, M., Ashworth, E., Strimbeck, R., and Palta, J. (2001). "Mechanisms of frost survival and freeze-damage in nature," in *Conifer Cold Hardiness Tree Physiology*, eds F. J. Bigras and S. J. Colombo (Dordrecht: Springer), 89–120. doi: 10.1007/978-94-015-9650-3_4

Sveshnikov, D., Ensminger, I., Ivanov, A. G., Campbell, D., Lloyd, J., Funk, C., et al. (2006). Excitation energy partitioning and quenching during cold acclimation in Scots pine. *Tree Physiol.* 26, 325–336. doi: 10.1093/treephys/26.3.325

Thayer, S. S., and Bjorkman, O. (1990). Leaf xanthophyll content and composition in sun and shade determined by HPLC. *Photosynth. Res.* 23, 331–343. doi: 10.1007/BF00034864

Verhoeven, A. (2014). Sustained energy dissipation in winter evergreens. *New Phytol.* 201, 57–65. doi: 10.1111/nph.12466

Verhoeven, A., Osmolak, A., Morales, P., and Crow, J. (2009). Seasonal changes in abundance and phosphorylation status of photosynthetic proteins in eastern white pine and balsam fir. *Tree Physiol.* 29, 361–374. doi: 10.1093/treephys/tpn031

Vogg, G., Heim, R., Hansen, J., Schäfer, C., and Beck, E. (1998). Frost hardening and photosynthetic performance of Scots pine (*Pinus sylvestris L.*) needles. I. Seasonal changes in the photosynthetic apparatus and its function. *Planta* 204, 193–200. doi: 10.1007/s004250050246

Wang, K.-Y. (1996). Canopy CO_2 exchange of Scots pine and its seasonal variation after four-year exposure to elevated CO_2 and temperature. *Agric. For. Meteorol.* 82, 1–27. doi: 10.1016/0168-1923(96)02342-8

Wang, T., Hamann, A., Spittlehouse, D., and Carroll, C. (2016). Locally downscaled and spatially customizable climate data for historical and future periods for North America. *PLoS One* 11:e0156720. doi: 10.1371/journal.pone.0156720

Wang, T., Hamann, A., Spittlehouse, D. L., and Murdock, T. Q. (2012). ClimateWNA–high-resolution spatial climate data for western North America. *J. Appl. Meteorol. Climatol.* 51, 16–29. doi: 10.1175/JAMC-D-11-043.1

Way, D. A., and Montgomery, R. A. (2015). Photoperiod constraints on tree phenology, performance and migration in a warming world. *Plant Cell Environ.* 38, 1725–1736. doi: 10.1111/pce.12431

Welling, A., Moritz, T., Palva, E. T., and Junttila, O. (2002). Independent activation of cold acclimation by low temperature and short photoperiod in hybrid aspen. *Plant Physiol.* 129, 1633–1641. doi: 10.1104/pp.003814

Wenny, D. L., and Dumroese, R. K. (1992). *A Growing Regime for Container-Grown Douglas-fir Seedlings, Report Number: Bulletin 49*. Moscow, ID: University of Idaho.

Wong, C. Y. S., D'Odorico, P., Bhathena, Y., Arain, M. A., and Ensminger, I. (2019). Carotenoid based vegetation indices for accurate monitoring of the phenology of photosynthesis at the leaf-scale in deciduous and evergreen trees. *Remote Sens. Environ.* 233:111407. doi: 10.1016/j.rse.2019.111407

Conflict of Interest: The authors declare that the research was conducted in the absence of any commercial or financial relationships that could be construed as a potential conflict of interest.

frontiers in Forests and Global Change

OPINION
published: 05 July 2021
doi: 10.3389/ffgc.2021.670797

Oaks as Beacons of Hope for Threatened Mixed Forests in Central Europe

Hilke Schroeder[1], Tetyana Nosenko[2], Andrea Ghirardo[2], Matthias Fladung[1], Jörg-Peter Schnitzler[2] and Birgit Kersten[1]*

[1] Thünen-Institute of Forest Genetics, Grosshansdorf, Germany, [2] Research Unit Environmental Simulation, Institute of Biochemical Plant Pathology, Helmholtz Zentrum München, Neuherberg, Germany

Keywords: ***Quercus*, resistance, tolerance, tree-insect interaction, genomics, phenotype, genotype**

OPEN ACCESS

Edited by:
Jeffrey M. Warren, Oak Ridge National Laboratory (DOE), United States

Reviewed by:
Christian Ammer, University of Göttingen, Germany

****Correspondence:***
Hilke Schroeder
hilke.schroeder@thuenen.de

Specialty section:
This article was submitted to Forest Ecophysiology, a section of the journal Frontiers in Forests and Global Change

Received: *22 February 2021*
Accepted: *03 June 2021*
Published: *05 July 2021*

Citation:
Schroeder H, Nosenko T, Ghirardo A, Fladung M, Schnitzler J-P and Kersten B (2021) Oaks as Beacons of Hope for Threatened Mixed Forests in Central Europe. Front. For. Glob. Change 4:670797. doi: 10.3389/ffgc.2021.670797

INTRODUCTION

Climate change has a severe impact on forest ecosystems (Seidl et al., 2017). Adaptation of trees to the rapidly changing regional climate is hampered by their longevity and late reproductive age. Therefore, the increases in frequency, duration and intensity of drought episodes, heat waves and heavy rainfall events (Spinoni et al., 2018; Hari et al., 2020) threaten many tree species of European forests. As a result, environmentally stressed trees will become vulnerable to pronounced damage from herbivorous insects and pathogens. Thus, the damage caused by insects increases the vulnerability of forests to fungal infections and secondary pests (Meyer et al., 2015), and conversely, fungal infections can promote the development of herbivores (Eberl et al., 2020). Both together then contribute to the higher overall vulnerability of forests.

With regional shifts in weather conditions and climate zones in Europe, complex combinations of abiotic and biotic stresses will likely occur. The quick succession of abiotic and biotic stresses can further worsen forest damage. A quantification of the vulnerability of European forests to windthrows (40% of losses), fires (34%), and insect outbreaks (26%) during the period 1979–2018 revealed that about 33.4 billion tons of forest biomass were seriously affected by these disturbances (Forzieri et al., 2021). There is a clear trend toward higher overall forest vulnerability driven by a warming-induced reduction in plant defenses against insect outbreaks, especially at high latitudes.

If forests fail to adapt to climate changes, there will be manifold consequences for the ecosystem function and services, productivity, biodiversity, and negative feedbacks to climate (Ammer, 2019).

IMPORTANCE OF EUROPEAN OAKS AND HISTORY OF OAK DECLINE

The two predominant oak species in Central Europe, English oak (*Quercus robur* L.) and sessile oak (*Q. petraea* Matt.) are two of about 50 tree species growing in European forests. Together their share of about 10% of the stands makes oaks the second most common deciduous tree species in Europe after beech (Bolte et al., 2007; BMEL., 2014). Among tree species native to Europe, oaks have the highest species diversity at all trophic levels. More than a thousand animal species (including insects, birds, small mammals) live on and with oaks (ProQuercus). Economically, oak wood has a special importance due to its high strength and resistance. It is used as construction timber, as well as processed into barrels, railroad sleepers, furniture, parquet, and veneers.

In Central Europe, frequent insect outbreaks are believed to be one of the causes of the oak decline observed in the last century (Gasow, 1925; Thomas et al., 2002; Denman and Webber, 2009). The first important oak dieback was observed already in 1911–1920 and later in the 1980s; oaks of all age groups died at a rate of 2–5 trees per hectare and per year due to insect defoliation often co-occurring with drought events (Hartmann and Blank, 1992; Denman and Webber, 2009).

The decline of European oaks can be explained by changing climatic conditions and their consequences like heavy rains, local floods, and pests (Keča et al., 2016). Root pathogens from the genus *Phytophthora* DeBary especially benefit from wet soils following heavy rain events. *Phytophthora* threats have been observed in oaks in North America and Europe since the 1990s with various impact on different species (Sturrock et al., 2011). For *Q. robur*, soil acidity was recognized as the main factor for enhanced susceptibility to *Phytophthora* infections (Jönsson et al., 2003).

A decline in growth rate was observed in the second or third year after drought events when comparing tree-ring series in *Q. robur* and *Q. petraea* stems at three different sites (Perkins et al., 2018). Being a ring-porous tree species, oaks are most likely categorized as anisohydric species which strive to regulate stomatal conductance to keep photosynthetic processes alive, even during drought periods. However, anisohydric traits may lead to a longer drought memory due to high investments to sustain photosynthetic activity, thus leading to a hangover of drought effects (Perkins et al., 2018).

Even more herbivorous insect species from Southern and Eastern Europe will likely migrate into central European forests (Sturrock et al., 2011; Pureswaran et al., 2018), as it has been observed for the oak processionary moth *Thaumetopoea processionea* L. (Bolte et al., 2009). Owing to climate change, also native species, such as the oak splendor beetle *Agrilus biguttatus* Fabr., increase their infestation ability and are predicted to cause more serious damage (Bolte et al., 2009; Sanders et al., 2013).

ADVANTAGES OF EUROPEAN OAKS (*QUERCUS* SPP.)

Temperature increase during the last decades caused changes in the abundance of broadleaved species in European forests, e.g., beech (*Fagus sylvatica* L.) forests have declined in several regions of Central Europe (Denmark: Huang et al., 2017; Germany: Dulamsuren et al., 2017; Austria: Corcobado et al., 2020). This decline of beech is only marginally caused by outbreaks of insects. This is not unexpected because compared to oaks, beech suffers only from a low number of insect pests as e.g., the splendor beetle *Agrilus viridis* L. (Bolte et al., 2009). A major threat for beeches are *Phytophthora* infections which are observed since the 1930s. In combination with drought periods and heatwaves since 2003, the beech decline has increased dramatically in comparison with oak (Corcobado et al., 2020).

A study covering 50 years of phenological data showed that oak and beech follow different phenological strategies with oaks having the better adaptation capacity to climate change due to a higher phenological plasticity (Wenden et al., 2019). Furthermore, oaks have the possibility to maintain their hydraulic status during dry summers due to their extensive root system reaching deep soil layers (Zapater et al., 2011; Scharnweber et al., 2013). Beech reacts with phenological maladaptation to changes in temperature and water regime, slightly compensated by within-population genetic diversity (Frank et al., 2017). Beech is threatened especially in its warmer distribution areas with potential reduction of its vitality (Wenden et al., 2019). Under future climate projection, 10–16% growth rate decline is predicted for *F. sylvatica* by 2100, while an increase of 12% growth rate is expected for *Q. robur* (Huang et al., 2017). Therefore, in climatically warmer areas, where beech is likely to reach its limits (Kramer et al., 2010), oak may prevail over beech because it is already adapted to the warmer climate (Delb, 2012; Cuervo-Alarcon et al., 2021). In more northern regions, on the other hand, a successful strategy should be to support oak and beech to maintain resilient mixed forests that help mitigate the effects of climate change because an adequate species mix can even lead to increased productivity (Pretzsch et al., 2013).

Increasing spring temperatures enhance seed production and dispersal in temperate oaks (Caignard et al., 2017). A higher reproduction success of temperate oaks is associated with improved fitness. Furthermore, the extension of the growing season leads to an increase in vegetative growth of *Q. petraea* and *Q. robur* (Saxe et al., 2001; Caignard et al., 2017). So, both higher seed production and vegetative growth seem possible in temperate oaks during climate change. A comparative analysis of genetic diversity in adult and offspring generations in beech and oak populations coexisting in a naturally established old-growth forest stand, revealed that adult generations of both species exhibited high levels of genetic diversity (He: 0.657 for beech; 0.821 for oak; depending on the sets of selected genetic markers) (Sandurska et al., 2017).

The high genetic diversity of oaks and beeches will facilitate adaptation to climate change. In addition, there is the adaptive potential in oaks resulting from introgression (hybridization of e.g., *Q. petraea* and *Q. robur* in overlapping habitats; Kremer and Hipp, 2020). It is increasingly recognized that hybrids play an important role in evolutionary processes. Thus, natural or man-made oak hybrids together with successful oak breeding programs and grafting of superior individuals may lead to novel traits that give oak decisive advantages in evolutionary processes, facilitating gene flow.

Due to massive anthropogenic activities in the past, natural regeneration of European tree species is mostly developed from remaining local stocks (Bradshaw, 2004). In our opinion, this may result in lower genetic diversity for naturally regenerating tree species as beech compared to bred and out-planted tree species as temperate oaks.

GENOMICS AND MOLECULAR MARKERS OF CLIMATE-CHANGE RELEVANT TRAITS

In oaks, phenotypic traits of particular importance include among others drought tolerance, resistance to insects and

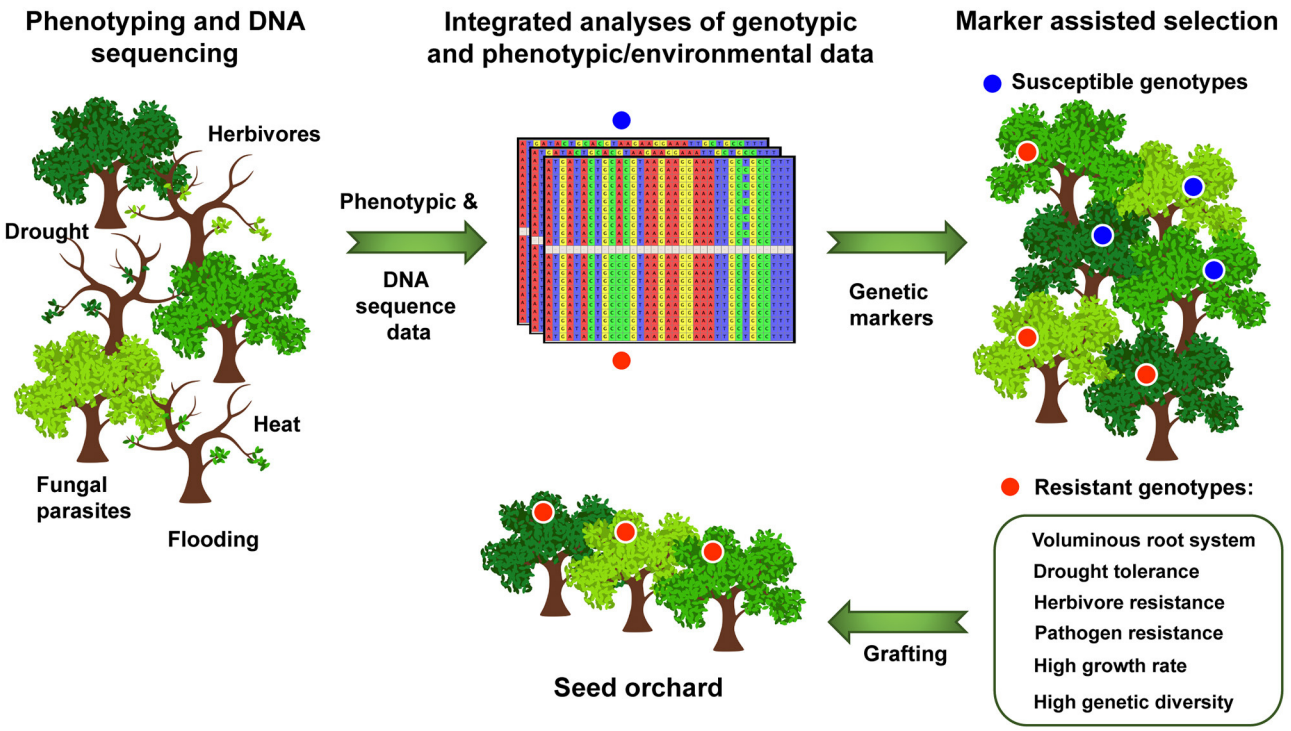

FIGURE 1 | Selection of resistant oak genotypes for regional seed orchards. Resistance of individual oak trees to pathogens and herbivores and their tolerance to abiotic factors are assessed based on a long-term monitoring in e.g., natural populations or common gardens. Genetic markers (e.g., SNPs: single nucleotide polymorphisms) associated with oak resistance to pathogens and herbivores and/or their tolerance to drought, heat, and flooding are identified based on genome-wide or targeted resequencing of selected oak trees in genotype-phenotype or genotype-environment association studies. The developed genetic markers enable a rapid genotyping of trees from genetically diverse oak populations and the subsequent selection of (at least partially) resistant/tolerant genotypes as a stock for establishing regional seed orchards (by grafting).

pathogens, and growth-related traits. These traits are expected to be influenced multi-factorially and inherited poly-genetically. The increasing availability of reference genomes for different oak species is the prerequisite to identify the underlying genes/genomic loci and develop diagnostic genetic markers for breeding programs (Badenes et al., 2016). First success is shown, for example, in the quantitative trait loci (QTL) study which identified two regions associated with *Erysiphe alphitoides* infection in the *Q. robur* genome (Bartholomé et al., 2020).

In addition to QTL studies, genome-wide association studies (GWAS) in natural populations, common gardens, or other experimental settings (e.g., McKown et al., 2018) provide new insights (**Figure 1**). Challenging in these studies is the lack of efficient methods for tree phenotyping (Dungey et al., 2018) and the modeling of complex genomic traits. Multi-trait GWAS approaches, as applied to *Populus trichocarpa* (Chhetri et al., 2019), may help to uncover potentially pleiotropic effects of individual genes in *Quercus*, especially when analyzing climate-relevant traits.

Analyzing genome-wide associations between single nucleotide polymorphisms and environmental/climate variables may be the key to identify adaptive genetic markers in *Quercus* (**Figure 1**). Alternatively, genomic selection approaches may help identifying genotypes with the climate change-relevant traits and their genotypic plasticity. Using a large-scale common garden experiment in combination with genome sequencing and calculation of genomic estimated breeding values, Browne et al. (2019) identified several *Q. lobata* genotypes that grow relatively fast under higher temperatures. These genotypes, which are presumably pre-adapted to future climates, were proposed by the authors to serve as seed sources for assisted gene flow programs.

An alternative approach is developing molecular markers for important traits in the genus *Quercus* based on transcriptome, proteome, and metabolome data. Examples include omics studies on signaling pathways induced in *Q. robur* by herbivory (e.g., Ghirardo et al., 2012; Kersten et al., 2013), which play a central role in plant defense against herbivorous insects (summarized in Erb and Reymond, 2019). Another example is cross-species comparative transcriptomics analysis of *Q. robur*, *Q. pubescens,* and the evergreen *Q. ilex* L. to reveal drought-related molecular patterns (Madritsch et al., 2019).

Once developed, molecular markers can be used to identify and select (at least partially) resistant/tolerant oak ecotypes/genotypes using marker-assisted selection (**Figure 1**). Among several modern strategies (Cortés et al., 2020), the use of molecular markers is one of the most promising

strategies to evaluate and breed oak adaptation to changing climatic conditions.

CONCLUSIONS

We need to prepare our forests for the impending climate change consequences through silvicultural and breeding measures to mitigate forest vulnerability. Ecosystems should increment genotypes that are characterized by an increased tolerance to various biotic and abiotic stresses. Overall, complex consideration of tree tolerance to different stressors is crucial for assessing their adaptive capacity to climate change.

Particularly in the more northern European forests, supporting oaks and beeches will help maintain resilient mixed forests to mitigate climate change effects on forest ecosystems. The asynchrony of drought responses between these tree species could stabilize productivity in forests where both species occur (Rubio-Cuadrado et al., 2018). *Q. robur*, *Q. petraea*, and related hybrids may play a crucial role in helping forests adapting to climate change. Therefore, silvicultural approaches for the climate-smart forestry should take advantage of these climate-stable properties of oaks by establishing the required light regime for this species to increase its proportion in European forests (Perkins et al., 2018). Future development and application of genetic markers will aid in assessing the adaptability and resilience of planted oak material in the face of the proposed shifts of the climate zones and in selecting material that can withstand the multiple challenges of climate change for the forest of the future.

AUTHOR CONTRIBUTIONS

HS and BK wrote the first draft of the manuscript. TN developed and designed the figure. All authors developed the concept, structure of the manuscript, accomplished, checked the first version, and read and approved the submitted version.

FUNDING

The project leading to this paper was financed by the Fachagentur Nachwachsende Rohstoffe e. V. (FNR) in the programme Waldklimafond (28W-B-4-113-01/2) funded by Federal Ministry of Food and Agriculture and Federal Ministry for Environment, Nature Conservation and Nuclear Safety, Germany.

ACKNOWLEDGMENTS

We like to thank all technical assistants, gardeners, and colleagues who contribute to our work over the last years.

REFERENCES

Ammer, C. (2019). Diversity and forest productivity in a changing climate. *New Phytol.* 221, 50–66. doi: 10.1111/nph.15263

Badenes, M. L., Marti, A. F. I., Rios, G., and Rubio-Cabetas, M. J. (2016). Application of genomic technologies to the breeding of trees. *Front. Genet.* 7:198. doi: 10.3389/fgene.2016.00198

Bartholomé, J., Brachi, B., Marçais, B., Mougou-Hamdane, A., Bodénés, C., Plomion, C., et al. (2020). The genetics of exapted resistance to two exotic pathogens in pedunculate oak. *New Phytol.* 226, 1088–1103. doi: 10.1111/nph.16319

BMEL. (2014). *Der Wald in Deutschland. Ausgewählte Ergebnisse der Dritten Bundeswaldinventur*. Berlin: BMEL.

Bolte, A., Ammer, C., Löf, M., Madsen, P., Nabuurs, G. J., Schall, P., et al. (2009). Adaptive forest management in central Europe: climate change impacts, strategies and integrative concept. *Scand. J. Forest Res.* 24, 473–482. doi: 10.1080/02827580903418224

Bolte, A., Czajkowski, T., and Kompa, T. (2007). The north-eastern distribution range of European beech - a review. *Forestry* 80, 413–429. doi: 10.1093/forestry/cpm028

Bradshaw, R. H. W. (2004). Past anthropogenic influence on European forests and some possible genetic consequences. *Forest Ecol. Manag.* 197, 203–212. doi: 10.1016/j.foreco.2004.05.025

Browne, L., Wright, J. W., Fitz-Gibbon, S., Gugger, P. F., and Sork,. V. L. (2019). Adaptational lag to temperature in valley oak (*Quercus lobata*) can be mitigated by genome-informed assisted gene flow. *Proc. Natl. Acad. Sci. U.S.A.* 116, 25179–25185. doi: 10.1073/pnas.1908771116

Caignard, T., Kremer, A., Firmat, C., Nicolas, M., Venner, S., and Delzon, S. (2017). Increasing spring temperatures favor oak seed production in temperate areas. *Sci. Rep.* 7:8555. doi: 10.1038/s41598-017-09172-7

Chhetri, H. B., Macaya-Sanz, D., Kainer, D., Biswal, A. K., Evans, L. M., Chen, J. G., et al. (2019). Multitrait genome-wide association analysis of *Populus trichocarpa* identifies key polymorphisms controlling morphological and physiological traits. *New Phytol.* 223, 293–309. doi: 10.1111/nph.15777

Corcobado, T., Cech, T. L., Brandstetter, M., Daxer, A., Hüttler, C., Kudlácek, T., et al. (2020). Decline of European Beech in Austria: involvement of *Phytophthora* spp. and contributing biotic and abiotic factors. *Forests* 11:895. doi: 10.3390/f11080895

Cortés, A. J., Restrepo-Montoya, M., and Bedoya-Canas, L. E. (2020). Modern strategies to assess and breed forest tree adaptation to changing climate. *Front. Plant Sci.* 11:583323. doi: 10.3389/fpls.2020.583323

Cuervo-Alarcon, L., Arend, M., Müller, M., Sperisen, C., Finkeldey, R., and Krutovsky, K. V. (2021). A candidate gene association analysis identifes SNPs potentially involved in drought tolerance in European beech (*Fagus sylvatica* L.). *Sci. Rep*. 11:2386. doi: 10.1038/s41598-021-81594-w

Delb, H. (2012). Eichenschädlinge im Klimawandel in Südwestdeutschland. *FVA-Einblick* 2, 11–14.

Denman, S., and Webber, J. (2009). Oak declines: new definitions and new episodes in Britain. *Q. J. Forest* 103, 285–290.

Dulamsuren, C., Hauck, M., Kopp, G., Ruff, M., and Leuschner, C. (2017). European beech responds to climate change with growth decline at lower, and growth increase at higher elevations in the center of its distribution range (SW Germany). *Trees* 31, 673–686. doi: 10.1007/s00468-016-1499-x

Dungey, H. S., Dash, J. P., Pont, D., Clinton, P. W., Watt, M. S., and Telfer, E. J. (2018). Phenotyping whole forests will help to track genetic performance. *Trends Plant Sci.* 23, 854–864. doi: 10.1016/j.tplants.2018.08.005

Eberl, F., Fernandez de Bobadilla, M., Reichelt, M., Hammerbacher, A., Gershenzon, J., and Unsicker, S. B. (2020). Herbivory meets fungivory: insect herbivores feed on plant pathogenic fungi for their own benefit. *Ecol. Lett.* 23, 1073–1084. doi: 10.1111/ele.13506

Erb, M., and Reymond, P. (2019). Molecular interactions between plants and insect herbivores. *Annu. Rev. Plant Biol.* 70, 527–557. doi: 10.1146/annurev-arplant-050718-095910

Forzieri, G., Girardello, M., Ceccherini, G., Spinoni, J., Feyen, L., Hartmann, H., et al. (2021). Emergent vulnerability to climate-driven disturbances in European forests. *Nat. Commun.* 12:1081. doi: 10.1038/s41467-021-21399-7

Frank, A., Pluess, A. R., Howe, G. T., Sperisen, C., and Heiri, C. (2017). Quantitative genetic differentiation and phenotypic plasticity of European beech in a heterogeneous landscape: indications for past climate adaptation. *Perspect. Plant Ecol.* 26, 1–13. doi: 10.1016/j.ppees.2017.02.001

Gasow, H. (1925). Der grüne Eichenwickler (*Tortrix viridana* Linne) als Forstschädling. *Arb. Biol. Reichsanst*. 12, 355–508.

Ghirardo, A., Heller, W., Fladung, M., Schnitzler, J. P., and Schroeder, H. (2012). Function of defensive volatiles in pedunculate oak (*Quercus robur*) is tricked by the moth *Tortrix viridana*. *Plant Cell Environ.* 35, 2192–2207. doi: 10.1111/j.1365-3040.2012.02545.x

Hari, V., Rakovec, O., Markonis, Y., Hanel, M., and Kumar, R. (2020). Increased future occurrences of the exceptional 2018-2019 Central European drought under global warming. *Sci. Rep.* 10:12207. doi: 10.1038/s41598-020-68872-9

Hartmann, G., and Blank, R. (1992). Winterfrost, Kahlfraß und Prachtkäferbefall als Faktoren im Ursachenkomplex des Eichensterbens in Norddeutschland. *Forst. Holz.* 15, 443–452.

Huang, W., Fonti, P., Larsen, J. B., Ræbild, A., Callesen, I., Pedersen, N. B., et al. (2017). Projecting tree-growth responses into future climate: a study case from a Danish-wide common garden. *Agric. For. Meteorol.* 247, 240–251. doi: 10.1016/j.agrformet.2017.07.016

Jönsson, U., Jung, T., Rosengren, U., Nihlgård, B., and Sonesson, K. (2003). Pathogenicity of Swedish isolates of *Phytophthora quercina* to *Quercus robur* in two different soils. *New Phytol.* 158, 355–364. doi: 10.1046/j.1469-8137.2003.00734.x

Keča, N., Koufakis, I., Dietershagen, J., Nowakowska, J. A., and Oszako, T. (2016). European oak decline phenomenon in relation to climatic changes. *Folia Forest. Polon. A* 58, 170–177. doi: 10.1515/ffp-2016-0019

Kersten, B., Ghirardo, A., Schnitzler, J. P., Kanawati, B., Schmitt-Kopplin, P., Fladung, M., et al. (2013). Integrated transcriptomics and metabolomics decipher differences in the resistance of pedunculate oak to the herbivore *Tortrix viridana* L. *BMC Genom.* 14:737. doi: 10.1186/1471-2164-14-737

Kramer, K., Degen, B., Buschbom, J., Hickler, T., Thuiller, W., Sykes, M. T., et al. (2010). Modelling exploration of the future of European beech (Fagus sylvatica L.) under climate change—Range, abundance, genetic diversity and adaptive response. *Forest Ecol. Manag.* 259, 2213–2222. doi: 10.1016/j.foreco.2009.12.023

Kremer, A., and Hipp, A. L. (2020). Oaks: An evolutionary success story. *New Phytol.* 226, 987–1011. doi: 10.1111/nph.16274

Madritsch, S., Wischnitzki, E., Kotrade, P., Ashoub, A., Burg, A., Fluch, S., et al. (2019). Elucidating drought stress tolerance in European oaks through cross-species transcriptomics. *G3* 9, 3181–3199. doi: 10.1534/g3.119.400456

McKown, A. D., Klápště, J., Guy, R. D., El-Kassaby, Y. A., and Mansfield, S. D. (2018). Ecological genomics of variation in bud-break phenology and mechanisms of response to climate warming in *Populus trichocarpa*. *New Phytol.* 220, 300–316. doi: 10.1111/nph.15273

Meyer, J. B., Gallien, L., and Prospero, S. (2015). Interaction between two invasive organisms on the European chestnut: does the chestnut blight fungus benefit from the presence of the gall wasp? *FEMS Microbiol. Ecol.* 91:fiv122. doi: 10.1093/femsec/fiv122

Perkins, D., Uhl, E., Biber, P., du Toit, B., Carraro, V., Rötzer, T., et al. (2018). Impact of climate trends and drought events on the growth of oaks (*Quercus robur* L. and *Quercus petraea* (Matt.) Liebl.) within and beyond their natural range. *Forests* 9:108. doi: 10.3390/f9030108

Pretzsch, H., Bielak, K., Block, J., Bruchwald, A., Dieler, J., Ehrhart, H. P., et al. (2013). Productivity of mixed versus pure stands of oak (*Quercus petraea* (M att.) L iebl. and *Quercus robur* L.) and European beech (*Fagus sylvatica* L.) along an ecological gradient. *Eur. J. For. Res.* 132, 263–280. doi: 10.1007/s10342-012-0673-y

ProQuercus. *Der Naturwert von eichenreichen Wäldern*. Available online at: https://www.proquercus.org/willkommen/die-eiche/biodiversit%C3%A4t/ (accessed May 27, 2021).

Pureswaran, D. S., Roques, A., and Battisti, A. (2018). Forest insects and climate change. *Curr. Forestry Rep*. 4, 35–50. doi: 10.1007/s40725-018-0075-6

Rubio-Cuadrado, A., Camarero, J.J., R}'ıo, M., Sánchez-González, M., Ruiz-Peinado, R., Bravo-Oviedo, A., et al. (2018). Drought modifies tree competitiveness in an oak-beech temperate forest. *For. Ecol. Manag.* 429, 7–17. doi: 10.1016/j.foreco.2018.06.035

Sanders, T. G. M., Pitman, R., and Broadmeadow, M. S. J. (2013). Species-specific climate response of oaks (*Quercus* spp.) under identical environmental conditions. *iForest* 7, 61–69. doi: 10.3832/ifor0911-007

Sandurska, E., Ulaszewski, B., and Burczyk, J. (2017). Genetic insights into ecological succession from oak- (*Quercus robur* L.) to beech- (*Fagus sylvatica* L.) dominated forest stands. *Acta Biol. Cracoviens. Ser. Bot.* 59/1, 23–33. doi: 10.1515/abcsb-2017-0002

Saxe, H., Cannell, M. G. R., Johnson, Ø., Ryan, M. G., and Vourlitis, G. (2001). Tree and forest functioning in response to global warming. *New Phytol.* 149, 369–400. doi: 10.1046/j.1469-8137.2001.00057.x

Scharnweber, T., Manthey, M., and Wilmking, M. (2013). Differential radial growth patterns between beech (*Fagus sylvatica* L.) and oak (*Quercus robur* L.) on periodically waterlogged soils. *Tree Physiol.* 33, 425–437. doi: 10.1093/treephys/tpt020

Seidl, R., Thom, D., Kautz, M., Martin-Benito, D., Peltoniemi, M., Vacchiano, G., et al. (2017). Forest disturbances under climate change. *Nat. Clim. Change* 7, 394–402. doi: 10.1038/nclimate3303

Spinoni, J., Vogt, J. V., Naumann, G., Barbosa, P., and Dosio, A. (2018). Will drought events become more frequent and severe in Europe? *Int. J. Climatol.* 38, 1718–1736. doi: 10.1002/joc.5291

Sturrock, R. N., Frankel, S. J., Brown, A. V., Hennon, P. E., and Kliejunas, J. T., Lewis, K. J., et al. (2011). Climate change and forest diseases. *Plant Pathol.* 60, 133–149. doi: 10.1111/j.1365-3059.2010.02406.x

Thomas, F. M., Blank, R., and Hartmann, G. (2002). Abiotic and biotic factors and their interactions as causes of oak decline in Central Europe. *For. Pathol.* 32, 277–307. doi: 10.1046/j.1439-0329.2002.00291.x

Wenden, B., Mariadassou, M., Chmielewski, F. M., and Vitasse, Y. (2019). Shifts in the temperature-sensitive periods for spring phenology in European beech and pedunculate oak clones across latitudes and over recent decades. *Glob. Change Biol.* 26, 1808–1819. doi: 10.1111/gcb.14918

Zapater, M., Hossann, C., Bréda, N., Bréchet, C., Bonal, D., and Granier, A. (2011). Evidence of hydraulic lift in a young beech and oak mixed forest using 18O soil water labelling. *Trees* 25, 885–894. doi: 10.1007/s00468-011-0563-9

Conflict of Interest: The authors declare that the research was conducted in the absence of any commercial or financial relationships that could be construed as a potential conflict of interest.

frontiers in Forests and Global Change

ORIGINAL RESEARCH
published: 01 September 2021
doi: 10.3389/ffgc.2021.704470

Antecedent Drought Condition Affects Responses of Plant Physiology and Growth to Drought and Post-drought Recovery

Ximeng Li[1,2,3], Jingting Bao[3,4], Jin Wang[5], Chris Blackman[3] and David Tissue[3]**

[1] College of Life and Environmental Science, Minzu University of China, Beijing, China, [2] Key Laboratory of Ecology and Environment in Minority Areas, Minzu University of China, National Ethnic Affairs Commission, Beijing, China, [3] Hawkesbury Institute for the Environment, Western Sydney University, Penrith, NSW, Australia, [4] School of Life Sciences and Engineering, Lanzhou University of Technology, Lanzhou, China, [5] Shapotou Desert Experiment and Research Station, Cold and Arid Regions Environmental and Engineering Research Institute, Chinese Academy of Sciences, Lanzhou, China

OPEN ACCESS

Edited by:
Nadine K. Ruehr,
Karlsruhe Institute of Technology, Germany

Reviewed by:
Leonie Schönbeck,
Swiss Federal Institute for Forest, Snow and Landscape Research (WSL), Switzerland
Makoto Watanabe,
Tokyo University of Agriculture and Technology, Japan

***Correspondence:**
Ximeng Li
liximeng2009@hotmail.com
David Tissue
D.Tissue@westernsydney.edu.au

Specialty section:
This article was submitted to Forests and the Atmosphere, a section of the journal Frontiers in Forests and Global Change

Received: 03 May 2021
Accepted: 11 August 2021
Published: 01 September 2021

Citation:
Li X, Bao J, Wang J, Blackman C and Tissue D (2021) Antecedent Drought Condition Affects Responses of Plant Physiology and Growth to Drought and Post-drought Recovery. Front. For. Glob. Change 4:704470. doi: 10.3389/ffgc.2021.704470

Antecedent environmental conditions may have a substantial impact on plant response to drought and recovery dynamics. Saplings of *Eucalyptus camaldulensis* were exposed to a range of long-term water deficit pre-treatments (antecedent conditions) designed to reduce carbon assimilation to approximately 50 (A_{50}) and 10% (A_{10}) of maximum photosynthesis of well-watered plants (A_{100}). Thereafter, water was withheld from all plants to generate three different levels of water stress before re-watering. Our objective was to assess the role of antecedent water limitations in plant physiology and growth recovery from mild to severe drought stress. Antecedent water limitations led to increased soluble sugar content and depletion of starch in leaves of A_{50} and A_{10} trees, but there was no significant change in total non-structural carbohydrate concentration (NSC; soluble sugar and starch), relative to A_{100} plants. Following re-watering, A_{50} and A_{10} trees exhibited faster recovery of physiological processes (e.g., photosynthesis and stomatal conductance) than A_{100} plants. Nonetheless, trees exposed to the greatest water stress (−5.0 MPa) were slowest to fully recover photosynthesis (A_{max}) and stomatal conductance (g_s). Moreover, post-drought recovery of photosynthesis was primarily limited by g_s, but was facilitated by biochemistry (V_{cmax} and J_{max}). During recovery, slow regrowth rates in A_{50} and A_{10} trees may result from insufficient carbon reserves as well as impaired hydraulic transport induced by the antecedent water limitations, which was dependent on the intensity of drought stress. Therefore, our findings suggest that antecedent water stress conditions, as well as drought severity, are important determinants of physiological recovery following drought release.

Keywords: *Eucalyptus camaldulensis*, drought, non-structural carbohydrate, photosynthesis, stem growth, post-drought recovery

INTRODUCTION

Understanding the impacts of drought stress on plant physiology and growth is essential for predicting the structure and function of plant communities (O'Brien et al., 2017a; Choat et al., 2018; Brodribb et al., 2020), especially within the context of global climate change in which drought episodes are projected to be more common in the future (Dai, 2013). Such impacts, however, can be complex to assess because the consequence of drought stress is a function of resistance and resilience (Stuart-Haëntjens et al., 2018; Li et al., 2020; Schmitt et al., 2020), and both components can be strongly modified by drought events that plants have previously experienced (i.e., antecedent drought) (Kannenberg et al., 2020). Adjustments in plant morphology and/or physiology triggered by antecedent, non-lethal water deficit can often result in divergent responses during subsequent drought stress, with potential impacts on plant performance during recovery (Kannenberg et al., 2020). This is particularly evident in field-grown trees, for which the growth response to recurring drought differs over time (Xu et al., 2010; O'Brien et al., 2017b; Wu et al., 2018; Anderegg et al., 2020). Although the immediate effects of drought stress on plant physiology have been well documented, knowledge gaps still exist on how drought response and post-drought recovery can be modified by antecedent drought conditions (Ruehr et al., 2019).

Leaves are the primary sites of CO_2 and water exchange for the majority of terrestrial plants. How leaves respond to and recover from drought stress can therefore have disproportionately critical effects on plants. Antecedent drought stress can generate multiple adjustments in leaf morphology, physiology, and biochemistry (Gessler et al., 2020). Biological processes related to growth, including cell division and enlargement, are highly sensitive to water stress, and are typically reduced prior to reductions in photosynthesis caused by water deficit (Chapin et al., 1990; Körner, 2015). Consequently, an increase in non-structural carbohydrates (NSCs) is commonly observed in plants subjected to drought stress due to an imbalance in source-sink strength (Sala and Hoch, 2009; Sala et al., 2012; Granda and Camarero, 2017; Piper et al., 2017). Additionally, drought induced variation in tissue NSCs contents may occur in all organs, and the importance of sugar enriched organ to plant performance during water deficit and post-drought recovery can be markedly species-specific (Hagedorn et al., 2016; Joseph et al., 2020; Ouyang et al., 2021). Here, we primarily focus on leaves, the NSCs variation of which have been shown to predominantly regulates plant response to drought stress in some species (Martínez-Vilalta et al., 2016; Signori-Müller et al., 2021)., and dominates the variation of whole plant carbohydrates contents in *Eucalyptus* species (Duan et al., 2013). Depending on its specific type (i.e., soluble sugar and starch), NSCs, together with other secondary metabolites derived from their soluble form, can be involved in physiological processes related to drought resistance such as osmotic regulation, or can be stored as carbon reserves for regrowth upon alleviation of drought stress (Sala et al., 2012; Trifilò et al., 2017; Tomasella et al., 2020). Hence, variation in NSCs induced by antecedent drought conditions can have important implications for the fate of plants during subsequent drought and recovery cycles.

Of the numerous physiological processes impacted by water limitation, photosynthesis is extensively studied because of its central role in determining plant fitness and sensitivity to water deficit (Flexas et al., 2006a). Leaf photosynthetic rate is co-determined by stomatal conductance and biochemical components of photosynthesis. During drought stress, leaf stomata will partially or completely close to minimize water loss. Given that CO_2 and water molecules share the same pathway at both leaf and cellular levels (e.g., aquaporins), reduced stomatal conductance (g_s) will inevitably constrain photosynthesis (Flexas et al., 2008) and is considered to be the major cause for downregulation of photosynthesis during drought stress (Flexas et al., 2004; Grassi and Magnani, 2005; Zait et al., 2019). On the other hand, the biochemical components of photosynthesis, including the capacity for Rubisco carboxylation (V_{cmax}) and electron transport (J_{max}), are generally less sensitive to dehydration, although a body of literature has shown that both biochemical components can be compromised during drought, and can show similar or even higher drought sensitivity compared to g_s (Zhou et al., 2014). Identifying the key limiting factor for photosynthesis during drought stress and recovery is of utmost importance, especially for modeling vegetation dynamics using ecosystem models. However, acclimation may occur during antecedent drought, thereby generating different physiological responses to subsequent stress conditions (Ruehr et al., 2019; Gessler et al., 2020). Antecedent drought conditions may also alter the relative contribution of each limiting factor during subsequent droughts (Flexas et al., 2009; Menezes-Silva et al., 2017).

The capacity to recover physiological function following the easing of drought stress upon re-watering represents a key dimension of plant drought resilience. However, little is known about the post-drought dynamics and interaction of two fundamental physiological processes, i.e., carbon and water relations (Ruehr et al., 2019). For a given species, the time required for recovery is typically contingent on the severity of drought stress given it determines the extent to which physiological functions are impaired (Flexas et al., 2004; Blackman et al., 2009; Brodribb and Cochard, 2009). With respect to post-drought carbon-relations, it has been shown that stomatal limitation of photosynthesis is prevailing when drought stress is mild or moderate, while biochemical limitation becomes more prominent as drought stress is exacerbated (Flexas et al., 2006a). This is anticipated to result in different recovery dynamics given that reopening of stomata is typically faster than the time it takes to repair photosynthetic machinery after water supply is resumed (Ruehr et al., 2019). Furthermore, rates of photosynthetic recovery from drought are determined by drought severity and its impact on hydraulic function. Recent studies emphasize the pivotal role of water relations in governing plant mortality during drought stress, showing that recovery is no longer possible once the water status has exceeded thresholds of hydraulic impairment due to embolism (Blackman et al., 2009; Brodribb and Cochard, 2009; Choat et al., 2018). Furthermore, plant hydraulics is also intimately coupled with carbon through its impacts on leaf gas

exchange (Brodribb and Holbrook, 2003; Skelton et al., 2017). Thus, assessing the interaction of antecedent drought conditions and drought severity on the recovery dynamics of photosynthesis is crucial for gaining a comprehensive understanding of impacts caused by droughts.

Early experiments studying the influences of drought on plant physiology often subject plants to drought stress differing in either duration (i.e., short or long-term) or severity (i.e., mild to severe), and mainly focused on physiological responses triggered by water limitation (Menezes-Silva et al., 2017). Here, we take a different approach by exposing plants to two drought cycles characterized by different physiological attributes before re-watering and assessing recovery. The first drought was chronic and relatively mild, which was aimed at reducing carbon assimilation and manipulating NSC storage, but not inducing significant impairment in hydraulic function. The second drought was more acute and designed to induce a range of stress levels associated with moderate to severe leaf hydraulic dysfunction. Our aim was to test the potential influences of antecedent drought conditions (i.e., the first drought stress) on the subsequent drought response and eventually the rate of recovery, with particular emphasis on carbon and water relations. We hypothesized that: (1) long-term, mild drought stress will but promote the accumulation of leaf NSC due the hysteresis in ceasing of photosynthesis relative to growth; (2) leaf photosynthesis in plants exposed to antecedent drought conditions will be less affected by subsequent drought than control plants; (3) both stomatal and non-stomatal limitations will restrict the rate of recovery of photosynthesis following re-watering; and (4) the time required for regaining physiological function is dependent on the severity of the drought.

MATERIALS AND METHODS

Plant Material and Experimental Design

Eucalyptus camaldulensis, commonly known as river red gum, is one of the most widely distributed tree species across Australia. *E. camaldulensis* can adapt to diverse climatic conditions, ranging from tropical to temperate ecosystems. At the local scale, the distribution of *E. camaldulensis* is primarily confined to locations where soil water availability is ample, such as riverbanks or floodplains, where it often appears as the dominant species, providing significant ecological functional services (Butcher et al., 2009; Doody et al., 2015).

Seeds of river red gum (*E. camaldulensis* subsp. *camaldulensis*) were obtained from the Australian Tree Seed Centre (Canberra, ACT) and germinated in forestry tubes placed in a sunlit poly-tunnel provided by Greening Australia (Richmond, NSW, Australia) for 2 months. On October 20, 2017, 40 similarly sized seedlings (approximately 15 cm tall) were transplanted into 15 × 40 cm (diameter × height) cylindrical pots filled with *ca.* 9 kg of moderately fertile sandy loam soil. Twenty pots were randomly selected and placed in one of the two adjacent naturally sunlit glasshouse bays located at the Hawkesbury Campus, Western Sydney University, Richmond, NSW Australia. Environmental conditions within both glasshouse bays were controlled, with temperature set to 26/18°C (day/night), which represents the local average air temperature during the growing season, and air CO_2 concentration set to 400 μmol mol^{-1}. This environmental condition was maintained throughout the experimental period. All seedlings were irrigated daily and fed with slow-release fertilizer biweekly (Osmocote, All-Purpose, Scotts, Australia) to ensure the absence of water and nutrient limitations.

Starting on November 28, 2017, 30 plants with similar height and basal diameter (75 cm and 0. 5 cm, respectively) were selected for the experiment. Plants were evenly divided into three groups, so that we could apply three levels of drought in the first round of drought treatment (i.e., antecedent drought condition). Levels of antecedent drought conditions were defined based on the photosynthetic rate measured under saturating light and ambient air CO_2 conditions (A_{max}), with A_{max} of stressed plants maintained at approximately 50 (A_{50}) and 10% (A_{10}) relative to that of the well-watered plants (A_{100}). For A_{50} and A_{10} plants, drought stress was imposed by withholding irrigation. Leaf A_{max} was monitored daily for each individual until the desired values were achieved. Pots were labeled and weighed immediately. During the period of antecedent drought treatment, pot-specific soil water content was maintained by weighing individual pots daily in the morning and replacing the water loss from the previous day. Leaf gas exchange was measured every 1–3 days during the same period to ensure that the targeted A_{max} could be maintained. It has been shown that complete stomatal closure in *E. camaldulensis* typically occurs when leaf water potential reaches approximately −1.5 MPa (Zhou et al., 2014), which is less negative than the water potential threshold for the incipient hydraulic dysfunction (see below). Given that the stomata remained open during the phase of antecedent drought treatment, no hydraulic impairment was likely incurred by the intensity of drought stress.

After 48 days of antecedent drought treatment, plants in each drought treatment group were further divided into three sub-groups to implement the second round of drought treatment, so that each sub-group contained 3–4 individuals. The second drought treatment aimed to generate dysfunction in water transport and was therefore applied based on previously determined hydraulic vulnerability curves of leaves. Hence, irrigation water was withheld until midday leaf water potential (Ψ_{leaf}) reached *ca.* −3.5, −4.5, or −5.0 MPa for the three drought groups; these values corresponded to the Ψ_{leaf} at which 12, 50, and 88% loss of leaf hydraulic conductivity (K_{Leaf}) occurred in this species (Blackman et al., unpublished data). For each individual, Ψ_{Leaf} was measured once daily. In the controlled environment of the glasshouse bays, the target Ψ_{Leaf} was typically achieved in 1–3 days. Once the targeted Ψ_{leaf} was attained, photosynthetic CO_2 response (AC_i) curves were measured; thereafter, the pot was re-watered to field capacity to alleviate the water stress and allow for recovery. Physiological measurements, including Ψ_{Leaf} and AC_i curves were repeated on 3, 7 and 14 days following re-watering during the recovery phase to assess the degree of physiological recovery over time.

Gas Exchange Measurements

Leaf gas exchange measurements, including A_{max}, stomatal conductance (g_s), and AC_i curves were measured between 9 am and noon with up to four cross-calibrated open gas exchange systems (LI-6400XT, Li-Cor, Lincoln, NE, United States) equipped with red-blue LED light sources (6400-02B) and an external CO_2 injector (6400-01). For each individual plant, one upper canopy, fully expanded leaf was tagged and consistently used for gas exchange measurements throughout the experiment. For spot measurements, gas exchange variables including A_{max} and g_s were recorded under saturating light (i.e., 1,500 μmol m^{-2} s^{-1}). Cuvette CO_2 concentration and temperature were set to match the ambient conditions (i.e., 400 μmol mol^{-1} and 26°C, respectively). Leaf AC_i curves were generated by recording A_{max} under varying cuvette CO_2 concentrations: 400, 300, 200, 100, 400, 600, 800, 1,000, and 1,200 μmol mol^{-1}, with other environmental parameters identical to the spot measurements. Before each measurement, leaves were allowed to acclimate in the cuvette for up to 20 min and data were recorded after the readings were stable. During all gas exchange measurements, relative humidity and leaf-to-air water vapor deficit in the cuvette typically varied between 50 and 60% and 1.5–2.0 kPa, respectively.

Leaf Non-structural Carbohydrate Concentrations

Leaf carbohydrate content was assessed at the beginning and the end of the antecedent drought stress phase. Within each antecedent drought treatment group, 2–4 upper canopy

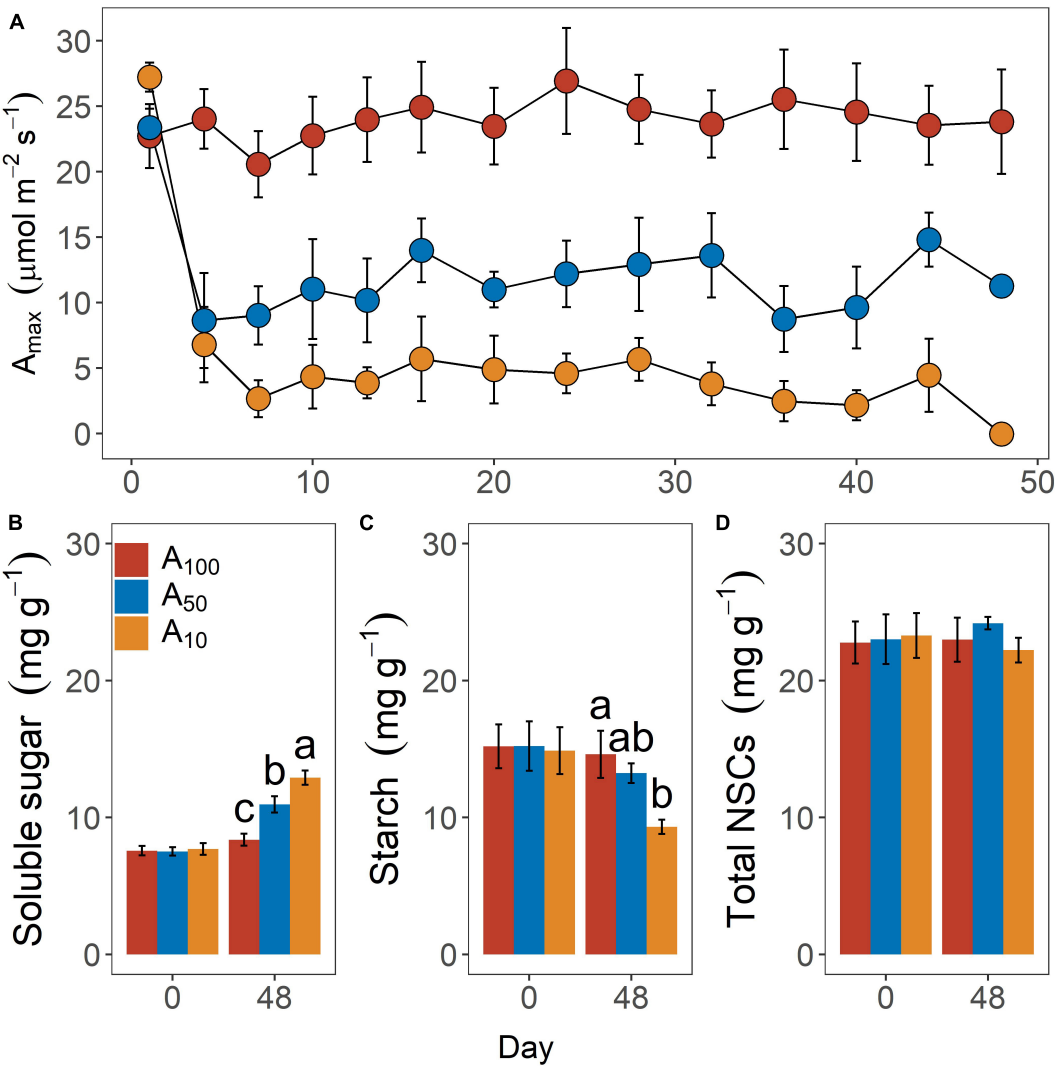

FIGURE 1 | Daily variation of leaf maximum photosynthetic rate (A_{max}) during pretreatment phase **(A)** and leaf soluble sugar **(B)**, starch **(C)**, and total non-structural carbohydrates (NSCs) content **(D)** at the inception and end of antecedent drought treatment. Colors indicate levels of antecedent drought conditions (i.e., A_{100}, A_{50}, and A_{10}). Error bars indicate standard error of mean [n = 10 for panel **(A)** and n = 4 for panels **(B–D)**]. Different letters above bars in panels **(B–D)** denote statistical significance at $p \leq 0.05$ level.

leaves were collected for each plant from 4 randomly selected individuals. The leaf samples were immediately oven-dried at 80°C for 24 h to stop metabolism and then stored in −20°C freezer until measurement. Leaf starch and soluble sugars concentrations were determined following the protocol described by Duan et al. (2013). Concisely, dried materials were grounded to a fine powder in a ball mill, and then weighed for 20 mg. Samples were extracted with 80% aqueous ethanol, then boiled at 95°C for 30 min and centrifuged at 3,000 rpm for 5 min. Supernatant was collected, re-extracted with ethanol and water, and then subjected to the procedures described above. The final supernatant was reserved and evaporated at 40°C using a rotational vacuum concentrator (RVC 2-25 CD, Christ, Germany). Starch content (mg g^{-1}) was determined from the remaining pellets after extraction and assayed with a total starch assay kit (Megazyme International Ireland Ltd., Wicklow, Ireland). Total soluble sugar content (mg g^{-1}) was measured from the supernatants by the anthrone method. Total NSCs content (mg g^{-1}) was calculated as the sum of soluble sugar and starch.

Growth Measurements

To minimize canopy leaf loss, leaf samples used for Ψ_{Leaf} determination were measured for leaf area using leaf area meter (LI-3100, Li-Cor, Lincoln, NE, United States). Samples were then oven-dried for at least 72 h to constant mass, and leaf mass per area (LMA, g m^{-2}) was calculated as the ratio of dry mass to leaf area.

Plant height (H, cm) and basal diameter (D, mm) were measured biweekly throughout the experimental period. Basal diameter was measured using digital calipers at *ca*. 3 cm above soil level, while plant height was considered as the distance from the soil level to the apex of the main stem. Stem volume was estimated as $H \times D^2$ (cm^3), and stem volume index growth rate (VIGR, cm^3 day^{-1}) was calculated as the increment of stem volume between measurement periods divided by the number of days.

Data Analysis

Leaf AC_i curve data were fitted to the FvCB model using *fitaci* function of the Plantecophys R Package to estimate the maximum carboxylation rate of Rubisco (V_{cmax}, μmol m^{-2} s^{-1}) and electron transport rate (J_{max}, μmol m^{-2} s^{-1}) (Duursma, 2015). The speed of recovery is assessed by calculating the time required for specific physiological variables to regain 50% of its maximum ($t_{1/2}$, day), according to Brodribb and Cochard (2009). In short, the percentage of recovery relative to its maximum, measured from each individual within the same treatment group, was pooled together and was plotted against the corresponding number of days. The relationship was fitted using a linear regression and $t_{1/2}$ was then extrapolated from the linear function. The estimation of $t_{1/2}$ was limited to A_{max} and g_s given that the reduction in other physiological variables never surpassed 50% of their maximum.

Leaf NSCs, including the content of soluble sugar, starch and total NSCs content at the end of antecedent drought treatment, were analyzed using one-way ANOVA to test the difference among treatment groups. Physiological data including the A_{max}, g_s, V_{cmax}, and J_{max} measured during the recovery phase were presented as the percentage relative to their corresponding values measured prior to the implementation of the antecedent drought treatment. All time-series data were analyzed using the one-way repeated measurement ANOVA with the *ezANVOA* function in the ezANVOA package, with the levels of drought treatment and time of measurement considered as between- and within-subject factors, respectively. In addition, within each measurement time point, one-way ANOVA was used to test the difference among antecedent drought treatment groups. Following all one-way ANOVA, Tukey's HSD *post hoc* was applied using the *HSD.test* function in the agricolae package for comparison among means. All data were tested for normality and homogeneity of variance before statistical analysis was performed. Statistically significant differences were considered when $p \leq 0.05$. Data process and analysis were performed under R 3.5.3 statistical computing environment (R Core Team, 2013).

RESULTS

Effects of Antecedent Drought Conditions on Leaf Photosynthesis, Carbohydrate Content, and Growth

Leaf photosynthetic rate under saturating light (A_{max}, μmol m^{-2} s^{-1}) differed significantly across levels of antecedent drought conditions (**Figure 1A**; $p < 0.01$). Consistent with our objective, A_{max} in drought-stressed plants (i.e., A_{50} and A_{10}) was constantly maintained at the desired levels during the period of antecedent drought treatment. Interaction between time and drought treatment was observed, but only limited to the first day of measurement, with A_{max} of A_{10} being slightly higher (*ca*. 4.0 μmol m^{-2} s^{-1}) than that of A_{100} and A_{50}.

Contents of leaf NSCs, including soluble sugar (**Figure 1B**), starch (**Figure 1C**), and total NSCs (**Figure 1D**) did not differ across groups before drought treatments were applied. Differences in these variables were observed after 48 days of water restriction during the antecedent treatment. Soluble sugar of A_{10} (12.9 ± 0.5 mg g^{-1}) and A_{50} (10.9 ± 0.6 mg g^{-1}) plants were significantly higher than that of A_{100} plants (8.4 ± 0.4 mg g^{-1}; $p = 0.02$). Starch content also differed significantly across groups but exhibited an inverse pattern ($p = 0.03$), with starch content being 9.3 ± 0.5 mg g^{-1}, 13.2 ± 0.7 mg g^{-1} and 14.6. ± 1.7 mg g^{-1} for A_{10}, A_{50}, and A_{100} plants. Growth rate was strongly impeded by drought treatment ($p < 0.01$; data not shown). The volume index growth rates (VIGR, cm^3 day^{-1}) were 5.23 ± 0.31 cm^3 day^{-1}, 0.99 ± 0.11 cm^3 day^{-1} and 0.39 ± 0.07 cm^3 day^{-1} for A_{100}, A_{50}, and A_{10} plants, respectively.

Responses of Leaf Photosynthesis and Water Relations to Subsequent Drought Stress

All physiological variables, including A_{max}, light saturated stomatal conductance (g_{smax}, mol m^{-2} s^{-1}), carboxylation rate of Rubisco (V_{cmax}, μmol m^{-2} s^{-1}) and electron transport rate (J_{max}, μmol m^{-2} s^{-1}) were significantly decreased by

subsequent drought stress (**Figure 2** and **Table 1**; day 0). In general, the percentage loss of function from maximum values for each physiological parameter, increased with drought severity; however, there was an exception in V_{cmax} and J_{max}, where the relative values for plants at −4.5 MPa were 25.4 and 15.4% higher, respectively, than plants at −3.5 MPa. All physiological variables in plants subjected to antecedent drought conditions, and subsequently to variable drought stress, were less affected compared with control plants that were well-watered and did not experience an antecedent drought stress (**Figure 2**).

Recovery Dynamics of Leaf Photosynthesis, Water Relations, and Plant Growth After Re-watering

Recovery in photosynthetic variables was dependent on the degree of antecedent water deficit and drought severity (**Figures 2**, **3** and **Table 1**). For A_{max} and associated components (i.e., g_s, V_{cmax} and J_{max}), A_{50} and A_{10} plants consistently showed faster rates of recovery compared to A_{100} plants; these effects were stronger as the intensity of subsequent drought stress increased. For example, for plants at −4.5 MPa, A_{max}, V_{cmax} and J_{max} attained nearly or complete recovery on the third day of re-watering, whereas full recovery of these variables in A_{100} plants was much slower; e.g., A_{max} and J_{max} did not reach the values measured before the implementation of the antecedent drought treatments even after 14 days of re-watering (**Figures 2E,G,H**). Notably, for V_{cmax} and J_{max}, the values during the recovery phase were up to 50% higher than their pre-stress levels, suggesting a compensatory response to the previous drought stress.

Upon re-watering, leaf water potential (Ψ_{Leaf}, −MPa) recovered rapidly, reaching pre-stress values within 3 days in most plants, regardless of antecedent and subsequent drought treatment (**Figure 4**). Across drought treatment, Ψ_{Leaf} of plants exposed to antecedent drought was generally less negative than that of control plants, although the difference was not significant.

Upon re-watering and release of the drought stress, all plants showed stem regrowth, but with differing rates of growth. For plants dried to −3.5 and −4.5 MPa, VIGR of A_{100} plants was significantly higher than that of A_{50} and A_{10} plants (**Table 2**; $p < 0.05$ in both cases), while VIGR did not vary across levels of antecedent drought treatment when exposed to severe water stress ($p = 0.17$).

The Relationships Between Recovery of Leaf Photosynthesis and Associated Physiological Variables

Recovery of leaf carbon assimilation was closely related to variables associated with CO_2 diffusion and biochemistry

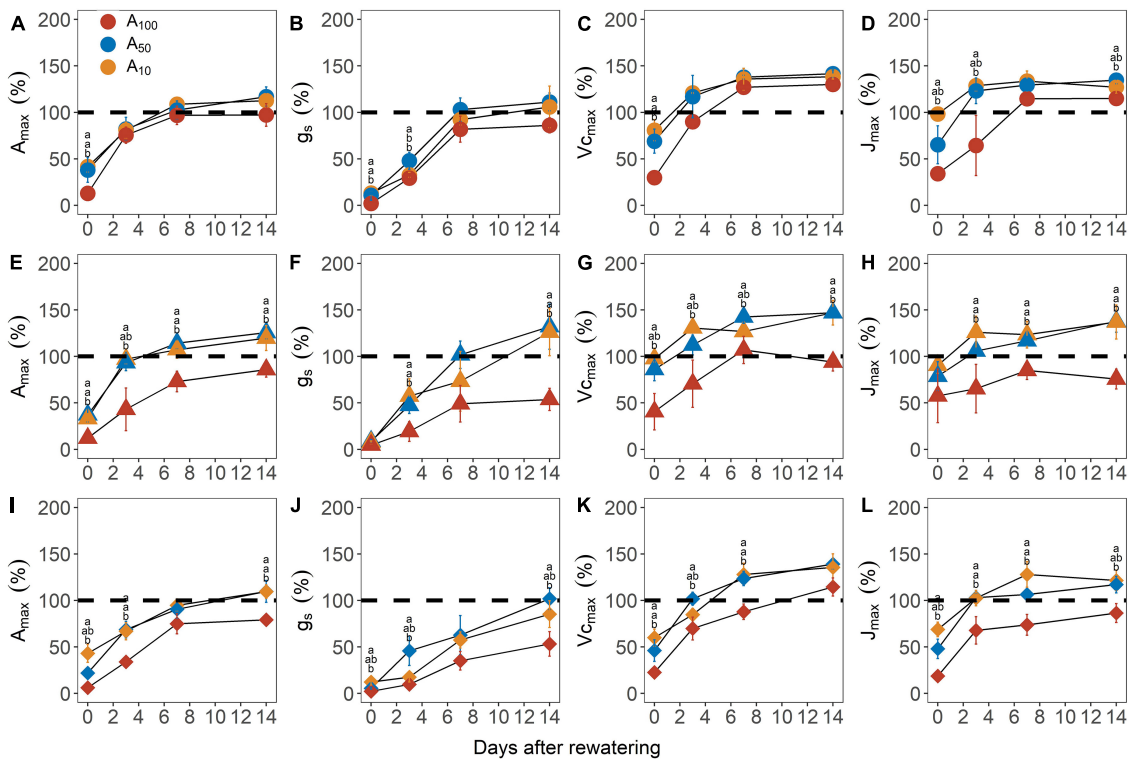

FIGURE 2 | Recovery of maximum photosynthetic rate [A_{max}, panels **(A,E,I)**], stomatal conductance [g_s; panels **(B,F,J)**], maximum Rubisco carboxylation rate [V_{cmax}; panels **(C,G,K)**] and maximum electron transport rate [J_{max}; panels **(D,H,J)**] from –3.5 MPa (circle), –4.5 MPa (triangle), and –5.0 MPa (diamond) during the recovery phase. All traits are given as the percentage of maximum (%). Colors denote levels of antecedent drought conditions (i.e., A_{100}, A_{50}, and A_{10}). Error bars indicate standard error of mean (n = 3–4). Different letters above data points represent statistically significant difference at $p \leq 0.05$ across pretreatment levels in each day.

TABLE 1 | Statistical analysis for the difference in the percentage of recovery in maximum photosynthetic rate (A_{max}), stomatal conductance (g_s), maximum carboxylation rate of Rubisco (V_{cmax}), maximum electron transport rate (J_{max}), and midday leaf water potential (Ψ_{Leaf}) across different drought treatments (i.e., −3.5,−4.5, and −5.0 MPa) during the phase of recovery (i.e., day 0, 3, 7, and 14).

Traits	Treatment (MPa)	Days of recovery											
		Day 0			Day 3			Day 7			Day 14		
		SS	*F*-value	*p*	SS	*F*-value	*p*	SS	*F*-value	*p*	SS	*F*-value	*p*
A_{max}	−3.5	1,480.42	$8.28_{[2,6]}$	0.02	74.60	$0.36_{[2,6]}$	0.71	213.61	$1.50_{[2,6]}$	0.30	647.07	$3.16_{[2,6]}$	0.12
	−4.5	1,085.27	$14.16_{[2,7]}$	<0.01	5,444.10	$13.00_{[2,7]}$	<0.01	2,926.70	$18.34_{[2,7]}$	<0.01	2,761.74	$14.25_{[2,7]}$	<0.01
	−5.0	2,051.82	$24.57_{[2,6]}$	<0.01	2,286.50	$17.75_{[2,6]}$	<0.01	660.54	$3.93_{[2,6]}$	0.08	1,843.29	$12.21_{[2,6]}$	<0.01
g_s	−3.5	206.62	$8.49_{[2,6]}$	0.02	590.78	$7.75_{[2,6]}$	0.02	666.74	$2.57_{[2,6]}$	0.16	1,051.10	$2.39_{[2,6]}$	0.17
	−4.5	28.31	$4.17_{[2,7]}$	0.07	2,338.60	$6.56_{[2,7]}$	0.03	4,182.90	$3.84_{[2,7]}$	0.08	11,410.70	$12.40_{[2,7]}$	<0.01
	−5.0	156.82	$17.52_{[2,6]}$	<0.01	2,154.52	$11.63_{[2,6]}$	<0.01	1,290.70	$3.15_{[2,6]}$	0.12	3,678.90	$10.63_{[2,6]}$	0.01
V_{cmax}	−3.5	4,267.40	$18.86_{[2,6]}$	<0.01	1,691.20	$4.88_{[2,6]}$	0.06	197.81	$2.06_{[2,6]}$	0.21	215.01	$3.83_{[2,6]}$	0.32
	−4.5	5,461.40	$14.96_{[2,7]}$	<0.01	5,689.90	$11.17_{[2,6]}$	<0.01	1,903.70	$10.20_{[2,7]}$	0.01	5,620.60	$28.28_{[2,7]}$	<0.001
	−5.0	2,148.16	$13.75_{[2,6]}$	<0.01	1,543.22	$9.49_{[2,6]}$	0.01	2,906.22	$16.11_{[2,6]}$	<0.01	1,064.80	$4.77_{[2,6]}$	0.06
J_{max}	−3.5	6,181.50	$19.36_{[2,6]}$	<0.01	7,646.80	$9.03_{[2,6]}$	0.02	599.52	$4.34_{[2,6]}$	0.07	588.69	$10.65_{[2,6]}$	0.01
	−4.5	1,678.40	$1,678.40_{[2,6]}$	0.19	5,729.80	$8.66_{[2,7]}$	0.02	2,536.37	$11.80_{[2,7]}$	<0.01	7,610.30	$19.41_{[2,6]}$	<0.01
	−5.0	3,821.10	$31.14_{[2,6]}$	<0.001	2,457.65	$12.08_{[2,6]}$	<0.01	4,486.60	$19.31_{[2,6]}$	<0.01	2,183.80	$10.77_{[2,6]}$	0.01
Ψ_{leaf}	−3.5	0.03	$3.23_{[2,6]}$	0.11	0.63	$8.58_{[2,6]}$	0.02	1.16	$13.41_{[2,6]}$	<0.01	0.37	$6.49_{[2,6]}$	0.03
	−4.5	0.01	$1.36_{[2,6]}$	0.33	1.92	$7.59_{[2,6]}$	0.02	2.71	$36.83_{[2,6]}$	<0.001	0.06	$1.20_{[2,6]}$	0.37
	−5.0	0.01	$0.36_{[2,6]}$	0.71	0.63	$9.35_{[2,6]}$	0.01	0.68	$20.40_{[2,6]}$	<0.01	0.07	$2.45_{[2,6]}$	0.17

Presented statistical outcomes including sum of squares (SS), F-value, and calculated value of probability (p). Subscripted numbers following the F values indicate degrees of freedom for between and within group factors. Post hoc analysis was applied when $p \leq 0.05$ with the resulting being reported in ***Figure 2****.*

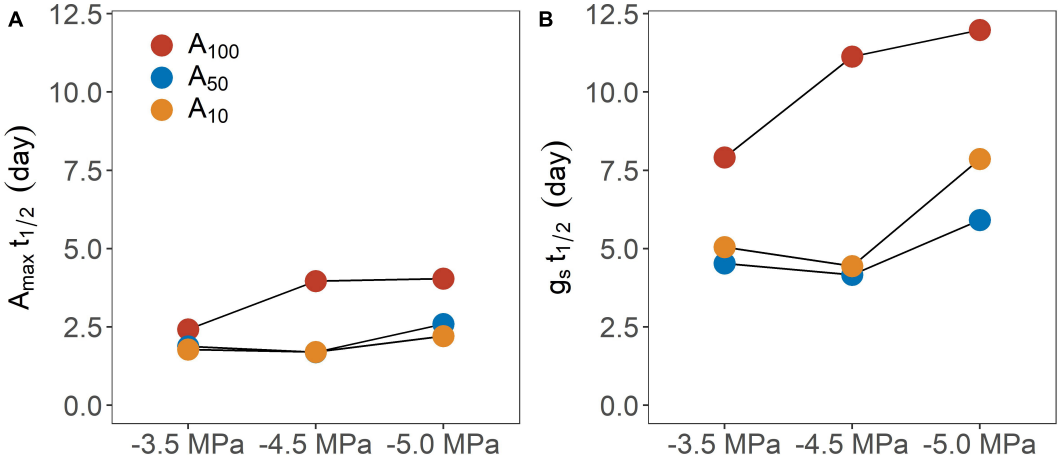

FIGURE 3 | Time (day) required for physiological traits [**(A)** maximum photosynthetic rate; **(B)** stomatal conductance) regain 50% of their maximum value following rewatering across different pretreatment (A_{100}, A_{50}, and A_{10}) and drought treatment levels (–3.5, –4.5, and –5.0 MPa).

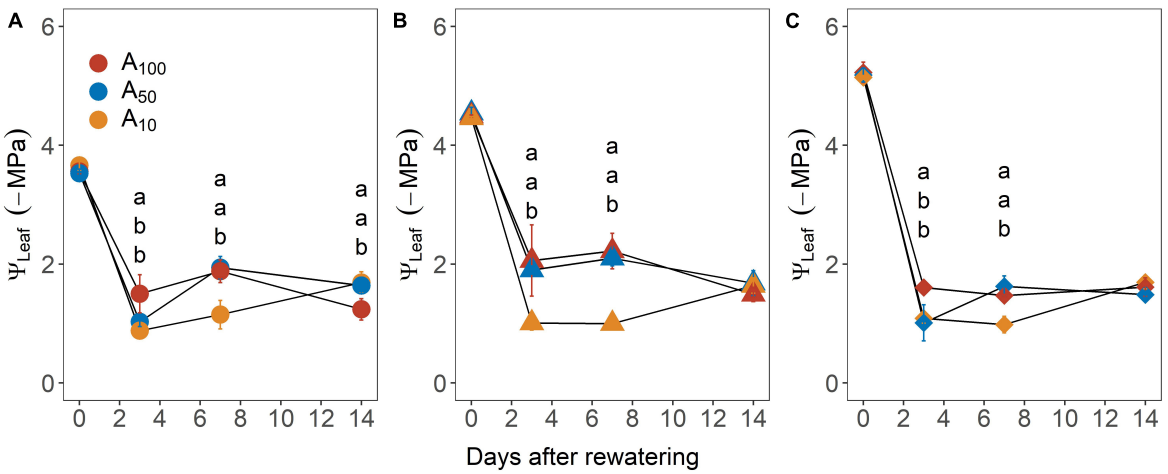

FIGURE 4 | Recovery of midday leaf water potential (Ψ_{Leaf}) from –3.5 MPa **(A)**, –4.5 MPa **(B)**, and –5.0 MPa **(C)** during the recovery phase. Colors denote levels of antecedent drought conditions (i.e., A_{100}, A_{50}, and A_{10}). Error bars indicate standard error of mean (n = 3–4).

TABLE 2 | Volume index growth rates (cm^3 day^{-1}; VIGR) of plants across all drought treatments during the recovery phase.

Pre-treatment	Drought treatment		
	–3.5 MPa	**–4.5 MPa**	**–5.0 MPa**
A_{100}	6.63 ± 0.85^{a}	5.10 ± 0.69^{a}	3.21 ± 0.08^{a}
A_{50}	3.36 ± 0.47^{b}	3.91 ± 0.42^{ab}	3.21 ± 0.38^{a}
A_{10}	3.24 ± 0.37^{b}	2.97 ± 0.50^{b}	3.58 ± 0.24^{a}

Data are shown as mean ± standard deviation of mean (n = 3–4). Superscripts indicate significant difference at p ≤ 0.05 level within each drought treatment group.

(**Figure 5**). When data were pooled together, a curvi-linear relationship was found between the percentage recovery of A_{max} and g_s. These two variables were linearly related up to 70% recovery of A_{max}, with a slope of 1.38. In addition, recovery of A_{max} was also linearly related to V_{cmax} ($r^2 = 0.91$, $p < 0.001$) and J_{max} ($r^2 = 0.77$, $p < 0.001$), with the slope of the linear regression being 0.94 and 0.97, respectively.

DISCUSSION

We applied different levels of drought stress and measured plant carbohydrates, gas exchange, plant water status and growth, to investigate the influences of antecedent drought conditions on the response of plants during subsequent drought stress and recovery dynamics. Although photosynthesis, growth and the form of leaf carbohydrate varied across different levels of antecedent drought treatment, total NSC content did not vary. During subsequent drought stress, plants that experienced antecedent drought conditions (i.e., A_{50} and A_{10}) were less affected compared with the control (i.e., A_{100}) in terms of carbon assimilation, maximum rate of Rubisco carboxylation and

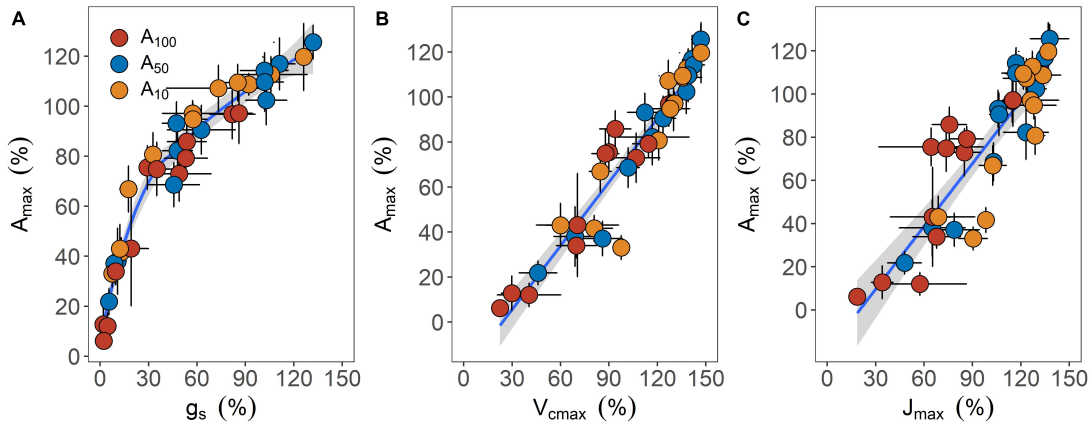

FIGURE 5 | The relationships between maximum photosynthetic rate (A_{max}) and stomatal conductance [g_s, panel **(A)**], maximum carboxylation rate of Rubisco [V_{cmax}, panel **(B)**] and maximum electron transport rate **(C)** during the recovery phase. All traits are expressed as the percentage of maximum relative to the values before drought treatment was applied. Error bars indicate standard error of mean (n = 3–4). Data are pooled across all drought treatment groups and are fitted with nonlinear [**(A)** $y = 28.86 \ln(x) - 25.57$, $R^2 = 0.95$] or linear regressions [**(B)** $y = 0.94x - 22.74$, $R^2 = 0.91$; and **(C)** $y = 0.97x - 19.46$, $R^2 = 0.78$] when possible. Shaded regions surrounding fitted lines represent 95% confident interval.

electron transport. Post-drought recovery of leaf photosynthesis was controlled by both stomatal and non-stomatal limitation. Importantly, time to recovery was dependent on both antecedent drought conditions and the severity of subsequent drought stress, with faster physiological recovery in antecedent plants compared to controls observed only when plants had been exposed to the more severe drought treatment. Overall, we found that antecedent drought conditions altered the response of leaf carbon assimilation to ensuing water limitation and resumption in *E. camaldulensis*, suggesting that both drought resistance and resilience are dependent on the exposure of plants to historical drought events.

Variation of Leaf Carbohydrate Content During Sustained Drought

Greater reductions in growth relative to photosynthesis will theoretically lead to carbohydrate accumulation (Chapin et al., 1990; Sala et al., 2012; Piper et al., 2017). However, experimental evidence regarding the impact of drought on leaf carbohydrate content is inconsistent (Klein et al., 2014; Martínez-Vilalta et al., 2016; Chuste et al., 2020; He et al., 2020). For example, leaves of *Eucalyptus saligna* seedlings exposed to drought exhibited higher NSC content compared to well-watered controls (Ayub et al., 2011), whereas an opposite pattern was observed in leaves of *Eucalyptus globulus* and *Eucalyptus smithii* (Duan et al., 2013; Mitchell et al., 2013). In the present study, growth nearly ceased while leaf photosynthesis continued during the phase of antecedent drought treatment, yet total NSC content remained stable across treatment groups (**Figure 1**), similar to the findings reported by Klein et al. (2014) in branches of *Pinus halepensis* subjected to drought. The lack of change in NSC content during drought may emerge due to several reasons. Firstly, the total NSC content can vary markedly among organs (He et al., 2020); therefore, the NSC content of a single organ does not comprehensively reflect drought-induced changes in whole plant carbon reserve, although it can be driven by one organ (e.g., Duan et al., 2013). Secondly, the carbohydrate content may be influenced by the duration of drought exposure. For example, initially accumulated carbohydrate due to growth cessation may be depleted due to increased rates of other carbon-consuming metabolic processes such as respiration or synthesis of compatible osmolytes, as drought stress proceeds (Flexas et al., 2005; Tomasella et al., 2020).

Although total NSC content was not affected by drought, the relative contribution of soluble sugar and starch content to NSC was consistent with the findings of earlier studies (He et al., 2020). It has been shown that the depolymerization of starch into soluble sugar during drought stress will facilitate osmotic regulation, thereby lowering the risk of hydraulic impairment by increasing water acquisition (Trifilò et al., 2017; Tomasella et al., 2020). The concomitant increase in soluble sugar and decrease in starch, therefore reflects the shift in the functionality of carbohydrate from growth to maintenance, in which starch primarily acts as carbon reserve while soluble sugar performs immediate metabolic functions (Martínez-Vilalta et al., 2016).

Antecedent Drought Condition Promotes Drought Resistance of Photosynthesis

Our second hypothesis was partially supported by the observation that leaf A_{max} was generally higher in plants exposed to antecedent drought conditions, and then exposed to subsequent drought. The smaller reduction in A_{max} was attributed to the biochemical components of photosynthesis rather than gas exchange, as g_s did not differ across levels of drought stress in plants exposed to antecedent drought (**Figure 2**). On the other hand, biochemical components of photosynthesis can also acclimate to drought. With respect to Rubisco carboxylation, it has been reported that water limitation, although uncommon, can increase the catalytic efficiency of Rubisco by increasing either the amount of enzyme or activation

state (Galmés et al., 2013; Menezes-Silva et al., 2017). Likewise, in some species, an increased electron transport rate has been found in leaves exposed to drought (Kitao et al., 2003), although the functional significance of the adjustment is unclear, given that photosynthesis is rarely limited by RuBP regeneration under drought stress.

Recovery Is Co-limited by Stomatal and Non-stomatal Limitation

The decreased g_s, V_{cmax}, and J_{max} relative to their pre-stress values, in conjunction with the correlations between the percentage recovery of A_{max} and these components, indicate stomatal and non-stomatal limitation of photosynthesis during both drought stress and post-drought recovery phase (**Figure 2**). Noticeably, after the resumption of irrigation, although the recovery of A_{max} was associated with recovery of both g_s and biochemical components, the slope of the $A_{max} - g_s$ relationship was much steeper than the slope of the $A_{max} - V_{cmax}$ or $A_{max} - J_{max}$ relationship, up to *ca.* 70% of full recovery (**Figure 5**); hence, the initial phase and major fraction of the full recovery of A_{max} was primarily driven by the restoration of g_s. It has been suggested that drought induced down-regulation of leaf photosynthesis is mainly attributed to diffusive limitation rather than biochemical limitation (Flexas et al., 2004, 2006b). However, down-regulation of photosynthesis due to decreased V_{cmax} caused by inactivation of Rubisco and RuBP content have been reported in a number of species (Parry et al., 2002; Carmo-Silva et al., 2010; Galmés et al., 2013). It is likely that the occurrence of biochemical limitation depends on the strength of water limitation. For instance, decreased V_{cmax} or J_{max} only emerged when drought stress was severe and g_s approached very low values, approximately 20% of the control (Flexas et al., 2004), suggesting that decreased biochemical efficiency of photosynthesis may have limited the recovery of photosynthesis as the highest g_s accounted for *ca.* 14% of the pre-stressed value even for plants subjected to the mildest drought stress (i.e., −3.5 MPa). Nonetheless, it could be argued that decreased biochemical function could be an artifact due to drought-induced reduction in mesophyll conductance (g_m). Indeed, V_{cmax} remains unaffected by water stress when the resistance of g_m to CO_2 diffusion is accounted for when calculating Rubisco carboxylation rate from response curves (Flexas et al., 2006a, 2008). However, by accounting for g_m, Zhou et al. (2014) found that both diffusive and biochemical limitation can contribute to down-regulation of photosynthesis during drought in a wide range of species, including *E. camaldulensis*; e.g., V_{cmax} can decrease by 50% at −2.0 MPa, regardless of the variation in the value of g_m under drought. Still, further work is clearly needed to confirm our observation by assessing the potential effects of g_m on the measurement of biochemical components of photosynthesis, using plants subjected to the same drought treatment.

Recovery From Drought Depends on Antecedent Condition and Severity

Shorter $T_{1/2}$ for A_{max} and g_s was found in seedlings exposed to antecedent drought conditions, which apparently generated drought-induced acclimation of photosynthesis, although the difference in $T_{1/2}$ for A_{max} at −3.5 MPa was less pronounced between well-watered control and plants exposed to antecedent drought treatment. Notably, A_{10} and A_{50} plants exhibited similar $t_{1/2}$ for both A_{max} and g_s at less negative water potentials (i.e., −3.5 and −4.5 MPa), while the time for recovery diverged at −5.0 MPa. Hence, increasing the level of antecedent drought conditions would not consistently confer rapid recovery, especially when subsequent drought stress was severe (**Figure 4**), suggesting an interaction between the intensity of consecutive drought conditions. Overall, trees exposed to more severe drought stress typically need longer $T_{1/2}$. This finding is consistent with early studies showing that the time required for recovery is dependent on the severity of drought stress (Blackman et al., 2009; Brodribb and Cochard, 2009). Given that the subsequent drought stress was designed to reduce K_{Leaf}, a mechanistic explanation bridging the time to recovery and drought severity may be the following: that the greater the impairment of K_{Leaf}, the longer it would take A_{max} and g_s to fully recover, thereby delaying whole plant recovery. Of note, two implicit assumptions behind this interpretation are: (a) recovery of leaf photosynthesis is driven by the alleviation of stomatal limitation; and (b) the recovery dynamics of g_s are primarily governed by the recovery in K_{Leaf}. As has been discussed above, stomatal limitation played a major role in limiting the recovery of photosynthesis during the recovery phase. On the other hand, it is known that the stomatal openness highly depends on leaf water status, which is a function of K_{Leaf} at a given stem-to-leaf water potential gradient. In support, the variation of K_{Leaf} has been found to synchronize with that of g_s at diurnal scales (Brodribb and Holbrook, 2004) and the restoration of leaf gas exchange has been facilitated by the recovery of K_{Leaf} following drought stress (Galmés et al., 2007; Skelton et al., 2017). In the current study, the recovery of g_s was slower as drought stress and in turn hydraulic impairments intensified, which is consistent with the established theory linking plant hydraulics and gas exchange.

CONCLUSION

Our findings demonstrate that antecedent drought conditions may modify leaf biochemistry and physiology, which can be translated into different responses upon subsequent drought stress and recovery dynamics, following the alleviation of water limitation. Antecedent drought triggered an increase in soluble sugar content, which may have facilitated the recovery of water status by osmotic regulation and the maintenance of hydraulic integrity by lowering the vulnerability to embolism (De Baerdemaeker et al., 2017). The recovery of carbon assimilation was ultimately limited by decreased gas exchange capacity because of hydraulic impairment, which depended on the severity of the subsequent drought. Growth following re-watering was limited by the lack of carbon reserves, thus highlighting the importance of plant hydraulics and carbohydrates in regulating plant drought resistance and resilience. Overall, the response of plants to drought stress appears to be a function of the antecedent conditions and the subsequent drought, which should be considered in combination when assessing the response of plants to drought.

DATA AVAILABILITY STATEMENT

The raw data supporting the conclusions of this article will be made available by the authors, without undue reservation.

AUTHOR CONTRIBUTIONS

DT and CB conceived and designed the research and revised the manuscript. JW and JB conducted the experiments. XL analyzed the data and wrote the early draft of the manuscript. All authors read and approved the manuscript.

FUNDING

The project was funded by the Science and Industry Endowment Fund (RP04-122) and XL was supported by the Innovation team in Ecology of Minzu University of China (2020CXTD).

REFERENCES

Anderegg, W. R., Trugman, A. T., Badgley, G., Konings, A. G., and Shaw, J. (2020). Divergent forest sensitivity to repeated extreme droughts. *Nat. Clim. Chang.* 10, 1091–1095. doi: 10.1038/s41558-020-00919-1

Ayub, G., Smith, R. A., Tissue, D. T., and Atkin, O. K. (2011). Impacts of drought on leaf respiration in darkness and light in *Eucalyptus saligna* exposed to industrial-age atmospheric CO2 and growth temperature. *New Phytol.* 190, 1003–1018. doi: 10.1111/j.1469-8137.2011.03673.x

Blackman, C. J., Brodribb, T. J., and Jordan, G. J. (2009). Leaf hydraulics and drought stress: response, recovery and survivorship in four woody temperate plant species. *Plant Cell Environ.* 32, 1584–1595. doi: 10.1111/j.1365-3040.2009.02023.x

Brodribb, T., and Holbrook, N. M. (2004). Diurnal depression of leaf hydraulic conductance in a tropical tree species. *Plant Cell Environ.* 27, 820–827. doi: 10.1111/j.1365-3040.2004.01188.x

Brodribb, T. J., and Cochard, H. (2009). Hydraulic failure defines the recovery and point of death in water-stressed conifers. *Plant Physiol.* 149, 575–584. doi: 10.1104/pp.108.129783

Brodribb, T. J., and Holbrook, N. M. (2003). Stomatal closure during leaf dehydration, correlation with other leaf physiological traits. *Plant Physiol.* 132, 2166–2173. doi: 10.1104/pp.103.023879

Brodribb, T. J., Powers, J., Cochard, H., and Choat, B. (2020). Hanging by a thread? Forests and drought. *Science* 368, 261–266.

Butcher, P., McDonald, M., and Bell, J. (2009). Congruence between environmental parameters, morphology and genetic structure in Australia's most widely distributed eucalypt, *Eucalyptus camaldulensis*. *Tree Genet. Genomes* 5, 189–210. doi: 10.1007/s11295-008-0169-6

Carmo-Silva, A. E., Keys, A. J., Andralojc, P. J., Powers, S. J., Arrabaça, M. C., and Parry, M. A. (2010). Rubisco activities, properties, and regulation in three different C4 grasses under drought. *J. Exp. Bot.* 61, 2355–2366. doi: 10.1093/jxb/erq071

Chapin, F. S. III, Schulze, E., and Mooney, H. A. (1990). The ecology and economics of storage in plants. *Annu. Rev. Ecol. Evol. Syst.* 21, 423–447. doi: 10.1146/annurev.es.21.110190.002231

Choat, B., Brodribb, T. J., Brodersen, C. R., Duursma, R. A., Lopez, R., and Medlyn, B. E. (2018). Triggers of tree mortality under drought. *Nature* 558, 531–539. doi: 10.1038/s41586-018-0240-x

Chuste, P. A., Maillard, P., Bréda, N., Levillain, J., Thirion, E., Wortemann, R., et al. (2020). Sacrificing growth and maintaining a dynamic carbohydrate storage are key processes for promoting beech survival under prolonged drought conditions. *Trees* 34, 381–394. doi: 10.1007/s00468-019-01923-5

Dai, A. (2013). Increasing drought under global warming in observations and models. *Nat. Clim. Chang.* 3, 52–58. doi: 10.1038/nclimate1633

De Baerdemaeker, N. J., Salomón, R. L., De Roo, L., and Steppe, K. (2017). Sugars from woody tissue photosynthesis reduce xylem vulnerability to cavitation. *New Phytol.* 216, 720–727. doi: 10.1111/nph.14787

Doody, T. M., Colloff, M. J., Davies, M., Koul, V., Benyon, R. G., and Nagler, P. L. (2015). Quantifying water requirements of riparian river red gum (*Eucalyptus camaldulensis*) in the Murray-Darling Basin, Australia-implications for the management of environmental flows. *Ecohydrology* 8, 1471–1487. doi: 10.1002/eco.1598

Duan, H., Amthor, J. S., Duursma, R. A., O'grady, A. P., Choat, B., and Tissue, D. T. (2013). Carbon dynamics of eucalypt seedlings exposed to progressive drought in elevated [CO2] and elevated temperature. *Tree Physiol.* 33, 779–792. doi: 10.1093/treephys/tpt061

Duursma, R. A. (2015). Plantecophys-an R package for analysing and modelling leaf gas exchange data. *PLoS One* 10:e0143346. doi: 10.1371/journal.pone.0143346

Flexas, J., Barón, M., Bota, J., Ducruet, J. M., Gallé, A., Galmés, J., et al. (2009). Photosynthesis limitations during water stress acclimation and recovery in the drought-adapted Vitis hybrid Richter-110 (V. berlandieri× V. rupestris). *J. Exp. Bot.* 60, 2361–2377. doi: 10.1093/jxb/erp069

Flexas, J., Bota, J., Galmes, J., Medrano, H., and Ribas-Carbó, M. (2006a). Keeping a positive carbon balance under adverse conditions: responses of photosynthesis and respiration to water stress. *Physiol. Plant* 127, 343–352. doi: 10.1111/j.1399-3054.2006.00621.x

Flexas, J., Bota, J., Loreto, F., Cornic, G., and Sharkey, T. (2004). Diffusive and metabolic limitations to photosynthesis under drought and salinity in C3 plants. *Plant Biol.* 6, 269–279. doi: 10.1055/s-2004-820867

Flexas, J., Galmes, J., Ribas-Carbo, M., and Medrano, H. (2005). "The effects of water stress on plant respiration," in *Plant Respiration*, eds H. Lambers and M. Ribas-Carbo (Dordrecht: Springer), doi: 10.1007/1-4020-3589-6_6

Flexas, J., Ribas-Carbó, M., Bota, J., Galmés, J., Henkle, M., Martínez-Cañellas, S., et al. (2006b). Decreased Rubisco activity during water stress is not induced by decreased relative water content but related to conditions of low stomatal conductance and chloroplast CO2 concentration. *New Phytol.* 172, 73–82. doi: 10.1111/j.1469-8137.2006.01794.x

Flexas, J., Ribas-Carbo, M., Diaz-Espejo, A., Galmes, J., and Medrano, H. (2008). Mesophyll conductance to CO2: current knowledge and future prospects. *Plant Cell Environ.* 31, 602–621. doi: 10.1111/j.1365-3040.2007.01757.x

Galmés, J., Aranjuelo, I., Medrano, H., and Flexas, J. (2013). Variation in Rubisco content and activity under variable climatic factors. *Photosynth. Res.* 117, 73–90. doi: 10.1007/s11120-013-9861-y

Galmés, J., Flexas, J., Savé, R., and Medrano, H. (2007). Water relations and stomatal characteristics of Mediterranean plants with different growth forms and leaf habits: responses to water stress and recovery. *Plant Soil* 290, 139–155. doi: 10.1007/s11104-006-9148-6

Gessler, A., Bottero, A., Marshall, J., and Arend, M. (2020). The way back: recovery of trees from drought and its implication for acclimation. *New Phytol.* 228, 1704–1709. doi: 10.1111/nph.16703

Granda, E., and Camarero, J. J. (2017). Drought reduces growth and stimulates sugar accumulation: new evidence of environmentally driven non-structural carbohydrate use. *Tree Physiol.* 37, 997–1000. doi: 10.1093/treephys/tpx097

Grassi, G., and Magnani, F. (2005). Stomatal, mesophyll conductance and biochemical limitations to photosynthesis as affected by drought and leaf ontogeny in ash and oak trees. *Plant Cell Environ.* 28, 834–849. doi: 10.1111/j.1365-3040.2005.01333.x

Hagedorn, F., Joseph, J., Peter, M., Luster, J., Pritsch, K., Geppert, U., et al. (2016). Recovery of trees from drought depends on belowground sink control. *Nat. Plants* 2:16111. doi: 10.1038/nplants.2016.111

He, W., Liu, H., Qi, Y., Liu, F., and Zhu, X. (2020). Patterns in nonstructural carbohydrate contents at the tree organ level in response to drought duration. *Glob. Chang. Biol.* 26, 3627–3638. doi: 10.1111/gcb.15078

Joseph, J., Gao, D., Backes, B., Bloch, C., Brunner, I., Gleixner, G., et al. (2020). Rhizosphere activity in an old-growth forest reacts rapidly to changes in soil moisture and shapes whole-tree carbon allocation. *Proc. Natl. Acad. Sci. U.S.A.* 117, 24885–24892. doi: 10.1073/pnas.2014084117

Kannenberg, S. A., Schwalm, C. R., and Anderegg, W. R. (2020). Ghosts of the past: how drought legacy effects shape forest functioning and carbon cycling. *Ecol. Lett.* 23, 891–901. doi: 10.1111/ele.13485

Kitao, M., Lei, T. T., Koike, T., Tobita, H., and Maruyama, Y. (2003). Higher electron transport rate observed at low intercellular CO2 concentration in long-term drought-acclimated leaves of Japanese mountain birch (*Betula ermanii*). *Physiol. Plant* 118, 406–413. doi: 10.1034/j.1399-3054.2003.00120.x

Klein, T., Hoch, G., Yakir, D., and Körner, C. (2014). Drought stress, growth and nonstructural carbohydrate dynamics of pine trees in a semi-arid forest. *Tree Physiol.* 34, 981–992. doi: 10.1093/treephys/tpu071

Körner, C. (2015). Paradigm shift in plant growth control. *Curr. Opin. Plant Biol.* 25, 107–114. doi: 10.1016/j.pbi.2015.05.003

Li, X., Piao, S., Wang, K., Wang, X., Wang, T., Ciais, P., et al. (2020). Temporal trade-off between gymnosperm resistance and resilience increases forest sensitivity to extreme drought. *Nat. Ecol. Evol.* 4, 1075–1083. doi: 10.1038/s41559-020-1217-3

Martínez-Vilalta, J., Sala, A., Asensio, D., Galiano, L., Hoch, G., Palacio, S., et al. (2016). Dynamics of non-structural carbohydrates in terrestrial plants: a global synthesis. *Ecol. Monogr.* 86, 495–516. doi: 10.1002/ecm.1231

Menezes-Silva, P. E., Sanglard, L. M., Ávila, R. T., Morais, L. E., Martins, S. C., Nobres, P., et al. (2017). Photosynthetic and metabolic acclimation to repeated drought events play key roles in drought tolerance in coffee. *J. Exp. Bot.* 68, 4309–4322. doi: 10.1093/jxb/erx211

Mitchell, P. J., O'Grady, A. P., Tissue, D. T., White, D. A., Ottenschlaeger, M. L., and Pinkard, E. A. (2013). Drought response strategies define the relative contributions of hydraulic dysfunction and carbohydrate depletion during tree mortality. *New Phytol.* 197, 862–872. doi: 10.1111/nph.12064

O'Brien, M. J., Engelbrecht, B. M., Joswig, J., Pereyra, G., Schuldt, B., Jansen, S., et al. (2017a). A synthesis of tree functional traits related to drought-induced mortality in forests across climatic zones. *J. Appl. Ecol.* 54, 1669–1686. doi: 10.1111/1365-2664.12874

O'Brien, M. J., Ong, R., and Reynolds, G. (2017b). Intra-annual plasticity of growth mediates drought resilience over multiple years in tropical seedling communities. *Glob. Chang. Biol.* 23, 4235–4244. doi: 10.1111/gcb.13658

Ouyang, S. N., Gessler, A., Saurer, M., Hagedorn, F., Gao, D. C., Wang, X. Y., et al. (2021). Root carbon and nutrient homeostasis determines downy oak sapling survival and recovery from drought. *Tree Physiol.* 41, 1400–1412. doi: 10.1093/treephys/tpab019

Parry, M. A., Andralojc, P. J., Khan, S., Lea, P. J., and Keys, A. J. (2002). Rubisco activity: effects of drought stress. *Ann. Bot.* 89, 833–839. doi: 10.1093/aob/mcf103

Piper, F. I., Fajardo, A., and Hoch, G. (2017). Single-provenance mature conifers show higher non-structural carbohydrate storage and reduced growth in a drier location. *Tree Physiol.* 37, 1001–1010. doi: 10.1093/treephys/tpx061

R Core Team (2013). *R: A Language and Environment for Statistical Computing*. Vienna: R Foundation for Statistical Computing. Available online at: http://www.R-project.org/

Ruehr, N. K., Grote, R., Mayr, S., and Arneth, A. (2019). Beyond the extreme: recovery of carbon and water relations in woody plants following heat and drought stress. *Tree Physiol.* 39, 1285–1299. doi: 10.1093/treephys/tpz032

Sala, A., and Hoch, G. (2009). Height-related growth declines in ponderosa pine are not due to carbon limitation. *Plant Cell Environ.* 32, 22–30. doi: 10.1111/j.1365-3040.2008.01896.x

Sala, A., Woodruff, D. R., and Meinzer, F. C. (2012). Carbon dynamics in trees: feast or famine? *Tree Physiol.* 32, 764–775. doi: 10.1093/treephys/tpr143

Schmitt, A., Trouvé, R., Seynave, I., and Lebourgeois, F. (2020). Decreasing stand density favors resistance, resilience, and recovery of *Quercus petraea* trees to a severe drought, particularly on dry sites. *Ann. For. Sci.* 77, 1–21. doi: 10.1007/s13595-020-00959-9

Signori-Müller, C., Oliveira, R. S., de Vasconcellos Barros, F., Tavares, J. V., Gilpin, M., Diniz, F. C., et al. (2021). Non-structural carbohydrates mediate seasonal water stress across Amazon forests. *Nat. Commun.* 12, 1–9. doi: 10.1038/s41467-021-22378-8

Skelton, R. P., Brodribb, T. J., McAdam, S. A., and Mitchell, P. J. (2017). Gas exchange recovery following natural drought is rapid unless limited by loss of leaf hydraulic conductance: evidence from an evergreen woodland. *New Phytol.* 215, 1399–1412. doi: 10.1111/nph.14652

Stuart-Haëntjens, E., De Boeck, H. J., Lemoine, N. P., Mänd, P., Kröel-Dulay, G., Schmidt, I. K., et al. (2018). Mean annual precipitation predicts primary production resistance and resilience to extreme drought. *Sci. Total Environ.* 636, 360–366. doi: 10.1016/j.scitotenv.2018.04.290

Tomasella, M., Petrussa, E., Petruzzellis, F., Nardini, A., and Casolo, V. (2020). The possible role of non-structural carbohydrates in the regulation of tree hydraulics. *Int. J. Mol. Sci.* 21:144. doi: 10.3390/ijms21010144

Trifilò, P., Casolo, V., Raimondo, F., Petrussa, E., Boscutti, F., Gullo, M. A. L., et al. (2017). Effects of prolonged drought on stem non-structural carbohydrates content and post-drought hydraulic recovery in *Laurus nobilis* L.: the possible link between carbon starvation and hydraulic failure. *Plant Physiol. Biochem.* 120, 232–241. doi: 10.1016/j.plaphy.2017.10.003

Wu, X., Liu, H., Li, X., Ciais, P., Babst, F., Guo, W., et al. (2018). Differentiating drought legacy effects on vegetation growth over the temperate Northern Hemisphere. *Glob. Chang. Biol.* 24, 504–516. doi: 10.1111/gcb.13920

Xu, Z., Zhou, G., and Shimizu, H. (2010). Plant responses to drought and rewatering. *Plant Signal Behav.* 5, 649–654. doi: 10.4161/psb.5.6.11398

Zait, Y., Shtein, I., and Schwartz, A. (2019). Long-term acclimation to drought, salinity and temperature in the thermophilic tree *Ziziphus spina-christi*: revealing different tradeoffs between mesophyll and stomatal conductance. *Tree Physiol.* 39, 701–716. doi: 10.1093/treephys/tpy133

Zhou, S., Medlyn, B., Sabaté, S., Sperlich, D., and Prentice, I. C. (2014). Short-term water stress impacts on stomatal, mesophyll and biochemical limitations to photosynthesis differ consistently among tree species from contrasting climates. *Tree Physiol.* 34, 1035–1046. doi: 10.1093/treephys/tpu072

Conflict of Interest: The authors declare that the research was conducted in the absence of any commercial or financial relationships that could be construed as a potential conflict of interest.

Publisher's Note: All claims expressed in this article are solely those of the authors and do not necessarily represent those of their affiliated organizations, or those of the publisher, the editors and the reviewers. Any product that may be evaluated in this article, or claim that may be made by its manufacturer, is not guaranteed or endorsed by the publisher.

frontiers in Forests and Global Change

MINI REVIEW
published: 20 September 2021
doi: 10.3389/ffgc.2021.742392

Mycorrhizal Symbiosis for Better Adaptation of Trees to Abiotic Stress Caused by Climate Change in Temperate and Boreal Forests

*Muhammad Usman[1], Tania Ho-Plágaro[1], Hannah E. R. Frank[2], Monica Calvo-Polanco[3], Isabelle Gaillard[1], Kevin Garcia[2] and Sabine D. Zimmermann[1]**

[1] BPMP, CNRS, INRAE, Institut Agro, Université de Montpellier, Montpellier, France, [2] Department of Crop and Soil Sciences, North Carolina State University, Raleigh, NC, United States, [3] Excellence Unit AGRIENVIRONMENT, Agribiotechnology Research Institute, University of Salamanca, Salamanca, Spain

OPEN ACCESS

Edited by:
Raffaella Balestrini, Institute for Sustainable Plant Protection, National Research Council (CNR), Italy

Reviewed by:
Walter Chitarra, Council for Agricultural and Economics Research (CREA), Italy
Antonella Gori, University of Florence, Italy

***Correspondence:**
Sabine D. Zimmermann
sabine.zimmermann@cnrs.fr

Specialty section:
This article was submitted to Forest Ecophysiology, a section of the journal Frontiers in Forests and Global Change

Received: *16 July 2021*
Accepted: *30 August 2021*
Published: *20 September 2021*

Citation:
Usman M, Ho-Plágaro T, Frank HER, Calvo-Polanco M, Gaillard I, Garcia K and Zimmermann SD (2021) Mycorrhizal Symbiosis for Better Adaptation of Trees to Abiotic Stress Caused by Climate Change in Temperate and Boreal Forests. Front. For. Glob. Change 4:742392. doi: 10.3389/ffgc.2021.742392

Global climate changes have serious consequences on natural ecosystems and cause diverse environmental abiotic stressors that negatively affect plant growth and development. Trees are dependent on their symbiosis with mycorrhizal fungi, as the hyphal network significantly improves the uptake of water and essential mineral nutrients by colonized roots. A number of recent studies has enhanced our knowledge on the functions of mycorrhizal associations between fungi and plant roots. Moreover, a series of timely studies have investigated the impact and benefit of root symbioses on the adaptation of plants to climate change-associated stressors. Trees in temperate and boreal forests are increasingly exposed to adverse environmental conditions, thus affecting their durable growth. In this mini-review, we focus our attention on the role mycorrhizal symbioses play in attenuating abiotic stressors imposed on trees facing climatic changes, such as high temperatures, drought, salinity, and flooding.

Keywords: mycorrhizal symbioses, trees, climate change, environmental abiotic stress, high temperature, drought, salinity, flooding

INTRODUCTION

Plant growth and development are dependent on intimate interspecific interactions and co-adaptation between plant species and soil microorganisms, and will be increasingly affected by environmental and climatic changes (van der Putten, 2012; Steidinger et al., 2019; Suz et al., 2021; Van Nuland et al., 2021). Trees, requiring sustained growth in fluctuating environmental conditions, are particularly vulnerable to increasing stress. Functional plant-microbe interactions are determinant drivers for plant adaptation to environmental stressors, among them severe and frequent climate-caused factors (Gehring et al., 2017; Lau et al., 2017). Such increasing abiotic stress conditions include high temperature waves associated with increasing solar radiation (Teskey et al., 2015), intensifying periods of drought (Cook et al., 2018), high levels of salinity (Corwin, 2021), and unpredictable events of flooding (Alfieri et al., 2017; Tabari, 2020; **Figure 1A**). Often, these conditions are tightly connected to poor soils with nutrient shortages. In temperate and boreal forest ecosystems, belowground beneficial interactions with plant roots are dominated by

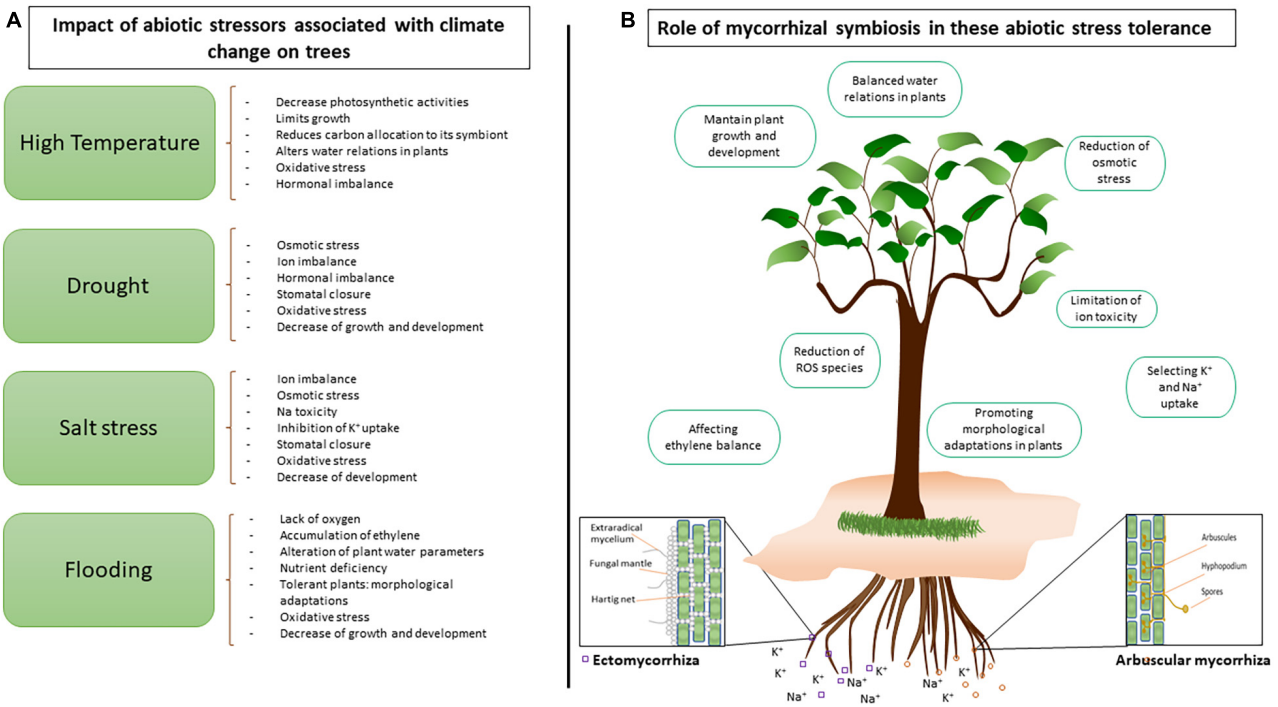

FIGURE 1 | Mycorrhizal fungi alleviate climate change-linked abiotic stress affecting tree growth in temperate and boreal forests. **(A)** Trees are affected by increasing abiotic stress linked to climate change such as high temperatures, drought, salt stress, and flooding. **(B)** However, tree-associated mycorrhizal (ECM, ectomycorrhizal and AM, arbuscular mycorrhizal) fungi improve plant water and mineral nutrition (among them potassium K^+) and help to adapt to stressful environmental conditions (among them elevated sodium Na^+ in saline conditions).

mycorrhizal symbioses. Trees are dependent on mycorrhizal fungi because they rely on the hyphal network, extending the root area of exploration beyond the rhizosphere, to increase the acquisition of essential macro- and microelements and water by colonized roots (Smith and Read, 2010; Becquer et al., 2019; Xu and Zwiazek, 2020).

Aside from the well described contribution to plant nutrition (Garcia et al., 2016, 2020), these root-associated beneficial symbionts are expected to improve the ability of their host trees to adapt to the stressor associated with climate change (Classen et al., 2015; van der Linde et al., 2018). Ectomycorrhizal (ECM) and arbuscular mycorrhizal (AM) fungi are widely associated with trees in natural forests and plantations (**Figure 1B**). ECM fungi, interacting with 60% of all trees (Steidinger et al., 2019) form a fungal sheath around fine roots, thus protecting the plant root and mediating direct interactions with the soil. AM fungi are more present in tropical environments than temperate and boreal forests, but do interact with several tree species, such as poplars (Fang et al., 2020), alders (Kilpeläinen et al., 2019), eucalyptus (Adjoud et al., 1996), or olive trees (Calvo-Polanco et al., 2016).

Herewith, we summarize recent reports on the role mycorrhizal symbioses play in tree growth and survival under increasingly prevalent climate change-driven abiotic stress conditions in temperate and boreal forests. In particular, we focus on publications, mainly from last few years, concerning those stressors that pose the most significant and increasing threat, namely high temperatures, drought, salinity, and flooding.

PLANT TOLERANCE TO ABIOTIC STRESS MEDIATED BY MYCORRHIZAL INTERACTIONS

Global climate change is primarily described by quantification of CO_2 rise causing increase of mean temperatures. Other abiotic stresses, such as drought, salt stress or flooding, are tightly linked and affect plants and associated microorganisms (**Figure 1**). Whether CO_2 rise will affect mycorrhizal tree symbioses in an indirect way by more carbon uptake (Godbold et al., 1997), other consequential stressors deteriorating plant growth might be alleviated by beneficial microbial root associations.

Increasing Temperatures

Frequency and intensity of high temperatures are increasing due to global warming. It can result in irreversible damages for many tree species, altering their growth and production, and sometimes leading to mortality (Teskey et al., 2015). To date, minimal research has explicitly explored the role of mycorrhizal fungi in heat stress alleviation in trees. Indeed, most studies have focused primarily on how increasing temperatures affect tree and fungal populations individually (Deslippe et al., 2011; Morgado et al., 2015; Treseder et al., 2016). However, the impacts of climate change on tree, fungal, and ecosystem health are connected and interdependent, and mycorrhizal fungi can also be directly affected by increasing soil temperatures

(Kipfer et al., 2010; Gavito and Azcón–Aguilar, 2012). Higher temperatures can lower a tree's photosynthetic activity, thereby limiting its growth and reducing carbon allocation to its ECM symbionts (Fernandez et al., 2017). Recently, Song et al. (2015) examined fungal partner changes in reaction to heat stress in two tree species, Douglas fir (*Pseudotsuga menziesii*) and ponderosa pine (*Pinus ponderosae*), and found that defoliation of the former resulted in stress signaling and resource sharing to the latter. In response to defoliation from heat and insect stress, photosynthetic carbon from *P. menziesii* was transferred to *P. ponderosae* plants via shared mycorrhizal networks (Song et al., 2015). Mueller et al. (2019) investigated growth-promoting effects of mature tree mortality on seedlings of pinyon pines and revealed increases in plant growth after mature trees died, and saw no significant loss of seedling establishment. One reason for this could be the inoculum of ECM symbionts provided by the older trees that the seedlings can utilize for acquiring the newly available resources. This indicates the importance of ECM communities in promoting the success of further generations, even as tree life expectancy may be cut short, as well as their role in promoting growth of other species following mortality. On the other hand, this ecosystem service depends on the presence of compatible species, and mortality from increasing temperatures simultaneous with heat-induced fungal community shifts, may threaten this resilience. Indeed, Fernandez et al. (2017) reported fungal taxonomic changes as a result of warming temperatures. An increased reliance on Ascomycetes and fungi that provided optimum benefits as photosynthesis capacity decreased was observed (Fernandez et al., 2017).

From these observations, it seems imperative that more research is conducted to understand how the positive effects conferred by mycorrhizal fungi will help host trees tackle the upcoming climatic variability. In particular: (i) identifying how ECM fungal communities will evolve, (ii) determining which tree-fungus combinations will be better adapted, and (iii) characterizing the underlying molecular mechanisms in both plant and fungi that prevent deleterious effects triggered by rising soil and ambient temperatures, could be promising ways to explore. Indeed, plant and ecosystem health are facing the pressure of changing global temperatures and will continue to do so to a greater extent in coming years. The respective success of each plant and microbial populations is integral in the success of the other, and further research into how ECM and AM fungi alleviate plant stress to climate change could shed light on how these interdependencies may provide ecosystem resilience through temperature increases.

Drought

Drought stress, partly linked to high temperatures, is one of the major abiotic stressors caused by climate change, and contributes to forest decline at a global level (Choat et al., 2012). Soil water deficiencies diminish plant physiological processes, including photosynthesis, enzyme structure, nutrient uptake and transport, and hormone balancing. This results in the triggering of other stressors such as nutritional, osmotic and oxidative stress. At the belowground level, roots have developed a variety of strategies to avoid and tolerate drought conditions, including root biomass adjustments, anatomical alterations and physiological acclimation, and interaction with mycorrhizal fungi.

Different mechanisms have been suggested for the improvement of plant drought tolerance by mycorrhizas. The most obvious direct mechanism to cope with water shortage is the increase of the absorbing surface in the soil through the development and ramification of an extraradical mycelium (Bogeat-Triboulot et al., 2004; Ruth et al., 2011; Zhang et al., 2018). Mycorrhizal fungi improve soil aggregate stability thanks to the structure of the hyphal network which, as part of the soil matrix, directly contributes to the formation and maintenance of soil water-macroaggregates (Ji et al., 2019), providing a better infiltration and storage of water. In the case of AM fungi, another well-identified mechanism that improves soil aggregate stability by carbon sequestration is the release of the glycoprotein glomalin by the fungus acting as soil-superglue (Kumar Singh et al., 2020; Cheng H. Q. et al., 2021).

Mycorrhizal colonization also has the ability to modify the root architecture to both enhance soil aggregate stability and increase the water and nutrient absorbing surface area, especially under drought conditions. For example, several studies in trifoliate orange suggested that mycorrhizal trees possess greater root hair growth to tolerate drought stress (Wu et al., 2016; Zou et al., 2017; Liu et al., 2018; Zhang et al., 2019). ECM fungi are reported to trigger structural changes in the root system of poplar trees by inducing lateral root formation (Felten et al., 2009; Wu et al., 2012). Finally, the modulation of root water transport under drought conditions in mycorrhizal plants has been commonly attributed to the aquaporin-mediated transport, as mycorrhizal colonization has been often shown to affect plant aquaporin gene expression (Calvo-Polanco et al., 2016, 2019; He et al., 2020).

In addition to the increased water uptake, mycorrhizal symbioses can indirectly improve nutrient acquisition under drought (Lehto and Zwiazek, 2011; Ouledali et al., 2018; Behrooz et al., 2019; Boutasknit et al., 2020). This is not only due to the increased absorption area of mycorrhizal roots, but also to factors such as the improved secretion of phosphatase to the soil, either directly by the extraradical hyphae as described for *Rhizophagus clarus* (Sato et al., 2019), or by stimulating the exudation of root phosphatase as observed in mycorrhizal citrus trees (Cheng H. Q. et al., 2021). These mechanisms could stimulate the decomposition and acquisition of organic orthophosphate and might thus partially alleviate the plant responses to drought stress.

Finally, mycorrhizal symbiosis also triggers numerous biochemical and physiological modifications in the plants that enhance plant drought tolerance. For example, some reports exist about the enhanced production of enzymatic (He et al., 2020; Huang et al., 2020) and non-enzymatic (Essahibi et al., 2018) antioxidants in mycorrhizal trees such as carob, trifoliate orange and apple trees under drought conditions. These enzymes and compounds may decrease the oxidative damage in the structure of carbohydrates, lipids, proteins, and DNA that result from

prolonged drought exposure. It has also been suggested that mycorrhizal symbiosis has the potential to lower the osmotic damage through the accumulation of soluble sugars and proline (Yin et al., 2018; Behrooz et al., 2019; Boutasknit et al., 2020; Huang et al., 2020; Wang et al., 2021). Similarly, the water-use efficiency is in most cases improved in colonized plants, as observed in AM poplar and in ECM pine and oak trees exposed to drought (Li L. et al., 2021; Li M. et al., 2021; Li Y. et al., 2021). This could be related to a better modulation of stomata closure and abscisic acid concentration and signaling (Wang et al., 2017; Ouledali et al., 2018; Chen et al., 2020).

Salt Stress

Climate change-associated salinity stress causes land degradation, decreased crop yields, and afforestation, thus severely impacting the global economy (Leisner, 2020; Zandalinas et al., 2021). In addition, due to deep changes in environmental conditions and the expansion of irrigated land (>20% worldwide), the negative impact of salinity is considerably increasing and will continue to do so (Yuan et al., 2016). Excessive sodium (Na^+) in soil competes for potassium (K^+) uptake by plant roots due to ion similarity (Liang et al., 2018; Wu, 2018). Moreover, within the cytoplasm, Na^+ has toxic effects on cellular functions and enzyme activation. Several endangered tree species (Bothe et al., 2010) evolved adaptations (Kijowska-Oberc et al., 2020), such as the exclusion or accumulation of the excess of Na^+ within the different plant tissues (Ottow et al., 2005; Thiem et al., 2018), the control of transpiration (Negrão et al., 2017), or the increase of vessel frequencies (Janz et al., 2012).

Although many plant species have evolved salt tolerance mechanisms, interaction with soil microorganisms, and particularly mycorrhizal fungi, can greatly improve plant growth and development under saline conditions (Weissenhorn, 2002; Yi et al., 2008; Yang et al., 2014; Hrynkiewicz et al., 2015; Zwiazek et al., 2019; Klinsukon et al., 2021). Improved water (Lee et al., 2010) and nutrient (Li et al., 2012) uptake, as well as the exclusion of Na^+ from roots and, consequently, shoots by mycorrhizal fungi are mechanisms that have been proposed to contribute to salt stress tolerance in colonized trees (Guerrero-Galán et al., 2019).

Improved acquisition of K^+ as an essential macroelement by AM and ECM fungi (Garcia and Zimmermann, 2014; Frank and Garcia, 2021) helps maintain a desirable K^+/Na^+ ratio. By contrast, the mobilization of Na^+ and chloride (Cl^-) by plant roots was attenuated by the presence of mycorrhizal fungi, particularly under salt stress (Giri et al., 2007; Calvo-Polanco et al., 2008; Hrynkiewicz et al., 2015; Garcia et al., 2017; Hashem et al., 2018; Abdelhamid et al., 2019). To elude the translocation of excessive Na^+ in photosynthetic organs, plants have adopted mechanisms to store Na^+ in intraradical mycelium or in root cell vacuoles (Acosta-Motos et al., 2020). Moreover, defense mechanisms using antioxidant enzymes in plants might be improved by AM symbiosis lifting up their activities to mitigate salt stress, like catalase, peroxidase, glutathione reductase, superoxide dismutase, and ascorbate peroxidase. Ait-El-Mokhtar et al. (2019) demonstrated this mechanism when *Phoenix dactylifera* L. was colonized by AM fungi in salt stress conditions. Improvement of physiological plant parameters by AM and ECM symbioses has been shown by several studies in recent years, however, mechanisms have been discussed mainly for AM symbioses in non-woody plants (Porcel et al., 2012; Evelin et al., 2019). In trees, Behmanesh et al. (2019) reported that pistachio seedlings (*Pistacia vera* L.) inoculated by *Rhizophagus irregularis* (formerly *Glomus intraradices*) and *Glomus mosseae* displayed improved vegetative growth, chlorophyll contents, and less deposition of Na^+ in shoots as compared to non-inoculated seedlings. Similar findings were reported by Frosi et al. (2018), when *Cenostigma pyramidale* was inoculated with AM fungi *Acaulospora longula* and *Claroideoglomus etunicatum*. Increases in shoot dry weight and chlorophyll contents, and less accumulation of Na^+ and Cl^- in photosynthetic organs were reported. Salt tolerance of almond rootstocks was increased by the AM fungi *R. intraradices* and *Funneliformis mosseae* through the improvement of diverse physiological parameters like chlorophyll, soluble sugars and proline content, osmotic parameters, and increased activity of antioxidant enzymes (Shahvali et al., 2020).

Likewise, several studies have shown improved salt tolerance in ECM trees as in white spruce in association with *Hebeloma crustuliniforme* (Muhsin and Zwiazek, 2002). When *Coccoloba uvifera* L., inoculated by *Scleroderma bermudense*, was grown in up to 500 mM of salt, the plants exhibited improved growth, water uptake, and shoot phosphorus and K^+ concentrations, while the upward movement of Na^+ and Cl^- ions was limited in comparison to non-inoculated plants (Bandou et al., 2006). Improved ECM-driven uptake of essential nutrients along with water was observed in poplar roots colonized by *Paxillus involutus* under saline conditions (Luo et al., 2011). Involvement of aquaporin-mediated water transport was shown in jack pine in association with *Suillus tomentosus* (Lee et al., 2010). A recent study revealing improved growth of *Alnus glutinosa* when inoculated by the ECM strain *P. involutus* OW-5 under saline conditions, showed proline accumulation in plant tissues that acts as an endogenous osmotic regulator to tolerate salt stress effects (Thiem et al., 2020).

Altogether, mechanisms behind plant salt tolerance in AM and ECM symbiosis are rather complex, including several direct and indirect effects, and need further studies.

Flooding

Extreme precipitation and floods are expected to intensify due to climate change (Alfieri et al., 2017; Tabari, 2020), with consequences in the structure, function and production of forest ecosystems, and their interactions with soil microorganisms (Barnes et al., 2018). The adaptation of plants to flooding is dependent on the accumulation of ethylene within the plant tissues (Reynoso et al., 2019). In the most tolerant species, plants display extensive morphological modifications, such as the formation of aerenchyma (Sou et al., 2021) and adventitious roots, the reduction of the endodermis (Calvo-Polanco et al., 2012; Voesenek and Bailey-Serres, 2015), and the formation of hypertrophied lenticels (Fougnies et al., 2007).

In addition to these plant adaptations, the associated microbiome is crucial. The tolerance of mycorrhizal fungal species to flooding varies according to their host tree species and the severity and length of the stress (Lodge, 1989; Yang et al., 2016; Barnes et al., 2018; Johnson, 2018). In general, AM fungi are believed to be more present in waterlogged environments than ECM fungi, as they have been shown to survive anaerobic conditions due to the presence of well-developed aerenchyma in the roots (Wang et al., 2010). However, recent studies have determined that ECM also display a certain degree of resilience dependent on the species (Cho et al., 2021). Differences between hydrophobic and hydrophilic ECM fungi have been observed (Barnes et al., 2018), and several fungal species recovered after long periods of waterlogged field conditions (Thomas, 2021), as was shown for *Thelephora terrestris*, *Laccaria laccata*, and *H. crustuliniforme* (Stenström, 1991).

The few studies on AM trees under flood conditions are related to improving growth and development (e.g., citrus, peach, or trifoliate orange trees) by acting on the phosphorus and nitrogen acquisition (Neto et al., 2006; Fougnies et al., 2007; Wu et al., 2012; Zou et al., 2014; Zheng et al., 2020) and on the expression of aquaporins (Cheng X. F. et al., 2021). Even that it is commonly known that ethylene accumulation within the plant tissues is one of the main responses of plants to waterlogged conditions, this information on mycorrhizal trees is largely lacking. Only one study reported for mycorrhizal tomato plants showed that AM fungi reduced root ethylene concentrations, while improving their water status through the action of fungal and tomato aquaporins and the regulation of ACC synthase and oxidase genes (Calvo-Polanco et al., 2014).

In conclusion, there is immense potential to improve our knowledge on how mycorrhizal fungi help trees to cope with flooding events, and their effect in the main mechanism of ethylene regulation for the initial sensing of flood, that involves the oxygen-dependent degradation of group VII Ethylene Response Factor transcription factors and Plant Cysteine Oxidase enzymes (van Dongen and Licausi, 2015). This information will contribute to the development of new technologies and management procedures to overcome flood stress in agricultural and forestry settings.

CONCLUSION

Overall, mycorrhizal fungi have the potential to conserve and restore temperate and boreal forest ecosystems and to maintain sustainable forestry crops under stress due to global changes (Bothe et al., 2010; Field et al., 2020; Li et al., 2020). Numerous studies have shown improved tolerance of mycorrhizal trees to numerous abiotic stresses, such as high temperatures, drought, high salinity, and flooding (**Figure 1**). In general, the identified mechanisms are similar to those ones found in non-woody plants. However, we need to consider that most of these experiments have been performed with tree seedlings grown in pots under controlled conditions, so further research is required to unravel the underlying mechanisms in natural environments and in mature trees. The influence of natural soil microbiome interactions on complex ecosystem functioning linked to conditions of climate change has been recently analyzed taking growth and foliar development of a tree species (*Populus angustifolia*) as a model (Van Nuland et al., 2021). Moreover, microbiome manipulation experiments in forest conditions (e.g., adding inoculum of adapted species isolated from not stressed forest environments) could be feasible and bring further insight.

One of the most outstanding particularities of large trees is that they possess a root system that penetrates several meters into the ground. Although mycorrhizas have been commonly described to be mostly concentrated in the top layer of the soil, some reports show that they are also present several meters underground (de Araujo Pereira et al., 2018; Robin et al., 2019). With this respect, further research is required to unravel other relevant roles of mycorrhizas in deeper soil horizons and in large trees, probably more related with ecosystem services, such as carbon storage, that may also help trees to cope with environmental stresses.

Clear evidence exists to consider local beneficial mycorrhizal fungi as an environmentally friendly tool with a high potential to protect trees, from both forest and sustainable agricultural systems, against environmental stressors that will only increase in intensity and frequency due to global climate change. Although our review is focused on the negative effects of climate change on trees, it is worth mentioning that the mycorrhizal fungi decline occurring nowadays might be also linked to climate change (Bennett and Classen, 2020). However, it is unclear if mycorrhizal populations are directly affected by climate change-derived stresses or if, by contrast, they are negatively affected by a lower performance of trees exposed to stresses (Sapsford et al., 2017). Thus, further research is required to decipher the links between trees and mycorrhizal fungi under stress conditions in a climate change scenario in order to design good strategies aimed at supporting the health of both partners, trees and mycorrhizal fungi.

AUTHOR CONTRIBUTIONS

MU, TH-P, HERF, MC-P, KG, and SDZ wrote the manuscript. MC-P, IG, KG, and SDZ revised and supervised this work. All authors contributed to the article and approved the submitted version.

FUNDING

SDZ and TH-P are supported by the French ANR project "MYCOTRANS" (AAP Générique 2019 PRC N° 193112). MU is financially supported by a Ph.D. fellowship from the Pakistan Higher Education Commission. MC-P acknowledges the support from FEDER-Junta de Castilla y León, Escalera de Excelencia (RIS3; CLU-2018-04). KG and HERF acknowledge support by the AFRI program (grant no. 2020-67013-31800) from the USDA National Institute of Food and Agriculture, the North Carolina Soybean Producers Association (2019–1656), and the North Carolina Agriculture Research Service (NCARS). The funders had no role in the decision to publish or in the preparation of the manuscript.

ACKNOWLEDGMENTS

We thank the whole research community contributing to the field and we apologize for further publications that we could have overlooked or are not included for space limitations. Contribution to research projects of former Ph.D. students Carmen Guerrero-Galán and Gabriella Houdinet is acknowledged.

REFERENCES

Abdelhamid, M. T., El-Masry, R. R., Darwish, D. S., Abdalla, M. M., Oba, S., and Ragab, R. (2019). "The mechanisms involved in improving the tolerance of plants to salt stress using arbuscular mycorrhizal fungi," in *Microorganisms in Saline Environments: Strategies and Functions*, eds B. Giri and A. Varma (Berlin: Springer), 303–327. doi: 10.1007/978-3-030-18975-4_13

Acosta-Motos, J. R., Penella, C., Hernández, J. A., Díaz-Vivancos, P., Sánchez-Blanco, M. J., Navarro, J. M., et al. (2020). Towards a sustainable agriculture: strategies involving phytoprotectants against salt stress. *Agronomy* 10:194. doi: 10.3390/agronomy10020194

Adjoud, D., Plenchette, C., Halli-Hargas, R., and Lapeyrie, F. (1996). Response of 11 eucalyptus species to inoculation with three arbuscular mycorrhizal fungi. *Mycorrhiza* 6, 129–135. doi: 10.1007/s005720050117

Ait-El-Mokhtar, M., Laouane, R. B., Anli, M., Boutasknit, A., Wahbi, S., and Meddich, A. (2019). Use of mycorrhizal fungi in improving tolerance of the date palm (*Phoenix dactylifera* L.) seedlings to salt stress. *Sci. Hortic.* 253, 429–438. doi: 10.1016/j.scienta.2019.04.066

Alfieri, L., Bisselink, B., Dottori, F., Naumann, G., de Roo, A., Salamon, P., et al. (2017). Global projections of river flood risk in a warmer world. *Earths Future* 5, 171–182. doi: 10.1002/2016EF000485

Bandou, E., Lebailly, F., Muller, F., Dulormne, M., Toribio, A., Chabrol, J., et al. (2006). The ectomycorrhizal fungus Scleroderma bermudense alleviates salt stress in seagrape (*Coccoloba uvifera* L.) seedlings. *Mycorrhiza* 16, 559–565. doi: 10.1007/s00572-006-0073-6

Barnes, C. J., van der Gast, C. J., McNamara, N. P., Rowe, R., and Bending, G. D. (2018). Extreme rainfall affects assembly of the root-associated fungal community. *New Phytol.* 220, 1172–1184. doi: 10.1111/nph.14990

Becquer, A., Guerrero-Galán, C., Eibensteiner, J. L., Houdinet, G., Bücking, H., Zimmermann, S. D., et al. (2019). The ectomycorrhizal contribution to tree nutrition. *Adv. Bot. Res.* 89, 77–126. doi: 10.1016/bs.abr.2018.11.003

Behmanesh, Z., Alaei, H., Mohammadi, A. H., and Dashti, H. (2019). Effect of arbuscular mycorrhizas *Glomus intraradices* and *Glomus mosseae* on pistachio root rot caused by Phytophthora under salinity stress. *Iran. J. Plant Protect. Sci.* 50, 197–212.

Behrooz, A., Vahdati, K., Rejali, F., Lotfi, M., Sarikhani, S., and Leslie, C. (2019). Arbuscular mycorrhiza and plant growth-promoting bacteria alleviate drought stress in walnut. *HortScience* 54, 1087–1092. doi: 10.21273/HORTSCI13961-19

Bennett, A. E., and Classen, A. T. (2020). Climate change influences mycorrhizal fungal–plant interactions, but conclusions are limited by geographical study bias. *Ecology* 101:e02978. doi: 10.1002/ecy.2978

Bogeat-Triboulot, M.-B., Bartoli, F., Garbaye, J., Marmeisse, R., and Tagu, D. (2004). Fungal ectomycorrhizal community and drought affect root hydraulic properties and soil adherence to roots of *Pinus pinaster* seedlings. *Plant Soil* 267, 213–223. doi: 10.1007/s11104-005-5349-7

Bothe, H., Turnau, K., and Regvar, M. (2010). The potential role of arbuscular mycorrhizal fungi in protecting endangered plants and habitats. *Mycorrhiza* 20, 445–457. doi: 10.1007/s00572-010-0332-4

Boutasknit, A., Baslam, M., Ait-El-Mokhtar, M., Anli, M., Ben-Laouane, R., Douira, A., et al. (2020). Arbuscular mycorrhizal fungi mediate drought tolerance and recovery in two contrasting carob (Ceratonia siliqua L.) ecotypes by regulating stomatal, water relations, and (in) organic adjustments. *Plants* 9:80. doi: 10.3390/plants9010080

Calvo-Polanco, M., Armada, E., Zamarreño, A. M., García-Mina, J. M., and Aroca, R. (2019). Local root ABA/cytokinin status and aquaporins regulate poplar responses to mild drought stress independently of the ectomycorrhizal fungus *Laccaria bicolor*. *J. Exp. Bot.* 70, 6437–6446. doi: 10.1093/jxb/erz389

Calvo-Polanco, M., Molina, S., Zamarreño, A. M., García-Mina, J. M., and Aroca, R. (2014). The symbiosis with the arbuscular mycorrhizal fungus *Rhizophagus irregularis* drives root water transport in flooded tomato plants. *Plant Cell Physiol.* 55, 1017–1029. doi: 10.1093/pcp/pcu035

Calvo-Polanco, M., Sánchez-Castro, I., Cantos, M., García, J. L., Azcón, R., Ruiz-Lozano, J. M., et al. (2016). Effects of different arbuscular mycorrhizal fungal backgrounds and soils on olive plants growth and water relation properties under well–watered and drought conditions. *Plant Cell Environ.* 39, 2498–2514. doi: 10.1111/pce.12807

Calvo-Polanco, M., Señorans, J., and Zwiazek, J. J. (2012). Role of adventitious roots in water relations of tamarack (*Larix laricina*) seedlings exposed to flooding. *BMC Plant Biol.* 12:99. doi: 10.1186/1471-2229-12-99

Calvo-Polanco, M., Zwiazek, J. J., and Voicu, M. C. (2008). Responses of ectomycorrhizal American elm (*Ulmus americana*) seedlings to salinity and soil compaction. *Plant Soil* 308, 189–200. doi: 10.1007/s11104-008-9619-z

Chen, W., Meng, P., Feng, H., and Wang, C. (2020). Effects of arbuscular mycorrhizal fungi on growth and physiological performance of *Catalpa bungei* CA Mey. under drought stress. *Forests* 11:1117. doi: 10.3390/f11101117

Cheng, H. Q., Giri, B., Wu, Q. S., Zou, Y. N., and Kuča, K. (2021). Arbuscular mycorrhizal fungi mitigate drought stress in citrus by modulating root microenvironment. *Arch. Agron. Soil Sci.* [Epub ahead of print]. doi: 10.1080/03650340.2021.1878497

Cheng, X.-F., Wu, H.-H., Zou, Y.-N., Wu, Q.-S., and Kuča, K. (2021). Mycorrhizal response strategies of trifoliate orange under well-watered, salt stress, and waterlogging stress by regulating leaf aquaporin expression. *Plant Physiol. Biochem.* 162, 27–35. doi: 10.1016/j.plaphy.2021.02.026

Cho, Y., Shinnam, Y., Park, M. S., Kim, J. S., Kim, C. S., and Lim, Y. W. (2021). Ectomycorrhizal fungi associated with *Pinus densiflora* seedlings under flooding stress. *Sustainability* 13:4367. doi: 10.3390/su13084367

Choat, B., Jansen, S., Brodribb, T. J., Cochard, H., Delzon, S., Bhaskar, R., et al. (2012). Global convergence in the vulnerability of forests to drought. *Nature* 491, 752–755. doi: 10.1038/nature11688

Classen, A. T., Sundqvist, M. K., Henning, J. A., Newman, G. S., Moore, J. A., Cregger, M. A., et al. (2015). Direct and indirect effects of climate change on soil microbial and soil microbial-plant interactions: what lies ahead? *Ecosphere* 6, 1–21. doi: 10.1890/ES15-00217.1

Cook, B. I., Mankin, J. S., and Anchukaitis, K. J. (2018). Climate change and drought: from past to future. *Curr. Clim. Change Rep.* 4, 164–179. doi: 10.1007/s40641-018-0093-2

Corwin, D. L. (2021). Climate change impacts on soil salinity in agricultural areas. *Eur. J. Soil Sci.* 72, 842–862. doi: 10.1111/ejss.13010

de Araujo Pereira, A. P., Santana, M. C., Bonfim, J. A., de Lourdes Mescolotti, D., and Cardoso, E. J. B. N. (2018). Digging deeper to study the distribution of mycorrhizal arbuscular fungi along the soil profile in pure and mixed *Eucalyptus grandis* and *Acacia mangium* plantations. *Appl. Soil Ecol.* 128, 1–11. doi: 10.1016/j.apsoil.2018.03.015

Deslippe, J. R., Hartmann, M., Mohn, W. W., and Simard, S. W. (2011). Long–term experimental manipulation of climate alters the ectomycorrhizal community of *Betula nana* in *Arctic tundra*. *Glob. Change Biol.* 17, 1625–1636. doi: 10.1111/j.1365-2486.2010.02318.x

Essahibi, A., Benhiba, L., Babram, M. A., Ghoulam, C., and Qaddoury, A. (2018). Influence of arbuscular mycorrhizal fungi on the functional mechanisms associated with drought tolerance in carob (*Ceratonia siliqua* L.). *Trees* 32, 87–97. doi: 10.1007/s00468-017-1613-8

Evelin, H., Devi, T. S., Gupta, S., and Kapoor, R. (2019). Mitigation of salinity stress in plants by arbuscular mycorrhizal symbiosis: current understanding and new challenges. *Front. Plant Sci.* 10:470. doi: 10.3389/fpls.2019.00470

Fang, F., Wang, C., Wu, F., Tang, M., and Doughty, R. (2020). Arbuscular mycorrhizal fungi mitigate nitrogen leaching under poplar seedlings. *Forests* 11:325. doi: 10.3390/f11030325

Felten, J., Kohler, A., Morin, E., Bhalerao, R. P., Palme, K., Martin, F., et al. (2009). The ectomycorrhizal fungus *Laccaria bicolor* stimulates lateral root formation in poplar and *Arabidopsis* through auxin transport and signaling. *Plant Physiol.* 151, 1991–2005. doi: 10.1104/pp.109.147231

Fernandez, C. W., Nguyen, N. H., Stefanski, A., Han, Y., Hobbie, S. E., Montgomery, R. A., et al. (2017). Ectomycorrhizal fungal response to warming is linked to poor host performance at the boreal–temperate ecotone. *Glob. Change Biol.* 23, 1598–1609. doi: 10.1111/gcb.13510

Field, K. J., Daniell, T., Johnson, D., and Helgason, T. (2020). Mycorrhizas for a changing world: sustainability, conservation, and society. *Plants People Planet* 2, 98–103. doi: 10.1002/ppp3.10092

Fougnies, L., Renciot, S., Muller, F., Plenchette, C., Prin, Y., de Faria, S. M., et al. (2007). *Arbuscular mycorrhizal* colonization and nodulation improve flooding tolerance in *Pterocarpus officinalis* Jacq. seedlings. *Mycorrhiza* 17, 159–166. doi: 10.1007/s00572-006-0085-2

Frank, H. E. R., and Garcia, K. (2021). Benefits provided by four ectomycorrhizal fungi to *Pinus taeda* under different external potassium availabilities. *Mycorrhiza*. doi: 10.1007/s00572-021-01048-z

Frosi, G., Barros, V. A., Oliveira, M. T., Santos, M., Ramos, D. G., Maia, L. C., et al. (2018). *Arbuscular mycorrhizal* fungi and foliar phosphorus inorganic supply alleviate salt stress effects in physiological attributes, but only arbuscular mycorrhizal fungi increase biomass in woody species of a semiarid environment. *Tree Physiol.* 38, 25–36. doi: 10.1093/treephys/tpx105

Garcia, K., Bücking, H., and Zimmermann, S. D. (2020). Editorial: importance of root symbiomes for plant nutrition: new insights, perspectives, and future challenges. *Front. Plant Sci.* 11:594. doi: 10.3389/fpls.2020.00594

Garcia, K., Chasman, D., Roy, S., and Ané, J. M. (2017). Physiological responses and gene co-expression network of mycorrhizal roots under K+ deprivation. *Plant Physiol.* 173, 1811–1823. doi: 10.1104/pp.16.01959

Garcia, K., Doidy, J., Zimmermann, S. D., Wipf, D., and Courty, P.-E. (2016). Take a trip through the plant and fungal transportome of mycorrhiza. *Trends Plant Sci.* 21, 937–950. doi: 10.1016/j.tplants.2016.07.010

Garcia, K., and Zimmermann, S. D. (2014). The role of mycorrhizal associations in plant potassium nutrition. *Front. Plant Sci.* 5:337. doi: 10.3389/fpls.2014.00337

Gavito, M. E., and Azcón–Aguilar, C. (2012). Temperature stress in arbuscular mycorrhizal fungi: a test for adaptation to soil temperature in three isolates of *Funneliformis mosseae* from different climates. *Agric. Food Sci.* 21, 2–11. doi: 10.23986/afsci.4994

Gehring, C. A., Sthultz, C. M., Flores-Rentería, L., Whipple, A. V., and Whitham, T. G. (2017). Tree genetics defines fungal partner communities that may confer drought tolerance. *Proc. Nat. Acad. Sci. U.S.A.* 114, 11169–11174. doi: 10.1073/pnas.1704022114

Giri, B., Kapoor, R., and Mukerji, K. G. (2007). Improved tolerance of *Acacia nilotica* to salt stress by *Arbuscular mycorrhiza*, *Glomus fasciculatum* may be partly related to elevated K/Na ratios in root and shoot tissues. *Microb. Ecol.* 54, 753–760. doi: 10.1007/s00248-007-9239-9

Godbold, D. L., Berntson, G. M., and Bazzaz, F. A. (1997). Growth and mycorrhizal colonization of three North American tree species under elevated atmospheric CO2. *New Phytol.* 137, 433–440. doi: 10.1046/j.1469-8137.1997.00842.x

Guerrero-Galán, C., Calvo-Polanco, M., and Zimmermann, S. D. (2019). Ectomycorrhizal symbiosis helps plants to challenge salt stress conditions. *Mycorrhiza* 29, 291–301. doi: 10.1007/s00572-019-00894-2

Hashem, A., Abd-Allah, E. F., Alqarawi, A. A., and Egamberdieva, D. (2018). "Arbuscular mycorrhizal fungi and plant stress tolerance," in *Plant Microbiome: Stress Response, Microorganisms for Sustainability*, eds D. Egamberdieva and P. Ahmad (Berlin: Springer), 81–103. doi: 10.1007/978-981-10-5514-0_4

He, J. D., Zou, Y. N., Wu, Q. S., and Kuča, K. (2020). Mycorrhizas enhance drought tolerance of trifoliate orange by enhancing activities and gene expression of antioxidant enzymes. *Sci. Hortic.* 262:108745. doi: 10.1016/j.scienta.2019.108745

Hrynkiewicz, K., Szymańska, S., Piernik, A., and Thiem, D. (2015). Ectomycorrhizal community structure of Salix and *Betula* spp. at a saline site in central Poland in relation to the seasons and soil parameters. *Water Air Soil Pollut.* 226, 1–15. doi: 10.1007/s11270-015-2308-7

Huang, D., Ma, M., Wang, Q., Zhang, M., Jing, G., Li, C., et al. (2020). Arbuscular mycorrhizal fungi enhanced drought resistance in apple by regulating genes in the MAPK pathway. *Plant Physiol. Biochem.* 149, 245–255. doi: 10.1016/j.plaphy.2020.02.020

Janz, D., Lautner, S., Wildhagen, H., Behnke, K., Schnitzler, J. P., Rennenberg, H., et al. (2012). Salt stress induces the formation of a novel type of 'pressure wood' in two Populus species. *New Phytol.* 194, 129–141. doi: 10.1111/j.1469-8137.2011.03975.x

Ji, L., Tan, W., and Chen, X. (2019). Arbuscular mycorrhizal mycelial networks and glomalin-related soil protein increase soil aggregation in Calcaric Regosol under well-watered and drought stress conditions. *Soil Tillage Res.* 185, 1–8. doi: 10.1016/j.still.2018.08.010

Johnson, D. (2018). Water, water everywhere…but how does it affect the functional diversity of ectomycorrhizal fungi? *New Phytol.* 220, 950–951. doi: 10.1111/nph.15086

Kijowska-Oberc, J., Staszak, A. M., Kamiński, J., and Ratajczak, E. (2020). Adaptation of forest trees to rapidly changing climate. *Forests* 11:123. doi: 10.3390/f11020123

Kilpeläinen, J., Barbero-López, A., Adamczyk, B., Aphalo, P. J., and Lehto, T. (2019). Morphological and ecophysiological root and leaf traits in ectomycorrhizal, arbuscular-mycorrhizal and non-mycorrhizal *Alnus incana* seedlings. *Plant Soil* 436, 283–297. doi: 10.1007/s11104-018-03922-w

Kipfer, T., Egli, S., Ghazoul, J., Moser, B., and Wohlgemuth, T. (2010). Susceptibility of ectomycorrhizal fungi to soil heating. *Fungal Biol.* 114, 467–472. doi: 10.1016/j.funbio.2010.03.008

Klinsukon, C., Lumyong, S., Kuyper, T. W., and Boonlue, S. (2021). Colonization by arbuscular mycorrhizal fungi improves salinity tolerance of eucalyptus (*Eucalyptus camaldulensis*) seedlings. *Sci. Rep.* 11:4362. doi: 10.1038/s41598-021-84002-5

Kumar Singh, A., Zhu, X., Chen, C., Wu, J., Yang, B., Zakari, S., et al. (2020). The role of glomalin in mitigation of multiple soil degradation problems. *Crit. Rev. Env. Sci. Technol.* doi: 10.1080/10643389.2020.1862561 [Epub ahead of print].

Lau, J. A., Lennon, J. T., and Heath, K. D. (2017). Trees harness the power of microbes to survive climate change. *Proc. Nat. Acad. Sci. U.S.A.* 114, 11009–11011. doi: 10.1073/pnas.1715417114

Lee, S. H., Calvo-Polanco, M., Chung, G. C., and Zwiazek, J. J. (2010). Role of aquaporins in root water transport of ectomycorrhizal jack pine (*Pinus banksiana*) seedlings exposed to NaCl and fluoride. *Plant Cell Environ.* 33, 769–780. doi: 10.1111/j.1365-3040.2009.02103.x

Lehto, T., and Zwiazek, J. J. (2011). Ectomycorrhizas and water relations of trees: a review. *Mycorrhiza* 21, 71–90. doi: 10.1007/s00572-010-0348-9

Leisner, C. P. (2020). Climate change impacts on food security-focus on perennial cropping systems and nutritional value. *Plant Sci.* 293:110412. doi: 10.1016/j.plantsci.2020.110412

Li, J., Bao, S., Zhang, Y., Ma, X., Mishra-Knyrim, M., Sun, J., et al. (2012). Paxillus involutus strains MAJ and NAU mediate K+/Na+ homeostasis in ectomycorrhizal Populus × canescens under sodium chloride stress. *Plant Physiol.* 159, 1771–1786. doi: 10.1104/pp.112.195370

Li, L., Zhang, H., Tang, M., and Chen, H. (2021). Nutrient uptake and distribution in mycorrhizal cuttings of *Populus× canadensis* 'Neva' under drought stress. *J. Soil Sci. Plant Nutr.* doi: 10.1007/s42729-021-00523-y [EPub ahead of print].

Li, M., Wang, H., Zhao, X., Lu, Z., Sun, X., and Ding, G. (2021). Role of *Suillus placidus* in improving the drought tolerance of Masson pine (*Pinus massoniana* Lamb.) seedlings. *Forests* 12:332. doi: 10.3390/f12030332

Li, Y., Zhang, T., Zhou, Y., Zou, X., Yin, Y., Li, H., et al. (2021). Ectomycorrhizal symbioses increase soil calcium availability and water use efficiency of *Quercus acutissima* seedlings under drought stress. *Eur. J. For. Res.* doi: 10.1007/s10342-021-01383-y [Epub ahead of print].

Li, Z., Wu, N., Meng, S., Wu, F., and Liu, T. (2020). Arbuscular mycorrhizal fungi (AMF) enhance the tolerance of *Euonymus maackii* Rupr. at a moderate level of salinity. *PLoS One* 15:e0231497. doi: 10.1371/journal.pone.0231497

Liang, W. J., Ma, X. L., Wan, P., and Liu, L. Y. (2018). Plant salt-tolerance mechanism: a review. *Biochem. Biophys. Res. Comm.* 495, 286–291. doi: 10.1016/j.bbrc.2017.11.043

Liu, C. Y., Zhang, F., Zhang, D. J., Srivastava, A., Wu, Q. S., and Zou, Y. N. (2018). Mycorrhiza stimulates root-hair growth and IAA synthesis and transport in trifoliate orange under drought stress. *Sci. Rep.* 8, 1–9. doi: 10.1038/s41598-018-20456-4

Lodge, D. (1989). The influence of soil moisture and flooding on formation of VA-endo-and ectomycorrhizae in Populus and Salix. *Plant Soil* 117, 243–253. doi: 10.1007/BF02220718

Luo, Z. B., Li, K., Gai, Y., Göbel, C., Wildhagen, H., Jiang, X., et al. (2011). The ectomycorrhizal fungus (*Paxillus involutus*) modulates leaf physiology of poplar towards improved salt tolerance. *Environ. Exp. Bot.* 72, 304–311. doi: 10.1016/j.envexpbot.2011.04.008

Morgado, L. N., Semenova, T. A., Welker, J. M., Walker, M. D., Smets, E., and Geml, J. (2015). Summer temperature increase has distinct effects on the ectomycorrhizal fungal communities of moist tussock and dry tundra in Arctic Alaska. *Glob. Change Biol.* 21, 959–972. doi: 10.1111/gcb.12716

Mueller, R. C., Scudder, C. M., Whitham, T. G., and Gehring, C. A. (2019). Legacy effects of tree mortality mediated by ectomycorrhizal fungal communities. *New Phytol.* 224, 155–165. doi: 10.1111/nph.15993

Muhsin, T. M., and Zwiazek, J. J. (2002). Colonization with *Hebeloma crustuliniforme* increases water conductance and limits shoot sodium uptake in white spruce (*Picea glauca*) seedlings. *Plant Soil* 238, 217–225. doi: 10.1023/A:1014435407735

Negrão, S., Schmöckel, S. M., and Tester, M. (2017). Evaluating physiological responses of plants to salinity stress. *Ann. Bot.* 119, 1–11. doi: 10.1093/aob/mcw191

Neto, D., Carvalho, L. M., Cruz, C., and Martins-Loucao, M. A. (2006). How do mycorrhizas affect C and N relationships in flooded *Aster tripolium* plants? *Plant Soil* 279, 51–63. doi: 10.1007/s11104-005-6333-y

Ottow, E. A., Brinker, M., Teichmann, T., Fritz, E., Kaiser, W., Brosché, M., et al. (2005). Populus euphratica displays apoplastic sodium accumulation, osmotic adjustment by decreases in calcium and soluble carbohydrates, and develops leaf succulence under salt stress. *Plant Physiol.* 139, 1762–1772. doi: 10.1104/pp.105.069971

Ouledali, S., Ennajeh, M., Zrig, A., Gianinazzi, S., and Khemira, H. (2018). Estimating the contribution of arbuscular mycorrhizal fungi to drought tolerance of potted olive trees (*Olea europaea*). *Acta Physiol. Plant.* 40, 1–13. doi: 10.1007/s11738-018-2656-1

Porcel, R., Aroca, R., and Ruiz-Lozano, J. M. (2012). Salinity stress alleviation using arbuscular mycorrhizal fungi. A review. *Agron. Sust. Dev.* 32, 181–200. doi: 10.1007/s13593-011-0029-x

Reynoso, M. A., Kajala, K., Bajic, M., West, D. A., Pauluzzi, G., Yao, A. I., et al. (2019). Evolutionary flexibility in flooding response circuitry in angiosperms. *Science* 20, 1291–1295. doi: 10.1126/science.aax8862

Robin, A., Pradier, C., Sanguin, H., Mahé, F., Lambais, G. R., de Araujo Pereira, A. P., et al. (2019). How deep can ectomycorrhizas go? A case study on *Pisolithus* down to 4 meters in a Brazilian eucalypt plantation. *Mycorrhiza* 29, 637–648. doi: 10.1007/s00572-019-00917-y

Ruth, B., Khalvati, M., and Schmidhalter, U. (2011). Quantification of mycorrhizal water uptake via high-resolution on-line water content sensors. *Plant Soil* 342, 459–468. doi: 10.1007/s11104-010-0709-3

Sapsford, S. J., Paap, T., Hardy, G. E. S. J., and Burgess, T. I. (2017). The 'chicken or the egg': which comes first, forest tree decline or loss of mycorrhizae? *Plant Ecol.* 218, 1093–1106. doi: 10.1007/s11258-017-0754-6

Sato, T., Hachiya, S., Inamura, N., Ezawa, T., Cheng, W., and Tawaraya, K. (2019). Secretion of acid phosphatase from extraradical hyphae of the arbuscular mycorrhizal fungus Rhizophagus clarus is regulated in response to phosphate availability. *Mycorrhiza* 29, 599–605. doi: 10.1007/s00572-019-00923-0

Shahvali, R., Shiran, B., Ravash, R., Fallahi, H., and Banović Đeri, B. (2020). Effect of symbiosis with arbuscular mycorrhizal fungi on salt stress tolerance in GF677 (peach×almond) rootstock. *Scientia Horticulturae* 272, 109535. doi: 10.1016/j.scienta.2020.109535

Smith, S. E., and Read, D. J. (2010). *Mycorrhizal Symbiosis*. Cambridge, MA: Academic Press.

Song, Y. Y., Simard, S. W., Carroll, A., Mohn, W. W., and Zeng, R. S. (2015). Defoliation of interior Douglas-fir elicits carbon transfer and stress signalling to ponderosa pine neighbors through ectomycorrhizal networks. *Sci. Rep.* 5, 1–9. doi: 10.1038/srep08495

Sou, H. D., Masumori, M., Yamanoshita, T., and Tange, T. (2021). Primary and secondary aerenchyma oxygen transportation pathways of Syzygium kunstleri (King) Bahadur & R. C. Gaur adventitious roots in hypoxic conditions. *Sci. Rep.* 11:4520. doi: 10.1038/s41598-021-84183-z

Steidinger, B. S., Crowther, T. W., Liang, J., Van Nuland, M. E., Werner, G., Reich, P. B., et al. (2019). Climatic controls of decomposition drive the global biogeography of forest-tree symbioses. *Nature* 569, 404–408. doi: 10.1038/s41586-019-1128-0

Stenström, E. (1991). The effects of flooding on the formation of ectomycorrhizae in *Pinus sylvestris* seedlings. *Plant Soil* 131, 247–250. doi: 10.1007/BF00009455

Suz, L. M., Bidartondo, M. I., van der Linde, S., and Kuyper, T. W. (2021). Ectomycorrhizas and tipping points in forest ecosystems. *New Phytol.* 231, 1700–1707. doi: 10.1111/nph.17547

Tabari, H. (2020). Climate change impact on flood and extreme precipitation increases with water availability. *Sci. Rep.* 10:13768. doi: 10.1038/s41598-020-74038-4

Teskey, R., Wertin, T., Bauweraerts, I., Ameye, M., McGuire, M. A., and Steppe, K. (2015). Responses of tree species to heat waves and extreme heat events. *Plant Cell Environ.* 38, 1699–1712. doi: 10.1111/pce.12417

Thiem, D., Piernik, A., and Hrynkiewicz, K. (2018). Ectomycorrhizal and endophytic fungi associated with *Alnus glutinosa* growing in a saline area of central Poland. *Symbiosis* 75, 17–28. doi: 10.1007/s13199-017-0512-5

Thiem, D., Tyburski, J., Gołębiewski, M., and Hrynkiewicz, K. (2020). Halotolerant fungi stimulate growth and mitigate salt stress in *Alnus glutinosa* Gaertn. *Dendrobiology* 83, 30–42. doi: 10.12657/denbio.083.003

Thomas, P. W. (2021). Ectomycorrhiza resilience and recovery to extreme flood events in *Tuber aestivum* and *Quercus robur*. *Mycorrhiza* 31, 511–517. doi: 10.1007/s00572-021-01035-4

Treseder, K. K., Marusenko, Y., Romero-Olivares, A. L., and Maltz, M. R. (2016). Experimental warming alters potential function of the fungal community in boreal forest. *Glob. Change Biol.* 22, 3395–3404. doi: 10.1111/gcb.13238

van der Linde, S., Suz, L. M., Orme, C. D. L., Cox, F., Andreae, H., Asi, E., et al. (2018). Environment and host as large-scale controls of ectomycorrizal fungi. *Nature* 558, 243–248. doi: 10.1038/s41586-018-0189-9

van der Putten, W. H. (2012). Climate change, aboveground–belowground interactions, and species' range shifts. *Ann. Rev. Ecol. Evol. Syst.* 43, 365–383. doi: 10.1146/annurev-ecolsys-110411-160423

van Dongen, J. T., and Licausi, F. (2015). Oxygen sensing and signaling. *Ann. Rev. Plant Biol.* 66, 345–367. doi: 10.1146/annurev-arplant-043014-114813

Van Nuland, M. E., Ware, I. M., Schadt, C. W., Yang, Z., Bailey, J. K., and Schweitzer, J. A. (2021). Natural soil microbiome variation affects spring foliar phenology with consequences for plant productivity and climate-driven range shifts. *New Phytol.* [Epub ahead of print]. doi: 10.1111/nph.17599

Voesenek, L. A. C. J., and Bailey-Serres, J. (2015). Flood adaptive traits and processes: an overview. *New Phytol.* 206, 57–73. doi: 10.1111/nph.13209

Wang, J., Zhang, H., Gao, J., Zhang, Y., Liu, Y., and Tang, M. (2021). Effects of ectomycorrhizal fungi (*Suillus variegatus*) on the growth, hydraulic function, and non-structural carbohydrates of *Pinus tabulaeformis* under drought stress. *BMC Plant Biol.* 21:171. doi: 10.1186/s12870-021-02945-3

Wang, W. X., Zhang, F., Chen, Z. L., Liu, J., Guo, C., He, J. D., et al. (2017). Responses of phytohormones and gas exchange to mycorrhizal colonization in trifoliate orange subjected to drought stress. *Arch. Agron. Soil Sci.* 63, 14–23. doi: 10.1080/03650340.2016.1175556

Wang, Y., Qiu, Q., Yang, Z., Hu, Z., Tam, N. F., and Xin, G. (2010). Arbuscular mycorrhizal fungi in two mangroves in South China. *Plant Soil* 331, 181–191. doi: 10.1007/s11104-009-0244-2

Weissenhorn, I. (2002). Mycorrhiza and Salt Tolerance of Trees. EU-project MYCOREM (QLK3-1999-00097) the Use of Mycorrhizal Fungi in Phytoremediation. Final Report of Partner 9. Available online at: https://www.servaplant.nl/new/wp-content/uploads/2015/10/MycoremReport.pdf (accessed June 2021).

Wu, A. S., Zou, Y. N., and Huang, Y. M. (2012). The arbuscular mycorrhizal fungus Diversispora spurca ameliorates effects of waterlogginig on growth, root system architecture and antioxidant enzyme activities of citrus seedlings. *Fungal Ecol.* 6, 37–43. doi: 10.1016/j.funeco.2012.09.002

Wu, H. (2018). Plant salt tolerance and Na+ sensing and transport. *Crop J.* 6, 215–225. doi: 10.1016/j.cj.2018.01.003

Wu, Q. S., Liu, C. Y., Zhang, D. J., Zou, Y. N., He, X. H., and Wu, Q. H. (2016). Mycorrhiza alters the profile of root hairs in trifoliate orange. *Mycorrhiza* 26, 237–247. doi: 10.1007/s00572-015-0666-z

Xu, H., and Zwiazek, J. J. (2020). Fungal aquaporins in ectomycorrhizal root water uptake. *Front. Plant Sci.* 11:302. doi: 10.3389/fpls.2020.00302

Yang, H., Koide, R. T., and Zhang, Q. (2016). Short-term waterlogging increases arbuscular mycorrhizal fungal species richness and shifts community composition. *Plant Soil* 404, 373–384. doi: 10.1007/s11104-016-2850-0

Yang, S. J., Zhang, Z. L., Xue, Y. X., Zhang, Z. F., and Shi, S. Y. (2014). *Arbuscular mycorrhizal* fungi increase salt tolerance of apple seedlings. *Bot. Stud.* 55, 1–7. doi: 10.1186/s40529-014-0070-6

Yi, H., Calvo-Polanco, M., MacKinnon, M. D., and Zwiazek, J. J. (2008). Responses of ectomycorrhizal *Populus tremuloides* and *Betula papyrifera* seedlings to salinity. *Env. Exp. Bot.* 62, 357–363. doi: 10.1016/j.envexpbot.2007.10.008

Yin, D., Song, R., Qi, J., and Deng, X. (2018). Ectomycorrhizal fungus enhances drought tolerance of *Pinus sylvestris* var. mongolica seedlings and improves soil condition. *J. For. Res.* 29, 1775–1788. doi: 10.1007/s11676-017-0583-4

Yuan, F., Leng, B., and Wang, B. (2016). Progress in studying salt secretion from the salt glands in Recretohalophytes: how do plants secrete salt? *Front. Plant Sci.* 7:977. doi: 10.3389/fpls.2016.00977

Zandalinas, S. I., Fritschi, F. B., and Mittler, R. (2021). Global warming, climate change, and environmental pollution: recipe for a multifactorial stress combination disaster. *Trends Plant Sci.* 26, 588–599. doi: 10.1016/j.tplants.2021.02.011

Zhang, F., Wang, P., Zou, Y. N., Wu, Q. S., and Kuča, K. (2019). Effects of mycorrhizal fungi on root-hair growth and hormone levels of taproot and lateral roots in trifoliate orange under drought stress. *Arch. Agron. Soil Sci.* 65, 1316–1330. doi: 10.1080/03650340.2018.1563780

Zhang, F., Zou, Y. N., and Wu, Q. S. (2018). Quantitative estimation of water uptake by mycorrhizal extraradical hyphae in citrus under drought stress. *Sci. Hortic.* 229, 132–136. doi: 10.1016/j.scienta.2017.10.038

Zheng, F.-L., Liang, S.-M., Chu, X.-N., Yang, Y. L., and Wu, Q. S. (2020). Mycorrhizal fungi enhance flooding tolerance of peach through inducing proline accumulation and improving root architecture. *Plant Soil Environ.* 66, 624–631. doi: 10.17221/520/2020-PSE

Zou, Y. N., Srivastava, K., Wu, Q. S., and Huang, Y. M. (2014). Increased tolerance of trifoliate orange (*Poncirus trifoliata*) seedlings to waterlogging after inoculation with arbuscular mycorrhizal fungi. *J. Anim. Plant Sci.* 24, 1415–1420.

Zou, Y. N., Wang, P., Liu, C. Y., Ni, Q. D., Zhang, D. J., and Wu, Q. S. (2017). Mycorrhizal trifoliate orange has greater root adaptation of morphology and phytohormones in response to drought stress. *Sci. Rep.* 7, 1–10. doi: 10.1038/srep41134

Zwiazek, J. J., Equiza, M. A., Karst, J., Senorans, J., Wartenbe, M., and Calvo-Polanco, M. (2019). Role of urban ectomycorrhizal fungi in improving the tolerance of lodgepole pine (*Pinus contorta*) seedlings to salt stress. *Mycorrhiza* 29, 303–312. doi: 10.1007/s00572-019-00893-3

Conflict of Interest: The authors declare that the research was conducted in the absence of any commercial or financial relationships that could be construed as a potential conflict of interest.

Publisher's Note: All claims expressed in this article are solely those of the authors and do not necessarily represent those of their affiliated organizations, or those of the publisher, the editors and the reviewers. Any product that may be evaluated in this article, or claim that may be made by its manufacturer, is not guaranteed or endorsed by the publisher.

frontiers in Forests and Global Change

MINI REVIEW
published: 04 November 2021
doi: 10.3389/ffgc.2021.731903

Do Growth-Limiting Temperatures at the High-Elevation Treeline Require an Adaptation of Phloem Formation and Anatomy?

*Dennis Marko Schröter and Walter Oberhuber**

Department of Botany, Leopold-Franzens-University of Innsbruck, Innsbruck, Austria

Low temperatures during the growing season restrict the growth of trees at high elevations and lead to the formation of the high-elevation treeline. To ensure the survival and growth of trees in such extreme locations, sufficient vascular transport capacity – enabled by vascular anatomical characteristics – is required. However, in contrast to the xylem, only little is known about the effects of low temperatures on the anatomy and formation of the phloem as important nutrient- and signal-conducting tissue. In this review, known findings of cold-induced changes in the anatomical and phenological properties of vascular tissues are used as starting points to discuss how low temperatures might affect phloem formation at the treeline and how this conductive tissue might adaptively respond to this growth-limiting environmental variable. Data currently available suggest that low temperatures lead to changes in the anatomy and phenological development of the phloem. In order to ensure the functionality of the phloem and thus the survival of trees at the high-elevation treeline, appropriate adaptations to the prevailing low temperatures are therefore to be expected and are discussed in this review.

Keywords: adaptation, intra-annual phloem formation, low temperature, phloem anatomy, phloem transport, phenology, tree growth, treeline

OPEN ACCESS

Edited by:
James Blande,
University of Eastern Finland, Finland

Reviewed by:
Drew Peltier,
Northern Arizona University, United States
Anirban Guha,
University of Florida, United States

***Correspondence:**
Walter Oberhuber
walter.oberhuber@uibk.ac.at

Specialty section:
This article was submitted to Forest Ecophysiology, a section of the journal Frontiers in Forests and Global Change

Received: *28 June 2021*
Accepted: *07 October 2021*
Published: *04 November 2021*

Citation:
Schröter DM and Oberhuber W (2021) Do Growth-Limiting Temperatures at the High-Elevation Treeline Require an Adaptation of Phloem Formation and Anatomy? Front. For. Glob. Change 4:731903. doi: 10.3389/ffgc.2021.731903

INTRODUCTION

Phloem is a highly complex vascular tissue that performs numerous functions for the growth and survival of trees. The long-distance transport of both phytohormones and RNAs as information signals between above- and belowground tissues (Lacombe and Achard, 2016; Kondhare et al., 2021) and carbohydrates as nutrients from source to sink (Savage et al., 2016) are considered to be important key functions, enabled by the anatomical properties of phloem (Schulz and Thompson, 2009; Knoblauch and Oparka, 2012; Liesche et al., 2015). The characteristics of the phloem in trees differ from those in herbaceous plants (for more details see De Schepper et al., 2013 and the literature therein). Phloem transport occurs along three functional units (i.e., collection, transport, and release phloem) via sieve cells and sieve tube elements in gymnosperms and angiosperms, respectively (van Bel, 2003; De Schepper et al., 2013). The water required for phloem transport is provided by the radial connection to the xylem via ray parenchyma (**Box 1**; Hölttä et al., 2009; Pfautsch et al., 2015; Sevanto, 2018). In this process, ray parenchyma cells provide not only the radial transport of water and carbohydrates between xylem and phloem (van Bel, 1990) but also

in and out of the axial parenchyma tissue (Pfautsch et al., 2015). Sieve elements and companion cells are laterally connected via sieve areas consisting of several sieve pores. Axially, sieve elements are connected by sieve areas in gymnosperms, which form a sieve plate with large sieve pores in angiosperms (Liesche et al., 2017). During the growing season, there is a transition from early phloem cells with wide lumen that have a conducting function to late phloem cells with narrow lumens that primarily have a storage function (Gričar et al., 2021). These phloem cells are separated by a band of axial parenchyma cells (**Figure 1**; Gričar and Čufar, 2008).

Although both the xylem and phloem arise from radial cell division of the cambium (Larson, 1994), the formation of both tissues is not synchronous and is driven by different factors (Prislan et al., 2013; Gričar et al., 2015, 2021). In contrast to the xylem, the phloem was found to be less susceptible to environmental influences and mainly endogenously controlled (Alfieri and Evert, 1968; Rosner et al., 2001; Gričar and Čufar, 2008; Prislan et al., 2013; Swidrak et al., 2014; Miller et al., 2020; Gričar et al., 2021). Even before the reactivation of cambial activity after dormancy, phloem formation starts with expansion and differentiation of overwintered phloem cells (Alfieri and Evert, 1968, 1973; Antonova and Stasova, 2006; Gričar and Čufar, 2008). After the reactivation of the cambium, the onset of phloem cell production precedes xylem production by approximately 2–3 weeks (Alfieri and Evert, 1968; Antonova and Stasova, 2006, 2008; Swidrak et al., 2014; Jyske et al., 2015), due to the short functional life span of sieve cells of 1–2 years before they collapse (Evert, 2006).

Because climate change strongly affects tree growth and the phloem fulfills important functions in carbon allocation, phloem anatomy and phenology gained increasing importance in the last decade (e.g., Liesche et al., 2015, 2017; Miller et al., 2020; Gričar et al., 2021). Surprisingly, no studies were published yet dealing with intra-annual development and anatomy of phloem cells at high-elevation treeline sites, where trees reach their uppermost distributional limit due to temperature constraints on tree growth. Globally, trees at high-elevation treelines are exposed to seasonal mean air temperature between 5.5 and 7.5°C (Körner, 1998). In this brief review, we will evaluate possible adaptations in phloem phenology and anatomy under low temperatures.

TEMPERATURE LIMITATION OF TREE GROWTH AT HIGH ELEVATIONS

Low temperatures are considered to be the main reason for the upper distributional boundary of trees (e.g., Körner and Paulsen, 2004; Rossi et al., 2007; Caccianiga et al., 2008; Körner, 2015). Only a few taxa are able to reach the uppermost high-elevational limit for trees – the treeline – which is a conspicuous climate-driven ecological boundary and occurs worldwide at high elevations (Körner, 2012). In the temperate climate zone, conifers of the genera *Pinus*, *Larix,* and *Picea*, as well as tree species belonging to Betulaceae and Fagaceae, are among the most successful tree taxa dominating at the high-elevation treeline (e.g., Körner and Paulsen, 2004; Caccianiga et al., 2008; Körner, 2012; Leuschner and Ellenberg, 2017).

At high elevations, the meristem activity, i.e., cell division, enlargement, and differentiation, is more sensitive to low-temperature conditions prevailing during the growing season than photosynthesis. The "carbon-sink-limitation hypothesis" is currently the most widely accepted hypothesis for explaining the formation of treelines (e.g., Körner and Paulsen, 2004; Rossi et al., 2007; Körner, 2015). While photosynthesis is still active at temperatures near the freezing point (e.g., Häsler, 1982; Weng et al., 2005), the exponential increase in cell doubling time below c. 5°C causes the upper elevational limit for the occurrence of trees (Körner, 2003, 2015). Numerous studies revealed that both aboveground and belowground growth is strongly reduced at temperatures below 5°C (Häsler et al., 1999; Alvarez-Uria and Körner, 2007, 2011; Rossi et al., 2007, 2008; Schenker et al., 2014). All growth processes, i.e., root, radial stem, and shoot growth as well as budburst, and subsequent leaf and flower development require water, carbon compounds, nutrients, and hormones via the vascular system, i.e., phloem and xylem (Savage and Chuine, 2021). Several findings have already demonstrated the effects of low temperatures on the xylem, i.e., reductions in wood formation, cell diameter, and cell wall thickness (e.g., Rossi et al., 2007, 2008; Castagneri et al., 2017; Babushkina et al., 2019). Therefore, it is necessary to consider low-temperature influences at high elevations on the anatomical characteristics and phenology of the phloem to comprehensively understand temperature-induced growth limitation.

ARE CARBON AVAILABILITY AND PHLOEM TRANSPORT REDUCED AT THE HIGH-ELEVATION TREELINE?

A continuous supply of carbohydrates is essential for tree growth (Cuny et al., 2015; Deslauriers et al., 2016), especially under extreme climatic conditions prevailing at the treeline. Several authors have shown that photosynthesis is less limited by low temperatures than growth (Grace et al., 2002, for a review, see Körner, 2015). Larcher (2003) reported that photosynthetic production in evergreen conifers commences at temperatures between −5 and −3°C. An excess of these assimilates are stored as non-structural carbohydrates (**Box 1**; NSC) like starch and other carbon compounds (sugar, alcohol, lipids, proteins) which can be later mobilized for growth, development, and regeneration (Palacio et al., 2014). Several studies have shown an increasing trend in the content of NSC in leaves, stem, and root along an elevational transect, i.e., decrease in air temperature, up to the treeline (e.g., Hoch et al., 2002; Hoch and Körner, 2003, 2009; Gruber et al., 2011). An increase in NSC storage is considered as an immediate physiological response to low temperatures and to compensate for the imbalance between carbon production and demand (Hoch and Körner, 2012).

As mentioned above, root growth decreases at temperatures below 5°C (Alvarez-Uria and Körner, 2007, 2011; Schenker et al., 2014). However, at the treeline, reduced nutrient availability due to low nutrient mineralization rates (e.g., Meentemeyer, 1977)

BOX 1 | *Glossary of terms.*
Axial parenchyma: Longitudinally arranged parenchyma cells for vertical transport and storage of carbohydrates.
Callose: Polysaccharide (β-1,3-glucan) found in cell walls of higher plants; involved in phloem transport and deposited as response to injury.
Companion cells: Specialized nucleated parenchyma cells regulating transport of substances in and out of sieve elements.
Early phloem: First formed phloem cells with large diameter primarily for transport of substances.
Initial early phloem: Undifferentiated overwintering cells formed at the end of the previous growing season, which differentiate to early phloem in spring.
Late phloem: Formed after early phloem with narrow diameter primarily for storage.
Non-structural carbohydrates: Comprise primarily soluble sugars and starch; provide substrates for growth, metabolism and osmoregulation.
Sieve area: Are developed in axial and lateral cell walls between sieve elements and between sieve elements and companion cells, respectively.
Sieve elements: Enucleate functional units for phloem transport connected via sieve plates and/or sieve areas.
Sieve plate: Are developed in angiosperms in transverse cell walls between axial connected sieve elements (cf., **Figure 1**).
Sieve pores: Pores lined with callose within sieve areas and sieve plates (cf., **Figure 1**).
Ray parenchyma: Radially arranged parenchyma cells for storage and lateral transport of water and carbohydrates between xylem and phloem.

as well as cold-related physical constraints in water and nutrient uptake from soil to root (Weih and Karlsson, 2001, 2002) require appropriate adaptive responses for an efficient nutrient uptake. In this regard Hertel and Schöling (2011) found an increase of fine root biomass with elevation in Norway spruce (*Picea abies*) resulting in a higher root to shoot ratio. Additionally, Kubisch et al. (2017) demonstrated an accelerated fine root turnover and higher production rate in *Pinus cembra* under soil temperatures lowered by self-shading, which underpin the previous results. This implies both a sufficient carbon availability and an efficient phloem transport in favor of root growth to ensure an adequate nutrient uptake at the treeline. Hence, phloem is able to remain functional even at the world's highest treeline formed by *Polylepis* sp. at c. 5,000 m a.s.l. (Hoch and Körner, 2005).

EXPECTED ADAPTATIONS OF PHLOEM ANATOMY AND PHENOLOGY AS A RESPONSE TO EXTREME CLIMATE CONDITIONS AT THE HIGH-ELEVATION TREELINE

In field experiments, several authors found that phloem formation and anatomy are less responsive to variability in environmental conditions compared to the xylem (Alfieri and Evert, 1968; Rosner et al., 2001; Gričar et al., 2014; Swidrak et al., 2014; Miller et al., 2020). However, extreme climate conditions might impair intra-annual phloem formation and/or phloem anatomy which would adversely affect carbon transport and dependent metabolic processes such as growth and development (e.g., Savage and Chuine, 2021). Salmon et al. (2019) described in detail the anatomical constraints of phloem under severe drought, whereas species-specific effects on phloem anatomy at low soil water availability were shown by Epron et al. (2019). This raises the question of how low temperatures can affect phloem formation and anatomy.

In a cooling treatment in the field, it was found that low temperatures (9–11°C) resulted in reduced cambial activity, indicated by a lower proportion of latewood in *Picea abies*, while the phloem anatomy and width of growth increments remained unaffected (Gričar et al., 2006). However, long-term cooling of a stem portion of *Picea abies* caused not only a significant reduction in cambial activity but low temperatures also led to anatomical alterations on the phloem side (Gričar et al., 2007). Specifically, early phloem was less affected, but the tangential band of axial parenchyma separating the early and late phloem was no longer continuous and the number of late phloem cells was reduced. Similar results were found at mid-elevation sites in *Picea abies* (1,200 m a.s.l.; Gričar et al., 2015, 2021). Based on these studies, it can be expected that comparable effects occur at the high-elevation treeline (**Figure 1**).

Does the Temperature-Induced Reduction in Cambial Activity Also Affect Phloem Anatomical Features?

Based on several studies on coniferous species, temperature-induced changes in xylem anatomy affect cell size, as well as cell wall thickness, the latter being related to carbon mobilization and deposition rates (e.g., Rossi et al., 2008; Lupi et al., 2010; Körner, 2012). Castagneri et al. (2017) and Babushkina et al. (2019) demonstrated along an elevational gradient, that low temperatures especially at high elevations are one of the key climatic factors affecting xylem cell enlargement and cell wall deposition, which subsequently are reflected in a reduction of cell diameter and cell wall thickness. Similar effects on phloem anatomy are to be expected at the treeline, where low temperatures prevail during the growing season (**Figure 1**). Moreover, it should be noted that possible low-temperature effects on phloem formation and anatomy may impair the carbon transport in some tree species. Liesche et al. (2015) demonstrated in their study a lower phloem transport rate in narrow sieve cells of gymnosperms compared to angiosperms, which supports this assumption. Additionally, Pfautsch et al. (2015) reported that phloem sap becomes increasingly viscous with decreasing temperature, which additionally increases resistance in phloem transport. Because at high elevation xylem cells were found to be highly vulnerable to cavitation (Mayr et al., 2002, 2003), impaired phloem transport could also have an impact on the repair of embolized xylem cells (cf., Pfautsch et al., 2015).

How Can Phloem Transport Efficiency Be Ensured Under Low Temperatures Prevailing at the High-Elevation Treeline?

Several findings conducted at mid-elevation sites (1,200 m a.s.l., Gričar et al., 2014, 2015, 2021; Miller et al., 2020)

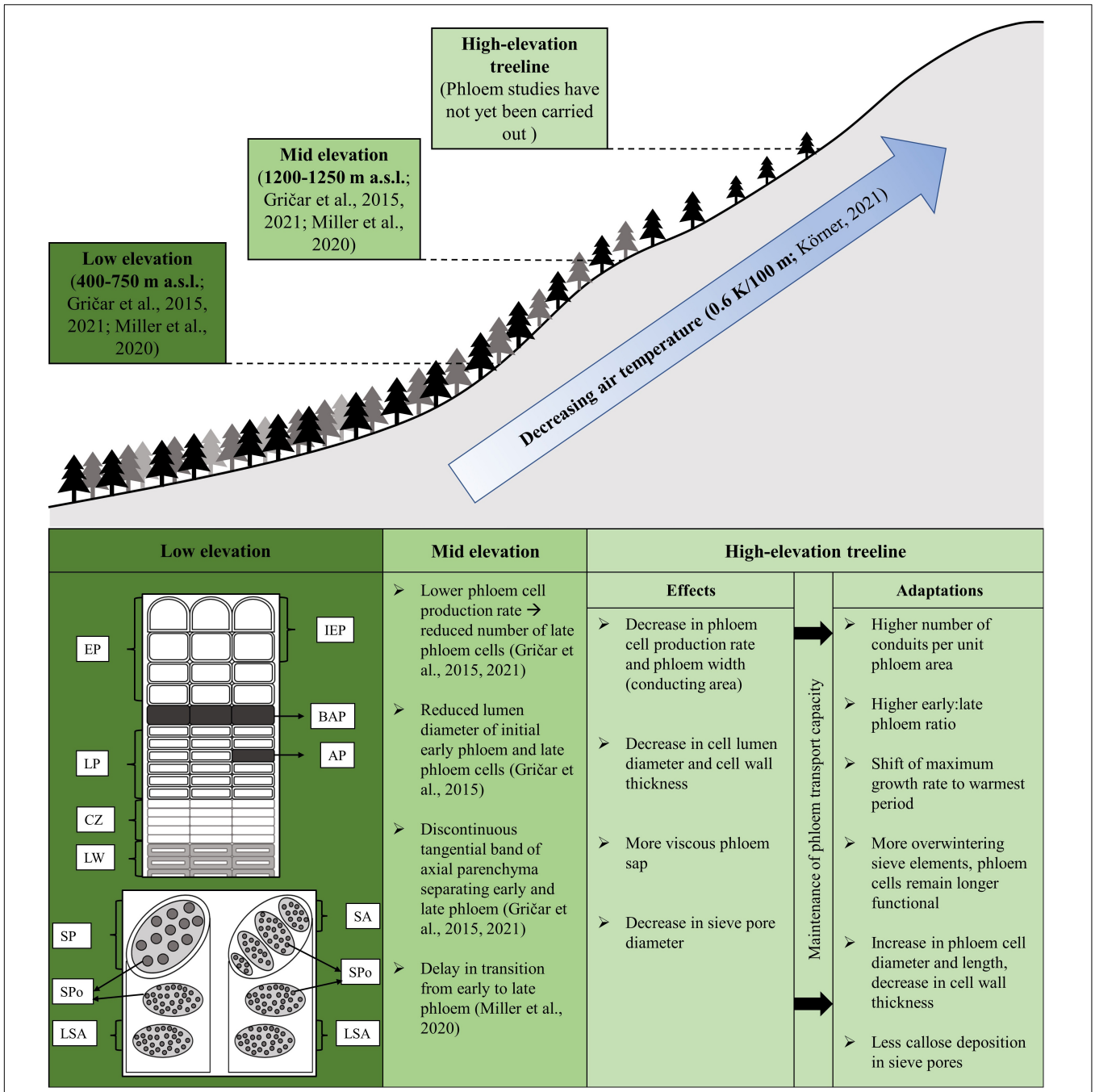

FIGURE 1 | Schematic illustration of known and assumed low-temperature effects on phloem anatomy and formation along an elevational transect. Upper graphic: Current studies dealing with environmental influence on the phloem conducted at different elevations. Below: General phloem structure at low-elevation sites, alterations caused by decrease in temperature at mid-elevation sites, and effects and possible phloem adaptations at the high-elevation treeline. Low elevation, top: Annual phloem ring exemplified by *Picea abies* after Gričar and Čufar (2008) consist of early phloem (EP) with initial early phloem (IEP), the continuous tangential band (BAP) of axial parenchyma cells (AP), late phloem (LP) with adjacent cambial zone (CZ) and latewood tracheids (LW); bottom: phloem cells (axial view) with lateral sieve areas (LSA) and sieve pores (SPo), as well as axial sieve areas (SA) in conifers (right) and sieve plates (SP) with larger sieve pores in angiosperms (left), respectively.

indicate plasticity in phloem formation, i.e., the ability to adapt structurally to ensure optimal function under local environmental conditions. Phloem cells show a tip-to-base widening (Jyske and Hölttä, 2015; Ryan and Robert, 2017), and to compensate for the smaller conducting area the number of conduits per unit phloem area increases (Jyske and Hölttä, 2015). Due to aerodynamic coupling of the shoot to the macroclimate, height growth at the treeline is

more strongly restricted than radial stem growth (Hoch and Körner, 2005; Körner, 2012; Wang et al., 2012). Therefore, it can be assumed that phloem responds with an increase in cell density resulting in an increased ratio of early to late phloem cells for better conductivity. The priority of the early phloem as the conductive part over the late phloem (storage) is shown by its robustness to environmental influences and underpins its greater importance for the survival of trees (Larson, 1994; Gričar et al., 2015, 2021). Temperature-related changes in radial dimension (lumen) of initial early phloem (**Box 1**; i.e., first tangential rows of cells at the phloem growth ring boundary formed in the previous year) and late phloem cells (Gričar et al., 2015), as well as a seasonal variability in length of sieve elements and axial parenchyma (Jyske et al., 2015), suggest an adaptive change in cell size for an efficient conductivity under low temperatures. Furthermore, several authors reported a decrease in cell wall thickness in earlywood and latewood tracheids at mid elevations (1,260 m a.s.l., Gindl et al., 2001; 1,200 m a.s.l., Gričar et al., 2015), and a similar effect in sieve cell wall thickness could be conceivable as another way to increase the sieve cell lumen diameter at high elevations. However, the conductive capacity of the phloem at the treeline may be favored not only by adaptations in the aforementioned anatomical traits but also by an increase in sieve pore size and frequency along the pathway (Mullendore et al., 2010). Sieve pores can be lined with callose or nearly occluded with it, which may play a significant role in transport regulation through the symplast (Neuberger and Evert, 1975; Knoblauch and van Bel, 1998). Callose is deposited as a response to cell injury, senescence, or dormancy (Evert, 1990) whereby not all pores are sealed with it (Montwe et al., 2019; Prislan et al., 2019). Due to the prevailing extreme climate conditions at the high-elevation treeline, less callose might accumulate as a temperature-dependent response to increase sieve pore size and create less resistance to ensure phloem transport capacity (cf., McNairn, 1972). Because of the severely time-limited lifespan of sieve elements, the priority for tree survival is in phloem production while xylem thickness can be reduced or become discontinuous (Evert, 2006). Especially under extreme environmental conditions, this is reflected in a lower xylem to phloem ratio (Larson, 1994; Plomion et al., 2001; Gričar et al., 2009).

Phenological adaptations can also influence anatomical properties of vascular tissues in favor of functional capacity, as demonstrated by Cuny et al. (2019). It became apparent, that in cold environments xylem differentiation rate (i.e., cell elongation and cell wall thickening) decreased but to mitigate the influence of low temperatures the duration of these processes was extended. Miller et al. (2020) reported a delay in the transition from early to late phloem in *Picea abies* along an elevational gradient extending from 450 m to 1,250 m a.s.l., which was related to the onset of cambial activity, cell production rate, and the number of cells in the early phloem. Findings in this study also provide the first evidence that in contrast to xylem formation (e.g., Rossi et al., 2006) maximum phloem cell production rate does not coincide with the summer solstice. These results suggest that at the high-elevation treeline the maximum phloem growth rate may shift to the warmest period instead of being controlled by photoperiod or endogenous factors. Furthermore, it is conceivable that more overwintering phloem cells are formed or that phloem cells remain functional for more than one to two growing seasons, which would correspond to the observations of Holdheide (1951). Hence, adaptations in intra-annual phloem formation and anatomy in response to low temperatures and climate extremes (e.g., the occurrence of frost drought) prevailing at the high-elevation treeline are to be expected (**Figure 1**; cf., Agusti and Greb, 2013; Gričar et al., 2015, 2021; Miller et al., 2020). This would also entail a shift from endogenous to exogenous control of phloem formation.

AREAS OF FUTURE RESEARCH

Expected adaptations of phloem phenology and anatomy induced by extreme climatic conditions prevailing at the high-elevation treeline are shown in **Figure 1**. In order to understand the effects of low temperatures on the phloem at high elevations, several questions need to be clarified, e.g., (i) How does phloem phenology and anatomy adapt to climate extremes (e.g., cold summer with shortened growing period, early or late frost events) at the treeline? (ii) To what extent is phloem transport capacity and efficiency affected by low temperatures? (iii) Is tip-to-base widening occurring at treeline (cf., Jyske and Hölttä, 2015; Ryan and Robert, 2017)? (iv) Are there organ specific differences in phloem formation and anatomy, e.g., in branches (twigs) vs. roots due to exposure to different temperature regimes, i.e., high vs. low daily temperature variability? (v) How sensitive is phloem formation to environmental stress (e.g., frost drought) within the treeline ecotone? (vi) Is there a year-to-year variability in phloem formation depending on weather conditions or does endogenous control of phloem formation also predominate at the high-elevation treeline? A combination of high measurement frequency and long-term observations in the field together with field chilling experiments, laboratory manipulations, and histo-anatomical analyses will be necessary to answer these questions. As there are differences in phloem anatomy between gymnosperms and angiosperms (Jensen et al., 2012; Liesche et al., 2015, 2017) the question arises if species-specific adaptations regarding phloem anatomy and/or phenology at the high-elevation treeline occur.

CONCLUSION

Phloem fulfills important functions for tree growth and development (Hölttä et al., 2009; Pfautsch et al., 2015;

Sevanto, 2018). However, compared to the xylem much less is known about the influence of growth-limiting temperatures at high elevations on the anatomy and intra-annual formation of the phloem. Therefore, to advance our knowledge about the characteristics of phloem tissue at the high-elevation treeline, field and experimental studies are urgently needed. This review is intended to highlight the existing gaps in knowledge regarding phloem adaptation to extreme climate conditions prevailing at the high-elevation treeline and to serve as a stimulus to open up a new area of research.

AUTHOR CONTRIBUTIONS

Both authors listed have made a substantial, direct and intellectual contribution to the work, and approved it for publication.

FUNDING

The publication of this manuscript was financially supported by the University of Innsbruck.

REFERENCES

Agusti, J., and Greb, T. (2013). Going with the wind–Adaptive dynamics of plant secondary meristems. *Mech. Dev.* 130, 34–44. doi: 10.1016/j.mod.2012.05.011

Alfieri, F. J., and Evert, R. F. (1968). Seasonal development of the secondary phloem in *Pinus*. *Am. J. Bot.* 55, 518–528. doi: 10.2307/2440583

Alfieri, F. J., and Evert, R. F. (1973). Structure and Seasonal development of the secondary phloem in the Pinaceae. *Bot. Gaz.* 134, 17–25. doi: 10.1086/336674

Alvarez-Uria, P., and Körner, C. (2007). Low temperature limits of root growth in deciduous and evergreen temperate tree species. *Funct. Ecol.* 21, 211–218. doi: 10.1111/j.1365-2435.2007.01231.x

Alvarez-Uria, P., and Körner, C. (2011). Fine root traits in adult trees of evergreen and deciduous taxa from low and high elevation in the Alps. *Alp. Bot.* 121, 107–112. doi: 10.1007/s00035-011-0092-6

Antonova, G. F., and Stasova, V. V. (2006). Seasonal development of phloem in Scots pine stems. *Russ. J. Dev. Biol.* 37, 306–320. doi: 10.1134/S1062360406050043

Antonova, G. F., and Stasova, V. V. (2008). Seasonal development of phloem in Siberian larch stems. *Russ. J. Dev. Biol.* 39, 207–218. doi: 10.1134/S1062360408040024

Babushkina, E. A., Belokopytova, L. V., Zhimova, D. F., and Vaganov, E. A. (2019). Siberian spruce tree ring anatomy: imprint of development processes and their high-temporal environmental regulation. *Dendrochronologia* 53, 114–124. doi: 10.1016/j.dendro.2018.12.003

Caccianiga, M., Andreis, C., Armiraglio, S., Leonelli, G., Pelfini, M., and Sala, D. (2008). Climate continentality and treeline species distribution in the Alps. *Plant Biosyst.* 142, 66–78. doi: 10.1080/11263500701872416

Castagneri, D., Fonti, P., von Arx, G., and Carrer, M. (2017). How does climate influence xylem morphogenesis over the growing season? Insights from long−term intra−ring anatomy in *Picea abies*. *Ann. Bot.* 119, 1011–1020. doi: 10.1093/aob/mcw274

Cuny, H. E., Fonti, P., Rathgeber, C. B. K., von Arx, G., Peters, R. L., and Frank, D. C. (2019). Couplings in cell differentiation kinetics mitigate air temperature influence on conifer wood anatomy. *Plant Cell. Environ.* 42, 1222–1232. doi: 10.1111/pce.13464

Cuny, H. E., Rathgeber, C. B. K., Frank, D., Fonti, P., Mäkinen, H., Prislan, P., et al. (2015). Woody biomass production lags stem-girth increase by over one month in coniferous forests. *Nat. Plants* 1:15160. doi: 10.1038/NPLANTS.2015.16

De Schepper, V., De Swaef, T., Bauweraerts, I., and Steppe, K. (2013). Phloem transport: a review of mechanisms and controls. *J. Exp. Bot.* 64, 4839–4850. doi: 10.1093/jxb/ert302

Deslauriers, A., Huang, J.-G., Balducci, L., Beaulieu, M., and Rossi, S. (2016). The contribution of carbon and water in modulating wood formation in black spruce saplings. *Plant Physiol.* 170, 2072–2084. doi: 10.1104/pp.15.01525

Epron, D., Dannoura, M., and Hölttä, T. (2019). Introduction to the invited issue on phloem function and dysfunction. *Tree Physiol.* 39, 167–172. doi: 10.1093/treephys/tpz007

Evert, R. F. (1990). "Dicotyledons," in *Sieve Elements. Comparative Structure, Induction and Development*, eds H.-D. Behnke and R. D. Sjolund (Berlin: Springer-Verlag), 103–137.

Evert, R. F. (2006). *Esau's Plant Anatomy. Meristems, Cells, and Tissues of the Plant Body: Their Structure, Function, and Development*, 3rd Edn. Hoboken, NJ: John Wiley & Sons, Inc.

Gindl, W., Grabner, M., and Wimmer, R. (2001). Effects of altitude on tracheid differentiation and lignification of Norway spruce. *Can. J. Bot.* 79, 815–821. doi: 10.1139/b01-060

Grace, J., Berninger, F., and Nagy, L. (2002). Impacts of climate change on the tree line. *Ann. Bot.* 90, 537–544. doi: 10.1093/aob/mcf222

Gričar, J., and Čufar, K. (2008). Seasonal dynamics of phloem and xylem formation in silver fir and Norway spruce as affected by drought. *Russ. J. Plant Physiol.* 55, 538–543. doi: 10.1134/S102144370804016X

Gričar, J., Čufar, K., Eler, K., Gryc, V., Vavrčík, H., de Luis, M., et al. (2021). Transition dates from earlywood to latewood and early phloem to late phloem in Norway Spruce. *Forests* 12:331. doi: 10.3390/f12030331

Gričar, J., Krže, L., and Čufar, K. (2009). Number of cells in xylem, phloem and dormant cambium in silver fir (*Abies alba*), in trees of different vitality. *IAWA J.* 30, 121–133. doi: 10.1163/22941932-90000208

Gričar, J., Prislan, P., De Luis, M., Gryc, V., Hacurova, J., Vavrčík, H., et al. (2015). Plasticity in variation of xylem and phloem cell characteristics of Norway spruce under different local conditions. *Front. Plant Sci.* 6:730. doi: 10.3389/fpls.2015.00730

Gričar, J., Prislan, P., Gryc, V., Vavrčík, H., de Luis, M., and Čufar, K. (2014). Plastic and locally adapted phenology in cambial seasonality and production of xylem and phloem cells in *Picea abies* from temperate environments. *Tree Physiol.* 34, 869–881. doi: 10.3832/ifor1771-008

Gričar, J., Zupančic, M., and Čufar, K. (2007). Regular cambial activity and xylem and phloem formation in locally heated and cooled stem portions of Norway spruce. *Wood Sci. Technol.* 41, 463–475. doi: 10.1007/s00226-006-0109-2

Gričar, J., Zupančic, M., Čufar, K., Koch, G., Schmitt, U., and Oven, P. (2006). Effect of local heating and cooling on cambial activity and cell differentiation in stem of Norway spruce. *Ann. Bot.* 97, 943–951. doi: 10.1093/aob/mcl050

Gruber, A., Pirkebner, D., Oberhuber, W., and Wieser, G. (2011). Spatial and seasonal variations in mobile carbohydrates in *Pinus cembra* in the timberline ecotone of the Central Austrian Alps. *Eur. J. For. Res.* 130, 173–179. doi: 10.1007/s10342-010-0419-7

Häsler, R. (1982). Net photosynthesis and transpiration of *Pinus montana* on east and north facing slopes at alpine timberline. *Oecologia* 54, 14–22. doi: 10.1007/BF00541102

Häsler, R., Streule, A., and Turner, H. (1999). Shoot and root growth of young *Larix decidua* in contrasting microenvironments near the alpine timberline. *Phyton* 39, 47–52.

Hertel, D., and Schöling, D. (2011). Norway spruce shows contrasting changes in below- versus above-ground carbon partitioning towards the alpine tree line: evidence from a central European case study. *Arct. Antarct. Alp. Res.* 43, 46–55. doi: 10.1657/1938-4246-43.1.46

Hoch, G., and Körner, C. (2003). The carbon charging of pines at the climatic treeline: a global comparison. *Oecologia* 135, 10–21. doi: 10.1007/s00442-002-1154-7

Hoch, G., and Körner, C. (2005). Growth, demography and carbon relations of *Polylepis* trees at the world's highest treeline. *Funct. Ecol.* 19, 941–951. doi: 10.1111/j.1365-2435.2005.01040.x

Hoch, G., and Körner, C. (2009). Growth and carbon relations of tree line forming conifers at constant vs. variable low temperatures. *J. Ecol.* 97, 57–66. doi: 10.1111/j.1365-2745.2008.01447.x

Hoch, G., and Körner, C. (2012). Global patterns of mobile carbon stores in trees at the high-elevation tree line. *Glob. Ecol. Biogeogr.* 21, 861–871. doi: 10.1111/j.1466-8238.2011.00731.x

Hoch, G., Popp, M., and Körner, C. (2002). Altitudinal increase of mobile carbon pools in *Pinus cembra* suggests sink limitation of growth at the Swiss treeline. *Oikos* 98, 361–374. doi: 10.1034/j.1600-0706.2002.980301.x

Holdheide, W. (1951). "Anatomie mitteleuropäischer Gehölzrinden (mit mikrophotographischem Atlas)," in *Handbuch der Mikroskopie in der Technik*, 5th Edn, ed. H. Freund (Frankfurt-am-Main: Unschau Verlag), 193–367.

Hölttä, T., Mencuccini, M., and Nikinmaaa, E. (2009). Linking phloem function to structure: analysis with a coupled xylem-phloem transport model. *J. Theor. Biol.* 259, 325–337. doi: 10.1016/j.jtbi.2009.03.039

Jensen, K. H., Liesche, J., Bohr, T., and Schulz, A. (2012). Universality of phloem transport in seed plants. *Plant Cell. Environ.* 35, 1065–1076. doi: 10.1111/j.1365-3040.2011.02472.x

Jyske, T., and Hölttä, T. (2015). Comparison of phloem and xylem hydraulic architecture in *Picea abies* stems. *New Phytol.* 205, 102–115. doi: 10.1111/nph.12973

Jyske, T. M., Suuronen, J.-P., Pranovich, A. V., Laakso, T., Watanabe, U., Kuroda, K., et al. (2015). Seasonal variation in formation, structure, and chemical properties of phloem in *Picea abies* as studied by novel microtechniques. *Planta* 242, 613–629. doi: 10.1007/s00425-015-2347-8

Knoblauch, M., and Oparka, K. (2012). The structure of the phloem: still more questions than answers. *Plant J.* 70, 147–156. doi: 10.1111/j.1365-313X.2012.04931.x

Knoblauch, M., and van Bel, A. J. E. (1998). Sieve tubes in action. *Plant Cell* 10, 35–50. doi: 10.2307/3870627

Kondhare, K. R., Patil, N. S., and Banerjee, A. K. (2021). A historical overview of long-distance signalling in plants. *J. Exp. Bot.* 72, 4218–4236. doi: 10.1093/jxb/erab048

Körner, C. (1998). A re-assessment of high elevation treeline positions and their explanation. *Oecologia* 115, 445–459. doi: 10.1007/s004420050540

Körner, C. (2003). Carbon limitation in trees. *J. Ecol.* 91, 4–17. doi: 10.1046/j.1365-2745.2003.00742.x

Körner, C. (2012). *Alpine Treelines. Functional Ecology of the Global High Elevation Tree Limits*. Basel: Springer.

Körner, C. (2015). Paradigm shift in plant growth control. *Curr. Opin. Plant Biol.* 25, 107–114. doi: 10.1016/j.pbi.2015.05.003

Körner, C. (2021). *Alpine Plant Life*, 3rd Edn. Berlin: Springer.

Körner, C., and Paulsen, J. (2004). A world-wide study of high altitude treeline temperatures. *J. Biogeogr.* 31, 713–732. doi: 10.1111/j.1365-2699.2003.01043.x

Kubisch, P., Leuschner, C., Coners, H., Gruber, A., and Hertel, D. (2017). Fine root abundance and dynamics of stone Pine (*Pinus cembra*) at the alpine treeline is not impaired by self-shading. *Front. Plant Sci.* 8:602. doi: 10.3389/fpls.2017.00602

Lacombe, B., and Achard, P. (2016). Long-distance transport of phytohormones through the plant vascular system. *Curr. Opin. Plant Biol.* 34, 1–8. doi: 10.1016/j.pbi.2016.06.007

Larcher, W. (2003). *Physiological Plant Ecology. Ecophysiology and Stress Physiology of Functional Groups*. Berlin: Springer-Verlag.

Larson, P. R. (1994). *The Vascular Cambium: Development and Structure*. Berlin: Springer-Verlag.

Leuschner, C., and Ellenberg, H. (2017). *Ecology of Central European forests. Vegetation Ecology of Central Europe*, Vol. 1. Berlin: Springer.

Liesche, J., Pace, M. R., Xu, Q., Li, Y., and Chen, S. (2017). Height-related scaling of phloem anatomy and the evolution of sieve element end wall types in woody plants. *New Phytol.* 214, 245–256. doi: 10.1111/nph.14360

Liesche, J., Windt, C., Bohr, T., Schulz, A., and Hartvig Jensen, K. (2015). Slower phloem transport in gymnosperm trees can be attributed to higher sieve element resistance. *Tree Physiol.* 35, 376–386. doi: 10.1093/treephys/tpv020

Lupi, C., Morin, H., Deslauriers, A., and Rossi, S. (2010). Xylem phenology and wood production: resolving the chicken-or-egg dilemma. *Plant Cell. Environ.* 33, 1721–1730. doi: 10.1111/j.1365-3040.2010.02176.x

Mayr, S., Schwienbacher, F., and Bauer, H. (2003). Winter at the Alpine timberline: why does embolism occur in Norway spruce but not in stone pine? *Plant Physiol.* 131, 780–792. doi: 10.1104/pp.011452

Mayr, S., Wolfschwenger, M., and Bauer, H. (2002). Winter-drought induced embolism in Norway spruce (*Picea abies*) at the Alpine timberline. *Physiol. Plant* 115, 74–80. doi: 10.1034/j.1399-3054.2002.1150108.x

McNairn, R. B. (1972). Phloem translocation and heat-induced callose formation in field-grown *Gossypium hirsutum* L. *Plant Physiol.* 50, 366–370. doi: 10.1104/pp.50.3.366

Meentemeyer, V. (1977). "Climatic regulation of decomposition rates of organic matter in terrestrial ecosystems," in *Proceedings of the Environmental Chemistry and Cycling Processes. Department of Energy Symposium Series CONF-760429*, eds D. C. Adrians and I. L. Brisbin (Washington, DC: U.S. Department of Energy), 779–789.

Miller, T. W., Stangler, D. F., Larysch, E., Seifert, T., Spiecker, H., and Kahle, H. P. (2020). Plasticity of seasonal xylem and phloem production of Norway spruce along an elevational gradient. *Trees* 34, 1281–1297. doi: 10.1007/s00468-020-01997-6

Montwe, D., Hacke, U., Schreiber, S. G., and Stanfield, R. C. (2019). Seasonal vascular tissue formation in four boreal tree species with a focus on callose deposition in the phloem. *Front. For. Glob. Change* 2:58. doi: 10.3389/ffgc.2019.00058

Mullendore, D. L., Windt, C. W., Van As, H., and Knoblauch, M. (2010). Sieve tube geometry in relation to phloem flow. *Plant Cell* 22, 579–593. doi: 10.1105/tpc.109.070094

Neuberger, D. S., and Evert, R. F. (1975). Structure and development of sieve areas in the hypocotyl of *Pinus resinosa*. *Protoplasma* 84, 109–125. doi: 10.1007/BF02075947

Palacio, S., Hoch, G., Sala, A., Körner, C., and Millard, P. (2014). Does carbon storage limit tree growth? *New Phytol.* 201, 1096–1100. doi: 10.1111/nph.12602

Pfautsch, S., Hölttä, T., and Mencuccini, M. (2015). Hydraulic functioning of tree stems–fusing ray anatomy, radial transfer and capacitance. *Tree Physiol.* 35, 706–722. doi: 10.1093/treephys/tpv058

Plomion, C., Leprovost, G., and Stokes, A. (2001). Wood formation in trees. *Plant Physiol.* 127, 1513–1523. doi: 10.1104/pp.010816

Prislan, P., Gričar, J., de Luis, M., Smith, K. T., and Čufar, K. (2013). Phenological variation in xylem and phloem formation in *Fagus sylvatica* from two contrasting sites. *Agric. For. Meteorol.* 180, 142–151. doi: 10.1016/j.agrformet.2013.06.001

Prislan, P., Mrak, P., Žnidaršič, N., Štrus, J., Humar, M., Thaler, N., et al. (2019). Intra-annual dynamics of phloem formation and ultrastructural changes in sieve tubes in *Fagus sylvatica*. *Tree Physiol.* 39, 262–274. doi: 10.1093/treephys/tpy102

Rosner, S., Baier, P., and Kikuta, S. (2001). Osmotic potential of Norway Spruce (*Picea abies* (L.) Karst.) secondary phloem in relation to anatomy. *Trees* 15, 472–482. doi: 10.1007/s00468-001-0131-9

Rossi, S., Deslauriers, A., Anfodillo, T., and Carraro, V. (2007). Evidence of threshold temperatures for xylogenesis in conifers at high altitudes. *Oecologia* 152, 1–12.

Rossi, S., Deslauriers, A., Anfodillo, T., Morin, H., Saracino, A., Motta, R., et al. (2006). Conifers in cold environments synchronize maximum growth rate of tree-ring formation with day length. *New Phytol.* 170, 301–310. doi: 10.1111/j.1469-8137.2006.01660.x

Rossi, S., Deslauriers, A., Gričar, J., Seo, J. W., Rathgeber, C. B. K., Anfodillo, T., et al. (2008). Critical temperatures for xylogenesis in conifers of cold climates. *Glob. Ecol. Biogeogr.* 17, 696–707. doi: 10.1111/j.1466-8238.2008.00417.x

Ryan, M. G., and Robert, E. M. R. (2017). Zero-calorie sugar delivery to roots. *Nat. Plants* 3, 922–923. doi: 10.1038/s41477-017-0070-0

Salmon, Y., Dietrich, L., Sevanto, S., Hölttä, T., Dannoura, M., and Epron, D. (2019). Drought impacts on tree phloem: from cell-level responses to ecological significance. *Tree Physiol.* 39, 173–191. doi: 10.1093/treephys/tpy153

Savage, J. A., and Chuine, I. (2021). Coordination of spring vascular and organ phenology in deciduous angiosperms growing in seasonally cold climates. *New Phytol.* 230, 1700–1715. doi: 10.1111/nph.17289

Savage, J. A., Clearwater, M. J., Haines, D. F., Klein, T., Mencuccini, M., Sevanto, S., et al. (2016). Allocation, stress tolerance and carbon transport in plants: how does phloem physiology affect plant ecology? *Plant Cell. Environ.* 39, 709–725. doi: 10.1111/pce.12602

Schenker, G., Lenz, A., Körner, C., and Hoch, G. (2014). Physiological minimum temperatures for root growth in seven common European broad-leaved tree species. *Tree Physiol.* 34, 302–313. doi: 10.1093/treephys/tpu003

Schulz, A., and Thompson, G. A. (2009). *Phloem Structure and Function: Encyclopedia of Life Sciences (eLS)*. 2nd Edn, Wiley. doi: 10.1002/9780470015902.a0001290.pub2

Sevanto, S. (2018). Drought impacts on phloem transport. *Curr. Opin. Plant Biol.* 43, 76–81. doi: 10.1016/j.pbi.2018.01.002

Swidrak, I., Gruber, A., and Oberhuber, W. (2014). Xylem and phloem phenology in co-occurring conifers exposed to drought. *Trees* 28, 1161–1171. doi: 10.1007/s00468-014-1026-x

van Bel, A. J. E. (1990). Xylem-phloem exchange via the rays: the undervalued route of transport. *J. Exp. Bot.* 41, 631–644. doi: 10.1093/jxb/41.6.631

van Bel, A. J. E. (2003). The phloem, a miracle of ingenuity. *Plant Cell. Environ.* 26, 125–149. doi: 10.1046/j.1365-3040.2003.00963.x

Wang, Y., Čufar, K., Eckstein, D., and Liang, E. (2012). Variation of maximum tree height and annual shoot growth of Smith fir at various elevations in the Sygera Mountains, southeastern Tibetan Plateau. *PLoS One* 7:e31725. doi: 10.1371/journal.pone.0031725

Weih, M., and Karlsson, P. S. (2001). Growth response of mountain birch to air and soil temperature: is increasing leaf-nitrogen content an acclimation to lower air temperature? *New Phytol.* 150, 147–155. doi: 10.1046/j.1469-8137.2001.00078.x

Weih, M., and Karlsson, P. S. (2002). Low winter soil temperature affects summertime nutrient uptake capacity and growth rate of mountain birch seedlings in the subarctic, Swedish Lapland. *Arct. Antarct. Alp. Res.* 34, 434–439. doi: 10.1080/15230430.2002.12003514

Weng, J. H., Liao, T. S., Sun, K. H., Chung, J. C., Lin, C. P., and Chu, C. H. (2005). Seasonal variations in photosynthesis of *Picea morrisonicola* growing in the subalpine region of subtropical Taiwan. *Tree Physiol.* 25, 973–979. doi: 10.1093/treephys/25.8.973

Conflict of Interest: The authors declare that the research was conducted in the absence of any commercial or financial relationships that could be construed as a potential conflict of interest.

Publisher's Note: All claims expressed in this article are solely those of the authors and do not necessarily represent those of their affiliated organizations, or those of the publisher, the editors and the reviewers. Any product that may be evaluated in this article, or claim that may be made by its manufacturer, is not guaranteed or endorsed by the publisher.

frontiers in Ecology and Evolution

ORIGINAL RESEARCH
published: 07 December 2021
doi: 10.3389/fevo.2021.722964

Directional Selection on Tree Seedling Traits Driven by Experimental Drought Differs Between Mesic and Dry Populations

João Costa e Silva[1], Rebecca Jordan[2,3], Brad M. Potts[3,4], Elizabeth Pinkard[2] and Suzanne M. Prober[5]*

[1] Centro de Estudos Florestais, Instituto Superior de Agronomia, Universidade de Lisboa, Lisbon, Portugal, [2] CSIRO, Land and Water, Sandy Bay, TAS, Australia, [3] School of Natural Sciences, University of Tasmania, Hobart, TAS, Australia, [4] ARC Training Centre for Forest Value, University of Tasmania, Hobart, TAS, Australia, [5] CSIRO, Land and Water, Floreat, WA, Australia

We evaluated population differences and drought-induced phenotypic selection on four seedling traits of the Australian forest tree *Eucalyptus pauciflora* using a glasshouse dry-down experiment. We compared dry and mesic populations and tested for directional selection on lamina length (reflecting leaf size), leaf shape, the node of ontogenetic transition to the petiolate leaf (reflecting the loss of vegetative juvenility), and lignotuber size (reflecting a recovery trait). On average, the dry population had smaller and broader leaves, greater retention of the juvenile leaf state and larger lignotubers than the mesic population, but the populations did not differ in seedling survival. While there was statistical support for directional selection acting on the focal traits in one or other population, and for differences between populations in selection gradient estimates for two traits, only one trait—lamina length—exhibited a pattern of directional selection consistent with the observed population differences being a result of past adaptation to reduce seedling susceptibility to acute drought. The observed directional selection for lamina length in the mesic population suggests that future increases in drought risk in the wild will shift the mean of the mesic population toward that of the dry population. Further, we provide evidence suggesting an early age trade-off between drought damage and recovery traits, with phenotypes which develop larger lignotubers early being more susceptible to drought death. Such trade-offs could have contributed to the absence of population mean differences in survival, despite marked differentiation in seedling traits.

Keywords: adaptation to drought, trade-off, leaf length and shape, vegetative juvenility, lignotuber size, selection gradient, generalized linear mixed model, *Eucalyptus pauciflora*

OPEN ACCESS

Edited by:
Carsten Kulheim, Michigan Technological University, United States

Reviewed by:
Daniel J. Ballhorn, Portland State University, United States
Matthew Larcombe, University of Otago, New Zealand

****Correspondence:***
João Costa e Silva
jces@isa.ulisboa.pt

Specialty section:
This article was submitted to Chemical Ecology, a section of the journal Frontiers in Ecology and Evolution

Received: *09 June 2021*
Accepted: *08 November 2021*
Published: *07 December 2021*

Citation:
Costa e Silva J, Jordan R, Potts BM, Pinkard E and Prober SM (2021) Directional Selection on Tree Seedling Traits Driven by Experimental Drought Differs Between Mesic and Dry Populations. Front. Ecol. Evol. 9:722964. doi: 10.3389/fevo.2021.722964

INTRODUCTION

Global warming is leading to major shifts in the distribution of plant and animal species globally (Chen et al., 2011). Sessile species, such as forest trees, are among the most vulnerable owing to their often poor dispersal abilities and long life histories (Petit and Hampe, 2006). Already, extreme climate events causing heat and drought stress have been linked directly (Allen et al., 2010; Matusick et al., 2013) and indirectly (Buotte et al., 2016) to forest dieback in many parts of the world. Ongoing climate change is expected to exacerbate such stresses (Allen et al., 2010; Schwalm et al., 2017), and it has long been argued that the rate of climate change may exceed the adaptive capacity of tree populations (Davis and Shaw, 2001; Jump and Peñuelas, 2005; Aitken et al., 2008).

Tree adaptation to major environmental gradients such as aridity is polygenic and genome-wide (Kramer et al., 2015; Jordan et al., 2017; Steane et al., 2017), involves diverse functional traits (Alberto et al., 2013; Kremer et al., 2014), and potentially also genetic constraints (Bourne et al., 2017; Costa e Silva et al., 2020). Detecting adaptive changes in local populations of long-lived organisms, such as forest trees, is difficult due to numerous factors (Alberto et al., 2013), including long-life cycles (Petit and Hampe, 2006), ontogenetic (Brunner et al., 2016) and plastic (Nicotra et al., 2010; McLean et al., 2014) changes in phenotype, superimposed on the normal selective filtering of mal-adapted inbred progeny during stand development (Koelewijn et al., 1999; Costa e Silva et al., 2011; Griffin et al., 2019). Molecular markers are often used to detect signatures of adaptive genetic variation in tree species (Keller et al., 2012; Alberto et al., 2013; Dillon et al., 2014; Pluess et al., 2016; Frachon et al., 2018) and, as the effects of putative adaptive markers/SNPs become validated, there will be increasing opportunity for their use to monitor adaptive changes in forest tree populations following selection. However, traditional analysis of phenotypic selection and quantitative genetic studies of functional traits continue to provide valuable insights into the effects of natural selection, and have been applied in many animal and plant species (Kingsolver et al., 2001, 2012; Shaw and Etterson, 2012; Merilä and Hendry, 2014). Despite this, there is a paucity of empirical studies in forest tree populations that address the adaptive value of functional traits through their impact on fitness components (Gómez, 2004; Alberto et al., 2013; Ramírez-Valiente et al., 2014, 2015; Costa e Silva et al., 2018; Warwell and Shaw, 2018, 2019), as is the case for most long-lived species (Monica and Lauren, 2003).

Lande and Arnold (1983) developed a least-squares multiple regression framework for the analysis of phenotypic selection based on the relationship between relative fitness (i.e., the fitness of an individual divided by the mean fitness of the population) and phenotypic measures for a set of traits. This approach assumes a causal fitness-trait relationship, such that a trait (or a trait combination) is expected to be under selection when significantly influencing fitness. The partial regression coefficients thus represent selection gradients that quantify the direct effects of trait variables on relative fitness, and the complete model with linear, quadratic and cross-product terms provides a quadratic approximation to the individual fitness surface (Phillips and Arnold, 1989). In particular, by characterizing directional selection, the linear selection gradient has a direct application in the prediction of evolutionary change between generations, under the assumption of multivariate normal distribution of breeding values (Lande, 1979). Fitness components used to evaluate selection commonly involve discrete variables (e.g., viability and fecundity measured by survival and the number of offspring), and generalized linear models have been described for the estimation of selection gradients with non-normal distributions of fitness responses (Janzen and Stern, 1998; Morrissey and Sakrejda, 2013).

Numerous studies have shown significant directional selection in wild populations (Kingsolver and Diamond, 2011; Kingsolver et al., 2012; Siepielski et al., 2013). Such selection can vary with time/seasons (Siepielski et al., 2009; Steele et al., 2011; Ramírez-Valiente et al., 2014, 2015; Warwell and Shaw, 2018, 2019) and environment (Dudley, 1996; Etterson, 2004; Heschel and Riginos, 2005; Donovan et al., 2009; Lau et al., 2014; Warwell and Shaw, 2018), and this variation drives population divergence and local adaptation within a species (Siepielski et al., 2013; Hendry, 2017). However, there are often multiple phenotypic solutions to the same adaptive requirement (e.g., drought survival—McDowell et al., 2011; Choat et al., 2018; Klein et al., 2018) and increasing evidence from common-garden trials that the focal traits under selection can be population specific (Dudley, 1996; Etterson, 2004; Heschel and Riginos, 2005; Donovan et al., 2009). Understanding population differences in the focal traits under selection following the same selection event can allow insights into functional traits that may be underlying local adaptation (Dudley, 1996; Monica and Lauren, 2003) and how these vary within a species. Such understanding is a key step toward evaluating the effects of selection due to, for example, climate change (Hoffmann and Sgro, 2011; Alberto et al., 2013; Merilä and Hendry, 2014), including outcomes for different populations or parts of the species distribution.

The present study focuses on the Australian tree species *Eucalyptus pauciflora* Sieber ex Spreng.. *Eucalyptus pauciflora* has one of the broadest altitudinal ranges of any eucalypt species (i.e., growing from sea-level to near the alpine tree line on both continental Australia and the island of Tasmania), and is one of the main tree species used for ecological restoration in the dry midlands of Tasmania (Prober et al., 2016; Bailey et al., 2021). Climate change is predicted to result in most Tasmanian *E. pauciflora* populations being outside the contemporary climate envelope of the species and at risk of maladaptation by 2080 (Harrison, 2017). This risk of maladaptation mainly reflects the predicted increasing temperatures and evapotranspiration across Tasmania (Corney et al., 2010; Harrison et al., 2017), and thus increased risk of drought stress. Both water deficit and high temperatures contribute to drought stress (Park Williams et al., 2013; Duan et al., 2014; Mitchell et al., 2014) and could, independently or combined, drive selection on plant traits (Costa e Silva et al., 2019). The challenge in understanding adaptation is to unravel these multiple effects. Here we focus on just a single factor—water deficit, which has both plastic (Cano et al., 2014; Duan et al., 2014; McKiernan et al., 2016) and genetic-based (Ammitzboll et al., 2020) selective impacts on eucalypt seedlings.

As with other forest tree studies on drought-induced selection (e.g., Warwell and Shaw, 2019), we focused on the seedling life stage as: (i) there is usually significant seedling mortality in wild and planted eucalypt populations, with water deficit being the most common cause (Battaglia and Reid, 1993; Stoneman, 1994; Tozer and Bradstock, 1998); (ii) the phenotypic and genetic variation in morphological traits at this life stage has been well-characterized in *E. pauciflora* (Gauli et al., 2015); and (iii) there are signals that variation in some seedling morphological traits of *E. pauciflora* is adaptive (Gauli et al., 2015; Costa e Silva et al., 2019). We specifically aimed to: (1) assess the difference between dry and mesic populations in four seedling traits that potentially may influence the plant's response to acute drought; (2) evaluate the consequences of the variation in the focal seedling traits on fitness in each population; and (3) estimate whether the

relationship between fitness and the focal traits differs between populations. We hypothesized that, if selection acting on the studied traits via seedling survival was driven by acute drought stress in wild populations, then an imposed artificial drought would elicit a shift in character states of the mesic population toward those of the dry population.

MATERIALS AND METHODS

Populations Studied

The current study used seedlings from two populations of *E. pauciflora*, which were grown in a common-garden glasshouse trial subject to an artificial drought. These two lowland Tasmanian populations were from Brushy Lagoon and Ross, and were from mesic and dry parts of the climatic range of *E. pauciflora* on the island, respectively. These populations were selected to accentuate rainfall differences and minimize the differences in other environmental factors. The mean annual precipitation at Ross is nearly 50% lower than at Brushy Lagoon, but Ross also has a slightly higher mean maximum temperature of the warmest period than Brushy Lagoon (**Table 1**). These populations are located over 90 km apart, well-exceeding the distance of significant genetic spatial autocorrelation in the species (i.e., 27 km—Gauli et al., 2013). The populations have similar high outcrossing rates (Gauli et al., 2013) and inbreeding levels in their open-pollinated progeny (Gauli et al., 2014), but differ markedly in numerous seedling traits (Gauli et al., 2015).

Drought Experiment

Each population was represented by 12 families corresponding to 12 mother-trees randomly selected within native stands and situated by more than two canopy heights apart. The seedlings of each family were obtained from open-pollinated seeds collected randomly from near the middle of the canopy of the mother-tree. Seedlings from these families were grown in soil-filled pots (9 cm × 9 cm × 18 cm) and, when the plants were 14-week-old, the pots were arranged into an experimental design for imposing drought stress under glasshouse conditions. The experiment was conducted in two glasshouses, though a large portion of window panels were removed so that seedlings were exposed to ambient air conditions. Temperature and relative humidity were similar between the two glasshouses, and temperature reflected external ambient air temperature over the duration of the experiment (**Supplementary Figure 1**). Over the course of the dry-down period, the average daily maximum temperature inside the glasshouses was 16.9 and 16.0°C, and the average daily minimum temperatures were 6.5 and 6.8°C. Daily maxima did not exceed 27°C and daily minima did not go below −1°C. Humidity ranged from an average daily maximum of 88.5 and 90.9% to an average daily minimum of 51.6 and 58.5% in the two glasshouses, respectively. The experimental layout was effectively a split-plot design comprising four replicates (blocks), two in each glasshouse. Each replicate included two main plots (hereafter denoted as population plots), one of the Brushy Lagoon families and one of the Ross families, and families were randomized as single-tree plots within these population plots. Overall, there were 387 and 386 seedlings in the Brushy Lagoon and Ross populations, respectively, available for analysis. Across the experiment, the sizes of the population plots varied between 92 and 101 seedlings in Brushy Lagoon, and between 93 and 100 seedlings in Ross. The family sizes across all four replicates ranged from 22 to 38 seedlings in Brushy Lagoon, and from 19 to 38 seedlings in Ross, with an average of 32 seedlings per family in both populations. The degree of unbalance in family sizes was moderate: the variation of family sizes as measured by the coefficient of variation was 16% in both populations.

The water deficit treatment was applied using floral foam, in a manner adapted from Fernández and Reynolds (2000) and Marchin et al. (2020). Each population plot consisted of a water basin containing a layer of floral foam (Oasis Ideal Standard Super 60; Apack Pty Ltd., Dandenong South, Australia). Potted seedlings were placed on the foam, with a small amount of fine washed sand in drainage holes to ensure effective contact with foam. Water basins were topped up twice daily to within approximately 10 cm from the top of the foam, enabling self-watering by wicking, though with reduced water availability for plants (see Marchin et al., 2020). Exposed foam, above the top of the water basins, was wrapped in plastic to minimize water loss through evaporation.

After placing seedlings in the experimental design, they were left to acclimate for 10 days, over which time morphometric measurements were taken from the seedlings (see below). After 10 days, no further water was added to the water basins, initiating the drought component of the experiment. At the end of the experiment 67 days later, seedling survival was scored as a binary outcome, based on the following assessments: a seedling was classified as dead (scored as 0) when all leaves, including laterals, and the apical meristem had dried out; otherwise it was classified as alive (scored as 1). As scored, seedling survival refers to observable "canopy" mortality immediately following termination of the dry-down experiment, and does not account for the possibility of differential recovery if rewatering had occurred. This measure of seedling survival was used as a fitness component for individuals in the analysis of phenotypic selection.

Trait Measurements

Phenotypic trait measurements were taken from the seedlings during the 10-day acclimation period. At this time, a single leaf was sampled from the third pair of leaves up the main stem (cotyledonary node = 0), and individually digitally photographed with a constant size scale for the measurement of leaf dimensions (see below). Following the removal of the third-node leaf, these seedlings were also measured for the lignotuber diameter—i.e., the diameter (mm) across the lignotubers developed in the axils of the cotyledons—and for the stem diameter (mm) perpendicular to the axis of maximum lignotuber diameter. The seedling height (cm) and the node number of the first petiolate leaf (counted from the cotyledonary node) were also recorded. The node number of the first petiolate leaf is a trait that reflects the ontogenetic transition from sessile (juvenile) to petiolate (mature) leaves in *Eucalyptus* spp., and is hereafter referred to as "vegetative juvenility" (i.e., the higher the node number, the later the petiole development is in nodes, and thus

TABLE 1 | Population information for the mesic (Brushy Lagoon) and dry (Ross) populations of *Eucalyptus pauciflora* used in the dry-down experiment.

Population	Latitude (°)	Longitude (°)	Altitude (m)	RANN (mm)	TMXWM (°C)	*n*
Brushy Lagoon	−41.4094	146.7470	265	974	22.6	387
Ross	−42.0017	147.5323	240	503	23.9	386

RANN = mean annual precipitation; TMXWM = mean maximum temperature of the warmest period (weekly values); n = number of seedlings used in final analysis.

the more the seedling is vegetatively juvenile). Leaf dimensions were manually measured from the digital images of the seedling leaves, and included the lamina length (mm) and lamina width (mm). In the present study, seedling leaf morphology, lignotuber size and vegetative juvenility were represented by four functional traits—lamina length, leaf shape index, adjusted lignotuber size and vegetative juvenility (see below). Photos of lignotubers and vegetative juvenility in seedlings of *E. pauciflora* are provided in Figure 3 of Costa e Silva et al. (2019).

Data Analyses

The data analyses entailed two main components. Firstly, population mean differentiation and variance estimation were addressed for the focal functional traits and seedling survival. Then, phenotypic selection analysis was pursued within populations to measure directional selection acting on the focal traits through seedling survival, and differences between populations in estimated selection gradients for a trait were subsequently evaluated. To account for the inherent positive allometric relationship between lamina length and lamina width, the lamina width measurements were adjusted for seedling differences in lamina length in the data analyses. The adjusted lamina width thus provides a measure that reflects leaf shape, and is hereafter denoted as "leaf shape index" (with increasing values meaning broader leaves). The lignotuber diameter measurement is also inherently dependent on stem diameter and, following Costa e Silva et al. (2019), was also adjusted in the data analyses to provide a measure independent of stem diameter, hereafter referred to as "adjusted lignotuber size." Finally, in addition to the focal traits, seedling height and stem diameter were modeled as "nuisance variables" in the phenotypic selection analysis. This was done to account for the effects of initial plant size on drought-induced mortality, as the seedlings were growing in pots with a defined soil volume, and bigger plants are expected to inherently use more water (Ammitzboll et al., 2020).

The SAS 9.4 software (SAS, 2017) was used in the data analyses. In particular, linear mixed models were estimated with the procedure MIXED, and generalized linear mixed models were estimated with the procedures GLIMMIX and NLMIXED.

Linear Mixed Model for the Continuous Variables (Lamina Length, Leaf Shape Index and Adjusted Lignotuber Size)

The following linear mixed model (LMM) was fitted for the continuous variables:

$$\mathbf{y} = \mathbf{X}\boldsymbol{\beta} + \mathbf{Z}_1\mathbf{b}_1 + \mathbf{Z}_2\mathbf{b}_2 + \mathbf{e} \quad (1)$$

where $\mathbf{y}$ is a n x 1 vector of observations (n = total number of seedlings in the experiment); $\boldsymbol{\beta}$ is a $p \times 1$ vector of fixed-effect parameters; $\mathbf{b}_1$ and $\mathbf{b}_2$ are $q \times 1$ vectors of random-effect parameters for families within the Brushy Lagoon and Ross populations, respectively; $\mathbf{X}$ is a design matrix relating $\mathbf{y}$ to the parameters in $\boldsymbol{\beta}$; $\mathbf{Z}_1$ and $\mathbf{Z}_2$ are design matrices relating $\mathbf{y}$ to the random effects in $\mathbf{b}_1$ and $\mathbf{b}_2$, respectively; $\mathbf{e}$ is a $n \times 1$ vector of residuals of the observations. The vector $\boldsymbol{\beta}$ included the intercept, and effects for population, block and population-by-block interaction for all traits. The analyses of leaf shape index and adjusted lignotuber size involved the adjustment of the lamina width and lignotuber diameter measurements using lamina length and stem diameter as covariates, respectively. In these cases, $\boldsymbol{\beta}$ included also the corresponding coefficients for the regression parameter and its interaction with population. The family effects and residuals were modeled by considering a heterogeneous variance structure at the population level. In this sense, it was assumed that $\begin{pmatrix}\mathbf{b}_1\\ \mathbf{b}_2\end{pmatrix} \sim MVN(\mathbf{0}, \mathbf{G})$, with $\mathbf{G} = \begin{bmatrix}\mathbf{I}_{q_1}\sigma^2_{b_1} & 0\\ 0 & \mathbf{I}_{q_2}\sigma^2_{b_2}\end{bmatrix}$, where $\sigma^2_{b_1}$ and $\sigma^2_{b_2}$ are family variances in Brushy Lagoon and Ross, respectively; $\mathbf{I}_{q_1}$ and $\mathbf{I}_{q_2}$ are identity matrices of dimension equal to the number of families in Brushy Lagoon (q_1) and Ross (q_2). Conditional on the family random effects, the residuals were assumed $\begin{pmatrix}\mathbf{e}_1\\ \mathbf{e}_2\end{pmatrix} \sim MVN(\mathbf{0}, \mathbf{R})$, with $\mathbf{R} = \begin{bmatrix}\mathbf{I}_{n_1}\sigma^2_{e_1} & 0\\ 0 & \mathbf{I}_{n_2}\sigma^2_{e_2}\end{bmatrix}$, where $\sigma^2_{e_1}$ and $\sigma^2_{e_2}$ are residual variances in Brushy Lagoon and Ross, respectively; $\mathbf{I}_{n_1}$ and $\mathbf{I}_{n_2}$ are identity matrices of dimension equal to the number of seedlings in Brushy Lagoon (n_1) and Ross (n_2); it was further assumed that the residuals and random effects were independent. Visual inspection of histograms and quantile-quantile plots of conditional studentized residuals showed residual distributions conforming reasonably well to a normal distribution for all traits. In addition, the residuals did not appear to co-vary with random effects, as generally indicated by small and statistically non-significant correlations estimated within either population. The (co)variance structure of $\mathbf{y}$ was defined by $\mathbf{V} = \mathbf{ZGZ}' + \mathbf{R}$, where $\mathbf{Z} = \begin{bmatrix}\mathbf{Z}_1 & 0\\ 0 & \mathbf{Z}_2\end{bmatrix}$; through $\mathbf{G}$, the $\mathbf{V}$-matrix captures the covariance of the observations within families, which will be reflected in the estimation of the fixed-effect parameters and their standard errors (Raudenbush and Bryk, 2002; see next paragraph).

The variances in $\mathbf{G}$ and $\mathbf{R}$ were estimated by restricted maximum likelihood (REML; Patterson and Thompson, 1971). Following the estimation of variance components, fixed-effect parameters were estimated by generalized least-squares, i.e. $\hat{\boldsymbol{\beta}} = (\mathbf{X}'\hat{\mathbf{V}}^{-1}\mathbf{X})^{-1}\mathbf{X}'\hat{\mathbf{V}}^{-1}\mathbf{y}$, with the associated

model-based sampling (co)variance matrix being given by $Var(\hat{\boldsymbol{\beta}}) = (\mathbf{X}'\hat{\mathbf{V}}^{-1}\mathbf{X})^{-1}$. This matrix was corrected by using the Kenward-Roger (KR) adjustment, to provide estimates of standard errors of $\hat{\boldsymbol{\beta}}$ that account for potential finite-sample bias and the uncertainty in the estimation of **G** and **R** (Kenward and Roger, 2009). Based on a corrected $Var(\hat{\boldsymbol{\beta}})$ matrix, the Kenward and Roger (1997, 2009) approximation to compute denominator degrees of freedom was applied to improve statistical inference about the fixed effects. For sample sizes comparable to the number of families and the within-family sizes in our study, simulation work with LMMs using REML indicated that applying the KR method to fixed-effect parameters produced accurate estimates of standard errors, and maintained Type-I error rates and confidence interval coverage close to the specified ($\alpha = 0.05$) nominal level (Ferron et al., 2009; Baldwin and Fellingham, 2013; McNeish and Stapleton, 2016a; see also **Supplementary Methods 1**).

Statistical inference about the fixed-effect model terms was based on *F*-tests, which indicated that the interactions of population with blocks, and with either lamina length or stem diameter used as covariates (in the LMM for leaf shape index or adjusted lignotuber size, respectively), were not statistically significant ($p > 0.05$). Thus, a final LMM without the interaction terms was then fitted for all traits. One-sided likelihood ratio tests (Self and Liang, 1987) were applied to assess whether estimated family variances were significantly greater than zero. In preliminary analyses, a one-sided likelihood ratio test was also used to test the variance estimate associated with a random term modeling a block-by-family interaction: as no significant effects were detected (suggesting an efficient randomization of seedlings within blocks), the interaction term was excluded in the LMM defined in Equation (1). The population least-squares mean (LS-Mean) for a trait was calculated with a linear function of $\hat{\boldsymbol{\beta}}$ estimates, i.e. $\mathbf{L}\hat{\boldsymbol{\beta}}$, where **L** is the coefficient matrix pertaining to the LS-Mean. The standard error of a LS-Mean estimate was approximated by the square-root of $\mathbf{L}Var(\hat{\boldsymbol{\beta}})\mathbf{L}'$. The KR approximation for computation of degrees of freedom was also applied to obtain the critical values for the student's *t*-distribution used for estimating the 95% confidence interval of a LS-Mean.

Generalized Linear Mixed Model for the Discrete Variables (Seedling Survival and Vegetative Juvenility)

The following generalized linear mixed model (GLMM) was fitted for the discrete variables:

$$g(E(\mathbf{y} \mid \mathbf{X},\ \mathbf{b}_1,\ \mathbf{b}_2)) = g(\boldsymbol{\mu}) = \mathbf{X}\boldsymbol{\beta} + \mathbf{Z}_1\mathbf{b}_1 + \mathbf{Z}_2\mathbf{b}_2 \quad (2)$$

where $g(.)$ is a link function relating the conditional expectation [i.e. $E(\mathbf{y} \mid \mathbf{X},\ \mathbf{b}_1,\ \mathbf{b}_2) = \boldsymbol{\mu}$, where $\boldsymbol{\mu}$ is the mean vector] of the response variable to the linear predictor $\boldsymbol{\eta} = \mathbf{X}\boldsymbol{\beta} + \mathbf{Z}_1\mathbf{b}_1 + \mathbf{Z}_2\mathbf{b}_2$; the vectors and matrices in $\boldsymbol{\eta}$ were defined as in Equation (1) (except that $\boldsymbol{\eta}$ does not contain a definite error term, nor continuous covariates in **X** as in the LMMs for leaf shape index and adjusted lignotuber size); for $\mathbf{b}_1$ and $\mathbf{b}_2$, the model specification with heterogeneous variances and the distributional assumptions were the same as in the LMM. Conditional on the random effects, the observations were assumed to be independently distributed, with Bernoulli and Poisson distributions for the binary (seedling survival) and count (vegetative juvenility) variables, respectively. For the binary variable, $E(\mathbf{y} \mid \mathbf{X},\ \mathbf{b}_1,\ \mathbf{b}_2)$ is also the conditional probability of seedling survival [i.e. $P(\mathbf{y} = 1 \mid \mathbf{X},\ \mathbf{b}_1,\ \mathbf{b}_2)$]. The probit link function was used to model survival, such that $P(\mathbf{y} = 1 \mid \mathbf{X},\ \mathbf{b}_1,\ \mathbf{b}_2) = g^{-1}(\boldsymbol{\eta}) = \Phi(\mathbf{X}\boldsymbol{\beta} + \mathbf{Z}_1\mathbf{b}_1 + \mathbf{Z}_2\mathbf{b}_2)$, where $g^{-1}(.)$ is the inverse of $g(.)$ and $\Phi(.)$ is the standard normal cumulative distribution function. For vegetative juvenility, $g(.)$ was the logarithmic link function, and thus $E(\mathbf{y} \mid \mathbf{X},\ \mathbf{b}_1,\ \mathbf{b}_2) = g^{-1}(\boldsymbol{\eta}) = exp(\mathbf{X}\boldsymbol{\beta} + \mathbf{Z}_1\mathbf{b}_1 + \mathbf{Z}_2\mathbf{b}_2)$, where *exp* denotes the exponential function. The choice of the probit link function for seedling survival was based on the conclusions obtained by Hahn and Soyer (2005) with a random-intercept GLMM [i.e., akin to the model described in Equation (2)]. Previous GLMM analyses conducted separately in each population showed that the variance of the Pearson residuals was close to one for seedling survival, but was clearly smaller than one for vegetative juvenility, thus indicating that the GLMM for the latter trait was under-dispersed relative to the Poisson distribution. Consequently, as an alternative to the standard Poisson model, we used a quasi-Poisson GLMM for vegetative juvenility, under which the equi-dispersion assumption can be relaxed (Wedderburn, 1974; Gardner et al., 1995). The quasi-Poisson GLMM considered heterogeneity of dispersion effects at the population level, and further details are provided in **Supplementary Methods 2**.

Parameter estimation under the GLMMs fitted for the discrete variables was based on the residual pseudo-likelihood (RSPL) method, which enables extension of the concept of REML variance component estimation to the non-normal case (Wolfinger and O'Connell, 1993). Estimates of $\boldsymbol{\beta}$ were obtained by generalized least-squares, and the KR approximations described above were used to improve the model-based standard errors of $\hat{\boldsymbol{\beta}}$ and the statistical inference concerning fixed-effect model terms. For conditions covering those in the current study (i.e., sample sizes, survival prevalence, and mean vegetative juvenility), simulation work with cross-sectional clustered data indicated that RSPL together with the KR adjustments performed better than maximum likelihood (ML) methods, regarding the accuracy of estimates of the random-intercept variance (e.g., family variance) and the coverage of fixed-effect confidence intervals for binary and count variables (McNeish, 2016, 2019; see also **Supplementary Methods 1**).

Results from *F*-tests indicated that the fixed-effect term for the population-by-block interaction was significant ($p < 0.05$) for seedling survival, but not for vegetative juvenility; thus, the interaction term was excluded in a final GLMM for the latter trait only. The population LS-Mean for a variable was estimated on the linked scale by $\mathbf{L}\hat{\boldsymbol{\beta}}$ and then converted to the original scale via the inverse link transformation. The standard error of a LS-Mean on the original scale was approximated by $\phi(\mathbf{L}\hat{\boldsymbol{\beta}})$. stde$(\mathbf{L}\hat{\boldsymbol{\beta}})$ and $exp(\mathbf{L}\hat{\boldsymbol{\beta}})$. stde$(\mathbf{L}\hat{\boldsymbol{\beta}})$ for seedling survival and vegetative juvenility, respectively, where: $\phi(\mathbf{L}\hat{\boldsymbol{\beta}})$ is the probability density function of the standard normal distribution evaluated at $\mathbf{L}\hat{\boldsymbol{\beta}}$; and stde$(\mathbf{L}\hat{\boldsymbol{\beta}})$ is the estimated standard error of the LS-Mean on the linked scale. The 95% confidence interval of a LS-Mean on the original scale

was obtained by applying the inverse link transformation to the confidence limits on the linked scale.

Under the RSPL method, the absence of a true log-likelihood function for the overall optimization process precludes the comparison of nested models using likelihood ratio tests (e.g., Hedeker and Gibbons, 2006; McNeish, 2016). Nevertheless, for comparison with RSPL estimates, family variances were also estimated for seedling survival and vegetative juvenility using ML, which enabled their statistical significance to be assessed by one-sided likelihood ratio tests. In this context, the Conway-Maxwell Poisson (CMP) distribution was assumed in the GLMM fitted for vegetative juvenility, since the estimation of a **R**-side multiplicative dispersion parameter as in the quasi-Poisson model (see **Supplementary Methods 2**) is not permitted with ML methods (e.g., Capanu et al., 2013). The CMP distribution is a two-parameter generalized form of the Poisson distribution that allows the modeling of empirical distributions of count variables that are over- or under-dispersed relative to the Poisson distribution (Shmueli et al., 2005; Guikema and Goffelt, 2008). Details on the parameterization of the CMP distribution, and on the GLMM for joint modeling the mean response and dispersion of vegetative juvenility, are given in **Supplementary Methods 3**. The GLMM fitted for seedling survival was defined as in Equation (2). ML estimation of the model parameters was based on an adaptive Gaussian quadrature, which entails a numerical integration method to approximate the marginal log-likelihood of the data (Pinheiro and Bates, 1995); 10 quadrature points were used to integrate the likelihood function over the random-effects distribution.

For both the LMMs and GLMMs, the intra-class correlation (ICC) coefficient was calculated as the proportion of the total variance attributable to the family variance, and thus was used to measure the relative importance of the family variance for each variable. In particular, for vegetative juvenility and seedling survival, the ICCs were estimated as described by Nakagawa et al. (2017) (see **Supplementary Methods 4**).

Analysis of Phenotypic Selection

In the present study, we focused on the estimation of linear selection gradients to measure the direction and strength of directional selection acting on traits in each population, and then we evaluated the difference between populations in selection gradient estimates for a given trait. The analysis of phenotypic selection assessed the fitness consequences of variation in four traits—lamina length, leaf shape index, adjusted lignotuber size and vegetative juvenility—using seedling survival as a fitness component. In addition to the target traits, seedling height and stem diameter were modeled as "nuisance variables." Prior to analyses, the data were pre-processed as follows: (i) linear least-squares regression was used to pre-adjust lamina width and lignotuber diameter in a population for seedling differences in lamina length and stem diameter, respectively, and the adjusted observations (obtained from the regression residuals) were then mean standardized—these data thus refer to leaf shape index and adjusted lignotuber size; and (ii) the remaining variables were centered at their means and then mean-standardized in a population. Mean standardization has been suggested for comparing the strengths of selection estimates on a similar scale (Hereford et al., 2004), and scaling in relation to the mean is both permissible and meaningful for the independent variables used in the current analysis (Houle et al., 2011).

The analysis of phenotypic selection was undertaken separately in each population, with the GLMM fitted for seedling survival including: a vector $\boldsymbol{\beta}$ with the intercept, block effects, and the linear regression coefficients for the focal and nuisance variables; and a vector $\mathbf{b}$ of random effects for families within the population, assuming $\mathbf{b} \sim MVN(\mathbf{0}, \mathbf{G})$, with $\mathbf{G} = \mathbf{I}_q\sigma_b^2$. Akin to the GLMM described in Equation (2), $g(.)$ was the probit link function, and the model parameters were estimated by the RSPL algorithm.

As opposed to least-squares multiple regression, the marginal effect of a predictor variable (i.e., the partial effect of a unit change in the predictor on the probability of seedling survival) cannot be directly obtained from the estimates of $\boldsymbol{\beta}$ in the GLMM. In this context, for a focal variable, the directional selection gradient can be obtained from the average gradient of the estimated fitness surface, which can be approximated by averaging the slope of the fitness surface over the distribution of the phenotypic observations (Janzen and Stern, 1998; Morrissey and Sakrejda, 2013). This procedure was undertaken as follows: (i) the marginal effect at each observation point in the data was estimated for a given focal variable; (ii) the estimated marginal effects were averaged over all observations in a population; and (iii) the average of the marginal effects was standardized to the relative fitness scale (i.e., division by the population mean of seedling survival), yielding a measure that can be quantitatively interpretable as a selection gradient. Following these sequential steps, **Supplementary Methods 5** provides the methodological details used to obtain directional selection gradients, based on the model parameters estimated from the random-intercept GLMM fitted to the data of a given population. The resulting selection gradient estimates have a population-averaged interpretation (see **Supplementary Methods 5**), although this does not apply to the estimates of $\boldsymbol{\beta}$ from the GLMM, which have a conditional interpretation (e.g., Molenberghs et al., 2002; Gardiner et al., 2009; McNeish, 2016; see also **Supplementary Methods 7**).

Non-parametric bootstrap was used to obtain standard errors and 95% confidence intervals for the directional selection gradient estimates in a population, and for their differences between populations for a trait. Bootstrap samples were generated while preserving the conditional independence of seedlings within families. Further details on this procedure, and on the estimation of standard errors and 95% confidence intervals, are given in **Supplementary Methods 6**. Statistical support against a null hypothesis being true (i.e., against the absence of an effect for either a selection gradient in a population or its difference between populations) was provided by a 95% confidence interval not overlapping with zero. Although directional selection was the main focus of the current study, we also computed 95% confidence intervals from bootstrapping for quadratic and correlational selection gradients (with their estimation based on second derivatives approximated at each observation by second-order central finite differences; e.g., see Supplemental File, point 8.4, in Franklin and Morrissey, 2017). As these confidence

intervals overlapped with zero, the effects of non-linear selection were judged to be unimportant, and they will not be further considered here.

RESULTS

A diagrammatic summary of the overall results is provided in **Figure 1**. **Table 2** presents the estimates of LS-Means, and related results from statistical tests of the population effect, for four functional traits and the fitness component, measured in the mesic (Brushy Lagoon) and dry (Ross) populations. Results from statistical inference about all the fixed-effect model terms included in the final LMMs and GLMMs fitted to the continuous and discrete variables are shown in **Supplementary Tables 1**, **2**, respectively. When compared to the mesic population, the LS-Means in the dry population were lower for lamina length, and higher for leaf shape index, adjusted lignotuber size and vegetative juvenility. Population-mean differences were statistically significant at the 0.1% (lamina length, adjusted lignotuber size, and vegetative juvenility) and 1% (leaf shape index) significance levels for the functional traits. The LS-Means for the probability of seedling survival were similar in the mesic and dry populations, and not statistically different ($p > 0.05$). For discrete variables (vegetative juvenility and seedling survival), LS-Means based on the conditional fixed-effect coefficients from the GLMM (as presented in **Table 2**) were similar to corresponding estimates calculated from fixed-effect coefficients with a marginal (i.e., population-averaged) interpretation (see **Supplementary Methods 7**).

REML estimates of family and residual variances are shown in **Table 3** for the continuous variables. Based on one-sided likelihood ratio tests, statistically significant ($p < 0.05$) family variance estimates were found for lamina length, leaf shape index and adjusted lignotuber size in both populations, suggesting significant genetic variation within each population for these traits. The proportion of the total variation explained by the family variance (i.e., ICC) was ≈ 0.2 for lamina length and leaf shape index, but lower for adjusted lignotuber size (i.e., 0.03 and 0.07 in Brushy Lagoon and Ross, respectively; **Table 3**). Two-sided likelihood ratio tests undertaken to evaluate whether residual variances differed between populations indicated significant variance heterogeneity for lamina length and adjusted lignotuber size ($p < 0.001$), but not for leaf shape index ($p > 0.05$). In addition, for the difference between populations in family variances, two-sided likelihood ratio tests did not indicate significant variance heterogeneity at the 5% significance level for any of the traits. However, the latter results may reflect the lack of statistical power to detect variance heterogeneity (see also below) for some traits, given that family variance estimates differed between populations by a factor of two for lamina length and three for adjusted lignotuber size (**Table 3**).

Table 4 provides the family variances estimated by RSPL and ML for the discrete variables. The ML estimates of family variances were noticeably smaller than their counterparts estimated by RSPL: for Brushy Lagoon and Ross, the differences of the ML estimates relative to the RSPL estimates were 33 and 18% for vegetative juvenility, and 16 and 11% for seedling survival (**Table 4**). Although the true parameter values are not known, these results are consistent with the downward finite-sample bias that may emerge for ML estimates of variance components in GLMMs with discrete variables when the number of clustering units is not large (see references in **Supplementary Methods 1**). RSPL estimates of family variances were thus considered to be more accurate than their ML counterparts, given that simulation studies (e.g., McNeish, 2016, 2019) using sample sizes comparable to the number of families and their sizes in the current study indicated substantial downward bias in ML estimates of variances for the random-intercept term, and no evidence of noticeable bias for corresponding RSPL estimates. Underestimation of variances will also lead to underestimation of standard errors for fixed-effect parameters, which may result in less conservative hypothesis tests for fixed-effect model terms. Nevertheless, for the examined vegetative juvenility and seedling survival data, the method to estimate model parameters was inconsequential regarding conclusions on the statistical significance of the population effect (although the *F*-value increased under ML estimation, particularly for vegetative juvenility; **Supplementary Table 2**).

Based on RSPL estimates of family variances, the ICC ranged from 0.25 to 0.28 for vegetative juvenility, and from 0.02 to 0.06 for seedling survival (**Table 4**). As RSPL applies linearization methods to approximate the model rather than the likelihood function, ML estimates were used to conduct one-sided likelihood ratio tests for family variances of vegetative juvenility and seedling survival. These tests detected statistically significant ($p < 0.05$) family variance estimates (and thus genetic variation) for vegetative juvenility in both populations, but only in Ross for seedling survival (**Table 4**). However, for seedling survival in Brushy Lagoon, the likelihood ratio test is likely to have a low statistical power: with our family sizes, the number of families would need to be larger for detecting a non-null family variance, as suggested by simulation work with binary variables and weak ICCs (Austin and Leckie, 2018). Lack of statistical power may also have affected two-sided likelihood ratio tests pursued to evaluate whether family variances differed between populations, as variance heterogeneity was not found to be statistically significant ($p > 0.05$), despite the $\approx$ three times difference between populations in family variances for seedling survival (**Table 4**). Conversely, under a GLMM using a CMP distribution for vegetative juvenility, two-sided likelihood ratio tests indicated statistically significant ($p < 0.001$) heterogeneity between populations in dispersion of the observations (see footnotes of **Supplementary Table 2**).

Table 5 shows the estimates of directional selection gradients and their population differences for the focal functional traits. For Brushy Lagoon, statistical support against the null hypothesis of no effect on relative fitness (i.e., as indicated by a 95% confidence interval not overlapping with zero) was found for the selection gradients of lamina length and vegetative juvenility, with directional selection favoring seedlings exhibiting lower values in these traits (i.e., a decrease of 1% from the mean of lamina length and vegetative juvenility was expected to increase relative fitness by 1.5 and 0.3%, respectively). For Ross, statistical

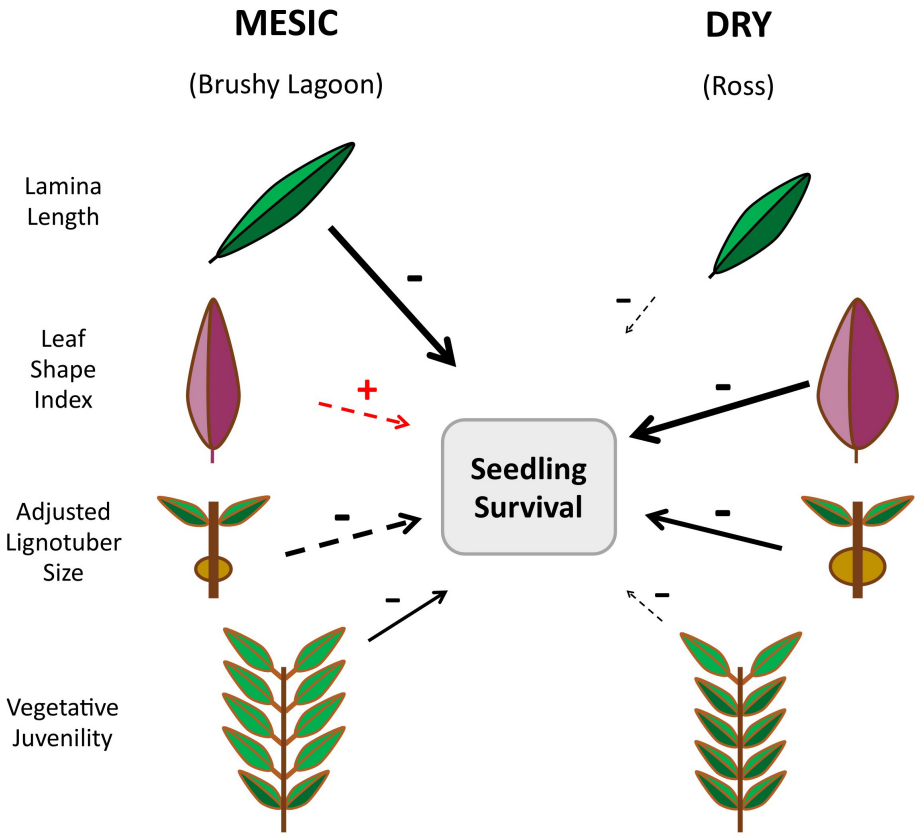

FIGURE 1 | Infographic summarizing the differences between the mesic (Brushy Lagoon) and dry (Ross) populations of *Eucalyptus pauciflora* for the least-squares means and directional selection gradients estimated for four seedling functional traits. Population-mean differences were statistically significantly ($p < 0.01$) for all focal traits assessed (**Table 2**). The directional selection gradient estimates for each population are symbolized by the arrows, which refer to the partial linear effect of a focal trait on seedling canopy (relative) survival evaluated after 67 days of dry-down. The increasing length and width of the arrows is indicative of increasing strength of the directional selection gradient estimates, and their directionality is shown by the +/− signs. In addition, a solid arrow indicates that the bootstrapped 95% confidence interval (CI) for the selection gradient estimate did not overlap with zero, providing statistical support against the null hypothesis of no effect on relative seedling survival (**Table 5**). A dashed arrow signifies that the bootstrapped 95% CI for the selection gradient estimate overlapped with zero, being indicative of no statistical support for the existence of fitness consequences of variation in the trait. The strong negative selection gradient estimated for lamina length in the mesic population suggests that a future occurrence of severe drought in the wild will shift the mean of the trait in the mesic population toward that of the dry population. The negative selection gradient estimated for adjusted lignotuber size in both populations suggests an early age trade-off between drought damage and recovery traits, with the canopies of phenotypes which develop larger lignotubers at the seedling stage being more susceptible to drought death.

support for the existence of fitness consequences of variation in the traits was provided for the selection gradients of leaf shape index and adjusted lignotuber size, indicating directional selection favoring phenotypes with lower values in these traits (i.e., an increase in 1.2 and 0.9% in relative fitness was expected from decreasing leaf shape index and adjusted lignotuber size by 1% from their means, respectively). Statistical support for the difference between populations in directional selection was observed in the selection gradient estimates for lamina length and leaf shape index, but not for adjusted lignotuber size and vegetative juvenility. Similar conclusions regarding the potential importance of directional selection acting on the traits within populations, and its difference between populations for a trait, were indicated from formal statistical inference about parameter estimates (on the probit scale) obtained from a GLMM fitted for data of the two populations combined (**Supplementary Table 3**).

DISCUSSION

This study identified significant functional trait differences and differing acute drought-induced phenotypic selection gradients between two populations from contrasting environments of the forest tree *E. pauciflora* (summarized in **Figure 1**). Significant genetic variation within populations, and significant mean differences between populations in all four focal traits studied suggest adaptive differences between the mesic and dry populations. While seedling survival did not differ between the two populations, when subject to acute drought stress, the traits under phenotypic selection varied between populations, suggesting different response strategies. Statistical support for the presence of fitness consequences of variation in the focal traits was detected for all traits in one or other population, but only one trait—lamina length—exhibited a pattern of directional selection consistent with a shift in the mean of the mesic population toward

TABLE 2 | Estimates of least-squares means and their standard errors (with 95% confidence intervals within parentheses) for four functional traits (lamina length, leaf shape index, adjusted lignotuber size and vegetative juvenility) and a fitness component (seedling survival) measured in the mesic (Brushy Lagoon) and dry (Ross) populations of *E. pauciflora*.

	Least-squares means		Population effect
	Brushy Lagoon	Ross	
Lamina length	75.17 ± 1.567 (71.71, 78.62)	60.40 ± 1.111 (57.96, 62.83)	$F = 59.12$; $p < 0.001$
Leaf shape index	30.45 ± 0.580 (29.18, 31.72)	32.81 ± 0.557 (31.60, 34.03)	$F = 8.35$; $p = 0.008$
Adjusted lignotuber size	5.09 ± 0.047 (4.99, 5.19)	5.68 ± 0.076 (5.51, 5.85)	$F = 43.13$; $p < 0.001$
Vegetative juvenility	2.38 ± 0.184 (2.01, 2.82)	5.13 ± 0.301 (4.51, 5.84)	$F = 63.02$; $p < 0.001$
Seedling survival	0.44 ± 0.034 (0.37, 0.51)	0.40 ± 0.044 (0.30, 0.50)	$F = 0.57$; $p = 0.458$

The results obtained from the significance test (F-statistic and p-value) undertaken for the population effect in the model are also given. Lamina length (mm); leaf shape index = adjusted lamina width (mm); adjusted lignotuber size = adjusted lignotuber diameter (mm); vegetative juvenility = node number of the first petiolate leaf; seedling survival = survival measured as a binary outcome (where 1 = alive and 0 = dead). Estimation of model parameters used restricted maximum likelihood in the linear mixed models (lamina length, leaf shape index and adjusted lignotuber size), and residual pseudo-likelihood in the generalized linear mixed models (vegetative juvenility and seedling survival). The analyses of leaf shape index and adjusted lignotuber size involved the adjustment of the lamina width and lignotuber diameter measurements using lamina length and stem diameter as covariates, respectively; thus their least-squares means are adjusted estimates for seedling differences in lamina length and radial stem growth, respectively. For vegetative juvenility and seedling survival, the tabulated values in the "Least-squares means" columns pertain to the inverse linked scale (i.e., the observed data scale).

TABLE 3 | Family and residual variances estimated by restricted maximum likelihood (REML), and estimates of intra-class correlation (ICC) coefficients, for continuous variables (lamina length, leaf shape index and adjusted lignotuber size) measured in the mesic (Brushy Lagoon) and dry (Ross) populations of *E. pauciflora*.

	Family variance		Residual variance		Intra-class correlation	
	Brushy Lagoon	Ross	Brushy Lagoon	Ross	Brushy Lagoon	Ross
Lamina length	26.50 ($p < 0.001$)	12.95 ($p < 0.001$)	94.23	58.21	0.220	0.182
Leaf shape index	3.51 ($p < 0.001$)	3.26 ($p < 0.001$)	12.33	10.48	0.222	0.237
Adjusted lignotuber size	0.014 ($p = 0.026$)	0.048 ($p < 0.001$)	0.392	0.647	0.034	0.069

*For family variances, a one-sided likelihood ratio test (Self and Liang, 1987) was applied to test whether a given estimate was significantly greater than zero (p-values are given within parentheses). Lamina length (mm); leaf shape index = adjusted lamina width (mm); adjusted lignotuber size = adjusted lignotuber diameter (mm) (see the footnotes of **Table 2** for further details). Standard error estimates for measuring the uncertainty of the estimated family variances are not presented. As the estimation of variance components usually constrains them to be positive, and their sampling distribution may thus be asymmetric, corresponding model-based estimates of standard errors may not provide accurate measures of uncertainty. The inaccuracy in standard error estimates is likely to occur for family variances, as the number of families sampled within each population was not large (Maas and Hox, 2004; McNeish and Stapleton, 2016b).*

that of the dry population following acute drought stress. Further, we provide evidence suggesting an early age trade-off between drought susceptibility and a recovery trait, with seedlings which develop larger lignotubers being more susceptible to drought death. Such trade-offs may have contributed to the observed similar population survival, despite the marked population differentiation in seedling traits.

Genetic variation within, and marked mean differences between, the mesic and dry populations for all four focal traits suggest adaptive differences between these populations, with seedlings of the dry population having on average smaller and broader leaves, longer vegetative juvenility, and larger lignotuber size than the mesic population. The mesic and dry populations compared were selected to accentuate rainfall differences and minimize the differences in other environmental factors. Accordingly, we expect that the observed population differences in the four functional traits reflect historic natural selection and adaptation to differences in water availability. Lamina length was strongly positively related to leaf area ($r = 0.88$, $n = 380$; unpublished data) and, as a surrogate of leaf size, its observed reduction in the dry population, for example, accords with the trait-environment associations reported in other *Eucalyptus* species (McLean et al., 2014). It is also consistent with species-level trends in south-eastern Australia, where species occurring in low rainfall areas tend to have smaller leaves through various changes in leaf length and width (McDonald et al., 2003). The longer vegetative juvenility observed in seedlings from the dry population also accords with the broader trends observed in a previous glasshouse trial with 37 *E. pauciflora* populations, where seedling vegetative

TABLE 4 | Family variances estimated by residual-pseudo likelihood (RSPL) and maximum likelihood (ML), and estimates of intra-class correlation (ICC) coefficients, for discrete variables (vegetative juvenility and seedling survival) measured in the mesic (Brushy Lagoon) and dry (Ross) populations of *E. pauciflora*.

	Family variance (RSPL)		Family variance (ML)		Intra-class correlation	
	Brushy Lagoon	**Ross**	**Brushy Lagoon**	**Ross**	**Brushy Lagoon**	**Ross**
Vegetative juvenility	0.066	0.038	0.044 ($p < 0.001$)	0.031 ($p < 0.001$)	0.278	0.252
Seedling survival	0.038	0.102	0.032 ($p = 0.105$)	0.091 ($p = 0.002$)	0.023	0.060

For family variances estimated by ML, a one-sided likelihood ratio test (Self and Liang, 1987) was applied to test whether a given estimate was significantly greater than zero (p-values are given within parentheses). Vegetative juvenility = node number of the first petiolate leaf; seedling survival = survival measured as a binary outcome (where 1 = alive and 0 = dead). Estimates of family variances refer to the linked scale (i.e., logarithmic and probit scales for vegetative juvenility and seedling survival, respectively). Likelihood ratio tests were not pursued to test family variances under RSPL estimation, since RSPL uses linearization methods to approximate the model rather than the likelihood function, which precludes the comparison of nested models using likelihood ratio tests (e.g., Hedeker and Gibbons, 2006; McNeish, 2016). Residual variances are not provided: the generalized linear mixed models (GLMMs) fitted for vegetative juvenility and seedling survival do not contain a definite error term, and thus the residual variance is not defined as in the linear mixed model for continuous traits. The ICCs presented above correspond to GLMMs estimated with RSPL, and were calculated as described by Nakagawa et al. (2017) (see also ***Supplementary Methods 4****). As in* ***Table 3****, standard error estimates for measuring the uncertainty of the estimated family variances are not given (see the footnotes in* ***Table 3****).*

TABLE 5 | Estimates of directional selection gradients, and their population differences, for four functional traits (lamina length, leaf shape index, adjusted lignotuber size and vegetative juvenility) measured in the mesic (Brushy Lagoon) and dry (Ross) populations of *E. pauciflora*.

	Directional selection gradient estimates		Differences between Brushy Lagoon and Ross in selection gradient estimates
	Brushy Lagoon	**Ross**	
Lamina length	−1.515 ± 0.382 *(−2.221, −0.720)*	−0.139 ± 0.425 (−0.963, 0.699)	−1.376 ± 0.569 *(−2.447, −0.206)*
Leaf shape index	0.376 ± 0.448 (−0.495, 1.278)	−1.176 ± 0.501 *(−2.161, −0.190)*	1.552 ± 0.677 *(0.218, 2.885)*
Adjusted lignotuber size	−0.765 ± 0.403 (−1.566, 0.031)	−0.873 ± 0.376 *(−1.622, −0.133)*	0.108 ± 0.550 (−0.987, 1.182)
Vegetative juvenility	−0.267 ± 0.116 *(−0.465, −0.010)*	−0.091 ± 0.160 (−0.411, 0.218)	−0.176 ± 0.196 (−0.522, 0.236)

Non-parametric bootstrapping was pursued to provide standard errors, and 95% confidence intervals (within parentheses), for the selection gradient estimates and their population differences. Lamina length (mm); leaf shape index = adjusted lamina width (mm); adjusted lignotuber size = adjusted lignotuber diameter (mm); vegetative juvenility = node number of the first petiolate leaf. As traits were mean-standardized, a given selection gradient pertains to the effect on relative fitness—i.e., percentage change in relative seedling survival—expected from increasing the focal trait by 1% from its mean, while holding all the other traits constant. Statistical support against a null hypothesis being true (i.e., against the absence of an effect for either a selection gradient in a population or its difference between populations) is provided by a 95% confidence interval not overlapping with zero (indicated in Italics).

juvenility was retained longer in populations from drier home-sites (Gauli et al., 2015; Costa e Silva et al., 2019). In this range-wide trial, the trait assessed was the percentage of nodes with petiolate leaves, which is negatively related to our measure of juvenility used in the present study. The difference between the dry and mesic populations is also consistent with trends in the *E. risdonii*/*tenuiramis* complex, where the retention of sessile juvenile leaves is extreme (into the reproductive stage) in populations from hot and dry environments (Costa e Silva et al., 2018). Populations of eucalypt species from hot/dry environments also have larger lignotubers than populations from mesic environments (Ladiges, 1974; Walters et al., 2005; Costa e Silva et al., 2019), as evident in our comparison.

Despite mean differences between the mesic and dry populations in putatively adaptive traits, the two populations did not differ significantly in survival following acute drought stress as induced in our dry-down experiment (**Table 2**). However, the two populations varied in the traits detected to be under directional selection, indicating that differences between the populations reside in the manner they selectively respond rather than in overall fitness under acute drought stress. Significant genetic-based family variance in survival was detected within the dry population, together with directional selection toward narrower leaves (smaller leaf shape index) and smaller lignotubers under acute drought stress. In contrast, no statistically significant family variance in survival was detected in the mesic population, and acute drought stress favored smaller leaf area (through shorter leaves) and earlier vegetative maturation (earlier development of petiolate leaves). However, statistical support for an important difference between the dry and mesic populations in directional selection gradients was

provided for lamina length and leaf shape index only. For a given trait, the population difference in the directional selection gradients could in part be due to a difference between populations in the phenotypic variance (Steele et al., 2011; De Lisle and Svensson, 2017). This would particularly apply to lamina length, where the statistical support for a difference between populations in directional selection (**Table 5**) could, to some extent, reflect a stronger selection in the more variable population (i.e., Brushy Lagoon; **Table 3**). Alternatively, the strength and direction of directional selection can be a function of the deviation of the population mean phenotype from the optimal phenotype for the environment (Steele et al., 2011; Hendry, 2017, p. 88). Regardless of the cause, given the significant genetic variation detected for all functional traits within each population (family variances in **Tables 3**, **4**), evolutionary change would be expected in these traits following the observed directional selection acting on them (Lande, 1979; Lande and Arnold, 1983).

The directional selection observed in lamina length, reflecting leaf area, is consistent with the hypothesis that the initial trait difference between the two populations could reflect, at least in part, the effects of past natural selection on the trait to reduce seedling susceptibility to events of acute drought stress. However, with drought risk likely to increase in the wild with climate change (and thus with more frequent episodes of severe drought), the direction and strength of the selection gradient estimates in the dry-down experiment suggest that, in the future, directional selection would shift the mean lamina length of the mesic population toward that of the dry population. A reduction in leaf area may also underlie directional selection favoring narrower leaves within the dry population (i.e., smaller leaf shape index) in the dry-down experiment. As noted above, reducing leaf area is well-recognized as an adaptation to drier conditions. In dry environments, selection has been shown to favor smaller leaves (Dudley, 1996; Ramírez-Valiente and Cavender-Bares, 2017). Smaller leaves may facilitate adaptation to drier conditions via greater main vein density reducing hydraulic vulnerability (Scoffoni et al., 2011) or through having a thinner boundary layer of still air allowing better heat shedding than larger leaves, and thus reducing the need for transpiration and associated water loss to shed heat (McDonald et al., 2003). As also mentioned above, the difference between the two populations in directional selection for a trait could reflect adaptation to different trait optima. For example, selection for narrower leaves, but not shorter leaves, in the dry population may be due to the already shorter leaves of this population being close to a phenotypic optimum, and thus only the variation in leaf shape index would determine selection mediated by seedling survival. In *Quercus*, narrow leaves were favored in a dry year but not in a wet year, although a statistically significant year-by-trait interaction could not be detected (Ramírez-Valiente et al., 2015). However, there was evidence in the current study for an important difference between the mesic and dry populations in directional selection gradient estimates for leaf shape index. In a species-level study in south-eastern Australia, combinations of reductions in leaf width in addition to leaf length were responsible for a reduction in leaf area in low rainfall areas (McDonald et al., 2003).

The selection gradient estimates for lignotuber size showed an opposite trend to what would be expected if the differences between the mesic and dry population means were the result of differences in adaptation arising from past natural selection to reduce susceptibility to acute drought stress. The dry population had larger lignotubers than the mesic population, but experienced directional selection in favor of seedlings with smaller lignotubers, shifting its mean toward the more mesic population. The same trend in directional selection, toward smaller lignotubers, was evident in the mesic population, but without statistical support for an important effect on seedling survival (as evaluated based on seedling canopy mortality). Susceptibility to drought damage and recovery can be considered as genetically different "traits" in eucalypts (Ammitzboll et al., 2020). While our unexpected finding is consistent with lignotubers having a key role in drought recovery, it signals a cost to their development. Such cost suggests a resistance vs. tolerance trade-off, common in the evolution of adaptations to periodic strong selection events arising from biotic (Best et al., 2008; Moreira et al., 2014) and abiotic (Vesk and Westoby, 2003; Agrawal et al., 2004; Ramírez-Valiente and Cavender-Bares, 2017) stress. In the present case, the observed cost may be transient and only evident at this early seedling stage (Orians et al., 2010; Hoque and Avila-Sakar, 2015), or persist through the life-cycle but out-weighed by the benefits of the better development of a recovery organ and gains in tolerance.

Lignotubers are generally considered a store of non-structural carbohydrates and dormant buds to enable basal re-sprouting following the death of the main stem (Walters et al., 2005; Borzak et al., 2016; Ammitzboll et al., 2020). If the main stem is not severely damaged, it is also possible that re-allocation of non-structural carbohydrates, such as starch, may help recover hydraulic function or photosynthetic activity (as suggested in Costa e Silva et al., 2019). However, the lignotuber does not appear to be an organ particularly specialized for the storage of non-structural carbohydrates such as starch, and likely serves primarily as a bud bank (Carrodus and Blake, 1970; Smith et al., 2018). The fact that selection favored smaller lignotuber sizes in the arid population under acute drought stress suggests that there is a cost associated with the early allocation of seedling resources to the development of this recovery organ. Non-structural carbohydrates support respiration and growth when photosynthesis is reduced during periods of water stress to avoid transpiration (McDowell et al., 2011; Mitchell et al., 2013). If the ready availability of non-structural carbohydrates is reduced due to resources being allocated to the lignotuber, or their storage within the lignotuber, then seedlings with larger lignotubers may be more susceptible to "carbon starvation" during prolonged water stress, and thus death of the seedling canopy. Lignotubers themselves have also been reported to have smaller and contorted vessels compared to those in the stems, and their resistance to water flow may be twice that of the stem (Myers, 1995). An alternative cause of drought-induced selection favoring small lignotubers may thus relate to their offering less resistance to water flow between the roots and the stem. Regardless of

the cause, with the arid population having significantly larger lignotubers than the mesic population, a trade-off between avoiding susceptibility to drought damage at the seedling stage vs. future seedling recovery could contribute to the absence of population differences in survival following the acute drought stress imposed. Indeed, with the evaluation of survival based on seedling canopy mortality at the termination of the experiment, re-watering and evaluation of recovery (Lu et al., 2010; Zhang et al., 2017; Ruehr et al., 2019) may well have provided the conditions under which population differences become manifest.

Drought-induced directional selection was found to favor early loss of vegetative juvenility in the mesic population, but had no effect on this trait in the dry population. There was thus no evidence from our phenotypic selection analysis that adaptation to acute drought stress would delay the development of the petiolate leaf in seedlings of the mesic population, and thus would shift the mean vegetative juvenility of the mesic population toward that of the dry population. Using growth performance as a fitness proxy, Costa e Silva et al. (2019) found no association between family-level variation in seedling juvenility and the fitness proxy in a *E. pauciflora* common-garden field trial established on a dry site, which is consistent with the results currently obtained in the dry population. In contrast, a common-garden trial of populations from the *E. risdonii*/*tenuiramis* complex established on a wet site showed that directional selection favored phenotypes with early ontogenetic transition to the petiolate "adult" leaf (Costa e Silva et al., 2018). This finding is consistent with the selection gradient estimate for vegetative juvenility in the mesic population. However, environmental context is important to the interpretation of trait-fitness relationships (MacColl, 2011), and this result from a wet site does not explain why such selection should also occur under acute drought stress.

Translating results of phenotypic selection analysis into mechanistic responses can be challenging (Wade and Kalisz, 1990; MacColl, 2011; Kingsolver et al., 2012). Whilst all four focal traits showed evidence of directional selection associated with acute drought stress in one or other of the tested populations, it is possible that selection on a measured trait may occur via indirect selection acting on unmeasured traits, correlated with the measured focal trait (Lande and Arnold, 1983; Mitchell-Olds and Shaw, 1987). Indeed, of the four traits studied, vegetative juvenility would be the one most likely to reflect indirect selection involving unmeasured ("hidden") traits that could also influence seedling survival. While we assessed vegetative juvenility of the seedlings based on the node at which the first petiolate leaf was produced, this is potentially a surrogate for a wide range of physical, chemical and physiological changes that can occur, as documented in other eucalypt species (James and Bell, 2001; Borzak et al., 2015; Vlasveld et al., 2018; Lucani et al., 2019). It is therefore possible that the directional selection detected against vegetative juvenility in the mesic population could reflect indirect selection on a "hidden" (unmeasured) trait with a negative phenotypic correlation with vegetative juvenility. Nevertheless, it is also possible that there is direct phenotypic selection on the early development of the petiole, which is only manifest in the early maturing mesic population and could be specific to the timing of the onset of acute drought stress with respect to the seedling ontogeny. Such direct selection could, for example, relate to the enhanced potential for changing leaf orientation, a key trait affecting light interception and heat avoidance in eucalypts and facilitated by the petiole (Cameron, 1970; King, 1997; James and Bell, 2000).

Our selection analysis focused on survival of acute drought stress as evaluated based on seedling canopy mortality. However, historic adaptation to long-term dry environments may be expected to involve a complexity of different selection forces driving a suite of adaptive differences associated with water availability more generally, not only acute drought stress. From an evolutionary perspective, growth in water limited environments may require different adaptations to those involved in surviving periodic acute drought stress. Xylem embolism is believed to be a key cause of tree mortality under severe water stress (Urli et al., 2013; Brodribb, 2017; Choat et al., 2018), including eucalypts (Li et al., 2018), although long periods of water stress and a prolonged reduction in photosynthetic activity can also contribute to mortality through "carbon starvation" and susceptibility to biotic attack (Galiano et al., 2011; McDowell et al., 2011; Mitchell et al., 2013). These selective mechanisms are part of a broader suite of traits which control water uptake and loss (Li et al., 2018), the potential coordination of leaf and stem traits (Bourne et al., 2017) and the important role of recovery mechanisms in drought adaptation (Zeppel et al., 2015; Ruehr et al., 2019). The different roles of such factors in adaptation to acute vs. chronic water stress may have contributed to the absence of our population difference in the studied fitness component, despite differences in focal trait mean values. In particular, historic adaptation in the dry population may potentially involve selection favoring seedling traits, as well as adult traits, that enhance survival in water limited environments more so than survival during periodic acute drought stress.

Nevertheless, it is possible that population differences in fitness following acute drought stress do exist, but depend upon their pattern of acclimation (also referred to as pre-conditioning and priming—McDowell et al., 2008; Wang et al., 2017). Non-lethal water stress has been shown to result in marked metabolic changes in *E. pauciflora* seedlings with, for example, leaf carbohydrate concentrations increasing and contributing to osmotic adjustment (Warren et al., 2012). In other eucalypts, differential plastic pre-adjustments to water stress have already been described for functional traits at the species (Warren et al., 2011, 2012), provenance (Li et al., 2000; McLean et al., 2014) and genotype (Pita and Pardos, 2001) levels in *Eucalyptus*. Further, it is possible that population differences in susceptibility to drought may only be expressed following a specific type of drought, such as one which includes water limitation combined with high temperature stress (Groom et al., 2004; Mitchell et al., 2014). This is particularly relevant as our dry-down experiment was conducted over autumn, and the maximum daily temperature the seedlings experienced averaged only 16–17°C, and did not exceed

27°C on any one day. The capacity to adapt to acute drought stress is likely to become more important into the future, with predictions of increasing extreme climate events. The results of this study suggest that: firstly, there may be genetic variation available in the focal traits (i.e., depending on the extent of genetic constraints in determining adaptive evolution; e.g., Costa e Silva et al., 2020) upon which they can respond to selection; and secondly, that the traits under phenotypic selection may vary between populations, reflecting in part differing historic selection pressures and adaptations, but also indicating potential different acute drought response strategies that may occur under future changes in the climate.

CONCLUSION

In conclusion, our dry-down experiment revealed different traits under directional selection between the studied dry and mesic populations, despite no difference in overall seedling survival. These results highlight the complexity of drought adaptation and the potential role of different traits and strategies in responses to acute drought stress. Further work on more populations from a wider range of environments, as well as replicated populations within the same environment, would help elucidate the various response strategies of *E. pauciflora* to drought stress, including key traits and mechanisms in different environments. Similarly, a better understanding of interacting factors, such as heat and drought pre-conditioning, in determining the dry-down tolerance of plants is required. Ultimately, a greater understanding of the variation in traits under selection and potential mechanisms across environments will contribute to predictions of resilience, or vulnerability, of populations to future climate stress.

DATA AVAILABILITY STATEMENT

The data upon which this research work is based is currently being used in another study, but can be requested from the corresponding author for consideration.

AUTHOR CONTRIBUTIONS

JCS conceived and conceptualized the research question and analytical design, performed the data analyses, and prepared the associated document provided in **Supplementary Material**. Data for this study was collected from a dry-down experiment designed and undertaken by RJ, EP, and SMP. BMP and RJ were responsible for data scoring of the experiment and compiling the datasets used in the analyses. JCS, RJ, and BMP wrote the manuscript. All authors contributed to the manuscript revision, read, and approved the submitted version.

FUNDING

The contribution of JCS to this research work was supported by *Fundação para a Ciência e a Tecnologia I.P.* (FCT), Portugal, through the *Norma Transitória* DL 57/2016/CP1382/CT0008 and UID/AGR/00239/2019. This research was also funded by the *Centro de Estudos Florestais*, Portugal, a research unit that is funded by FCT (Unit Project Reference: UIDB/00239/2020). BMP acknowledges support of the Australian Research Discovery (ARC) grant DP190102053.

ACKNOWLEDGMENTS

We thank and acknowledge Dorothy Steane's contribution to the design and implementation of the dry-down experiment, and Tim Brodribb for helpful discussion. We also thank Paul Tilyard, Fiona Walsh, and Dale Worledge for assistance with running and scoring the dry-down experiment. We are grateful to all institutions mentioned for their financial support, which provided the opportunity to complete this study.

SUPPLEMENTARY MATERIAL

The Supplementary Material for this article can be found online at: https://www.frontiersin.org/articles/10.3389/fevo.2021.722964/full#supplementary-material

REFERENCES

Agrawal, A. A., Conner, J. K., and Stinchcombe, J. R. (2004). Evolution of plant resistance and tolerance to frost damage. *Ecol. Lett.* 7, 1199–1208. doi: 10.1111/j.1461-0248.2004.00680.x

Aitken, S. N., Yeaman, S., Holliday, J. A., Wang, T., and Curtis-McLane, S. (2008). Adaptation, migration or extirpation: climate change outcomes for tree populations. *Evol. Appl.* 1, 95–111. doi: 10.1111/j.1752-4571.2007.00013.x

Alberto, F. J., Aitken, S. N., Alía, R., González-Martínez, S. C., Hänninen, H., Kremer, A., et al. (2013). Potential for evolutionary responses to climate change–evidence from tree populations. *Glob. Chang. Biol.* 19, 1645–1661. doi: 10.1111/gcb.12181

Allen, C. D., Macalady, A. K., Chenchouni, H., Bachelet, D., McDowell, N., Vennetier, M., et al. (2010). A global overview of drought and heat-induced tree mortality reveals emerging climate change risks for forests. *For. Ecol. Manage.* 259, 660–684. doi: 10.1016/j.foreco.2009.09.001

Ammitzboll, H., Vaillancourt, R. E., Potts, B. M., Harrison, P. A., Brodribb, T., Sussmilch, F. C., et al. (2020). Independent genetic control of drought resistance, recovery, and growth of *Eucalyptus globulus* seedlings. *Plant Cell Environ.* 43, 103–115. doi: 10.1111/pce.13649

Austin, P. C., and Leckie, G. (2018). The effect of number of clusters and cluster size on statistical power and type I error rates when testing random effects variance components in multilevel linear and logistic regression models. *J. Stat. Comput. Simul.* 88, 3151–3163. doi: 10.1080/00949655.2018.1504945

Bailey, T., Harrison, P., Davidson, N., Weller-Wong, A., Tilyard, P., Steane, D., et al. (2021). Embedding genetics experiments in restoration to guide plant choice for a degraded landscape with a changing climate. *Ecol. Manage. Restor.* (in press).

Baldwin, S. A., and Fellingham, G. W. (2013). Bayesian methods for the analysis of small sample multilevel data with a complex variance structure. *Psychol. Methods* 18, 151–164. doi: 10.1037/a0030642

Battaglia, M., and Reid, J. (1993). The effect of microsite variation on seed-germination and seedling survival of *Eucalyptus delegatensis*. *Aust. J. Bot.* 41, 169–181. doi: 10.1071/BT9930169

Best, A., White, A., and Boots, M. (2008). Maintenance of host variation in tolerance to pathogens and parasites. *Proc. Natl. Acad. Sci. U.S.A.* 105, 20786–20791. doi: 10.1073/pnas.0809558105

Borzak, C. L., Potts, B. M., Davies, N. W., and O'Reilly-Wapstra, J. M. (2015). Population divergence in the ontogenetic trajectories of foliar terpenes of a *Eucalyptus* species. *Ann. Bot.* 115, 159–170. doi: 10.1093/aob/mcu222

Borzak, C. L., Potts, B. M., and O'Reilly-Wapstra, J. M. (2016). Survival and recovery of *Eucalyptus globulus* seedlings from severe defoliation. *For. Ecol. Manage.* 379, 243–251. doi: 10.1016/j.foreco.2016.08.025

Bourne, A. E., Creek, D., Peters, J. M. R., Ellsworth, D. S., and Choat, B. (2017). Species climate range influences hydraulic and stomatal traits in *Eucalyptus* species. *Ann. Bot.* 120, 123–133. doi: 10.1093/aob/mcx020

Brodribb, T. J. (2017). Progressing from 'functional' to mechanistic traits. *New Phytol.* 215, 9–11. doi: 10.1111/nph.14620

Brunner, A. M., Varkonyi-Gasic, E., and Jones, R. C. (2016). "Phase change and phenology in trees," in *Plant Genetics and Genomics: Crops and Models*, Vol. 21, eds A. Groover and Q. Cronk (Cham: Springer), 227–274.

Buotte, P. C., Hicke, J. A., Preisler, H. K., Abatzoglou, J. T., Raffa, K. F., and Logan, J. A. (2016). Climate influences on whitebark pine mortality from mountain pine beetle in the greater yellowstone ecosystem. *Ecol. Appl.* 26, 2507–2524. doi: 10.1002/eap.1396

Cameron, R. (1970). Light intensity and the growth of *Eucalyptus* seedlings. I. Ontogenetic variation in *E. fastigata*. *Aust. J. Bot.* 18, 29–43.

Cano, F. J., López, R., and Warren, C. R. (2014). Implications of the mesophyll conductance to CO2 for photosynthesis and water-use efficiency during long-term water stress and recovery in two contrasting *Eucalyptus* species. *Plant Cell Environ.* 37, 2470–2490. doi: 10.1111/pce.12325

Capanu, M., Gönen, M., and Begg, C. B. (2013). An assessment of estimation methods for generalized linear mixed models with binary outcomes. *Stat. Med.* 32, 4550–4566. doi: 10.1002/sim.5866

Carrodus, B. B., and Blake, T. J. (1970). Studies on the lignotubers of *Eucalyptus obliqua* L'Heri. *New Phytol.* 69, 1069–1072.

Chen, I.-C., Hill, J. K., Ohlemüller, R., Roy, D. B., and Thomas, C. D. (2011). Rapid range shifts of species associated with high levels of climate warming. *Science* 333, 1024–1026. doi: 10.1126/science.1206432

Choat, B., Brodribb, T. J., Brodersen, C. R., Duursma, R. A., López, R., and Medlyn, B. E. (2018). Triggers of tree mortality under drought. *Nature* 558, 531–539. doi: 10.1038/s41586-018-0240-x

Corney, S., Katzfey, J., McGregor, J., Grose, M., Bennett, J., White, C., et al. (2010). *Climate Futures for Tasmania: Climate Modelling Technical Report*. Hobart, TAS: Antartic Climate & Ecosystem CRC.

Costa e Silva, J., Hardner, C., Tilyard, P., and Potts, B. M. (2011). The effects of age and environment on the expression of inbreeding depression in *Eucalyptus globulus*. *Heredity* 107, 50–60. doi: 10.1038/hdy.2010.154

Costa e Silva, J., Harrison, P. A., Wiltshire, R., and Potts, B. M. (2018). Evidence that divergent selection shapes a developmental cline in a forest tree species complex. *Ann. Bot.* 122, 181–194. doi: 10.1093/aob/mcy064

Costa e Silva, J., Potts, B., Harrison, P. A., and Bailey, T. (2019).). Temperature and rainfall are separate agents of selection shaping population differentiation in a forest tree. *Forests* 10:1145. doi: 10.3390/f10121145

Costa e Silva, J., Potts, B. M., and Harrison, P. A. (2020). Population divergence along a genetic line of least resistance in the tree species *Eucalyptus globulus*. *Genes* 11:1095.

Davis, M. B., and Shaw, R. G. (2001). Range shifts and adaptive responses to quaternary climate change. *Science* 292, 673–679.

De Lisle, S. P., and Svensson, E. I. (2017). On the standardization of fitness and traits in comparative studies of phenotypic selection. *Evolution* 71, 2313–2326. doi: 10.1111/evo.13325

Dillon, S., McEvoy, R., Baldwin, D. S., Rees, G. N., Parsons, Y., and Southerton, S. (2014). Characterisation of adaptive genetic diversity in environmentally contrasted populations of *Eucalyptus camaldulensis* Dehnh. (river red gum). *PLoS One* 9:e103515. doi: 10.1371/journal.pone.0103515

Donovan, L. A., Ludwig, F., Rosenthal, D. M., Rieseberg, L. H., and Dudley, S. A. (2009). Phenotypic selection on leaf ecophysiological traits in *Helianthus*. *New Phytol.* 183, 868–879. doi: 10.1111/j.1469-8137.2009.02916.x

Duan, H., Duursma, R. A., Huang, G., Smith, R. A., Choat, B., O'Grady, A. P., et al. (2014). Elevated [CO2] does not ameliorate the negative effects of elevated temperature on drought-induced mortality in *Eucalyptus radiata* seedlings. *Plant Cell Environ.* 37, 1598–1613. doi: 10.1111/pce.12260

Dudley, S. A. (1996). Differing selection on plant physiological traits in response to environmental water availability: a test of adaptive hypotheses. *Evolution* 50, 92–102. doi: 10.1111/j.1558-5646.1996.tb04475.x

Etterson, J. R. (2004). Evolutionary potential of *Chamaecrista fasciculata* in relation to climate change. I. Clinal patterns of selection along an environmental gradient in the Great Plains. *Evolution* 58, 1446–1458. doi: 10.1554/04-053

Fernández, R. J., and Reynolds, J. F. (2000). Potential growth and drought tolerance of eight desert grasses: lack of a trade-off? *Oecologia* 123, 90–98. doi: 10.1007/s004420050993

Ferron, J. M., Bell, B. A., Hess, M. R., Rendina-Gobioff, G., and Hibbard, S. T. (2009). Making treatment effect inferences from multiple-baseline data: the utility of multilevel modeling approaches. *Behav. Res. Methods* 41, 372–384. doi: 10.3758/BRM.41.2.372

Frachon, L., Bartoli, C., Carrère, S., Bouchez, O., Chaubet, A., Gautier, M., et al. (2018). A genomic map of climate adaptation in *Arabidopsis thaliana* at a micro-geographic scale. *Front. Plant Sci.* 9:967. doi: 10.3389/fpls.2018.00967

Franklin, O. D., and Morrissey, M. B. (2017). Inference of selection gradients using performance measures as fitness proxies. *Methods Ecol. Evol.* 8, 663–677. doi: 10.1111/2041-210X.12737

Galiano, L., Martínez-Vilalta, J., and Lloret, F. (2011). Carbon reserves and canopy defoliation determine the recovery of scots pine 4 yr after a drought episode. *New Phytol.* 190, 750–759. doi: 10.1111/j.1469-8137.2010.03628.x

Gardiner, J. C., Luo, Z., and Roman, L. A. (2009). Fixed effects, random effects and GEE: what are the differences? *Stat. Med.* 28, 221–239. doi: 10.1002/sim.3478

Gardner, W., Mulvey, E. P., and Shaw, E. C. (1995). Regression analyses of counts and rates: poisson, overdispersed poisson, and negative binomial models. *Psychol. Bull.* 118, 392–404. doi: 10.1037/0033-2909.118.3.392

Gauli, A., Steane, D. A., Vaillancourt, R. E., and Potts, B. M. (2014). Molecular genetic diversity and population structure in *Eucalyptus pauciflora* subsp pauciflora (Myrtaceae) on the island of Tasmania. *Aust. J. Bot.* 62, 175–188. doi: 10.1071/bt14036

Gauli, A., Vaillancourt, R. E., Bailey, T. G., Steane, D. A., and Potts, B. M. (2015). Evidence for local climate adaptation in early-life traits of Tasmanian populations of *Eucalyptus pauciflora*. *Tree Genet. Genomes* 11:104. doi: 10.1007/s11295-015-0930-6

Gauli, A., Vaillancourt, R. E., Steane, D. A., Bailey, T. G., and Potts, B. M. (2013).). Effect of forest fragmentation and altitude on the mating system of *Eucalyptus pauciflora* (Myrtaceae). *Aust. J. Bot.* 61, 622–632.

Gómez, J. M. (2004). Bigger is not always better: conflicting selective pressures on seed size in *Quercus ilex*. *Evolution* 58, 71–80. doi: 10.1111/j.0014-3820.2004.tb01574.x

Griffin, A. R., Potts, B. M., Vaillancourt, R. E., and Bell, J. C. (2019). Life cycle expression of inbreeding depression in *Eucalyptus regnans* and inter-generational stability of its mixed mating system. *Ann. Bot.* 124, 179–187. doi: 10.1093/aob/mcz059

Groom, P. K., Lamont, B. B., Leighton, S., Leighton, P., and Burrows, C. (2004). Heat damage in sclerophylls is influenced by their leaf properties and plant environment. *Ecoscience* 11, 94–101. doi: 10.1080/11956860.2004.11682813

Guikema, S. D., and Goffelt, J. P. (2008). A flexible count data regression model for risk analysis. *Risk Anal.* 28, 213–223. doi: 10.1111/j.1539-6924.2008.01014.x

Hahn, E. D., and Soyer, R. (2005). *Probit and Logit Models: Differences in the Multivariate Realm*. Available online at: http://home.gwu.edu/~{}soyer/mv1h.pdf (accessed December 29, 2020).

Harrison, P. (2017). *Integrating Climate Change into Conservation and Restoration Strategies : The Case of the Tasmanian Eucalypts*. Ph.D. thesis. Hobart, TAS: University of Tasmania.

Harrison, P. A., Vaillancourt, R. E., Harris, R. M. B., and Potts, B. M. (2017). Integrating climate change and habitat fragmentation to identify candidate seed sources for ecological restoration. *Restor. Ecol.* 25, 524–531. doi: 10.1111/rec.12488

Hedeker, D., and Gibbons, R. D. (2006). *Longitudinal Data Analysis*. Hoboken, NJ: Wiley.

Hendry, A. P. (2017). *Eco-Evolutionary Dynamics*. Oxford: Princeton University Press.

Hereford, J., Hansen, T. F., and Houle, D. (2004). Comparing strengths of directional selection: how strong is strong? *Evolution* 58, 2133–2143. doi: 10.1111/j.0014-3820.2004.tb01592.x

Heschel, M. S., and Riginos, C. (2005). Mechanisms of selection for drought stress tolerance and avoidance in *Impatiens capensis* (Balsaminaceae). *Am. J. Bot.* 92, 37–44. doi: 10.3732/ajb.92.1.37

Hoffmann, A. A., and Sgro, C. M. (2011). Climate change and evolutionary adaptation. *Nature* 470, 479–485. doi: 10.1038/nature09670

Hoque, S., and Avila-Sakar, G. (2015). Trade-offs and ontogenetic changes in resistance and tolerance to insect herbivory in *Arabidopsis*. *Int. J. Plant Sci.* 176, 150–158. doi: 10.1086/679478

Houle, D., Pélabon, C., Wagner, G. P., and Hansen, T. F. (2011). Measurement and meaning in biology. *Q. Rev. Biol.* 86, 3–34. doi: 10.1086/658408

James, S. A., and Bell, D. T. (2000). Leaf orientation, light interception and stomatal conductance of *Eucalyptus globulus* ssp. globulus leaves. *Tree Physiol.* 20, 815–823. doi: 10.1093/treephys/20.12.815

James, S. A., and Bell, D. T. (2001). Leaf morphological and anatomical characteristics of heteroblastic *Eucalyptus globulus* ssp globulus (Myrtaceae). *Aust. J. Bot.* 49, 259–269.

Janzen, F. J., and Stern, H. S. (1998). Logistic regression for empirical studies of multivariate selection. *Evolution* 52, 1564–1571. doi: 10.1111/j.1558-5646.1998.tb02237.x

Jordan, R., Hoffmann, A. A., Dillon, S. K., and Prober, S. M. (2017). Evidence of genomic adaptation to climate in *Eucalyptus microcarpa*: implications for adaptive potential to projected climate change. *Mol. Ecol.* 26, 6002–6020. doi: 10.1111/mec.14341

Jump, A. S., and Peñuelas, J. (2005). Running to stand still: adaptation and the response of plants to rapid climate change. *Ecol. Lett.* 8, 1010–1020. doi: 10.1111/j.1461-0248.2005.00796.x

Keller, S. R., Levsen, N., Olson, M. S., and Tiffin, P. (2012). Local adaptation in the flowering-time gene network of balsam poplar, *Populus balsamifera* L. *Mol. Biol. Evol.* 29, 3143–3152. doi: 10.1093/molbev/mss121

Kenward, M. G., and Roger, J. H. (1997). Small sample inference for fixed effects from restricted maximum likelihood. *Biometrics* 53, 983–997.

Kenward, M. G., and Roger, J. H. (2009). An improved approximation to the precision of fixed effects from restricted maximum likelihood. *Comput. Stat. Data Anal.* 53, 2583–2595. doi: 10.1016/j.csda.2008.12.013

King, D. A. (1997). The functional significance of leaf angle in *Eucalyptus*. *Aust. J. Bot.* 45, 619–639. doi: 10.1071/BT96063

Kingsolver, J. G., and Diamond, S. E. (2011). Phenotypic selection in natural populations: what limits directional selection? *Am. Nat.* 177, 346–357. doi: 10.1086/658341

Kingsolver, J. G., Diamond, S. E., Siepielski, A. M., and Carlson, S. M. (2012). Synthetic analyses of phenotypic selection in natural populations: lessons, limitations and future directions. *Evol. Ecol.* 26, 1101–1118. doi: 10.1007/s10682-012-9563-5

Kingsolver, J. G., Hoekstra, H. E., Hoekstra, J. M., Berrigan, D., Vignieri, S. N., Hill, C. E., et al. (2001). The strength of phenotypic selection in natural populations. *Am. Nat.* 157, 245–261. doi: 10.1086/319193

Klein, T., Zeppel, M. J. B., Anderegg, W. R. L., Bloemen, J., De Kauwe, M. G., Hudson, P., et al. (2018). Xylem embolism refilling and resilience against drought-induced mortality in woody plants: processes and trade-offs. *Ecol. Res.* 33, 839–855. doi: 10.1007/s11284-018-1588-y

Koelewijn, H. P., Koski, V., and Savolainen, O. (1999). Magnitude and timing of inbreeding depression in scots pine (*Pinus sylvestris* L.). *Evolution* 53, 758–768.

Kramer, K., van der Werf, B., and Schelhaas, M.-J. (2015). Bring in the genes: genetic-ecophysiological modeling of the adaptive response of trees to environmental change. With application to the annual cycle. *Front. Plant Sci.* 5:742. doi: 10.3389/fpls.2014.00742

Kremer, A., Potts, B. M., and Delzon, S. (2014). Genetic divergence in forest trees: understanding the consequences of climate change. *Funct. Ecol.* 28, 22–36. doi: 10.1111/1365-2435.12169

Ladiges, P. Y. (1974). Differentiation in some populations of *Eucalyptus viminalis* Labill. in relation to factors affecting seedling establishment. *Aust. J. Bot.* 22, 471–487. doi: 10.1071/bt9740471

Lande, R. (1979). Quantitative genetic analysis of multivariate evolution, applied to brain:body size allometry. *Evolution* 33, 402–416.

Lande, R., and Arnold, S. J. (1983). The measurement of selection on correlated characters. *Evolution* 37, 1210–1226. doi: 10.2307/2408842

Lau, J. A., Shaw, R. G., Reich, P. B., and Tiffin, P. (2014). Indirect effects drive evolutionary responses to global change. *New Phytol.* 201, 335–343. doi: 10.1111/nph.12490

Li, C. Y., Berninger, F., Koskela, J., and Sonninen, E. (2000). Drought responses of *Eucalyptus microtheca* provenances depend on seasonality of rainfall in their place of origin. *Aust. J. Plant Physiol.* 27, 231–238.

Li, X., Blackman, C. J., Choat, B., Duursma, R. A., Rymer, P. D., Medlyn, B. E., et al. (2018). Tree hydraulic traits are coordinated and strongly linked to climate-of-origin across a rainfall gradient. *Plant Cell Environ.* 41, 646–660. doi: 10.1111/pce.13129

Lu, Y., Equiza, M. A., Deng, X., and Tyree, M. T. (2010). Recovery of *Populus tremuloides* seedlings following severe drought causing total leaf mortality and extreme stem embolism. *Physiol. Plant.* 140, 246–257.

Lucani, C. J., Brodribb, T. J., Jordan, G. J., and Mitchell, P. J. (2019). Juvenile and adult leaves of heteroblastic *Eucalyptus globulus* vary in xylem vulnerability. *Trees Struct. Funct.* 33, 1167–1178. doi: 10.1007/s00468-019-01851-4

Maas, C. J. M., and Hox, J. J. (2004). Robustness issues in multilevel regression analysis. *Stat. Neerl.* 58, 127–137. doi: 10.1046/j.0039-0402.2003.00252.x

MacColl, A. D. (2011). The ecological causes of evolution. *Trends Ecol. Evol.* 26, 514–522. doi: 10.1016/j.tree.2011.06.009

Marchin, R. M., Ossola, A., Leishman, M. R., and Ellsworth, D. S. (2020). A simple method for simulating drought effects on plants. *Front. Plant Sci.* 10:1715. doi: 10.3389/fpls.2019.01715

Matusick, G., Ruthrof, K. X., Brouwers, N. C., Dell, B., and Hardy, G. S. J. (2013). Sudden forest canopy collapse corresponding with extreme drought and heat in a mediterranean-type eucalypt forest in southwestern Australia. *Eur. J. For. Res.* 132, 497–510. doi: 10.1007/s10342-013-0690-5

McDonald, P. G., Fonseca, C. R., Overton, J. M., and Westoby, M. (2003). Leaf-size divergence along rainfall and soil-nutrient gradients: is the method of size reduction common among clades? *Funct. Ecol.* 17, 50–57. doi: 10.1046/j.1365-2435.2003.00698.x

McDowell, N., Pockman, W. T., Allen, C. D., Breshears, D. D., Cobb, N., Kolb, T., et al. (2008). Mechanisms of plant survival and mortality during drought: why do some plants survive while others succumb to drought? *New Phytol.* 178, 719–739.

McDowell, N. G., Beerling, D. J., Breshears, D. D., Fisher, R. A., Raffa, K. F., and Stitt, M. (2011). The interdependence of mechanisms underlying climate-driven vegetation mortality. *Trends Ecol. Evol.* 26, 523–532. doi: 10.1016/j.tree.2011.06.003

McKiernan, A. B., Potts, B. M., Brodribb, T. J., Hovenden, M. J., Davies, N. W., McAdam, S. A. M., et al. (2016). Responses to mild water deficit and rewatering differ among secondary metabolites but are similar among provenances within *Eucalyptus* species. *Tree Physiol.* 36, 133–147. doi: 10.1093/treephys/tpv106

McLean, E. H., Prober, S. M., Stock, W. D., Steane, D. A., Potts, B. M., Vaillancourt, R. E., et al. (2014). Plasticity of functional traits varies clinally along a rainfall gradient in *Eucalyptus tricarpa*. *Plant Cell Environ.* 37, 1440–1451. doi: 10.1111/pce.12251

McNeish, D. (2016). Estimation methods for mixed logistic models with few clusters. *Multivariate Behav. Res.* 51, 790–804. doi: 10.1080/00273171.2016.1236237

McNeish, D. (2019). Poisson multilevel models with small samples. *Multivariate Behav. Res.* 54, 444–455. doi: 10.1080/00273171.2018.1545630

McNeish, D. M., and Stapleton, L. M. (2016a). Modeling clustered data with very few clusters. *Multivariate Behav. Res.* 51, 495–518. doi: 10.1080/00273171.2016.1167008

McNeish, D. M., and Stapleton, L. M. (2016b). The effect of small sample size on two-level model estimates: a review and illustration. *Educ. Psychol. Rev.* 28, 295–314. doi: 10.1007/s10648-014-9287-x

Merilä, J., and Hendry, A. P. (2014). Climate change, adaptation, and phenotypic plasticity: the problem and the evidence. *Evol. Appl.* 7, 1–14. doi: 10.1111/eva.12137

Mitchell, P. J., O'Grady, A. P., Hayes, K. R., and Pinkard, E. A. (2014). Exposure of trees to drought- induced die- off is defined by a common climatic threshold

across different vegetation types. *Ecol. Evol.* 4, 1088–1101. doi: 10.1002/ece3.1008

Mitchell, P. J., O'Grady, A. P., Tissue, D. T., White, D. A., Ottenschlaeger, M. L., and Pinkard, E. A. (2013). Drought response strategies define the relative contributions of hydraulic dysfunction and carbohydrate depletion during tree mortality. *New Phytol.* 197, 862–872. doi: 10.1111/nph.12064

Mitchell-Olds, T., and Shaw, R. G. (1987). Regression analysis of natural selection: statistical inference and biological interpretation. *Evolution* 41, 1149–1161. doi: 10.2307/2409084

Molenberghs, G., Didier, R., and Verbeke, G. (2002). A review of generalized linear mixed models. *J. Soc. Fr. Statistique* 143, 53–57.

Monica, A. G., and Lauren, R. G. (2003). Inheritance and natural selection on functional traits. *Int. J. Plant Sci.* 164, S21–S42. doi: 10.1086/368233

Moreira, X., Mooney, K. A., Rasmann, S., Petry, W. K., Carrillo-Gavilan, A., Zas, R., et al. (2014). Trade-offs between constitutive and induced defences drive geographical and climatic clines in pine chemical defences. *Ecol. Lett.* 17, 537–546. doi: 10.1111/ele.12253

Morrissey, M. B., and Sakrejda, K. (2013). Unification of regression-based methods for the analysis of natural selection. *Evolution* 67, 2094–2100. doi: 10.1111/evo.12077

Myers, B. (1995). The Influence of the lignotuber on hydraulic conductance and leaf conductance in *Eucalyptus behriana* seedlings. *Funct. Plant Biol.* 22, 857–863. doi: 10.1071/PP9950857

Nakagawa, S., Johnson, P. C. D., and Schielzeth, H. (2017). The coefficient of determination R2 and intra-class correlation coefficient from generalized linear mixed-effects models revisited and expanded. *J. R. Soc. Interface* 14:20170213. doi: 10.1098/rsif.2017.0213

Nicotra, A. B., Atkin, O. K., Bonser, S. P., Davidson, A. M., Finnegan, E. J., Mathesius, U., et al. (2010). Plant phenotypic plasticity in a changing climate. *Trends Plant Sci.* 15, 684–692.

Orians, C. M., Hochwender, C. G., Fritz, R. S., and Snall, T. (2010). Growth and chemical defense in willow seedlings: trade-offs are transient. *Oecologia* 163, 283–290. doi: 10.1007/s00442-009-1521-8

Park Williams, A., Allen, C. D., Macalady, A. K., Griffin, D., Woodhouse, C. A., Meko, D. M., et al. (2013). Temperature as a potent driver of regional forest drought stress and tree mortality. *Nat. Clim. Chang.* 3, 292–297. doi: 10.1038/nclimate1693

Patterson, H. D., and Thompson, R. (1971). Recovery of inter-block information when block sizes are unequal. *Biometrika* 58, 545–554.

Petit, R. J., and Hampe, A. (2006). Some evolutionary consequences of being a tree. *Annu. Rev. Ecol. Evol. Syst.* 37, 187–214. doi: 10.1146/annurev.ecolsys.37.091305.110215

Phillips, P. C., and Arnold, S. J. (1989). Visualizing multivariate selection. *Evolution* 43, 1209–1222. doi: 10.1111/j.1558-5646.1989.tb02569.x

Pinheiro, J. C., and Bates, D. M. (1995). Approximations to the log-likelihood function in the nonlinear mixed-effects model. *J. Comput. Graph. Stat.* 4, 12–35. doi: 10.1080/10618600.1995.10474663

Pita, P., and Pardos, J. A. (2001). Growth, leaf morphology, water use and tissue water relations of *Eucalyptus globulus* clones in response to water deficit. *Tree Physiol.* 21, 599–607.

Pluess, A. R., Frank, A., Heiri, C., Lalagüe, H., Vendramin, G. G., and Oddou-Muratorio, S. (2016). Genome–environment association study suggests local adaptation to climate at the regional scale in *Fagus sylvatica*. *New Phytol.* 210, 589–601. doi: 10.1111/nph.13809

Prober, S. M., Potts, B. M., Bailey, T., Byrne, M., Dillon, S., Harrison, P. A., et al. (2016). Climate adaptation and ecological restoration in eucalypts. *Proc. R. Soc. Vic.* 128, 40–53.

Ramírez-Valiente, J. A., and Cavender-Bares, J. (2017). Evolutionary trade-offs between drought resistance mechanisms across a precipitation gradient in a seasonally dry tropical oak (*Quercus oleoides*). *Tree Physiol.* 37, 889–901. doi: 10.1093/treephys/tpx040

Ramírez-Valiente, J. A., Valladares, F., Delgado, A., Nicotra, A. B., and Aranda, I. (2015). Understanding the importance of intrapopulation functional variability and phenotypic plasticity in *Quercus suber*. *Tree Genet. Genomes* 11:35. doi: 10.1007/s11295-015-0856-z

Ramírez-Valiente, J. A., Valladares, F., Sanchez-Gomez, D., Delgado, A., and Aranda, I. (2014). Population variation and natural selection on leaf traits in cork oak throughout its distribution range. *Acta Oecol. Int. J. Ecol.* 58, 49–56. doi: 10.1016/j.actao.2014.04.004

Raudenbush, S. W., and Bryk, A. S. (2002). *Hierarchical Linear Models: Applications and Data Analysis Methods*. Thousand Oaks, CA: Sage Publications.

Ruehr, N. K., Grote, R., Mayr, S., and Arneth, A. (2019). Beyond the extreme: recovery of carbon and water relations in woody plants following heat and drought stress. *Tree Physiol.* 39, 1285–1299.

SAS (2017). *SAS/STAT$14.3 User's Guide*. Cary, NC: SAS Institute Inc.

Schwalm, C. R., Anderegg, W. R. L., Michalak, A. M., Fisher, J. B., Biondi, F., Koch, G., et al. (2017). Global patterns of drought recovery. *Nature* 548, 202–205. doi: 10.1038/nature23021

Scoffoni, C., Rawls, M., McKown, A., Cochard, H., and Sack, L. (2011). Decline of leaf hydraulic conductance with dehydration: relationship to leaf size and venation architecture. *Plant Physiol.* 156, 832–843. doi: 10.1104/pp.111.173856

Self, S. G., and Liang, K.-Y. (1987). Asymptotic properties of maximum likelihood estimators and likelihood ratio tests under nonstandard conditions. *J. Am. Stat. Assoc.* 82, 605–610. doi: 10.1080/01621459.1987.10478472

Shaw, R. G., and Etterson, J. R. (2012). Rapid climate change and the rate of adaptation: insight from experimental quantitative genetics. *New Phytol.* 195, 752–765. doi: 10.1111/j.1469-8137.2012.04230.x

Shmueli, G., Minka, T. P., Kadane, J. B., Borle, S., and Boatwright, P. (2005). A useful distribution for fitting discrete data: revival of the Conway–Maxwell–Poisson distribution. *J. Roy. Stat. Soc. Ser. C. (Appl. Stat.)* 54, 127–142. doi: 10.1111/j.1467-9876.2005.00474.x

Siepielski, A. M., DiBattista, J. D., and Carlson, S. M. (2009). It's about time: the temporal dynamics of phenotypic selection in the wild. *Ecol. Lett.* 12, 1261–1276. doi: 10.1111/j.1461-0248.2009.01381.x

Siepielski, A. M., Gotanda, K. M., Morrissey, M. B., Diamond, S. E., DiBattista, J. D., and Carlson, S. M. (2013). The spatial patterns of directional phenotypic selection. *Ecol. Lett.* 16, 1382–1392. doi: 10.1111/ele.12174

Smith, M. G., Arndt, S. K., Miller, R. E., Kasel, S., and Bennett, L. T. (2018). Trees use more non-structural carbohydrate reserves during epicormic than basal resprouting. *Tree Physiol.* 38, 1779–1791.

Steane, D. A., Potts, B. M., McLean, E. H., Collins, L., Holland, B. R., Prober, S. M., et al. (2017). Genomic scans across three eucalypts suggest that adaptation to aridity is a genome-wide phenomenon. *Genome Biol. Evol.* 9, 253–265. doi: 10.1093/gbe/evw290

Steele, D. B., Siepielski, A. M., and McPeek, M. A. (2011). Sexual selection and temporal phenotypic variation in a damselfly population. *J. Evol. Biol.* 24, 1517–1532. doi: 10.1111/j.1420-9101.2011.02284.x

Stoneman, G. L. (1994). Ecology and physiology of establishment of eucalypt seedlings from seed: a review. *Aust. For.* 57, 11–29. doi: 10.1080/00049158.1994.10676109

Tozer, M. G., and Bradstock, R. A. (1998). Factors influencing the establishment of seedlings of the mallee, *Eucalyptus luehmanniana* (Myrtaceae). *Aust. J. Bot.* 45, 997–1008. doi: 10.1071/BT96111

Urli, M., Porté, A. J., Cochard, H., Guengant, Y., Burlett, R., and Delzon, S. (2013). Xylem embolism threshold for catastrophic hydraulic failure in angiosperm trees. *Tree Physiol.* 33, 672–683. doi: 10.1093/treephys/tpt030

Vesk, P. A., and Westoby, M. (2003). Drought damage and recovery–a conceptual model [2]. *New Phytol.* 160, 7–14.

Vlasveld, C., O'Leary, B., Udovicic, F., and Burd, M. (2018). Leaf heteroblasty in eucalypts: biogeographic evidence of ecological function. *Aust. J. Bot.* 66, 191–201. doi: 10.1071/BT17134

Wade, M. J., and Kalisz, S. (1990). The causes of natural selection. *Evolution* 44, 1947–1955. doi: 10.2307/2409605

Walters, J. R., Bell, T. L., and Read, S. (2005). Intra-specific variation in carbohydrate reserves and sprouting ability in *Eucalyptus obliqua* seedlings. *Aust. J. Bot.* 53, 195–203.

Wang, X., Liu, F.l., and Jiang, D. (2017). Priming: a promising strategy for crop production in response to future climate. *J. Integr. Agric.* 16, 2709–2716. doi: 10.1016/S2095-3119(17)61786-6

Warren, C. R., Aranda, I., and Cano, F. J. (2011). Responses to water stress of gas exchange and metabolites in *Eucalyptus* and *Acacia* spp. *Plant Cell Environ.* 34, 1609–1629. doi: 10.1111/j.1365-3040.2011.02357.x

Warren, C. R., Aranda, I., and Cano, F. J. (2012). Metabolomics demonstrates divergent responses of two *Eucalyptus* species to water stress. *Metabolomics* 8, 186–200. doi: 10.1007/s11306-011-0299-y

Warwell, M. V., and Shaw, R. G. (2018). Phenotypic selection on growth rhythm in whitebark pine under climatic conditions warmer than seed origins. *J. Evol. Biol.* 31, 1284–1299. doi: 10.1111/jeb.13301

Warwell, M. V., and Shaw, R. G. (2019). Phenotypic selection on ponderosa pine seed and seedling traits in the field under three experimentally manipulated drought treatments. *Evol. Appl.* 12, 159–174. doi: 10.1111/eva.12685

Wedderburn, R. W. M. (1974). Quasi-likelihood functions, generalized linear models, and the Gauss-Newton method. *Biometrika* 61, 439–447. doi: 10.1093/biomet/61.3.439

Wolfinger, R., and O'Connell, M. (1993). Generalized linear mixed models a pseudo-likelihood approach. *J. Stat. Comput. Simul.* 48, 233–243. doi: 10.1080/00949659308811554

Zeppel, M. J. B., Harrison, S. P., Adams, H. D., Kelley, D. I., Li, G., Tissue, D. T., et al. (2015). Drought and resprouting plants. *New Phytol.* 206, 583–589. doi: 10.1111/nph.13205

Zhang, Y., Xie, J.-B., and Li, Y. (2017). Effects of increasing root carbon investment on the mortality and resprouting of *Haloxylon ammodendron* seedlings under drought. *Plant Biol.* 19, 191–200.

Conflict of Interest: The authors declare that the research was conducted in the absence of any commercial or financial relationships that could be construed as a potential conflict of interest.

Publisher's Note: All claims expressed in this article are solely those of the authors and do not necessarily represent those of their affiliated organizations, or those of the publisher, the editors and the reviewers. Any product that may be evaluated in this article, or claim that may be made by its manufacturer, is not guaranteed or endorsed by the publisher.

Advantages of publishing in Frontiers

OPEN ACCESS
Articles are free to read for greatest visibility and readership

FAST PUBLICATION
Around 90 days from submission to decision

HIGH QUALITY PEER-REVIEW
Rigorous, collaborative, and constructive peer-review

TRANSPARENT PEER-REVIEW
Editors and reviewers acknowledged by name on published articles

Frontiers
Avenue du Tribunal-Fédéral 34
1005 Lausanne | Switzerland

Visit us: www.frontiersin.org
Contact us: frontiersin.org/about/contact

REPRODUCIBILITY OF RESEARCH
Support open data and methods to enhance research reproducibility

DIGITAL PUBLISHING
Articles designed for optimal readership across devices

FOLLOW US
@frontiersin

IMPACT METRICS
Advanced article metrics track visibility across digital media

EXTENSIVE PROMOTION
Marketing and promotion of impactful research

LOOP RESEARCH NETWORK
Our network increases your article's readership